Immunotherapy with T cells:

new strategies and improved designs

Eline van Diest

Immunotherapy with T cells:

new strategies and improved designs

Eline van Diest

Immunotherapy with T cells:
new strategies and improved designs

Immunotherapie met T cellen:
nieuwe strategieën en verbeterde ontwerpen
(met een samenvatting in het Nederlands)

Proefschrift

ter verkrijging van de graad van doctor aan de
Universiteit Utrecht
op gezag van de
rector magnificus, prof.dr. H.R.B.M. Kummeling,
ingevolge het besluit van het college voor promoties
in het openbaar te verdedigen op

donderdag 13 april 2023 des middags te 2.15 uur

door

Eline van Diest

geboren op 27 juli 1993
te Maastricht

Promotor:
Prof. dr. J.H.E. Kuball

Copromotoren:
Dr. D. Beringer
Dr. Z. Sebestyen

Beoordelingscommissie:
Prof. dr. P.A.J.T. Robe (voorzitter)
Prof. dr. R.M. Schiffelers
Prof. dr. F.G. Förster
Prof. dr. P.W.H.I. Parren
Dr. J.H.W. Leusen

Contents

CHAPTER 1

General introduction

Despite all the steps that have been made during the last decades towards the improvement of cancer treatment, for many patients the disease remains incurable. Moreover, the standard treatments such as irradiation, chemotherapy and surgery can cause a lot discomfort and unwanted side effects for patients. Therefore, there has been a large focus on the development of novel cancer treatments during the past decades. Cancer immunotherapy has proven to be a very promising alternative therapy for several tumor types. The initial success of immune checkpoint inhibitors, illustrated by the 2018 Nobel prize in physiology or Medicine being awarded to Professor James Allison and Professor Tasuku Honjo for their work on the checkpoint inhibitors CTLA-4 and PD1 [1], also initiated the development of other strategies for cancer immunotherapy [2]. These novel therapies include for example adoptive cellular therapies, therapeutic antibodies and cancer vaccines.

Immunotherapy using T cells

The importance of T cells in tumor surveillance was recognized in 1995 by Halliday et al., who found that spontaneous regression of melanoma correlated with infiltration of activated CD4+ T lymphocytes [3]. In this same period, Rosenberg and colleagues attempted to utilize these Tumor Infiltrated T cells (TILs) as therapy, by isolating TILs from tumor tissue and reinfusing them into melanoma patients [4, 5]. These studies showed very promising results, with complete tumor regression seen in several patients, but overall response rates were only between 20-30%. Although adoptive cell transfer (ACT) with TILs is still successfully used mainly for patients suffering from melanoma, for other tumor types it has proven to be very difficult to isolate and expand tumor reactive TILs.

Adoptive transfer with genetically engineered T cells

In 1986 researchers succeeded in the isolation an αβTCR from a T lymphocyte and subsequent transfer into another T cell clone [6], this initial discovery led to several reports showing that it is possible to transfer tumor reactivity of a specific T cell clone by αβTCR gene transfer[7-9]. A major breakthrough in the field of genetically engineered T cells for immunotherapy came from research showing that tumor regression could be induced in metastatic melanoma patients after ACT of T cells engineered to express a tumor reactive MART-1 αβTCR [10]. Currently different promising adoptive T cell strategy's using αβTCR gene transfer are being developed, with some showing durable responses in patients [11, 12]. There are however also several issues of concern related to this type of therapy, currently still hampering treatment effectivity. The risk of mispairing of the endogenous and introduced αβTCR chains [13], and optimization of strategies for expansion and purification of the engineered αβT cells remain point of attention. Furthermore the identification

of suitable target antigens and epitopes, as well as the isolation of tumor reactive αβTCRs are challenging for many tumor types [14]. Another drawback of αβTCR based therapy that has to be considered is the sensitivity to MHC downregulation, an immune-escape mechanism often seen on tumor cells [15]. Furthermore, as there is a high diversity of MHC-haplotype within the population, tumor reactive TCRs will only be suitable for a limited number of patients [16].

Chimeric antigen receptor engineered T cells (CAR-T cells) are an alternative approach in therapeutic T cell engineering, CAR-T cells express a chimeric receptor made by the fusion of an antibody derived single chain variable fragment (scFv) specific for a tumor antigen, coupled to a transmembrane and intracellular signaling domain. Since the initial studies describing such CAR-T cells [17, 18], the receptor design has further developed to second and third generation CARs, incorporating one or two co-stimulation domains in addition to the CD3ζ signaling domain [19]. CAR-T cells targeting CD19 have now been implemented successfully in the clinic for the treatment of different B cell malignancies [20]. Major success criteria likely included modulation of the signaling domains to optimize induction of T cell activation and proliferation, and the targeting of the self-antigen CD19, which allowed to expand CAR-T cells even in the absence of tumors, with an acceptable toxicity profile. Currently researchers are attempting to develop CAR-T cells therapy also for other malignancies, but as for αβTCR engineered T cells, several hurdles need to be overcome first. These include occurrence of toxicities due to cytokine release syndrome (CRS) or on-target off-tumor targeting [21], relapse due to antigen loss [22], and the lack of effectivity in solid tumors [23].

Gamma delta T cells for immunotherapy

During the past decade, the interest in the use of γδT cells for cancer immunotherapeutic purposes has increased significantly, illustrated by the large number of current efforts to bring γδT cells to the clinic [24, 25]. γδT cells are divided in two major subsets, γ9δ2T positive T cells comprise approximately 1-5% of the total T lymphocyte compartment in peripheral blood, while the other subset consisting of δ2 negative γδT cells resides preferentially in tissue, where they can be more abundant [26]. Different from conventional αβT cells, γδT cells do not require MHC mediated peptide presentation for target cell recognition. Several ligands have been identified for specific δ2-negative TCRs over the past years, including several MHC or MHC-like molecules, this recognition is however independent of specific antigen presentation, and rather seems to resemble immunoglobulin like binding [27]. Despite the importance of the discovery of these ligands for the overall understanding of γδT cell biology, it does not provide the definite answer as to how γδT cell recognize their targets [28].

Historically, γ9δ2T cells have been described to recognize phosphoantigen (pAg) accumulation in cells [29]. Presence of these pAgs can be caused by bacterial or viral infection but is also often found early in malignant transformation of cells, due to metabolic dysregulation [30]. A decade ago the transmembrane protein BTN3A1 on target cells was identified to be necessary for pAg dependent γ9δ2T cell recognition [31], it has now been shown that the intracellular BTN3A1 domain 30.1 can bind pAgs which probably leads to conformational changes in the extracellular domain of BTN3A1 [32-34], while BTN3A1 localization and turnover is most likely orchestrated by RhoB [35, 36]. Direct interaction between BTN3A1 and a γ9δ2TCR was however never found, and expression of BNT3A1 alone is not sufficient to induce pAg dependent recognition. More recently BTN2A1 was identified as direct ligand for the γ9TCR chain [37, 38], this interaction was also found to be essential but not sufficient for pAg mediated target cell recognition. All these findings together have led to a proposed model where intracellular pAg accumulation leads to γ9δ2TCR mediated recognition via an inside out mechanism involving both BTN2A1 and BTN3A1, and potentially a third, yet to be defined, δ2-chain ligand[36, 38].

In addition to the γδTCR, γδT cells also express several activating natural killer (NK) receptors, such as NKG2D and NKp30/44, that can also induce γδT cell activation by the recognition of stress induced ligands that are often expressed on tumor cells [39, 40]. Meaning that γδT cells have at least two independent mechanisms to recognize and target tumor cells.

The tumor protective phenotype of γδT cells was first shown by the observation that γδT cell deficient mice were more susceptible to the development of cutaneous carcinoma's [41]. Later Gentles et al. showed that in humans, infiltration of γδT in tumors correlated with a favorable prognosis [42]. Based on these key findings several clinical trials with cancer patients started in an attempt to either activate and expand γδT cells *in vivo*, or to use autologous transplantation of *in vitro* expanded γδT cells. Overall, these trials showed that γδT cell based therapies are safe to use and clinical responses were recorded in most studies [39, 43]. However, in general the clinical efficacy of these studies was only limited, underlining the need for novel improved therapeutic approaches using γδT cells. Currently different approaches to improve efficacy of γδT cell based therapies are being developed, including the use of an anti BTN3A antibody to induce γ9δ2T cell mediated tumor lysis *in vivo* [44], or a bispecific antibody to retarget γδT cells towards tumor cells [45, 46]. These therapies might however not be beneficial for patients with tumors that have little γδT cell infiltration or only have a dysfunctional and exhausted γδT cell population [47]. In attempt to overcome these limitations, we introduced a novel concept: αβT cells engineered to express a defined γδT cell receptor (TEGs) [48, 49]. TEGs are αβT cells engineered with a preselected tumor reactive γδTCR, they preserve the proliferation and memory capacity of αβT cells while obtaining γδTCR mediated tumor reactivity[50].

A first clinical candidate, TEG001, is currently tested in a phase 1 clinical trial against relapsed and refractory AML and multiple myeloma (NTR6541).

Bispecific antibodies

Historically, monoclonal antibodies (mAbs) have formed a significant share of all immunotherapeutic strategies, with the anti-CD3 mAb OKT3 being the first mAb approved for the clinic already in 1985 [51]. Since then, a large number of therapeutic antibodies have been approved for clinical use, it is expected that this number will increase to over a hundred in 2021 [52]. A significant part of these therapies is developed for the immune-oncology field, with the antibodies targeting the immune checkpoints CTLA-4 and PD1 on T cells and the anti-CD20 Ab rituximab for treatment of B-cell malignancies as some of the most successful examples [53, 54].

Parallel to more in depth research into characteristics and possibilities of mAbs, came the notion that it was also possible to engineer antibodies with dual specificity[55]. The potential of this discovery for the oncology field was recognized quickly, and the first reports on bispecific antibodies (bsAbs) used to target T cells towards tumor cells date from 1985 [56, 57]. Since then, advancements in technology have made expression and purification of bsAbs more efficient [58], leading to a larger number of publications showing that bsAbs can be used to retarget effector cells towards tumor cells, inducing effector cell activation and subsequent tumor cell lysis [59]. Most of these efforts were focused on T cells, with many bsAbs combining binding to a tumor antigen with engagement of CD3 on T cells. The use of bsAbs to redirect a polyclonal population of T cells towards tumor cells exempts the need for specific TCR-MHC presented antigen recognition, overcoming several often seen tumor immune-escape mechanisms [60]. Furthermore, bsAbs do not require the costly and time-consuming *ex vivo* genetic engineering strategies used for TCR- and CAR-T cell therapy [61], potentially making this approach a more efficient, off-the shelf alternative.

The first bispecific T cell engager (TCE) approved for the clinic came in 2010 with the introduction of catumaxomab for EPCAM positive tumors [62]. However, treatment with catumaxomab led to liver toxicity, which was later found to be caused by Fc mediated off-target immune cell activation, ultimately leading to a retraction from the market [63]. Fortunately, other bsAb designs were more successful, with the CD19xCD3 bispecific T cell engager blinatumomab being approved for treatment of B-cell ALL [64, 65]. Blinatumomab is a bsAb of the BiTE design, two Ab derived scFv's covalently linked via a short flexible linker, showing remarkable potency *in vitro* which also translated to potent tumor control *in vivo* [66]. Blinatumomab is now implemented in treatment of several B-cell malignancies, showing impressive responses, however, there are also concerns about the occurrence of treatment

related toxicities including CRS and neurotoxicity [67]. While neurotoxicity for B cell targeting immunological strategies is most likely caused by the low expression of CD19 in the brain [68], thus less expected when other targets are used, these data do imply that careful selection of targets will be crucial, and clinical trials will be needed to truly assess side effects. Similar to experience with CAR-T cells, relapse due to antigen loss is seen in 10-20% of patients treated with blinatumomab [69]. Additionally, as the half-life of blinatumomab is very short in patients, continuous infusion is required for the optimal treatment effects [70].

Based on the success of, and lessons learned from, blinatumomab, a plethora of TCE's has been developed over the past years, currently in different stages of clinical development. These include bsAbs with different designs, target antigens and effector recruitment domains [71]. While the initial interest in the field lay mainly on the engagement of T-cells, this is now also expanding to other immune cells, e.g. NK- or γδ-T cells, as these subsets have now also been recognized as vital players in tumor immunology, and might circumvent some of the T cell related toxicities and/or resistance seen during TCE treatment [72]. Furthermore, to broaden the applicability of bsAbs beyond hematological tumors, researchers are constantly in pursuit of novel target antigens that are exclusively expressed on tumor cells and absent from healthy tissue [73]. Recently several studies have shown that TCE mediated on- target off-tumor reactivity could also be prevented by decreasing the target binding affinity combined with increasing binding avidity, making it possible to more selectively target the tumors and leaving healthy tissue intact [74,75]. A novel class of TCE's also developed to expand the range of target antigens, called ImmTACs, make use of an affinity enhanced soluble tumor reactive αβTCR as cancer binding domain, making is possible to target intracellular (neo)antigens with a TCE [76]. In January 2022, the FDA approved the use of a Gp100 peptide reactive ImmTAC (tebentafusp-tebn) [77] for the treatment of HLA-A*02:01-positive adult patients with unresectable or metastatic uveal melanoma. This is the first TCR based therapy to be approved for clinical use.
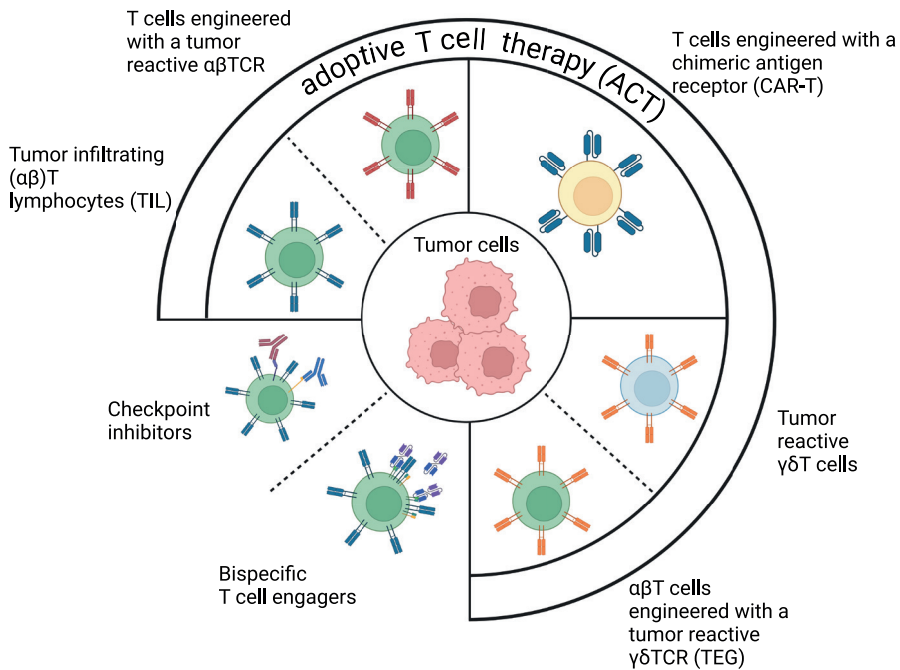
1

Figure 1. Immunotherapeutic strategies using T lymphocytes. Adoptive T cell therapy (ACT) for cancer can be divided in different treatment strategies. Treatment with tumor reactive αβTCRs, either using endogenous tumor infiltrating lymphocytes (TILs) or T cells genetically engineered with a tumor reactive αβTCRs. T cells engineered with an chimeric antigen receptor (CAR-T) are an alternative approach. ACT with γδTCRs can be divided in therapy using endogenous tumor reactive γδT cells or αβT cells engineered with a tumor reactive γδTCRs (TEG). Checkpoint inhibitors and bispecific T cell engagers, are alternative strategies to employ T lymphocytes as anti-cancer therapy.

Thesis outline

Overall, as described in this chapter, there are several potential game-changing cancer immunotherapies currently implemented in clinical practice, and many more in different stages of preclinical and clinical development (Figure 1). While these will undoubtedly change treatment outcome for many patients, unfortunately probably only a minor fraction of all cancer patients will benefit from these treatments. Issues currently still limiting broad implementation of immunotherapies include, amongst others, the lack of appropriate targets, occurrence of non-responding or relapsed patients, and the challenging manufacturing logistics plus the high costs of these therapies. Therefore, further improvement of at-present used therapies, development of novel concepts as well as efforts to combine different treatments to increase overall efficacy is needed [78]. In this thesis we aim to contribute to the improvement of immunotherapeutic

strategies using adoptive transfer of TCR engineered T cells that are currently under development. Furthermore, we introduce a novel concept to the fast-growing field of γδTCR mediated immunotherapy, and explore strategies to further improve this new treatment.

In **chapter 2** a novel method to purify αβTCR engineered T cells during GMP production is described. Our group previously developed a method to deplete non-and poorly engineered cells after transduction of a γδTCR into αβT cells using a GMP grade anti- αβTCR antibody[49]. In this chapter we show that by mutating two amino acids in the introduced βTCR constant chain, this purification method can be translated to αβTCR gene transfer. Furthermore, we showed that by extending the mutated interface in the βTCR constant domain to nine amino acids, binding of an anti-murine βTCR antibody could be achieved, providing the opportunity to further develop depletion strategies of engineered immune cells.

During the past decade our group has developed a novel CAR-T concept called TEGs, αβT cells engineered to express a defined γδTCR. TEGs combine the best properties of αβT and γδT cells, and their potential in targeting both hematological and solid tumors has been described in several publications [49, 50, 79-81]. **Chapter 3** describes the addition of a chimeric co-receptor, with the extracellular domain of NKG2D fused to an intracellular co-stimulation domain, to the TEG cells. We show that addition of a NKG2D-CD28 or NKG2D-41BB chimeric co-receptor results in enhanced TEG proliferation and target cell killing *in vitro.* This is translated to improved tumor control and enhanced mouse survival, shown in a hematologic and solid tumor model.

Chapter 4 focusses on the development of a novel immunotherapeutic strategy using tumor reactive γ9δ2TCR. The development of a bispecific molecule by linking the extracellular domains of tumor-reactive γ9δ2TCRs to a CD3-binding moiety, creating gamma delta TCR anti-CD3 bispecific molecules (GABs), is described. By careful selection of a high affinity γ9δ2TCR, GABs can be created that efficiently induce αβT cell mediated phosphoantigen-dependent recognition and lysis of tumor cell lines and primary patient material *in vitro* and in a subcutaneous myeloma xenograft model. This approach might overcome cumbersome genetic engineering efforts needed for TCR or CAR transfer. Furthermore, GABs and TEGs could be two complementary or even additive strategies, as reported for CAR-T and bsAbs [82], to harvest the full potential of the new universe of tumor targets identified for γδT cells.

In **chapter 5** a strategy that could potentially increase GAB potency is presented. We explore different strategies to design a multivalent GAB molecule, and show that it is possible to induce dimerization of the GAB design described in chapter 4,

1

resulting in a higher avidity molecule harboring two tumor- and T cell binding domains. GAB dimer shows increased potency *in vitro* compared the original monomeric GAB. These findings provide a first proof of principle that increasing avidity of target and/or T cell binding can enhance activity of GABs. Based on the results, potential novel avenues to follow for further development of such higher valency GABs are discussed.

In **chapter 6** we address the effect of the affinity of the CD3 binding moiety in the GAB on the *in vitro* and *in vivo* potency. We show that the incorporation of a higher affinity anti-CD3 scFv in the GAB leads to improved potency in induction of cytokine release and tumor cell lysis by T cells *in vitro.* Furthermore, the higher affinity anti-CD3 scFv also improved GAB mediated tumor control in a multiple myeloma xenograft model. These findings are discussed in the light of recent literature on the effect of CD3 affinity on *in vitro and in vivo* potency on other T cell engager designs.

Chapter 7 summarizes the findings of the previous chapters, and discusses these in the context of recent literature on T cell engineering, bispecific T cell engagers and γδT cells in immunotherapy.

References

1. Huang PW, Chang JW. Immune checkpoint inhibitors win the 2018 Nobel Prize. Biomed J. 2019;42(5):299-306.

2. Hoos A. Development of immuno-oncology drugs - from CTLA4 to PD1 to the next generations. Nat Rev Drug Discov. 2016;15(4):235-47.

3. Halliday GM, Patel A, Hunt MJ, Tefany FJ, Barnetson RS. Spontaneous regression of human melanoma/nonmelanoma skin cancer: association with infiltrating CD4+ T cells. World J Surg. 1995;19(3):352-8.

4. Rosenberg SA, Yannelli JR, Yang JC, Topalian SL, Schwartzentruber DJ, Weber JS, et al. Treatment of patients with metastatic melanoma with autologous tumor-infiltrating lymphocytes and interleukin 2. J Natl Cancer Inst. 1994;86(15):1159-66.

5. Rosenberg SA, Packard BS, Aebersold PM, Solomon D, Topalian SL, Toy ST, et al. Use of tumor-infiltrating lymphocytes and interleukin-2 in the immunotherapy of patients with metastatic melanoma. A preliminary report. N Engl J Med. 1988;319(25):1676-80.

6. Dembić Z, Haas W, Weiss S, McCubrey J, Kiefer H, von Boehmer H, et al. Transfer of specificity by murine alpha and beta T-cell receptor genes. Nature. 1986;320(6059):232-8.

7. Clay TM, Custer MC, Sachs J, Hwu P, Rosenberg SA, Nishimura MI. Efficient transfer of a tumor antigen-reactive TCR to human peripheral blood lymphocytes confers anti-tumor reactivity. J Immunol. 1999;163(1):507-13.

8. Kessels HW, Wolkers MC, van den Boom MD, van der Valk MA, Schumacher TN. Immunotherapy through TCR gene transfer. Nat Immunol. 2001;2(10):957-61.

9. Stanislawski T, Voss RH, Lotz C, Sadovnikova E, Willemsen RA, Kuball J, et al. Circumventing tolerance to a human MDM2-derived tumor antigen by TCR gene transfer. Nat Immunol. 2001;2(10):962-70.

10. Morgan RA, Dudley ME, Wunderlich JR, Hughes MS, Yang JC, Sherry RM, et al. Cancer regression in patients after transfer of genetically engineered lymphocytes. Science. 2006;314(5796):126-9.

11. Chandran SS, Klebanoff CA. T cell receptor-based cancer immunotherapy: Emerging efficacy and pathways of resistance. Immunol Rev. 2019;290(1):127-47.

12. Manfredi F, Cianciotti BC, Potenza A, Tassi E, Noviello M, Biondi A, et al. TCR Redirected T Cells for Cancer Treatment: Achievements, Hurdles, and Goals. Front Immunol. 2020;11:1689.

13. van Loenen MM, de Boer R, Amir AL, Hagedoorn RS, Volbeda GL, Willemze R, et al. Mixed T cell receptor dimers harbor potentially harmful neoreactivity. Proc Natl Acad Sci U S A. 2010;107(24):10972-7.

14. Arnaud M, Duchamp M, Bobisse S, Renaud P, Coukos G, Harari A. Biotechnologies to tackle the challenge of neoantigen identification. Curr Opin Biotechnol. 2020;65:52-9.

15. Cornel AM, Mimpen IL, Nierkens S. MHC Class I Downregulation in Cancer: Underlying Mechanisms and Potential Targets for Cancer Immunotherapy. Cancers (Basel). 2020;12(7).

16. Schipper RF, D'Amaro J, Bakker JT, Bakker J, van Rood JJ, Oudshoorn M. HLA gene haplotype frequencies in bone marrow donors worldwide registries. Hum Immunol. 1997;52(1):54-71.

17. Gross G, Waks T, Eshhar Z. Expression of immunoglobulin-T-cell receptor chimeric molecules as functional receptors with antibody-type specificity. Proc Natl Acad Sci U S A. 1989;86(24):10024-8.

18. Kuwana Y, Asakura Y, Utsunomiya N, Nakanishi M, Arata Y, Itoh S, et al. Expression of chimeric receptor composed of immunoglobulin-derived V regions and T-cell receptor-derived C regions. Biochem Biophys Res Commun. 1987;149(3):960-8.

19. June CH, O'Connor RS, Kawalekar OU, Ghassemi S, Milone MC. CAR T cell immunotherapy for human cancer. Science. 2018;359(6382):1361-5.

20. FDA approves CAR-T cell therapy to treat adults with certain types of large B-cell lymphoma. 2017.

21. Rafiq S, Hackett CS, Brentjens RJ. Engineering strategies to overcome the current roadblocks in CAR T cell therapy. Nat Rev Clin Oncol. 2020;17(3):147-67.

22. Si Lim SJ, Grupp SA, DiNofia AM. Tisagenlecleucel for treatment of children and young adults with relapsed/refractory B-cell acute lymphoblastic leukemia. Pediatr Blood Cancer. 2021;68(9):e29123.

23. Newick K, O'Brien S, Moon E, Albelda SM. CAR T Cell Therapy for Solid Tumors. Annu Rev Med. 2017;68:139-52.

24. Sebestyen Z, Prinz I, Déchanet-Merville J, Silva-Santos B, Kuball J. Translating gammadelta (γδ) T cells and their receptors into cancer cell therapies. Nat Rev Drug Discov. 2020;19(3):169-84.

25. Garber K. γδ T cells bring unconventional cancer-targeting to the clinic - again. Nat Biotechnol. 2020;38(4):389-91.

26. Chien YH, Meyer C, Bonneville M. γδ T cells: first line of defense and beyond. Annu Rev Immunol. 2014;32:121-55.

27. Deseke M, Prinz I. Ligand recognition by the γδ TCR and discrimination between homeostasis and stress conditions. Cell Mol Immunol. 2020;17(9):914-24.

28. Willcox BE, Willcox CR. γδ TCR ligands: the quest to solve a 500-million-year-old mystery. Nat Immunol. 2019;20(2):121-8.

29. Poupot M, Fournié JJ. Non-peptide antigens activating human Vgamma9/Vdelta2 T lymphocytes. Immunol Lett. 2004;95(2):129-38.

30. Morita CT, Jin C, Sarikonda G, Wang H. Nonpeptide antigens, presentation mechanisms, and immunological memory of human Vgamma2Vdelta2 T cells: discriminating friend from foe through the recognition of prenyl pyrophosphate antigens. Immunol Rev. 2007;215:59-76.

31. Harly C, Guillaume Y, Nedellec S, Peigné CM, Mönkkönen H, Mönkkönen J, et al. Key implication of CD277/butyrophilin-3 (BTN3A) in cellular stress sensing by a major human γδ T-cell subset. Blood. 2012;120(11):2269-79.

32. Sandstrom A, Peigné CM, Léger A, Crooks JE, Konczak F, Gesnel MC, et al. The intracellular B30.2 domain of butyrophilin 3A1 binds phosphoantigens to mediate activation of human Vγ9Vδ2 T cells. Immunity. 2014;40(4):490-500.

33. Gu S, Sachleben JR, Boughter CT, Nawrocka WI, Borowska MT, Tarrasch JT, et al. Phosphoantigen-induced conformational change of butyrophilin 3A1 (BTN3A1) and its implication on Vγ9Vδ2 T cell activation. Proc Natl Acad Sci U S A. 2017;114(35):E7311-e20.

34. Peigné CM, Léger A, Gesnel MC, Konczak F, Olive D, Bonneville M, et al. The Juxtamembrane Domain of Butyrophilin BTN3A1 Controls Phosphoantigen-Mediated Activation of Human Vγ9Vδ2 T Cells. J Immunol. 2017;198(11):4228-34.

35. Sebestyen Z, Scheper W, Vyborova A, Gu S, Rychnavska Z, Schiffler M, et al. RhoB Mediates Phosphoantigen Recognition by Vγ9Vδ2 T Cell Receptor. Cell Rep. 2016;15(9):1973-85.

36. Vyborova A, Beringer DX, Fasci D, Karaiskaki F, van Diest E, Kramer L, et al. γδ2T cell diversity and the receptor interface with tumor cells. J Clin Invest. 2020;130(9):4637-51.

37. Rigau M, Ostrouska S, Fulford TS, Johnson DN, Woods K, Ruan Z, et al. Butyrophilin 2A1 is essential for phosphoantigen reactivity by γδ T cells. Science. 2020;367(6478).

38. Karunakaran MM, Willcox CR, Salim M, Paletta D, Fichtner AS, Noll A, et al. Butyrophilin-2A1 Directly Binds Germline-Encoded Regions of the Vγ9Vδ2 TCR and Is Essential for Phosphoantigen Sensing. Immunity. 2020;52(3):487-98.e6.

39. Kabelitz D, Serrano R, Kouakanou L, Peters C, Kalyan S. Cancer immunotherapy with γδ T cells: many paths ahead of us. Cell Mol Immunol. 2020;17(9):925-39.

40. Correia DV, Lopes A, Silva-Santos B. Tumor cell recognition by γδ T lymphocytes: T-cell receptor vs. NK-cell receptors. Oncoimmunology. 2013;2(1):e22892.

41. Girardi M, Oppenheim DE, Steele CR, Lewis JM, Glusac E, Filler R, et al. Regulation of cutaneous malignancy by gammadelta T cells. Science. 2001;294(5542):605-9.

42. Gentles AJ, Newman AM, Liu CL, Bratman SV, Feng W, Kim D, et al. The prognostic landscape of genes and infiltrating immune cells across human cancers. Nat Med. 2015;21(8):938-45.

43. Liu Y, Zhang C. The Role of Human γδ T Cells in Anti-Tumor Immunity and Their Potential for Cancer Immunotherapy. Cells. 2020;9(5).

44. De Gassart A, Le KS, Brune P, Agaugué S, Sims J, Goubard A, et al. Development of ICT01, a first-in-class, anti-BTN3A antibody for activating Vγ9Vδ2 T cell-mediated antitumor immune response. Sci Transl Med. 2021;13(616):eabj0835.

45. de Bruin RCG, Veluchamy JP, Lougheed SM, Schneiders FL, Lopez-Lastra S, Lameris R, et al. A bispecific nanobody approach to leverage the potent and widely applicable tumor cytolytic capacity of Vγ9Vδ2-T cells. Oncoimmunology. 2017;7(1):e1375641.

46. Ganesan R, Chennupati V, Ramachandran B, Hansen MR, Singh S, Grewal IS. Selective recruitment of γδ T cells by a bispecific antibody for the treatment of acute myeloid leukemia. Leukemia. 2021;35(8):2274-84.

47. Vyborova A, Janssen A, Gatti L, Karaiskaki F, Yonika A, van Dooremalen S, et al. γ9δ2 T-Cell Expansion and Phenotypic Profile Are Reflected in the CDR3δ Repertoire of Healthy Adults. Front Immunol. 2022;13:915366.

48. Straetemans T, Kierkels GJJ, Doorn R, Jansen K, Heijhuurs S, Dos Santos JM, et al. GMP-Grade Manufacturing of T Cells Engineered to Express a Defined γδTCR. Front Immunol. 2018;9:1062.

49. Straetemans T, Gründer C, Heijhuurs S, Hol S, Slaper-Cortenbach I, Bönig H, et al. Untouched GMP-Ready Purified Engineered Immune Cells to Treat Cancer. Clin Cancer Res. 2015;21(17):3957-68.

50. Marcu-Malina V, Heijhuurs S, van Buuren M, Hartkamp L, Strand S, Sebestyen Z, et al. Redirecting αβ T cells against cancer cells by transfer of a broadly tumor-reactive γδT-cell receptor. Blood. 2011;118(1):50-9.

51. Kuhn C, Weiner HL. Therapeutic anti-CD3 monoclonal antibodies: from bench to bedside. Immunotherapy. 2016;8(8):889-906.

52. Kaplon H, Reichert JM. Antibodies to watch in 2021. MAbs. 2021;13(1):1860476.

53. Salles G, Barrett M, Foà R, Maurer J, O'Brien S, Valente N, et al. Rituximab in B-Cell Hematologic Malignancies: A Review of 20 Years of Clinical Experience. Adv Ther. 2017;34(10):2232-73.

54. Sharma P, Allison JP. The future of immune checkpoint therapy. Science. 2015;348(6230):56-61.

55. Fudenberg HH, Drews G, Nisonoff A. SEROLOGIC DEMONSTRATION OF DUAL SPECIFICITY OF RABBIT BIVALENT HYBRID ANTIBODY. J Exp Med. 1964;119(1):151-66.

56. Staerz UD, Kanagawa O, Bevan MJ. Hybrid antibodies can target sites for attack by T cells. Nature. 1985;314(6012):628-31.

57. Perez P, Hoffman RW, Shaw S, Bluestone JA, Segal DM. Specific targeting of cytotoxic T cells by anti-T3 linked to anti-target cell antibody. Nature. 1985;316(6026):354-6.

58. Labrijn AF, Janmaat ML, Reichert JM, Parren P. Bispecific antibodies: a mechanistic review of the pipeline. Nat Rev Drug Discov. 2019;18(8):585-608.

59. de Gast GC, van de Winkel JG, Bast BE. Clinical perspectives of bispecific antibodies in cancer. Cancer Immunol Immunother. 1997;45(3-4):121-3.

60. Spranger S, Gajewski TF. Mechanisms of Tumor Cell–Intrinsic Immune Evasion. Annual Review of Cancer Biology. 2018;2(1):213-28.

61. Chabannon C, Kuball J, McGrath E, Bader P, Dufour C, Lankester A, et al. CAR-T cells: the narrow path between hope and bankruptcy? Bone Marrow Transplant. 2017;52(12):1588-9.

62. Linke R, Klein A, Seimetz D. Catumaxomab: clinical development and future directions. MAbs. 2010;2(2):129-36.

63. Borlak J, Länger F, Spanel R, Schöndorfer G, Dittrich C. Immune-mediated liver injury of the cancer therapeutic antibody catumaxomab targeting EpCAM, CD3 and Fcγ receptors. Oncotarget. 2016;7(19):28059-74.

64. Pulte ED, Vallejo J, Przepiorka D, Nie L, Farrell AT, Goldberg KB, et al. FDA Supplementary Approval: Blinatumomab for Treatment of Relapsed and Refractory Precursor B-Cell Acute Lymphoblastic Leukemia. Oncologist. 2018;23(11):1366-71.

65. Przepiorka D, Ko CW, Deisseroth A, Yancey CL, Candau-Chacon R, Chiu HJ, et al. FDA Approval: Blinatumomab. Clin Cancer Res. 2015;21(18):4035-9.

66. Nagorsen D, Kufer P, Baeuerle PA, Bargou R. Blinatumomab: a historical perspective. Pharmacol Ther. 2012;136(3):334-42.

67. Goebeler ME, Bargou R. Blinatumomab: a CD19/CD3 bispecific T cell engager (BiTE) with unique anti-tumor efficacy. Leuk Lymphoma. 2016;57(5):1021-32.

68. Parker KR, Migliorini D, Perkey E, Yost KE, Bhaduri A, Bagga P, et al. Single-Cell Analyses Identify Brain Mural Cells Expressing CD19 as Potential Off-Tumor Targets for CAR-T Immunotherapies. Cell. 2020;183(1):126-42.e17.

1

69. Braig F, Brandt A, Goebeler M, Tony HP, Kurze AK, Nollau P, et al. Resistance to anti-CD19/CD3 BiTE in acute lymphoblastic leukemia may be mediated by disrupted CD19 membrane trafficking. Blood. 2017;129(1):100-4.

70. Zhu M, Wu B, Brandl C, Johnson J, Wolf A, Chow A, et al. Blinatumomab, a Bispecific T-cell Engager (BiTE(®)) for CD-19 Targeted Cancer Immunotherapy: Clinical Pharmacology and Its Implications. Clin Pharmacokinet. 2016;55(10):1271-88.

71. Krishnamurthy A, Jimeno A. Bispecific antibodies for cancer therapy: A review. Pharmacol Ther. 2018;185:122-34.

72. Demaria O, Cornen S, Daëron M, Morel Y, Medzhitov R, Vivier E. Harnessing innate immunity in cancer therapy. Nature. 2019;574(7776):45-56.

73. Middelburg J, Kemper K, Engelberts P, Labrijn AF, Schuurman J, van Hall T. Overcoming Challenges for CD3-Bispecific Antibody Therapy in Solid Tumors. Cancers (Basel). 2021;13(2).

74. Bacac M, Klein C, Umana P. CEA TCB: A novel head-to-tail 2:1 T cell bispecific antibody for treatment of CEA-positive solid tumors. Oncoimmunology. 2016;5(8):e1203498.

75. Slaga D, Ellerman D, Lombana TN, Vij R, Li J, Hristopoulos M, et al. Avidity-based binding to HER2 results in selective killing of HER2-overexpressing cells by anti-HER2/CD3. Sci Transl Med. 2018;10(463).

76. Oates J, Hassan NJ, Jakobsen BK. ImmTACs for targeted cancer therapy: Why, what, how, and which. Mol Immunol. 2015;67(2 Pt A):67-74.

77. Nathan P, Hassel JC, Rutkowski P, Baurain JF, Butler MO, Schlaak M, et al. Overall Survival Benefit with Tebentafusp in Metastatic Uveal Melanoma. N Engl J Med. 2021;385(13):1196-206.

78. Hegde PS, Chen DS. Top 10 Challenges in Cancer Immunotherapy. Immunity. 2020;52(1):17-35.

79. Johanna I, Straetemans T, Heijhuurs S, Aarts-Riemens T, Norell H, Bongiovanni L, et al. Evaluating in vivo efficacy - toxicity profile of TEG001 in humanized mice xenografts against primary human AML disease and healthy hematopoietic cells. J Immunother Cancer. 2019;7(1):69.

80. Gründer C, van Dorp S, Hol S, Drent E, Straetemans T, Heijhuurs S, et al. γ9 and δ2CDR3 domains regulate functional avidity of T cells harboring γ9δ2TCRs. Blood. 2012;120(26):5153-62.

81. Dekkers JF, Alieva M, Cleven A, Keramati F, Wezenaar AKL, van Vliet EJ, et al. Uncovering the mode of action of engineered T cells in patient cancer organoids. Nat Biotechnol. 2022.

82. Choi BD, Yu X, Castano AP, Bouffard AA, Schmidts A, Larson RC, et al. CAR-T cells secreting BiTEs circumvent antigen escape without detectable toxicity. Nat Biotechnol. 2019;37(9):1049-58.
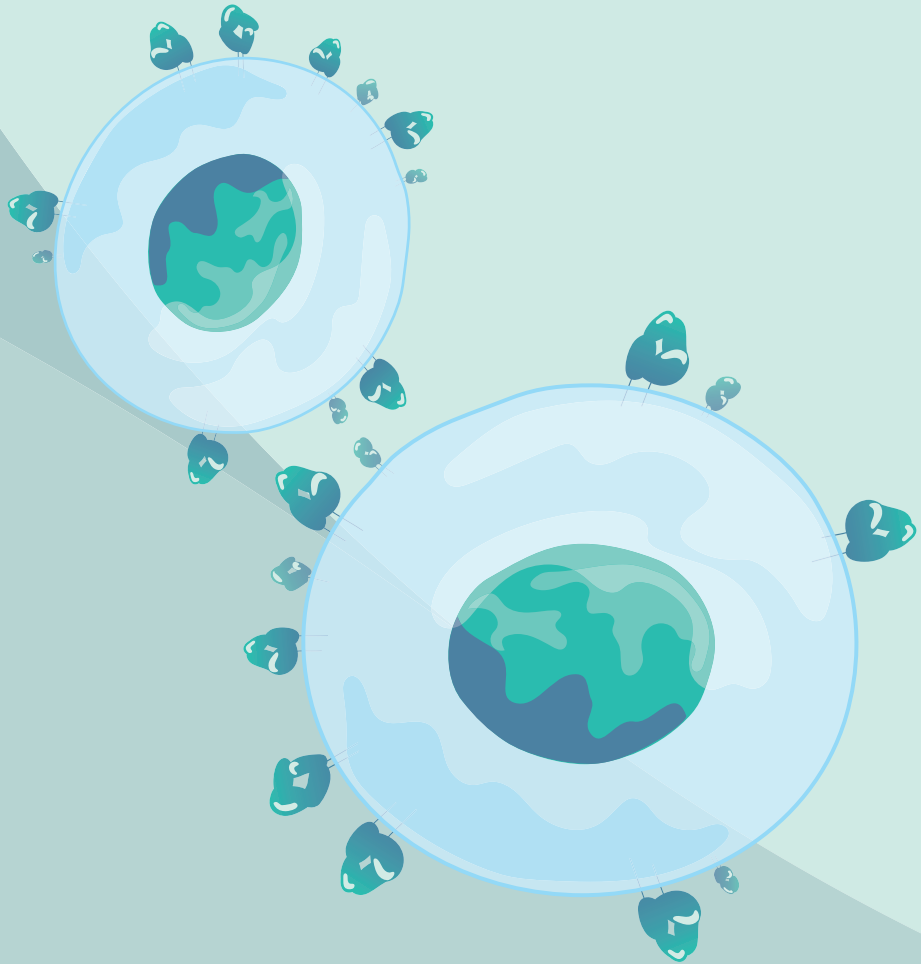
CHAPTER 2

Characterization and modulation of anti-αβTCR antibodies and their respective binding sites at the βTCR chain to enrich engineered T cells

G.J.J. Kierkels[1*], E. van Diest[1*], P. Hernández-López[1*], W. Scheper[1*], A.C.M. de Bruin[1],
E. Frijlink[1], T. Aarts-Riemens[1], S.F.J. van Dooremalen[1], D.X. Beringer[1],
R. Oostvogels[2], L. Kramer[1], T. Straetemans[1], W. Uckert[3], Z. Sebestyén[1], J. Kuball[1,2]

*¹Center for Translational Immunology, University Medical Center Utrecht,
Utrecht University, Heidelberglaan 100 3584 CX, The Netherlands*
*²Department of Hematology, University Medical Center Utrecht, Heidelberglaan 100
3584 CX, The Netherlands*
*³Max-Delbrück-Centrum für Molekulare Medizin (MDC), Robert-Rössle-Str. 10
13125, Berlin, Germany*

* Equally contributed

Abstract

T cell engineering strategies offer cure to patients and entered clinical practice with chimeric antibody-based receptors, αβT cell receptors (αβTCR)-based strategies are however lagging behind. To allow a more rapid and successful translation to successful concepts also using αβTCRs for engineering, incorporating a method for the purification of genetically modified T cells, as well as engineered T cell deletion after transfer into patients, could be beneficial. This would allow to increase efficacy, reduce potential side effects, and improve safety of newly, to be tested, lead structures. By characterizing the antigen binding interface of a GMP-grade anti-αβTCR antibody, usually used for depletion of αβT cells from stem cell transplantation products, we developed a strategy which allows for the purification of untouched αβTCR engineered immune cells by changing two amino acids only in the TCR β chain constant domain of introduced TCR chains. Vice versa, we engineered an antibody, which targets an extended mutated interface of nine amino acids in the TCR β chain constant domain, and provides the opportunity to further develop depletion strategies of engineered immune cells.

Characterization and modulation of anti- αβTCR antibodies and their respective binding sites at the βTCR chain to enrich engineered T cells

2

Introduction

The FDA approval of the first engineered T cells expressing chimeric antigen receptors has paved the way for new cellular interventions in the clinic [1, 2]. A next wave of cell therapy will come with T cell receptor (TCR) engineered T cells specific for targets on both solid and hematological malignancies [3]. Most clinical trials using αβTCR engineered T cells are directed against cancer/testis antigens, such as NY-ESO-1 [4]. Although the clinical response rates are very encouraging, only a small proportion of the patients benefit from these novel treatments [5, 6]. Disappointing response rates can be partially attributed to the presence of non- and poorly-engineered T cells in the administered cell product [7]. These non- and poorly-engineered T cells can hamper the therapeutic efficiency of engineered immune effector cells because of e.g. insufficient expression of the introduced receptor, mispairing of introduced αβTCR with endogenous αβTCR [8], or by competition for endogenous homeostatic cytokines [7, 9]. Furthermore, in an allogenic setting, the presence of T cells still expressing the endogenous αβTCR can lead to severe graft versus host disease. Purification of engineered T cells before infusion can overcome these hurdles, ultimately resulting in enhanced *in vivo* activity. Current methods for purification of engineered T cells often depend on the expression of artificial molecules such as truncated CD34 [10] or truncated NGFR [11], in addition to the tumor specific receptor. However, bigger transgene cassettes used to introduce multiple proteins are relatively difficult to express, and additional transgenes can add immunogenic properties to the engineered cell product [12]. Besides purification of engineered T cells to increase effectivity, elimination of engineered T cells after adoptive transfer might be needed, in case of cytokine release syndrome [13] or off-target toxicities e.g. due to peptide mimicry [5, 14], expression of the antigen at low levels in healthy tissues [15], or mispairing of introduced with endogenous αβTCR chains resulting in unwanted specificities [8]. A currently explored solution for the elimination of transferred cells, is the co-expression of HSV-TK along with the transgene of interest [16], mainly limited by the immunogenicity and relatively large size of the HSV-TK gene [17], An alternative elegant solution is to introduce a myc-tag into the αβTCR sequence itself, followed by *in vivo* depletion through myc-specific antibodies [18]. However, introducing artificial genes into the αβTCR might alter downstream signaling by modifying e.g. its glycosylation [19]. Selection of engineered T cells and subsequent *in vivo* elimination achieved with a single marker, which has previously been described for CD20 [20], would be favorable, due to the relatively small transgene cassette, and therefore better expression. Even better would be a method where the introduced tumor specific TCR could also be used for both purification and *in vivo* depletion, and thereby combines all three properties in one gene: tumor specificity, a selection opportunity of cells expressing the transgene at high levels, as well as an *in vivo* depletion option, which allows for the elimination of the engineered immune cells in case of toxicities caused by the introduced receptor. Within this context we have explored a strategy based

on the recent development of purified T cells engineered to express a defined γδT cell receptor (TEGs) [21-29]. In this strategy we took advantage of the observation that an anti-human αβTCR antibody used for the purification of TEGs does not cross-react with γδTCR chains, and can thereby differentiate between engineered and non-engineered cells. This anti-human αβTCR antibody is routinely used to deplete αβTCR T cells from apheresis products using CliniMACS depletion before allogeneic stem cell transplantation [3, 30]. Here we describe the translation of the TEG purification procedure into a purification procedure for αβTCR engineered T cells. We also provide the rationale for the additional development of elimination strategies of engineered immune cells by further modulating the binding site to be selectively targeted by a second independent antibody.

Materials and methods

Cells and cell lines

Phoenix-Ampho cells (CRL-3213) were obtained from ATCC and cultured in DMEM (Thermo Fisher Scientific, Breda, The Netherlands) containing 1% Pen/Strep (Invitrogen by Thermo Scientific, Breda, The Netherlands) and 10% FCS (Bodinco, Alkmaar, The Netherlands). The TCRβ-/- Jurma cell line (a derivate of Jurkat J.RT3-T3.5 cells [31]), a kind gift from Erik Hooijberg (VU Medical Center, Amsterdam, The Netherlands), TCRβ-/- Jurkat-76, a kind gift from Miriam Heemskerk (LUMC, Leiden The Netherlands) and the T2 cell line (ATCC CRL-1992) were cultured in RPMI 1640 + GlutaMAX (Thermo Fisher Scientific, Breda, The Netherlands) containing 1% Pen/ Strep and 10% FCS. Cell lines were authenticated by short tandem repeat profiling/ karyotyping/isoenzyme analysis. All cells were passaged for a maximum of 2 months, after which new seed stocks were thawed for experimental use. In addition, all cell lines were routinely verified by growth rate, morphology, and/or flow cytometry and tested negative for mycoplasma using MycoAlert Mycoplasma Kit (Lonza, Breda, The Netherlands). Peripheral Blood Mononuclear Cells (PBMCs) were obtained from Sanquin Blood Bank (Amsterdam, The Netherlands) and isolated by Ficoll-Paque (GE Healthcare, Eindhoven, The Netherlands) from buffy coats. PBMCs were cultured using the previously described Rapid Expansion Protocol (REP; [32]) in RPMI containing 5% non-typed human serum (Sanquin Blood Bank, Amsterdam, The Netherlands), 1% Pen/Strep (Invitrogen by Thermo Scientific, Breda, The Netherlands) and 50 µM Gibco™ β-Mercaptoethanol (Fisher scientific, Thermo Fisher Scientific, Breda, The Netherlands) (collectively called HuRPMI).

Cloning of TCR chains into single retroviral vectors

The "minimally murinized" Vα16.1 and Vβ4.1 chains from an NY-ESO1$_{157-165}$/HLA*02 specific TCR, respectively named M2.2.3 and M1.KA,4.1, were generated as previously described [33]. Additional partially murinized (regions or single residues)

TCR chains were ordered from GeneArt (Life Technologies, Thermo Fisher Scientific, Breda, The Netherlands) or constructed via mutagenesis PCR. Cysteine modified chains were designed as reported previously [34]. Variants of chimeric αβ/γδ TCRs were composed using the IMGT database [35]. Sequences were codon optimized and ordered in an industrial resistance-gene harboring vector or as DNA strings (Geneart Life Technologies, Thermo Fisher Scientific, Breda, The Netherlands). DNA strings were processed using the TA TOPO cloning kit (Thermo Fisher Scientific, Breda, The Netherlands) and cloned into the pCR™2.1-TOPO® vector, according to the manufacturer's protocol. All TCR chains were cloned separately into the retroviral vector pMP71 between the EcoRI and NotI restriction sites, using the indicated restriction enzymes and T4 DNA ligase (all from New England Biolabs, Ipswich MA, United States). Transformation of ligated constructs was performed in JM109 competent E. Coli (Promega, Leiden, The Netherlands), and subsequent plasmid DNA isolation was conducted using Nucleobond® PC500, according to the manufacturer's protocol (Macherey-Nagel, Düren, Germany).

Retroviral transduction of primary T cells and T cell lines

Phoenix-Ampho packaging cells were transfected using Fugene-HD (Promega, Leiden, The Netherlands) with env (pCOLT-GALV), gagpol (pHIT60), and separate pMP71 constructs containing α or β chains from a NY-ESO1$_{157-165}$/HLA-A*02 specific TCR (isolated from clone ThP2 [36]) kindly provided by Wolfgang Uckert [37], or containing TCRγ(G115)-T2A-TCRδ(G115)LM1 [21]. PBMCs (preactivated with 50 IU/ml IL-2 (Proleukin, Novartis, Arnhem, The Netherlands) and 30 ng/ml anti-CD3 (clone OKT-3, Miltenyi Biotec, Bergisch Gladbach, Germany), CD4/CD8 T cells selected from PBMCs with REAlease CD4/CD8 (TIL)microbead kit (Miltenyi Biotec, Bergisch Gladbach, Germany) preactivated with anti-CD3/CD28 Dynabeads bead to T cell ratio 1:5 (Thermo Fisher Scientific, Breda, The Netherlands) and 1.7 × 10^3 IU/ml of MACS GMP Recombinant Human interleukin (IL)-7, and 1.5 × 10^2 IU/ml MACS GMP Recombinant Human IL-15 (Milteny Biotec, Bergisch Gladbach, Germany), Jurma or Jurkat-76 cells were transduced twice within 48 hours with viral supernatant in 6-well plates (4x10^6 cells/well) in the presence of 50 IU/ml IL-2 (PBMCs only), 1.7 × 10^3 IU/ml IL-7, 1.5 × 10^2 IU/ml IL-15 and CD3/CD28 dynabeads 1:5 bead to T cell ratio (CD4/CD8 selected T cells only) and 6 μg/ml polybrene (all) (Sigma-Aldrich, Munich, Germany). After transduction, primary T cells were expanded by the addition of 50 μl/well anti-CD3/CD28 Dynabeads (Thermo Fisher Scientific, Breda, The Netherlands) and 50 IU/ml IL-2 or 1.7 × 10^3 IU/ml IL-7, 1.5 × 10^2 IU/ml IL-15.

Purification of engineered T cells by MACS depletion of poorly and non-engineered immune cells

Transduced primary T cells were incubated with biotin-labeled anti-human αβTCR antibody (clone BW242/412; Miltentyi Biotec, Bergisch Gladbach, Germany),

followed by incubation with an anti-biotin antibody coupled to magnetic beads (anti-biotin MicroBeads; Miltentyi Biotec, Bergisch Gladbach, Germany) [21]. Next, the cell suspension was applied to an LD column in a QuadroMACS™ Separator. αβTCR-positive T cells were depleted by MACS cell separation according to the manufacturer's protocol (Miltentyi Biotec, Bergisch Gladbach, Germany).

In silico TCR modelling

The structure of different murinized constant domains was predicted using SWISS-MODEL [38] on the modeled template of the β chain of the human JKF6 T-cell receptor (PDB entry code: 4ZDH). The structure of the murinized constant domains when binding H57-597 was modeled on the template of the β chain of the murine N15 T-cell receptor (PDB entry code: 1NFD) [39]. Structure visualizations were performed using PyMol Molecular Graphics System [40].

Chimeric antibody production and purification

Hamster-human (IgG1) chimeric H57-597 antibody was generated using Lonza expression vectors (pEE14·4-kappaLC, pEE14·4-IgG1) [41,42]. The antibody was produced by transient transfection of HEK293F cells with the heavy chain coding plasmid, the light chain coding plasmid and pAdVAntage (Accession Number U47294; Promega, Leiden, The Netherlands), using 293fectin transfection reagent (Invitrogen, Thermo Scientific, Breda, The Netherlands)) following the manufacturer's instructions. Antibody-containing supernatant was harvested 4 days after transfection and purified by affinity chromatography using HiTrap Protein G HP antibody purification columns (GE Healthcare, Eindhoven, The Netherlands).

Sequencing

DNA sequences of cloning intermediates and final constructs in pMP71 were verified by Barcode Sequencing (Baseclear, Leiden, The Netherlands). 75 µg plasmid DNA and 25 pmol primer specific for the pCR™2.1-TOPO® vector or pMP71 vector were premixed in a total of 20 µl and sent to Baseclear for Sanger sequencing.

Flow cytometry

Cells were stained with Vβ4-FITC (TRBV29-1, clone WJF24; Beckman Coulter, Brea, California), αβTCR-PE (clone BW242/412; Miltentyi Biotec, Bergisch Gladbach, Germany) CD3-PB (clone UCHT1; BD), CD4-PeCy7 (clone RPA-T4; eBioscience, Thermo Fisher Scientific, Breda, The Netherlands), CD8-APC (clone RPA-T8; BD), CD8-PB (clone SK1; Biolegend, San Diego, California), or RPE-conjugated NY-ESO-1$_{157-165}$ HLA*02:01 (SLLMWITQV) pentamer (ProImmune, Oxford, United Kingdom). Samples were fixed using 1% PFA in PBS, measured on a FACSCanto-II

flow cytometer (BD, Eysins, Switzerland), and analyzed using FACSDiva (BD, Eysins, Switzerland) or FlowJo (BD, Eysins, Switzerland) software.

ELISA

Effector and target cells (E:T 50,000:50,000) were incubated for 16 hours after which supernatant was harvested. IFNγ ELISA was performed using ELISA-ready-go! Kit (eBioscience, Thermo Fisher Scientific, Breda, The Netherlands) following the manufacturer's instructions.

MMAE ADC construction

Chimeric H57-MC-VC-PAB-MMAE was constructed using a kit from CellMosaic, (Woburn, Massachusetts) following the manufacturer's instructions.

Statistical analysis

Statistical analyses were performed using GraphPad Prism 8.3.0 for Windows (GraphPad Software, La Jolla, California). Differences between groups was calculated using a one- or two tailed paired T test (Figure 3, 5) or a repeated measure One-way Anova (Figure 4). Normal distribution of input data was assumed.

Results

Anti-human αβTCR binds an epitope on the TCRβ chain of human αβT cells

The GMP-grade anti-human αβT cell receptor (TCR) monoclonal antibody clone BW242/412 (from now on referred to as anti-human αβTCR) recognizes a common determinant of the human TCRα/β-CD3 complex, which has not yet been characterized. In order to allow for further epitope mapping of the interface between the anti-human αβTCR clone BW242/412 and a human αβTCR, we first tested the antibody's ability to bind to murine αβTCRs. Therefore, Jurma T cells, a TCR-deficient T cell line, were transduced with human αβTCRs directed against the cancer/testis antigen NY-ESO-1$_{157-165}$ [37] or with a murine nonsense αβTCR composed of the TCRα chain of an MDM2-specific αβTCR [43], and the TCRβ chain of a p53-specific αβTCR [44]. Specific binding of the anti-human αβTCR was only observed to the human (αHuHu/βHuHu) but not the murine (αMuMu/βMuMu) TCR transduced Jurma cells (Figure 1A). To rule out that parts of the human variable domain of the αβTCR bind to the anti-human αβTCR antibody, the human NY-ESO-1 αβTCR variable domain was grafted on the murine constant domain to create a chimeric αβTCR (αHuMu/βHuMu). Replacing only the human TCRα and TCRβ constant domains by murine equivalents completely abrogated binding of anti-human

αβTCR, to levels resembling binding to a fully murine αβTCR (αMuMu/βMuMu). This indicates that the human constant domain contains the binding epitope. Comparable transgenic expression of murine and human TCRs was confirmed by anti-MuTCRβ and anti-Vβ4 respectively (Figure 1A). Infusion of T cells expressing TCRs with complete murine constant domains into patients can generate immunogenic effects, and lead to a decreased persistence of the engineered cells *in vivo* [45]. To minimize these undesirable effects, we aimed to map the minimal amount of murine residues needed to disrupt binding of anti-human αβTCR, by making use of previously described chimeric-TCRα and β chains, with mutational blocks covering all amino acid differences between the constant regions of human and mouse αβTCRs [37]. We tested three NY-ESO-1 TCRα chain variants, and four NY-ESO-1 TCRβ chain variants, each containing one murine domain, flanked by complete human amino acid sequences. Every TCRα chain was paired with the fully human TCRβ chain (βHuHu) (Figure 1B), and every TCRβ chain was paired with the fully human TCRα chain (αHuHu) (Figure 1C) and introduced into Jurma cells, after which binding of anti-human αβTCR was determined by flow cytometry. Antibody binding was significantly impaired in T cells expressing the αβTCR, which includes murine domain 3 (βHuM3), while none of the other chimeric αβTCRs substantially impaired anti-human αβTCR binding (Figure 1B and C). βHuM3 TCR expression was confirmed by staining for anti-Vβ4, and was comparable to αHuHu/βHuHu (Supplementary Figure 1) These results indicate that domain 3 of the TCRβ chain (βHuM3) dictates the binding of anti-human αβTCR.

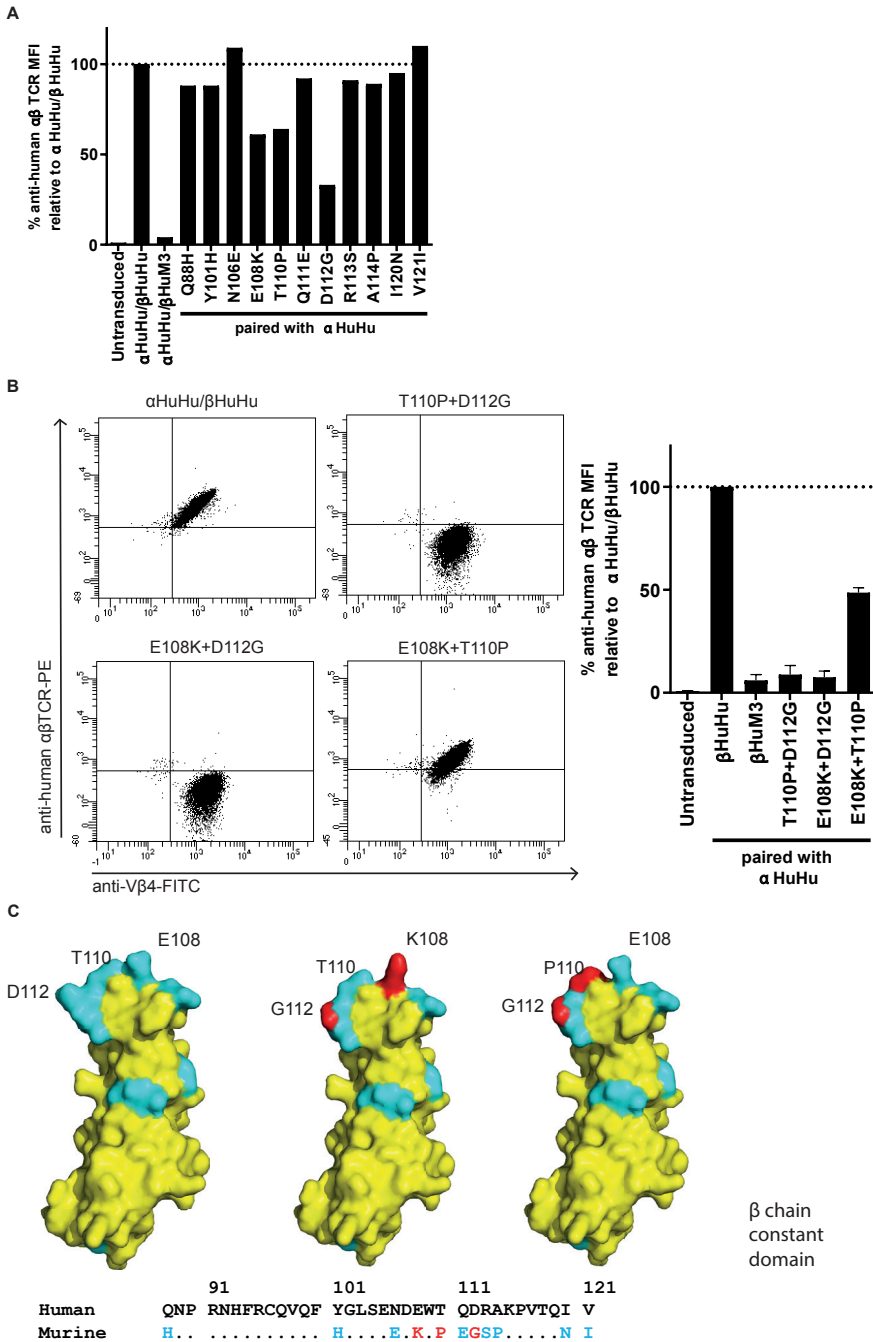**Figure 1. Partial murinization of the TCRβ chain constant domain abrogates binding of the anti-human αβTCR antibody clone BW242/412**. (A) Jurma cells were transduced with fully murine (αMuMu/βMuMu), fully human NY-ESO-1 specific (αHuHu/βHuHu) or chimeric αβTCR, in which the α- and β- constant domains were murine, and the variable domains were human NY-ESO-1 specific. Binding of anti-human αβTCR, anti-MuTCRβ and Vβ4 was assessed by flow cytometry. Schematic representation of the constructed variable (V) and constant (C) domains of αβTCRs that cover all amino acid differences in the (B) TCRα chain and (C) TCRβ chain (upper panels). The constant domain of the TCRα and β chain have been divided in respectively 3 or 4 different regions, based on the comparison of human and murine regions revealing clustered differences flanked by homologous regions as described.[35] Jurma cells were transduced with the different murinized αβTCRs after which anti-human αβTCR antibody binding was assessed by flow cytometry, the bar graphs (B&C lower panels) show the anti-human αβTCR MFI relative to the fully human TCR . Untransduced Jurma cells served as a negative control. The data correspond to 2 independent experiments and a representative figure is shown (A) or as average with standard deviation (B+C)

A

B

TCRα

C

TCRβ
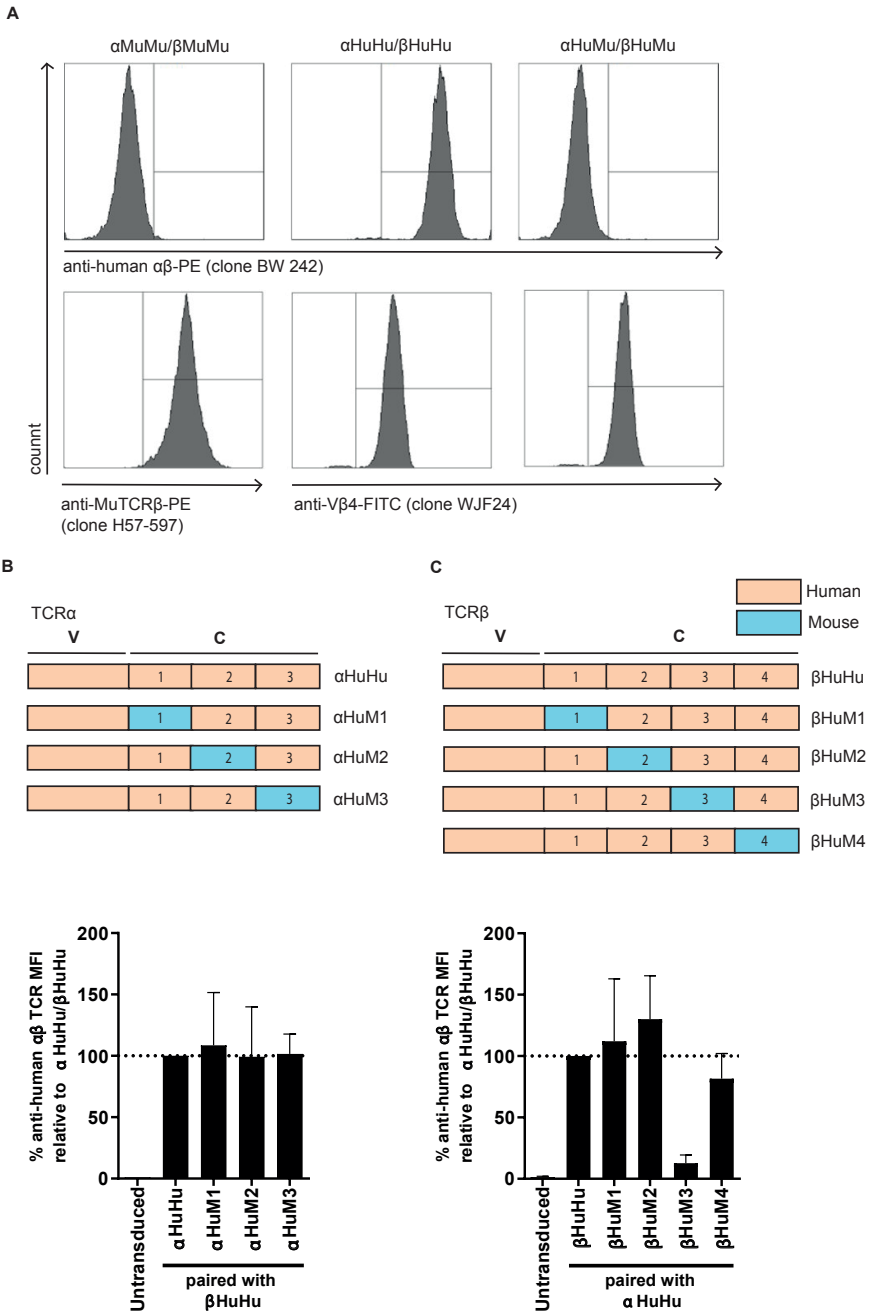
Anti-human αβTCR binding can be abrogated by mutating 2 residues

Analysis of the sequence of domain 3 of the TCRβ chain constant domain revealed eleven residues which are non-homologous between murine and human species (Supplementary Figure 2). To determine which residues are essential for anti-human αβTCR binding, we constructed eleven variants of the TCRβ chain, in which each one of the non-homologous amino acids was replaced by the murine counterpart. These eleven constructs were paired with the completely human αTCR chain (αHuHu), introduced in Jurma cells, and tested for binding by the anti-human αβTCR antibody. Of the eleven generated mutants, the substitutions of 'human' glutamic acid (E108) to the 'murine' lysine (K), 'human' threonine (T110) to the 'murine' proline (P), and 'human' aspartic acid (D112) to the 'murine' glycine (G), showed a substantial abrogation of anti-human αβTCR binding (Figure 2A). However, none of these substitutions was sufficient to induce total abrogation, as shown by the TCR consisting of αHuHu/βHuM3 (Figure 2A). Therefore, we constructed TCRβ chains with a combination of the aforementioned mutations. The TCRβ chains with a D112G mutation combined with E108K or T110P were both effective in abrogating binding of the anti-human αβTCR antibody (Figure 2B), which can be explained by a substantial decrease in bulkiness, thus a decrease in size of these residues (Figure 2C and Supplementary Table 1). For further engineered T cell experiments, the combination of T110P and D112G murinization was selected.

Figure 2. A combination of two specific murine amino acids in the TCRβ chain constant domain is sufficient to abrogate binding of the anti-human αβTCR antibody clone BW242/412. (A) Jurma cells were transduced with αβTCRs containing single murine amino acid substitutions in the 3rd domain of the β chain, after which binding of the anti-human αβTCR antibody was assessed using flow cytometry. Untransduced Jurma cells served as a negative control while fully human αβTCR transduced Jurma cells served as a positive control. (B) Jurma cells were transduced with αβTCRs containing combinations of murine amino acids in the 3rd domain of the β chain, after which binding of anti-human αβTCR antibody was assessed using flow cytometry. (C) Visualization of the eleven non-homologous amino acids between human and mouse β chain 3rd domain in cyan using SWISS-MODEL [57] on the modeled template of the β chain of the human JKF6 T-cell receptor (PDB entry code: 4ZDH). Effective single murine amino acid substitutions are displayed in red. The data correspond to 1 experiment (A) or 2 independent experiments shown with representative image (B) and average with standard deviation (B bar graph).

2

A

B

C

β chain constant domain

		91		101		111		121	
Human	QNP	RNHFRCQVQF		YGLSENDEWT		QDRAKPVTQI		V	
Murine	H..	....		H....E.K.P		EGSP.....N		I	

Enrichment of αβTCR engineered T cells utilizing fragments of murine αβTCR chains

Murine αβTCRs, or residues derived from murine αβTCRs introduced into human αβTCRs, and expressed in human T cells, have been reported to outcompete endogenous human TCR chains [33, 46, 47]. These murine and murinized αβTCRs preferentially pair with each other, thereby decreasing the occurrence of mispairing with endogenous human αβTCRs. Therefore, we utilized single murine amino acids to enhance the expression of introduced TCRs [33]. These "minimally murinized" constant domain variants (from now on referred to as mm) contain murine amino acids which are both critical and sufficient to improve pairing between the two chains [33]. Next, we introduced the above-identified murine residues (T110P+D112G) in the TCRβ chain constant domain in order to test whether this was sufficient to disrupt the binding of anti-human αβTCR in human primary T cells. To test this concept, healthy donor T cells were transduced with mm NY-ESO-1 specific αβTCRs as a negative control, or mm NY-ESO-1 specific αβTCRs, including the two identified mutations T110P+D112G. Magnetic-activated cell sorting (MACS) depletion using anti-human αβTCR resulted an increased cell fraction not able to bind anti-human αβTCR after an expansion of two weeks, in order to assess stability of the phenotype (Figure 3A). However, we also observed outgrowth of a large fraction of Vβ4 and αβTCR negative cells, mainly consisting of NK and γδ T cells, as reported previously [22]. To further increase purity of engineered immune cells, T cells were selected by CD4/CD8 MACS from PBMCs prior to the transduction. This indeed prevented the outgrowth of NK and γδ T cells after αβTCR depletion and expansion (Figure 3B). Next, we quantified the fraction of NY-ESO-1$_{157-165}$ HLA*02:01 pentamer positive cells before and after depletion, showing a significant increase in pentamer positive cells after depletion (Figure 3C), further proving successful enrichment of engineered immune cells when using T110P+D112G modified αβTCRs.

Figure 3. Primary αβT cells engineered with murinized αβTCRs can be successfully selected by using anti-human αβTCR antibody clone BW242/412 to delete non- and poorly engineered immune cells. (A) PBMCs were transduced with minimally murinized αβTCRs with (middle panel) and without (left panel) the "TPDG" mutations. Primary αβT cells with the "TPDG" mutations were MACS-depleted and expanded (right-panel). Endogenous αβTCR expression and expression of the introduced αβTCR without the "TPDG" mutations were determined by flow cytometry using anti-human αβTCR antibody, expression of the introduced βTCR chain was assessed with an anti-Vβ4 antibody. (B) Prior to transduction with minimally murinized abTCRs T cells were selected from PBMCs using CD4/CD8 MACS selection. (CD4/CD8+) (C) Expression of correctly paired αβTCR chains was assessed before and after depletion and expansion by NY-ESO-1 pentamers (CD8+) for both transduction strategies combined. The data correspond to 3 independent experiments and are shown as representative figure (A+B) or as average with standard deviation (C). Statistical significance (* p≤ 0.05, ** p≤ 0.01) was calculated using a paired T test.

A

Transduction of PBMCs

B

Transduction of CD4/CD8 selected lymphocytes

C

2
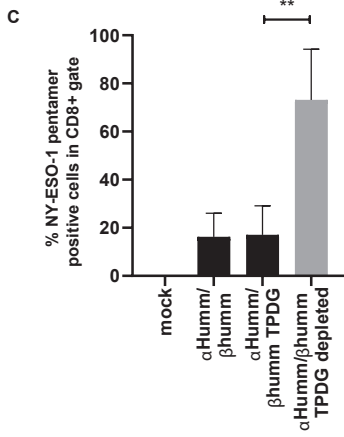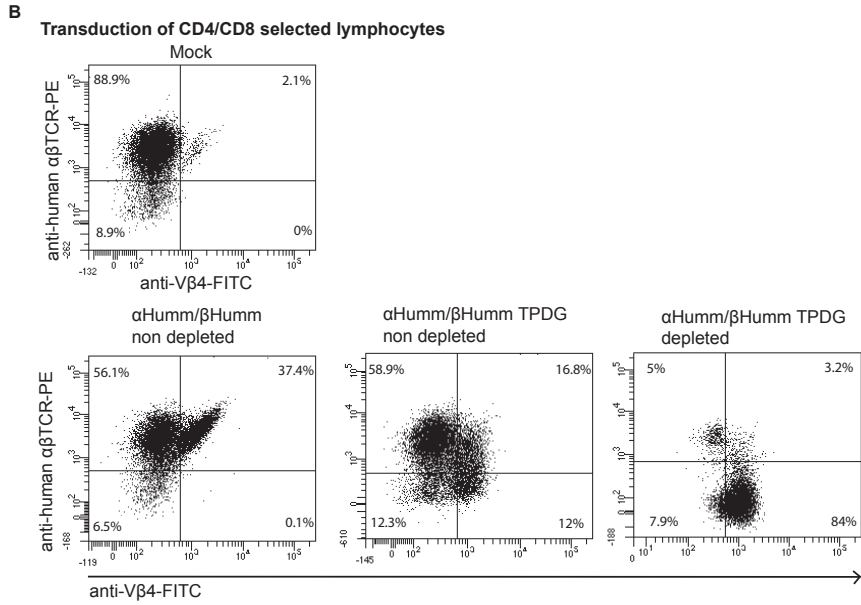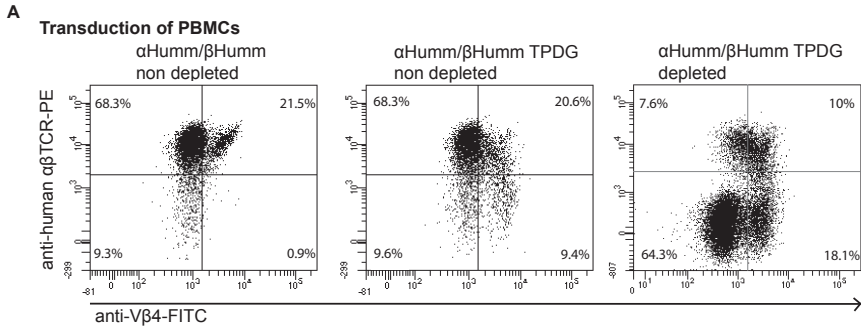
Enrichment strategy within the context of alternative αβTCR stabilization procedures

Multiple alternative strategies to prevent αβTCR chain mispairing and thereby increase the expression of the introduced tumor specific αβTCR have been reported. E.g., adding an additional cysteine residue, to introduce a disulfide bridge between the α and β chains, has been shown to increase expression and decrease mispairing [34]. Also, human γδTCRs introduced in human T cells do not pair with endogenous αβTCRs [32]. Therefore, it was attractive to use γδTCR transmembrane domains for engineering αβT cells in a similar way. We tested whether our enrichment strategy could also be combined with these alternative pairing solutions. Firstly, we constructed an NY-ESO-1 specific TCR with an additional disulfide bridge by the mutation of one specific residue in each chain; T48C in TCRCα and S57C in TCRCβ [34]. Secondly, we constructed an NY-ESO-1 specific TCR with the same additional disulfide bridge, and with a human γδTCR trans-membrane domain. These TCRs were compared to the previously used minimally murinized (mm) TCR strategy (schematic representation Figure 4A). To later make use of the αβTCR depletion method, we introduced the mutations T110P+D112G in the β chains. We then assessed the expression of the different TCRs in primary T cells by measuring the percentage of Vβ4+ and NY-ESO-1$_{157-165}$ HLA*02:01 pentamer+ cells within the CD8+ population (Figure 4B). All three conditions resulted in a NY-ESO-1$_{157-165}$ HLA*02:01 pentamer+ CD8+ fraction comparable in size to the Vβ4+ CD8+ fraction, indicating that in all cases the introduced TCR chains are preferentially paired (Figure 4B and Supplementary Figure 3). A modest, but significant, increase in expression of the introduced TCR was observed when using a combination of cysteine bridge and γδ-transmembrane domain when compared to the mm variant (Figure 4C). The increase in expression of Vβ4 was associated with an increase of the single Vβ4 positive cells to Vβ4/ endogenous αβTCR double positive cells (Figure 4D), indicating that the combination of cysteine bridge and γδ-transmembrane domain was most potent in the downregulation of the endogenous αβTCR. Next, the three different conditions were αβTCR depleted in the same way as before, and the percentage of Vβ4+ cells (Figure 5A) and NY-ESO-1$_{157-165}$ HLA*02:01 pentamer+ cells within the CD8+ population (Figure 5B) was measured by flow cytometry, showing successful enrichment for transduced cells in all conditions. After depletion however, we did not see significant differences in %Vβ4 or pentamer positive cells between the three tested constructs. In summary, all three described methods were suitable for creating preferential pairing and subsequent purification by our αβTCR depletion method with a slight advantage of the combination of cysteine bridge and γδ-transmembrane domain when assessed by TCR expression.
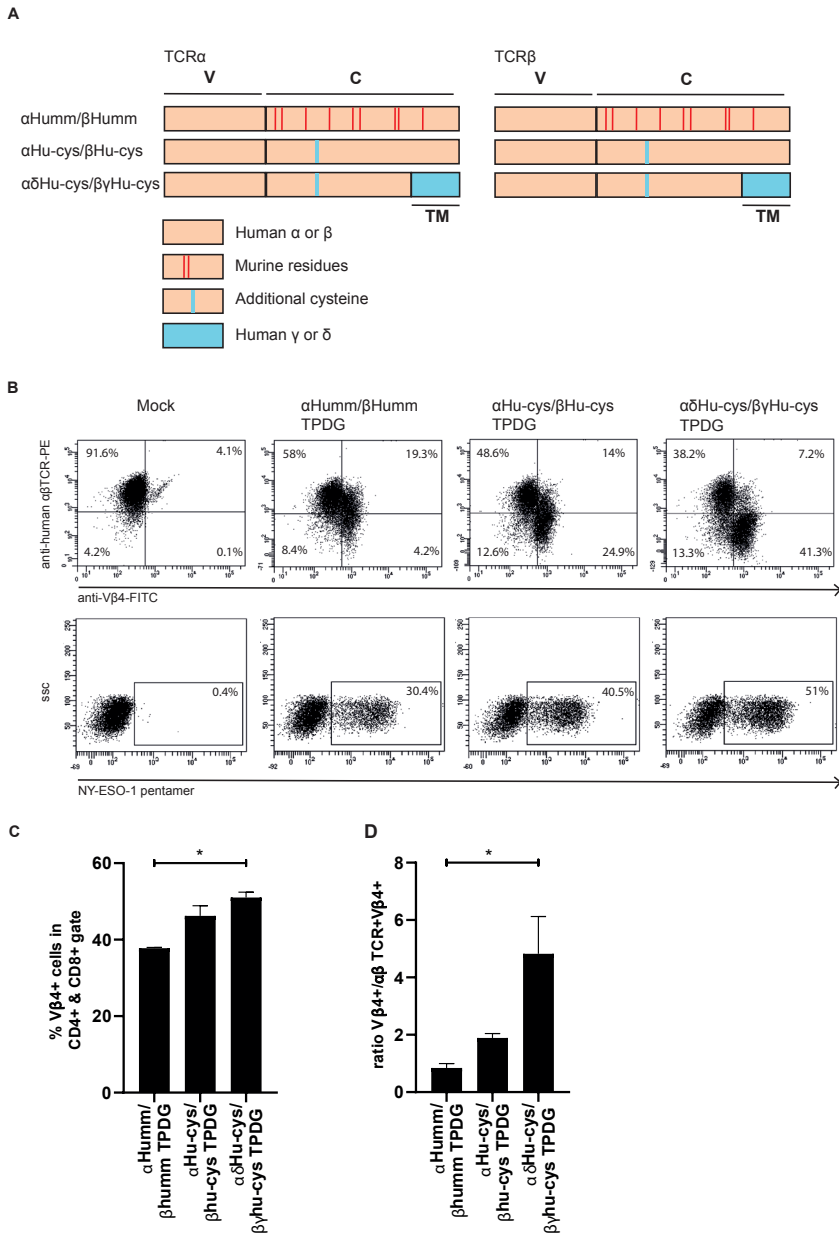
Figure 4. Efficacy of different strategies to induce preferential pairing of introduced α and βTCR chains. (A) Schematic representation of the three different methods for creating preferential pairing between the introduced α and βTCR chains. TM indicates the transmembrane domain, V the variable domain and C the constant domain. (B) Primary αβT cells were transduced with the 3 differentially modified αβTCRs as indicated in (A) and expression of the introduced βTCR was determined by an anti-Vβ4 antibody. Pairing of the introduced α and βTCR chains were assessed by NY-ESO-1 pentamers (C)

percentage Vβ4 + cells was quantified for the differently modified abTCRs (D) ratio between Vβ4 single positive/ Vβ4/ αβTCR double positive cells was determined. The data correspond to 2 independent experiments and are shown as representative figure (B) or as average with standard deviation (C+D). Statistical significance (* p≤ 0.05, ** p≤ 0.01) was calculated using a One-way ANOVA.
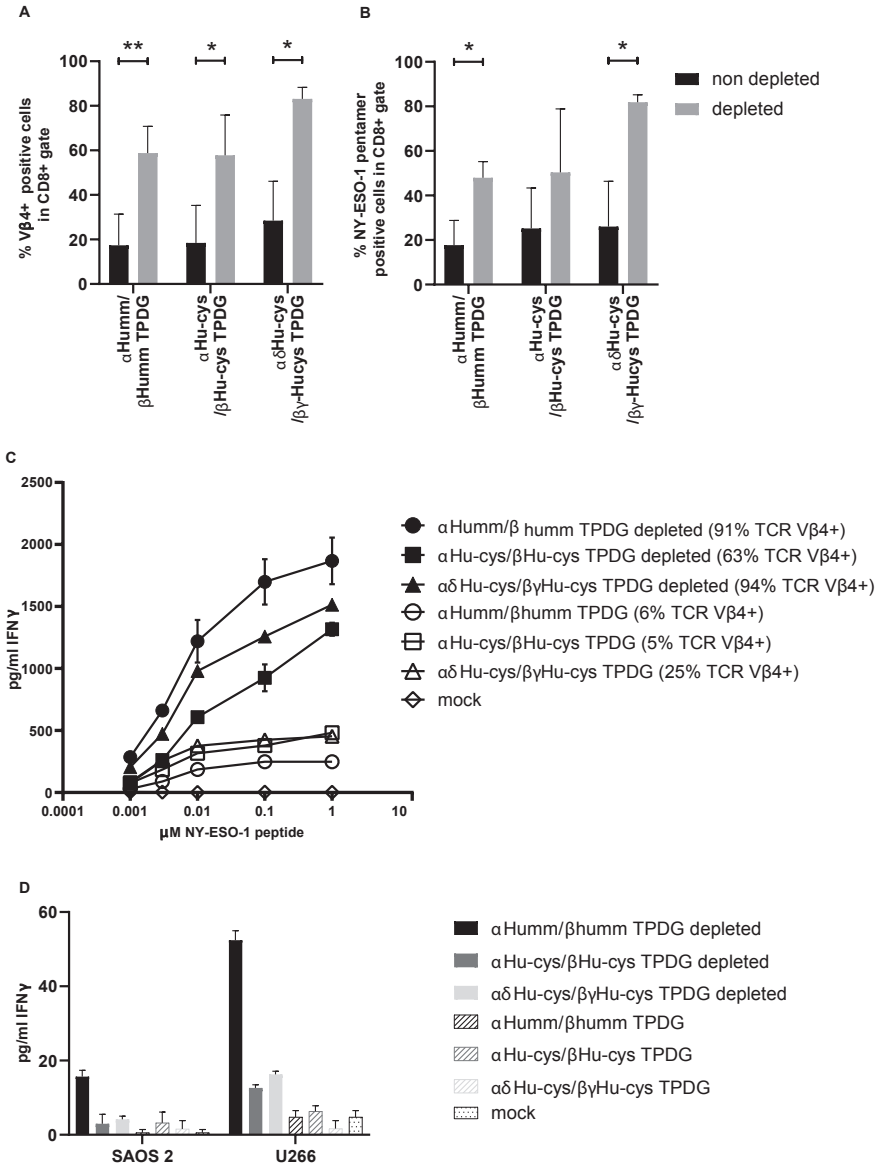

Figure 5. Depletion of non- and poorly- engineered T cells within the context of different preferential αβTCR pairing strategies. Primary αβT cells were transduced with the 3 differently modified αβTCRs as indicated in Figure 4A and depleted with the anti-human αβTCR antibody clone BW242/412. (A) Directly

before and after depletion, expression of the introduced βTCR was determined by an anti-Vβ4 antibody. (B) Expression of appropriately paired introduced α and βTCR chains was determined by NY-ESO-1 pentamers. (C+D) Functionality of purified or non-purified engineered immune cells was assessed in a stimulation assay after co-incubation with NY-ESO-1$_{157-165}$ peptide pulsed T2 cells (C) or tumor cell lines with endogenous expression of NY-ESO peptide (D). IFNγ production was measured in the supernatant by ELISA. The data correspond to 3 (A, B) or 2 (C, D) independent experiments and are shown as average with standard deviation (A, B) or representative figure (C, D). Statistical significance (* p≤ 0.05, ** p≤ 0.01) was calculated using a one tailed paired T test.

2

Augmented *in vitro* tumor cell recognition by purified engineered T cells

To assess whether purified NY-ESO-1$_{157-165}$ αβTCR engineered T cells were superior in target cell recognition compared to non-purified cells, we pulsed T2 cells with multiple concentrations of NY-ESO-1$_{157-165}$ peptide. Purified engineered T cells showed a stronger response to the peptide loaded T2 cells than the non-purified cells. Furthermore, we observed that IFNγ release associated with positivity for the different introduced TCRs (Figure 5C). Purification also resulted in the improved recognition of endogenously processed and presented peptide in the NY-ESO-1 positive tumor cell lines Saos-2 and U226 when assessed by IFNγ release (Figure 5D). As we observed varying, and only minor differences between the three strategies (Figure 4 and 5), and wanted to introduce as little changes as possible in engineered TCRs , the mm approach was used in the next set of experiments to prevent mispairing and increase expression of the introduced TCR as reported [33]. The placement of these 9 murine aminoacids, not on the surface but rather buried within the TCR, makes it unlikely that they would cause immunogenicity of the mmTCR as suggested by Sommermeyer et al [33].

Developing an antibody recognizing the introduced mutated region

The infusion of engineered T cells can potentially be toxic, due to the occurrence of cytokine release syndrome [13] or the off-target toxicity of the receptor used [14]. To be able to deplete infused engineered T cells *in vivo* when deemed necessary, we first aimed to raise an antibody specific for the T110P+D112G murinized variant of the αβTCR, by immunizing three Wistar rats with a human-mouse chimeric peptide. Despite the fact that antibodies were formed against the chimeric peptide (Supplementary Figure 4A), no antibody binding to surface-expressed αβTCRs could be detected (Supplementary Figure 4B). Therefore, we assessed if the commercially available anti-murine TCRβ chain antibody clone H57-597 (from now on referred to as anti-MuTCRβ), was able to bind the murinized αβTCRs on Jurkat-76 cells generated so far. Jurkat-76 cells expressing the T110P+D112G murinized variant of the αβTCR (indicated by βHumm 2/11; two out of the eleven non-homologous amino acids in the 3rd domain are murinized) were not bound by anti-MuTCRβ, however, Jurkat-76 cells expressing the βHummM3 murinized

variant of the αβTCR (indicated by βHumm 11/11; all eleven non-homologous amino acids in the 3rd domain are murinized) were bound by anti-MuTCRβ (Figure 6A). To limit the amount of murine amino acids introduced, we also constructed a variant in which 9/11 non-homologous amino acids in the 3rd domain are murinized (Supplementary Figure 4C). Both 11/11 and 9/11 non-homologous murine amino acids in β chain of domain 3 were sufficient to reestablish binding of anti-MuTCRβ, however, not to the same extent as the HuMu αβTCR (Figure 6A). Surprisingly, 9/11 caused a higher MFI than 11/11. Structural analyses suggested that this differential binding could be a consequence of the fact that 9/11 contains one less negatively charged residue, and therefore results in a more focused electrostatic potential to attract the lysine on CDR1 of anti-MuTCRβ (Figure 6B). To confirm that the anti-MuTCRβ antibody binds to the Vβ4+ cells, a co-staining was performed with both antibodies on transduced primary T cells. The MFI of anti-MuTCRβ-PE was plotted for the Vβ4+ gated cells, this showed that the anti-MuTCRβ antibody bound best to the 9/11 or complete murine constant domain (Figure 6C). As expected, there was no binding to the 2/11 variant but surprisingly also not to the 11/11 variant. This might suggest some interference when both antibodies are used in a co-staining, mainly affecing the suboptimal anti-muTCRβ binding to the 11/11 variant.
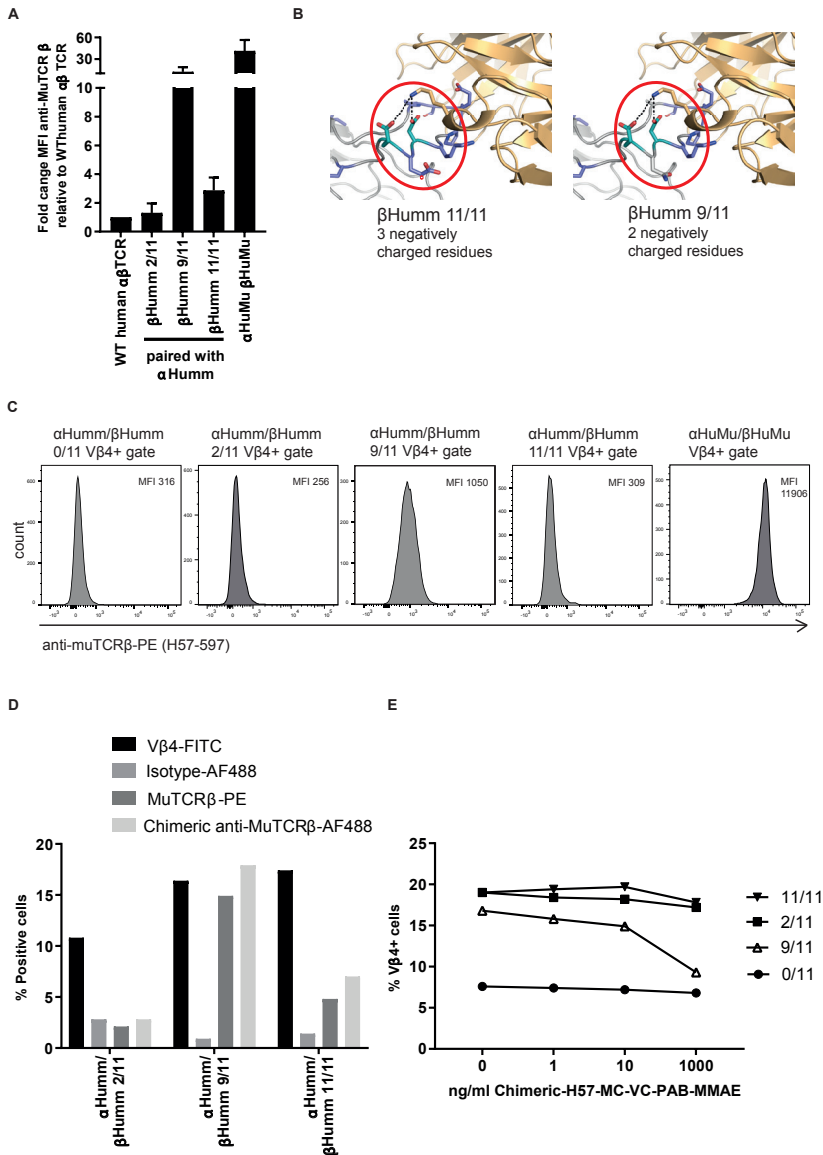
2

Figure 6. Opportunities for depletion of engineered T cells by using a mutation-specific antibody. (A) Jurkat-76 cells were transduced with 5 different murinized αβTCRs to assess binding of anti-MuTCRβ. Wild-type (WT) αβTCR transduced Jurkat-76 cells served as a negative control, while Jurkat-76 transduced with a TCR containing a complete murine constant domain served as a positive control. (B) The structure of the murinized constant domains (βHumm 11/11 and βHumm 9/11) when binding of H57-597 was modeled on the template of the β chain of the murine N15 T-cell receptor (PDB entry code: 1NFD) [53]. (C) Primary αT cells were transduced with the 5 different murinized αβTCRs and a co-staining was performed with anti muTCR and anti Vβ4 antibodies. Cells were first gated for Vβ4 positivity, and plots of the anti muTCR MFI in Vβ4 positive gate are shown (D) Primary αT cells expressing 3 different murinized αβTCRs were used to

assess binding of wild-type and chimeric anti-MuTCRβ. Anti-Vβ4 and anti-Human IgG1-AF488 isotype were included as a positive and a negative control respectively. (E) Jurkat-76 expressing 4 different murinized αβTCRs were incubated with chimeric H57-MC-VC-PAB-MMAE for 24 hours and then stained with an anti-Vβ4 antibody. The data correspond to 1 experiment (C), 2 independent experiments (D, E) for which a representative figure is shown or 3 independent experiments (A) shown in a bar graph representing average and standard deviation.

Since the clone of anti-MuTCRβ antibody is of Armenian Hamster origin and presumably induces severe side effects once administered to humans, comparable to anti-thymocyte globulin,[48] we aimed to generate a humanized variant of anti-MuTCRβ. We generated chimeric variants of anti-MuTCRβ (H57-597, PDB entry code: 1NFD) by exchanging the hamster IgG2 constant domain for the human IgG1 constant domain (referred to as chimeric anti-MuTCRβ). We tested binding of this newly constructed antibody in engineered Jurkat-76 cells, which resulted in specific antibody binding to the 9/11 murinized TCRβ chain expressed on Jurkat-76 (Supplementary Figure 5). To determine the capacity of the chimeric anti-MuTCRβ antibody to bind to primary T cells expressing the murinized αβTCRs, we conjugated this antibody and an isotype control, to Alexa Fluor 488 (AF488), and determined binding by flow cytometry. The chimeric anti-MuTCRβ antibody was able to bind both 9/11 and 11/11 murinized TCRs and, as observed in Figure 6A, the binding to 9/11 was stronger than to 11/11 (Figure 6D). To assess if the chimeric variant of anti-MuTCRβ was able to selectively deplete engineered T cells *in vitro,* the antibody was coupled to monomethyl auristatin E (MMAE), a cell cycle inhibitor, using the protease cleavable linker VC-PAB,[49] to create an antibody-drug conjugate (ADC). Jurkat-76 cells transduced with different murinized TCRs were incubated with multiple concentrations of the ADC. The highest concentration of chimeric H57-MC-VC-PAB-MMAE led to a decrease of Vβ4 positivity in the 9/11 condition only (Figure 6E). This specific decrease indicated that the ADC is able to selectively deplete 9/11, and not 11/11 αβTCR engineered Jurkat-76 *in vitro,* most likely due to the weaker binding of the engineered antibody to the 11/11 αβTCR (Figure 6D). However, depletion was far from complete, indicating that although this binding site is interesting, it is far from being developed for a kill-strategy.

Discussion

The main finding of our study is that replacing only two amino acids within the constant domain of the TCR β chain allows for the purification of αβTCR engineered T cells with GMP-ready tools, [50] without the need for additional complex genetic engineering. The very same region on the TCR β chain can also serve as a targeting interface for antibodies, which can be used to develop strategies to eliminate engineered immune cells. These new insights provide the molecular basis for developing select-kill strategies for increasing purity and augmenting safety of αβTCR engineered T cells, with only minor engineering steps.

A sufficient down-regulation of the endogenous αβTCR chains by the introduced αβTCR chains is essential for this method to work. Therefore, strategies interfering with endogenous αβTCRs or utilizing knock out of the α or β locus to enhance expression of introduced αβTCRs [51] will benefit from this strategy. However, engineering of T cells via ZFN, CRISPR or TALENs [52] requires additional engineering steps and therefore is an additional hurdle for GMP grade production. We accomplished dominance of the introduced receptors by using a previously described method where human residues are replaced by key murine counterparts [37]. Furthermore, we successfully assessed whether the introduction of an additional disulfide bridge [8] or the exchange of the human αβTCR transmembrane domain for the human γδTCR counterpart [21] could also lead to enhanced expression. Thus, we found, in line with our recently published solution for TEGs [21], an elegant and minimalistic strategy to purify αβTCR engineered T cells.

We observed, as reported previously for purification of TEGs [21, 22], that αβT cells double positive for endogenous and introduced TCR are also depleted. This is most likely due to the high affinity of the GMP-grade depletion antibody to the natural βTCR chain. This resulted in a substantial loss of engineered immune cells with residual endogenous αβTCR expression. Although the purified population represented only a small fraction of the initial population, we have shown when using this process for γδTCRs engineered immune cells, that the recovery is sufficient to reach therapeutic cell numbers in a full GMP grade process [22]. Furthermore, we observed enrichment of NK and γδT cells after depletion, previously reported for γδTCRs engineered immune cells [22] and transplantation products [53] as well. Therefore, selection of CD4+ and CD8+ T cells prior to transduction is recommended when applying our strategy. Selection of CD4+ and CD8+ T cells is used already successfully during the full grade GMP production process of approved CAR T products [54]. Overall, our strategy can further improve the current practice for infused engineered products that harbor only between 15-55% engineered immune cells [55, 56], since the lack of purity of infusion products can become a major clinical obstacle in terms of efficacy [21] as well as toxicity [13, 57].

Many tumor-associated antigens targeted by αβTCR gene therapy are not exclusively expressed on tumor cells [58]. Thus, depending on the type of antigen targeted by the introduced αβTCR, depletion strategies can be useful. This is illustrated by multiple clinical trials, which have led to devastating results caused by off-target or on-target but off-tumor toxicities [5, 14]. Preclinical strategies to predict off-target toxicities by affinity enhanced TCRs provide an important tool to minimize these risks [59]. However, these strategies are not infallible, and therefore an additional safe guard would be extremely valuable when e.g. targeting novel antigens or antigens which are also partially expressed on healthy tissues. Methods described so far for introducing a safety switch in engineered

T cell products rely on the introduction of additional genes for the expression of (truncated) targetable proteins, the introduction of inducible caspase proteins [60] or sensitivity to ganciclovir in the case of the widely used HSV-TK suicide gene [17]. The strategy described here, using minimal murine amino acid substitutions, is not only suitable for creating an untouched population of purified T cells, but also has the potential to develop strategies which will allow an *in vivo* depletion when needed. However, to accomplish this goal, the two identified murine amino acids that enable αβTCR depletion needed to be expanded with an additional seven amino acids, to create a chimeric TCR β chain with a total of nine murine amino acids. The major advantage of our strategy, as compared to strategies using e.g. myc-tags introduced into the TCR α chain [18], would be its combined property as a selection and a safeguard system, as well as its use of natural αβTCR domains, which most likely do not affect signaling or impair pairing. However, a major remaining limitation of our approach at this stage is the reduced binding efficacy of our engineered depletion antibody to the murine mutants when compared to the murine wild type, implying that further engineering of the TCR domain or affinity maturation of the antibody will be needed to enable translation of this strategy into an efficient killing strategy *in vivo*. As binding of the antibody is also partially driven by residues in the Cβ-TCR M1 domain [39], additional introduction of several murine amino acids in this domain could therefore be considered.

In conclusion, the murinization of two specific residues in the TCRβ constant domain allows for the untouched isolation of αβTCR engineered T cell products, and can be easily introduced in existing GMP-procedures. When a safeguard of engineered immune cells is required, mutating an additional seven human amino acids to murine residues in the TCRβ constant domain allows for binding of an antibody, which has the potential to, after further optimization, selectively recognize engineered T cells. However, the second step will require additional engineering of the TCR-antibody interface as well as carefully selecting the appropriate killing mechanism to reach its full potential.

Acknowledgement

Funding

Conflict of Interest Statement

GK, DB, ZS and JK are inventors on different patents with γδTCR sequences, recognition mechanisms and isolation strategies. JK is the scientific cofounder and a shareholder of Gadeta (www.gadeta.nl). No potential conflicts of interest were disclosed by the other authors.

2

References

1. Chabannon C, Kuball J, Bondanza A, Dazzi F, Pedrazzoli P, Toubert A, et al. Hematopoietic stem cell transplantation in its 60s: A platform for cellular therapies. Sci Transl Med. 2018;10(436).

2. McGrath E, Chabannon C, Terwel S, Bonini C, Kuball J. Opportunities and challenges associated with the evaluation of chimeric antigen receptor T cells in real-life. Curr Opin Oncol. 2020;32(5):427-33.

3. de Witte MA, Kierkels GJ, Straetemans T, Britten CM, Kuball J. Orchestrating an immune response against cancer with engineered immune cells expressing alphabetaTCRs, CARs, and innate immune receptors: an immunological and regulatory challenge. Cancer Immunol Immunother. 2015;64(7):893-902.

4. Gnjatic S, Nishikawa H, Jungbluth AA, Gure AO, Ritter G, Jager E, et al. NY-ESO-1: review of an immunogenic tumor antigen. Adv Cancer Res. 2006;95:1-30.

5. Morgan RA, Chinnasamy N, Abate-Daga D, Gros A, Robbins PF, Zheng Z, et al. Cancer regression and neurological toxicity following anti-MAGE-A3 TCR gene therapy. J Immunother. 2013;36(2):133-51.

6. Rapoport AP, Stadtmauer EA, Binder-Scholl GK, Goloubeva O, Vogl DT, Lacey SF, et al. NY-ESO-1-specific TCR-engineered T cells mediate sustained antigen-specific antitumor effects in myeloma. Nat Med. 2015;21(8):914-21.

7. de Witte MA, Jorritsma A, Kaiser A, van den Boom MD, Dokter M, Bendle GM, et al. Requirements for effective antitumor responses of TCR transduced T cells. J Immunol. 2008;181(7):5128-36.

8. Kuball J, Dossett ML, Wolfl M, Ho WY, Voss RH, Fowler C, et al. Facilitating matched pairing and expression of TCR chains introduced into human T cells. Blood. 2007;109(6):2331-8.

9. Abad JD, Wrzensinski C, Overwijk W, De Witte MA, Jorritsma A, Hsu C, et al. T-cell receptor gene therapy of established tumors in a murine melanoma model. J Immunother. 2008;31(1):1-6.

10. Fehse B, Richters A, Putimtseva-Scharf K, Klump H, Li Z, Ostertag W, et al. CD34 splice variant: an attractive marker for selection of gene-modified cells. Mol Ther. 2000;1(5 Pt 1):448-56.

11. Orchard PJ, Blazar BR, Burger S, Levine B, Basso L, Nelson DM, et al. Clinical-scale selection of anti-CD3/CD28-activated T cells after transduction with a retroviral vector expressing herpes simplex virus thymidine kinase and truncated nerve growth factor receptor. Hum Gene Ther. 2002;13(8):979-88.

12. Lamers CH, Willemsen R, van EP, van Steenbergen-Langeveld S, Broertjes M, Oosterwijk-Wakka J, et al. Immune responses to transgene and retroviral vector in patients treated with ex vivo-engineered T cells. Blood. 2011;117(1):72-82.

13. Neelapu SS, Tummala S, Kebriaei P, Wierda W, Gutierrez C, Locke FL, et al. Chimeric antigen receptor T-cell therapy - assessment and management of toxicities. Nat Rev Clin Oncol. 2018;15(1):47-62.

14. Linette GP, Stadtmauer EA, Maus MV, Rapoport AP, Levine BL, Emery L, et al. Cardiovascular toxicity and titin cross-reactivity of affinity-enhanced T cells in myeloma and melanoma. Blood. 2013;122(6):863-71.

15. Linette GP, Stadtmauer EA, Maus MV, Rapoport AP, Levine BL, Emery L, et al. Cardiovascular toxicity and titin cross-reactivity of affinity-enhanced T cells in myeloma and melanoma. Blood. 2013;122(6):863-71.

16. Traversari C, Marktel S, Magnani Z, Mangia P, Russo V, Ciceri F, et al. The potential immunogenicity of the TK suicide gene does not prevent full clinical benefit associated with the use of TK-transduced donor lymphocytes in HSCT for hematologic malignancies. Blood. 2007;109(11):4708-15.

17. Traversari C, Marktel S, Magnani Z, Mangia P, Russo V, Ciceri F, et al. The potential immunogenicity of the TK suicide gene does not prevent full clinical benefit associated with the use of TK-transduced donor lymphocytes in HSCT for hematologic malignancies. Blood. 2007;109(11):4708-15.

18. Kieback E, Charo J, Sommermeyer D, Blankenstein T, Uckert W. A safeguard eliminates T cell receptor gene-modified autoreactive T cells after adoptive transfer. Proc Natl Acad Sci U S A. 2008;105(2):623-8.

19. Kuball J, Hauptrock B, Malina V, Antunes E, Voss RH, Wolfl M, et al. Increasing functional avidity of TCR-redirected T cells by removing defined N-glycosylation sites in the TCR constant domain. JExpMed. 2009;206(2):463-75.

20. Introna M, Barbui AM, Bambacioni F, Casati C, Gaipa G, Borleri G, et al. Genetic modification of human T cells with CD20: a strategy to purify and lyse transduced cells with anti-CD20 antibodies. Hum Gene Ther. 2000;11(4):611-20.

2

21. Straetemans T, Gründer C, Heijhuurs S, Hol S, Slaper-Cortenbach I, Bönig H, et al. Untouched GMP-Ready Purified Engineered Immune Cells to Treat Cancer. Clin Cancer Res. 2015;21(17):3957-68.

22. Straetemans T, Kierkels GJJ, Doorn R, Jansen K, Heijhuurs S, Dos Santos JM, et al. GMP-Grade Manufacturing of T Cells Engineered to Express a Defined gammadeltaTCR. Front Immunol. 2018;9:1062.

23. Sebestyen Z, Prinz I, Dechanet-Merville J, Silva-Santos B, Kuball J. Translating gammadelta (gammadelta) T cells and their receptors into cancer cell therapies. Nat Rev Drug Discov. 2020;19(3):169-84.

24. Straetemans T, Janssen A, Jansen K, Doorn R, Aarts T, van Muyden ADD, et al. TEG001 Insert Integrity from Vector Producer Cells until Medicinal Product. Mol Ther. 2020;28(2):561-71.

25. Vyborova A, Beringer DX, Fasci D, Karaiskaki F, van Diest E, Kramer L, et al. gamma9delta2T cell diversity and the receptor interface with tumor cells. J Clin Invest. 2020;130(9):4637-51.

26. Johanna I, Hernandez-Lopez P, Heijhuurs S, Bongiovanni L, de Bruin A, Beringer D, et al. TEG011 persistence averts extramedullary tumor growth without exerting off-target toxicity against healthy tissues in a humanized HLA-A*24:02 transgenic mice. J Leukoc Biol. 2020;107(6):1069-79.

27. Janssen A, Villacorta Hidalgo J, Beringer DX, van Dooremalen S, Fernando F, van Diest E, et al. gammadelta T-cell Receptors Derived from Breast Cancer-Infiltrating T Lymphocytes Mediate Antitumor Reactivity. Cancer Immunol Res. 2020;8(4):530-43.

28. Johanna I, Straetemans T, Heijhuurs S, Aarts-Riemens T, Norell H, Bongiovanni L, et al. Evaluating in vivo efficacy - toxicity profile of TEG001 in humanized mice xenografts against primary human AML disease and healthy hematopoietic cells. J Immunother Cancer. 2019;7(1):69.

29. Kierkels GJJ, Scheper W, Meringa AD, Johanna I, Beringer DX, Janssen A, et al. Identification of a tumor-specific allo-HLA-restricted gammadeltaTCR. Blood Adv. 2019;3(19):2870-82.

30. Schumm M, Lang P, Bethge W, Faul C, Feuchtinger T, Pfeiffer M, et al. Depletion of T-cell receptor alpha/beta and CD19 positive cells from apheresis products with the CliniMACS device. Cytotherapy. 2013;15(10):1253-8.

31. Aarnoudse CA, Kruse M, Konopitzky R, Brouwenstijn N, Schrier PI. TCR reconstitution in Jurkat reporter cells facilitates the identification of novel tumor antigens by cDNA expression cloning. Int J Cancer. 2002;99(1):7-13.

32. Marcu-Malina V, Heijhuurs S, van Buuren M, Hartkamp L, Strand S, Sebestyen Z, et al. Redirecting alphabeta T cells against cancer cells by transfer of a broadly tumor-reactive gammadeltaT-cell receptor. Blood. 2011;118(1):50-9.

33. Sommermeyer D, Uckert W. Minimal amino acid exchange in human TCR constant regions fosters improved function of TCR gene-modified T cells. JImmunol. 2010;184(11):6223-31.

34. Kuball J, Dossett ML, Wolfl M, Ho WY, Voss RH, Fowler C, et al. Facilitating matched pairing and expression of TCR chains introduced into human T cells. Blood. 2007;109(6):2331-8.

35. IMGT®, the international ImMunoGeneTics information system®. http://www.imgt.org.

36. Kronig H, Hofer K, Conrad H, Guilaume P, Muller J, Schiemann M, et al. Allorestricted T lymphocytes with a high avidity T-cell receptor towards NY-ESO-1 have potent anti-tumor activity. Int J Cancer. 2009;125(3):649-55.

37. Sommermeyer D, Uckert W. Minimal amino acid exchange in human TCR constant regions fosters improved function of TCR gene-modified T cells. J Immunol. 2010;184(11):6223-31.

38. Bertoni M, Kiefer F, Biasini M, Bordoli L, Schwede T. Modeling protein quaternary structure of homo- and hetero-oligomers beyond binary interactions by homology. Sci Rep. 2017;7(1):10480.

39. Wang J, Lim K, Smolyar A, Teng M, Liu J, Tse AG, et al. Atomic structure of an alphabeta T cell receptor (TCR) heterodimer in complex with an anti-TCR fab fragment derived from a mitogenic antibody. EMBO J. 1998;17(1):10-26.

40. Schrodinger, LLC. The PyMOL Molecular Graphics System, Version 1.8. 2015.

41. Boross P, Lohse S, Nederend M, Jansen JH, van Tetering G, Dechant M, et al. IgA EGFR antibodies mediate tumour killing in vivo. EMBO Mol Med. 2013;5(8):1213-26.

42. Meyer S, Evers M, Jansen JHM, Buijs J, Broek B, Reitsma SE, et al. New insights in Type I and II CD20 antibody mechanisms-of-action with a panel of novel CD20 antibodies. Br J Haematol. 2018;180(6):808-20.

43. Stanislawski T, Voss RH, Lotz C, Sadovnikova E, Willemsen RA, Kuball J, et al. Circumventing tolerance to a human MDM2-derived tumor antigen by TCR gene transfer. Nat Immunol. 2001;2(10):962-70.

44. Kuball J, Schmitz FW, Voss RH, Ferreira EA, Engel R, Guillaume P, et al. Cooperation of human tumor-reactive CD4+ and CD8+ T cells after redirection of their specificity by a high-affinity p53A2.1-specific TCR. Immunity. 2005;22(1):117-29.

45. Davis JL, Theoret MR, Zheng Z, Lamers CH, Rosenberg SA, Morgan RA. Development of human anti-murine T-cell receptor antibodies in both responding and nonresponding patients enrolled in TCR gene therapy trials. Clin Cancer Res. 2010;16(23):5852-61.

46. Voss RH, Kuball J, Theobald M. Designing TCR for Cancer Immunotherapy. Methods MolMed. 2005;109:229-56.

47. Voss RH, Kuball J, Engel R, Guillaume P, Romero P, Huber C, et al. Redirection of T cells by delivering a transgenic mouse-derived MDM2 tumor antigen-specific TCR and its humanized derivative is governed by the CD8 coreceptor and affects natural human TCR expression. ImmunolRes. 2006;34(1):67-87.

48. Admiraal R, Nierkens S, de Witte MA, Petersen EJ, Fleurke GJ, Verrest L, et al. Association between anti-thymocyte globulin exposure and survival outcomes in adult unrelated haemopoietic cell transplantation: a multicentre, retrospective, pharmacodynamic cohort analysis. Lancet Haematol. 2017;4(4):e183-e91.

49. Caculitan NG, Dela Cruz Chuh J, Ma Y, Zhang D, Kozak KR, Liu Y, et al. Cathepsin B Is Dispensable for Cellular Processing of Cathepsin B-Cleavable Antibody-Drug Conjugates. Cancer Res. 2017;77(24):7027-37.

50. Locatelli F, Merli P, Pagliara D, Li Pira G, Falco M, Pende D, et al. Outcome of children with acute leukemia given HLA-haploidentical HSCT after alphabeta T-cell and B-cell depletion. Blood. 2017;130(5):677-85.

51. Provasi E, Genovese P, Lombardo A, Magnani Z, Liu PQ, Reik A, et al. Editing T cell specificity towards leukemia by zinc finger nucleases and lentiviral gene transfer. NatMed. 2012;18(5):807-15.

52. Gaj T, Gersbach CA, Barbas CF, III. ZFN, TALEN, and CRISPR/Cas-based methods for genome engineering. Trends Biotechnol. 2013.

53. Handgretinger R, Schilbach K. The potential role of gammadelta T cells after allogeneic HCT for leukemia. Blood. 2018.

54. Shah NN, Highfill SL, Shalabi H, Yates B, Jin J, Wolters PL, et al. CD4/CD8 T-Cell Selection Affects Chimeric Antigen Receptor (CAR) T-Cell Potency and Toxicity: Updated Results From a Phase I Anti-CD22 CAR T-Cell Trial. J Clin Oncol. 2020;38(17):1938-50.

55. Lock D, Mockel-Tenbrinck N, Drechsel K, Barth C, Mauer D, Schaser T, et al. Automated Manufacturing of Potent CD20-Directed Chimeric Antigen Receptor T Cells for Clinical Use. Hum Gene Ther. 2017;28(10):914-25.

56. Hodi FS, O'Day SJ, McDermott DF, Weber RW, Sosman JA, Haanen JB, et al. Improved survival with ipilimumab in patients with metastatic melanoma. N Engl J Med. 2010;363(8):711-23.

57. Smith M, Zakrzewski J, James S, Sadelain M. Posttransplant chimeric antigen receptor therapy. Blood. 2018;131(10):1045-52.

58. Schmitt TM, Stromnes IM, Chapuis AG, Greenberg PD. New Strategies in Engineering T-cell Receptor Gene-Modified T cells to More Effectively Target Malignancies. Clin Cancer Res. 2015;21(23):5191-7.

59. Bijen HM, van der Steen DM, Hagedoorn RS, Wouters AK, Wooldridge L, Falkenburg JHF, et al. Preclinical Strategies to Identify Off-Target Toxicity of High-Affinity TCRs. Mol Ther. 2018.

60. Di Stasi A, Tey SK, Dotti G, Fujita Y, Kennedy-Nasser A, Martinez C, et al. Inducible apoptosis as a safety switch for adoptive cell therapy. N Engl J Med. 2011;365(18):1673-83.

Supplementary Figures and Tables
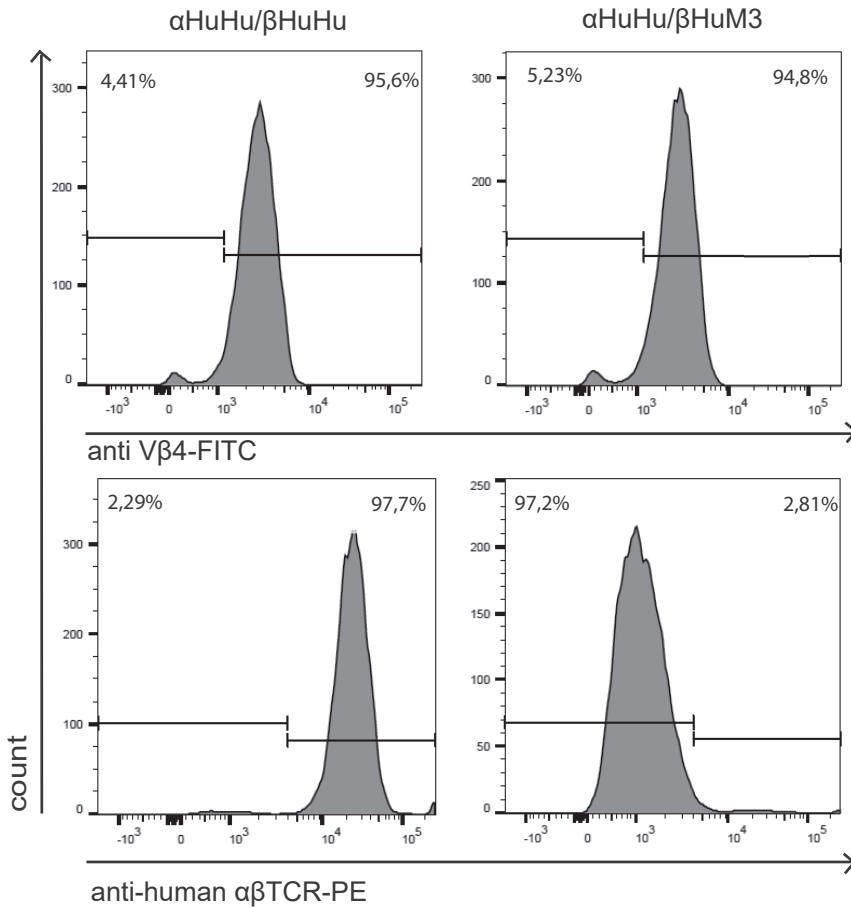
Supplementary Figure 1. αhuhu/βhuM3 murinized TCR is expressed at the cell surface. (A) Jurma cells were transduced with the αhuhu/βhuhu and αhuhu/βhuM3 murinized TCR after which TCR expression was confirmed with an anti-Vβ4 antibody (upper panel) and binding of the anti-human αβTCR antibody was assessed (lower panel), by flow cytometry. The data correspond to 2 independent experiments and a representative figure is shown.

TCRα

```
                          1
        1         11        21        31        41        51        61
Hu  IQNPDPAVYQ LRDSKSSDKS VCLFTDFDSQ TNVSQSKDSD VYITDKTVLD MRSMDFKSNS AVAWSNKSDF
Mu  ****E***** *K*PR*O*ST L********** I**PKTME*G TF******** *KA**S***G *I****OTS*

                2                    3
        71        81        91        101       111       121       131
Hu  ACANAFNNSI IPEDTFFPSP ESSCDVKLVE KSFETDTNLN FQNLSVIGFR ILLLKVAGFN LLMTLRLWSS
Mu  T*QDI*K--- -ETNATY**S DVP**AT*T* *****M*** *****M*L* ********** **********
```

TCRβ

```
                        1                                                2
        1         11        21        31        41        51        61
Hu  EDLKNVFPPE VAVFEPSEAE ISHTQKATLV CLATGFYPDH VELSWWVNGK EVHSGVSTDP QPLKEQPALN
Mu  ***R**T**K *SL****K** *ANK****** ***R**F*** ********** ********** *AY**---S*

            3
        71        81        91        101       111       121       131
Hu  DSRYCLSSRL RVSATFWQNP RNHFRCQVQF YGLSENDEWT QDRAKPVTQI VSAEAWGRAD CGFTSESYQQ
Mu  Y*-******* *******H** ********** H****E*K*P EGSP*****N I********* **I**A**H*

                    4
        141       151       161       171
Hu  GVLSATILYE ILLGKATLYA VLVSALVLMA MVKRKDSRG
Mu  ********** ********** ****G***** ***K*N*--
```
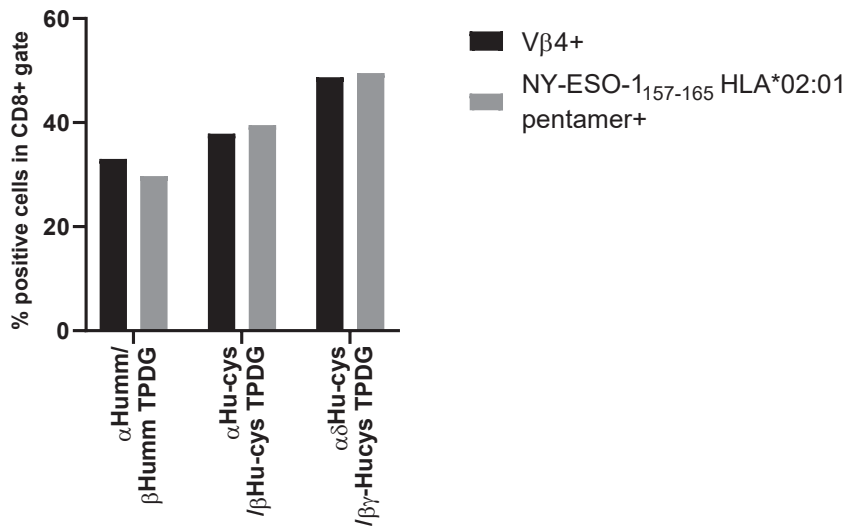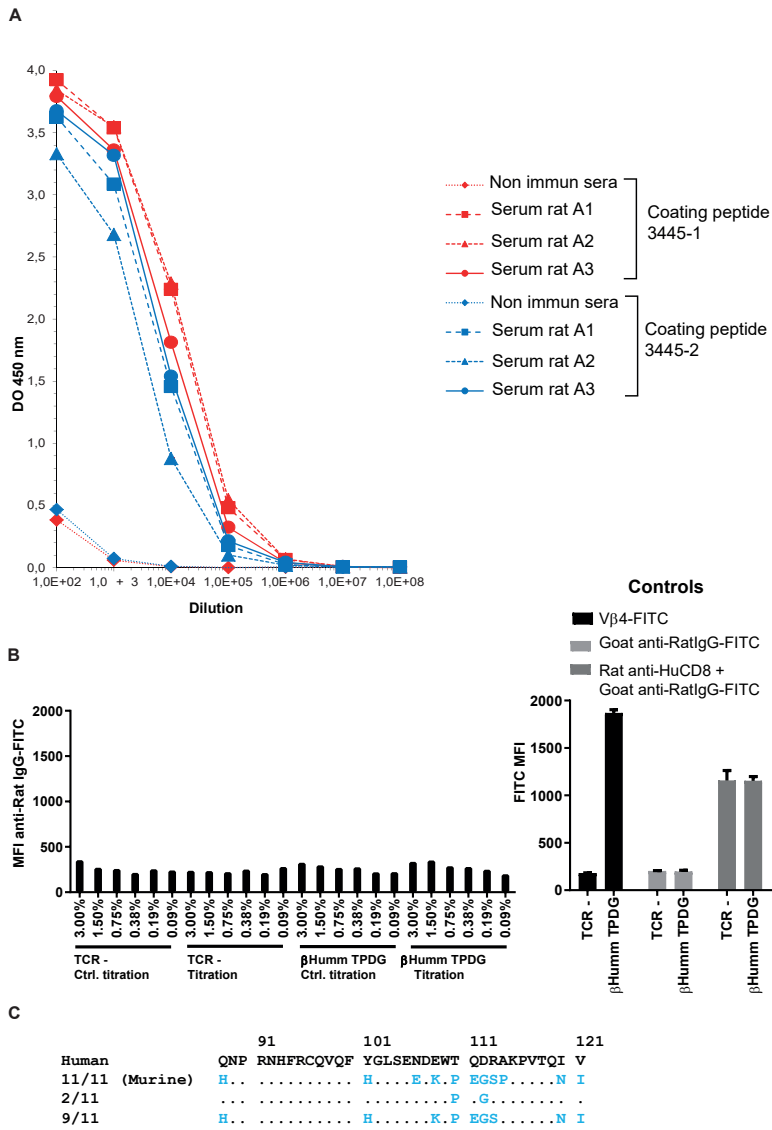
Supplementary Figure 2. Extensive homology between human and murine TCR chains. Sequence alignment of the Human (Hu) and Murine (Mu) TCR α (upper panel) or β (lower panel) constant chains. The three (TCRα) or four (TCRβ) TCR constant regions with clustered Hu-Mu sequence differences are indicated above the alignment.

Supplementary Figure 3. Comparable efficacy of different strategies to induce preferential pairing of introduced α and βTCR chains. Primary αβT cells were transduced with the 3 differentially modified αβ TCRs and expression of the introduced βTCR was determined by an anti-Vβ4 antibody. Pairing of the introduced α and βTCR chains was assessed by staining with NY-ESO-1 pentamers. The data correspond to 2 independent experiments and a representative figure is shown.

2

A

B

C

```
                 91         101         111         121
Human            QNP RNHFRCQVQF YGLSENDEWT QDRAKPVTQI V
11/11 (Murine)   H.. .......... H....E.K.P EGSP.....N I
2/11             ... .......... .........P .G........ .
9/11             H.. .......... H......K.P EGS......N I
```

Supplementary Figure 4. Attempting to raise an antibody specific for the T110P+D112G murinized variant of the αβTCR by immunizing 3 Wistar rats with a human-mouse chimeric peptide. (A) Determining the presence of peptide-specific antibodies in the serum of the immunized rats. (B) Assessing the ability of the generated antibodies to bind surface-expressed TCRs. aHumm/βHumm TPDG transduced or non-transduced Jurkat-76 cells were incubated with the indicated percentage of rat serum, after which flow cytometry using anti-RatIgG-FITC was performed. In the controls panel, the functionality of this secondary antibody was confirmed by staining the Jurkat-76 cells with rat anti-HuCD8 followed by anti-RatIgG-FITC. Expression of the TCR was confirmed using anti-Vβ4-FITC. (C) Sequence alignment of the human and murine 3rd domain of the TCRβ chain and the constructed 2/11 and 9/11 murinized variants.
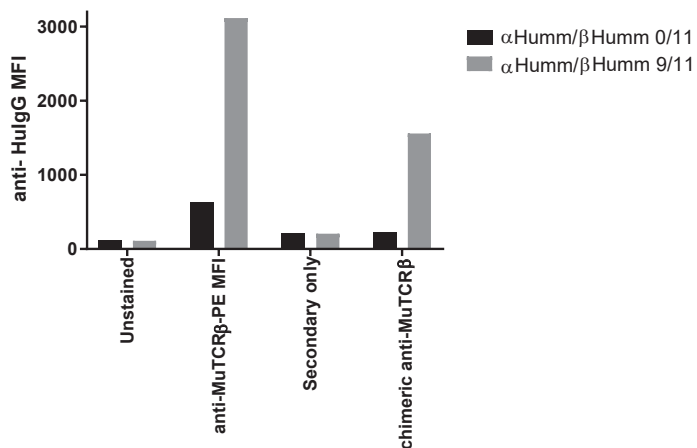
Supplementary Figure 5. Chimeric anti-MuTCRβ antibody binds to primary T cells expressing the murinized TCR containing 9 out of 11 murine residues in the 3rd domain of the β chain. Jurkat-76 cells were transduced with 2 different αβTCRs, containing 0/11 or 9/11 murine residues in the 3rd domain of the β chain, to assess binding of the newly generated chimeric and CDR grafted anti-MuTCRβ antibodies. As negative controls, unstained and secondary antibody only conditions were used. As a positive control, wild-type PE-conjugated anti-MuTCRβ was used The data correspond to 2 independent experiments and a representative figure is shown.

Supplementary Table 1 Differences between the eleven human-mouse non-homologous amino acids in the third domain of the β chain (βM3). In red the mutations that abrogated binding of the anti-human αβTCR antibody

	Change in		
Mutation	Size	Charge	Hydrophobicity
$Q_{88}H$	-	Uncharged to positive charge	Hydrophilic to hydrophobic
$T_{101}H$	-	Uncharged to positive charge	-
$N_{106}E$	-	Uncharged to positive charge	-
$E_{108}K$	-	Negative to positive charge	Slightly more hydrophilic
$T_{110}P$	Less bulky	Uncharged	-
$Q_{111}E$	-	Uncharged to positive charge	-
$D_{112}G$	Less bulky	Negative charge to uncharged	Less hydrophobic
$R_{113}S$	Less bulky	Positive charge to uncharged	-
$A_{114}P$	-	Uncharged	Less hydrophobic
$I_{120}N$	-	Uncharged	Hydrophobic to hydrophilic
$V_{121}I$	-	Uncharged	-

2
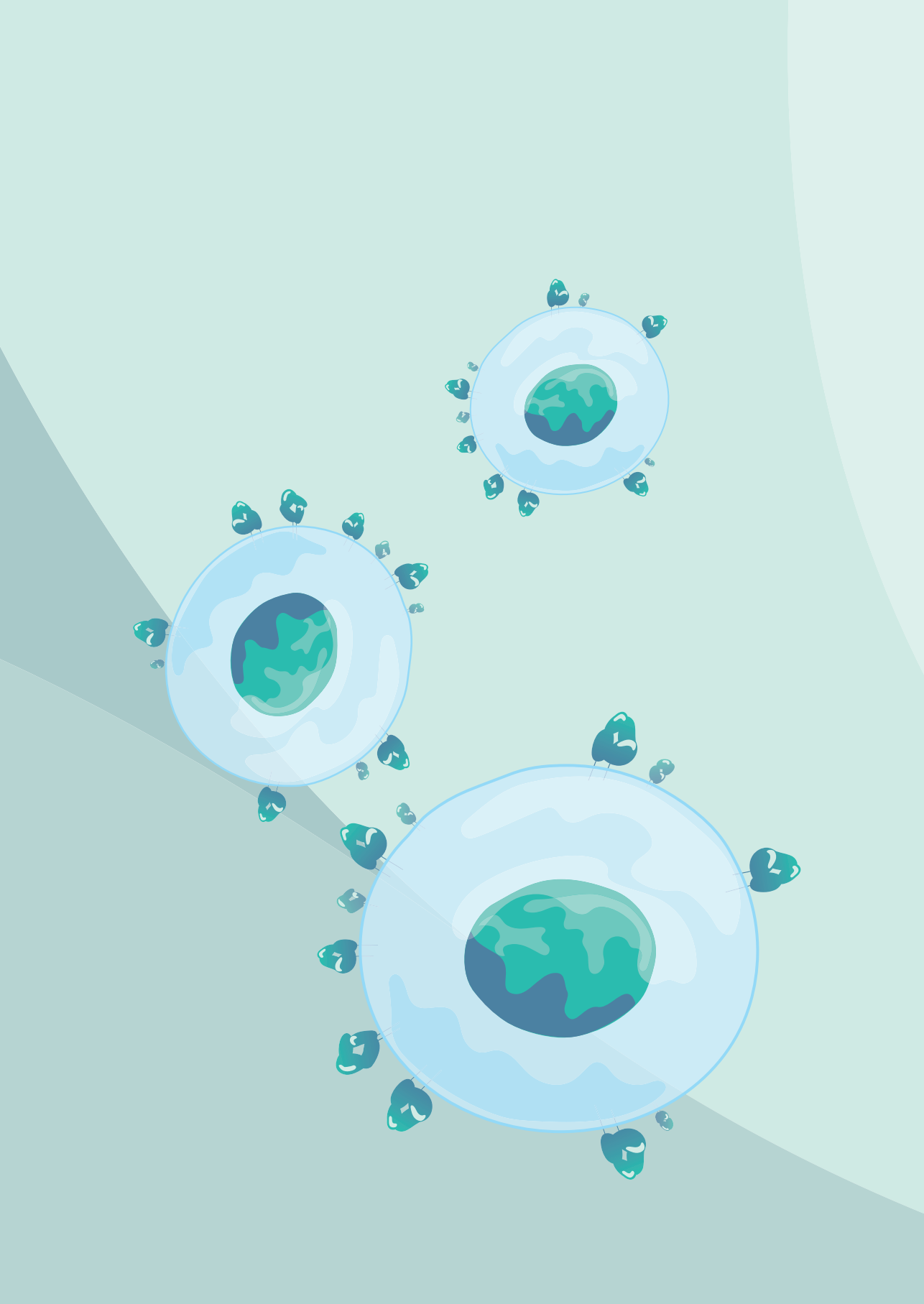
CHAPTER 3

Combining targeting of the cancer metabolome and cancer-associated stress antigens impacts engineered T cell dynamics and efficacy

Patricia Hernández-López[1†], Eline van Diest[1†], Peter Brazda[2], Inez Johanna[1], Angelo Meringa[1], Sabine Heijhuurs[1], Mara J.T. Nicolasen[1], Thomas A. Kluiver[2], Rosemary Millen[3], Effrosyni Karaiskaki[1], Trudy Straetemans[1], Hans Clevers[3], Remco de Bree[4], Hendrik G Stunnenberg[2], Weng Chuan Peng[2], Zsolt Sebestyén[1], Dennis X. Beringer[1x], and Jürgen Kuball[1,5x]

[1]*Center for Translational Immunology, University Medical Center Utrecht, Utrecht University; Utrecht, The Netherlands.*
[2]*Princess Máxima Center for Pediatric Oncology, Utrecht, The Netherlands.*
[3]*Hubrecht Institute, Utrecht, The Netherlands*
[4]*Department of Head and Neck Surgical Oncology, University Medical Center Utrecht, Utrecht, The Netherlands*
[5]*Department of Hematology, University Medical Center Utrecht; Utrecht, The Netherlands.*

† These authors contributed equally to this work
[x] Shared senior authors

Manuscript in preparation

Abstract

Broad antitumor-reactivity of γ9δ2T cells can be augmented by transfer of high affinity γ9δ2TCRs into αβT cells, resulting in a new generation of CAR-T cells called TEGs. We hypothesized that TEG activity can be enhanced by the addition of extra co-stimulation provided by chimeric co-receptors in which the extracellular domain of NKG2D, that recognizes stress-induced ligands expressed by 70-80% of tumors, is fused to the cytoplasmic signaling domains of different costimulatory proteins. The NKG2D-CD28$_{WT}$ and NKG2D-4-1BB$_{CD28TM}$ co-stimulatory chimeras were able to overcome suboptimal γ9δ2TCR engagement and enhance serial killing by- and proliferation capacity of the engineered T cells. Combining cancer-metabolome and stress-targeting resulted in an improved persistence and tumor targeting of TEG001 in an *in vitro* bone marrow niche model without harming resting or stressed healthy tissues, and increased survival rate compared to TEG001 in an *in vivo* multiple myeloma model. The mechanisms underlying this increased survival differed between both chimeras. The NKG2D-CD28$_{WT}$ chimera enhanced initial tumor control, at the expense of a large drop in T cell numbers, while NKG2D-4-1BB$_{CD28TM}$ chimera prolonged *in vivo* persistence of TEG001 due to an increased proliferation rate. For solid tumors, this prolonged persistence of TEG001-NKG2D-4-1BB$_{CD28TM}$ seems to be key for enhanced tumor control in an *in vivo* solid tumor model.

Introduction

To overcome scarceness of tumor antigens for many solid tumors, as well as the poor function and diversity of natural γδT cells, we introduced a novel class of CAR-T cells called TEGs (αβT cells engineered to express a defined γδTCR). TEGs sense an intracellular accumulation of phosphoantigens (pAg) in tumor cells by recognizing an in inside-out mechanism involving RhoB [1], BTN2A1 [2, 3] and BTN3A1 [1, 4-7] through a carefully selected high affinity γ9δ2TCR [8-11]. TEGs are currently being explored in a phase I clinical trial (NTR6541). However, although TEGs depend on the αβT cells, that have been clinically proven to be effective for hematological malignancies, as carrier [7, 9, 12, 13] , they are not unaffected by the many weaknesses observed for engineered αβT cells, in particular when targeting solid tumors [14]. To improve activity of engineered αβT cells, several CAR designs as well as combination of standard CAR constructs with co-stimulatory chimeric receptors have been employed [15-19]. Design strategies for single CAR designs frequently depend on trial and error to find the right balance between spacer and signaling domain for the CAR itself. In addition, different signaling domains, expressed as CAR-like co-stimulatory domains, are being explored [14].

 Within this context we made use of cancer-metabolome targeting TEGs (later referred to as TEG001), to address whether providing costimulatory signals in addition to the initial γ9δ2TCR mediated signal, by NKG2D chimeric co-receptors, could improve performance to CD4+ and CD8+ TEGs. Our concept relies on the combination of cancer-metabolome targeting of TEG001 and cancer-stress targeting, by designing NKG2D co-receptor chimeras interacting with NKG2D-ligands (MICA/B and ULBP1-6) given their broad expression in many tumor cells [20, 21].

It has been shown before that TEG activity benefits from endogenous NKG2D expression in CD8+ T cells [12]. NKG2D based CAR-T cells have also been explored in clinical trials, but showed no substantial efficacy in patients suffering from acute myeloid leukemia [22]. Reasons of failure might be that NKG2D engagement alone, without additional co-receptor support, does not exploit its full activity. Alternatively, the used design, partially depending on DAP10 signaling, might rapidly exhaust T cells [23, 24], an important mechanism to protect inflamed tissues from attack by T cells that recognize the expressed NKG2D ligands. However, given their broad expression on tumor cells, alternative strategies to target NKG2D ligands are still interesting for anti-cancer therapies [21].

Herein, we observed that while most of the studied NKG2D co-receptor chimeras impacted TEG001 function in different read outs, and could overcome suboptimal TCR engagement *in vitro,* only TEGs expressing the NKG2D-4-1BB$_{CD28TM}$ co-receptor, made by the fusion of NKG2D to CD28 transmembrane- and 4-1-BB co-stimulation domain, showed improved targeting of liquid and solid tumors *in vivo.*

3

Material and Methods

Antibodies

The following antibodies were used: CD8a-PerCP-Cy5.5 (1:100; clone RPA-T8; 301032), CD4-AF700 (1:40; clone RPA-T4; 300526), αβTCR-PE-Cy5 (1:80; clone IP26; 11-9986-42) and huNKG2D (clone 1D11; 320802) from Biolegend. γδTCR-PE-Cy7 (1:20; clone IMMU510; B10247) from Beckman Coulter. NKG2D-BV650 (1:40; clone 1D11; 563408) and γδTCR-APC (1:5; clone B1; 555718) from BD Biosciences. Pan-γδTCR-PE (1:10; clone IMMU510; B49176) from Beckman-Coulter. huCD45-PB (1:30; clone HI30; 2120145), mCD45-APC (1:30; clone 30-F11S; 1115560), and huCD69-APC(1:25; clone FN50; 2154550) from Sony Biotechnology. αβTCR-FITC (1:10; clone IP26; 11-9986-42) from Invitrogen. CD4-PE-Cy7 (1:100; clone RPA-T4; 25-0049-42), NKG2D-PE (1:25; clone 1D11; 12-5878-42) and Fixable Viability Dye eFluor506 from eBioscience. huCD28 (clone 15E8; 130-093-375) and huCD3 (clone OKT3; 130-093-387) from Miltenyi Biotec.

Cell lines and cell culture

Daudi, K562, HL60, RPMI-8226, SCC9 and Phoenix-Ampho cells were obtained from ATCC. Phoenix-Ampho and SCC9 cells were cultured in DMEM supplemented with 1% Pen/Strep (Invitrogen) and 10% FCS (Bodinco, Alkmaar, The Netherlands). All other cell lines were cultured in RPMI with 1% Pen/Strep and 10% FCS. Primary fresh PBMCs were isolated by Ficoll-Paque (GE Healthcare, Eindhoven, The Netherlands) from buffy coats supplied by Sanquin Blood Bank (Amsterdam, The Netherlands). Liver and head and neck patient derived organoids were established and cultured as described previously [25, 26]. For co-culture assays liver tumor-derived organoids were released from their BME matrix using dispase. For co-culture assays using head and neck tumor organoids, organoids were recovered from the BME by resuspension in TrypLE Express and collected in adDMEM/F12+++.

Construction of chimeric NKG2D receptors

cDNAs for the type I NKG2D co-receptors were synthetized by BaseClear (Leiden, Netherlands). Type II co-receptors were created using overlap extension PCR. Both designs were cloned into pBullet. For the second version of the type I NKG2D chimeric co-receptors, the transmembrane and linker domains of the co-receptors NKG2D-ICOS$_{wt}$ and NKG2D-4-1BB$_{wt}$ were replaced by the transmembrane and linker domains of NKG2D-CD28$_{wt}$ chimera using overlap extension PCR. They were all subcloned into pMP71 already containing γδTCR-Cl5, using XhoI and HindIII. All restriction enzymes were supplied by NEB (Massachusetts, USA).

Retroviral transduction of αβ T cells and cell lines

Briefly, packaging cells (Phoenix-Ampho) were transfected with helper constructs gag-pol (pHIT60), env (pCOLT-GALV) and pMP71 or pBullet retroviral vectors containing genes codifying for the different proteins. In the case of human PBMCs, they were pre-activated with anti-CD3 (30 ng/mL; Orthoclone OKT3; Janssen-Cilag) and IL-2 (50 IU/mL; Proleukin, Novartis). Both, PBMCs and cell lines, were transduced twice with viral supernatant within 48 or 3 hours respectively, in presence of 6 μg/mL polybrene (Sigma-Aldrich). For PMBCs 50 IU/mL of IL-2 was added. TCR-transduced T cells were expanded by stimulation with anti-CD3/CD28 Dynabeads (500,000 beads/10^6 cells; Life Technologies) and IL-2 (50 IU/mL). Thereafter, TCR-transduced T cells were depleted of the non-engineered T cells.

Depletion of non-engineered T cells

αβT cells transduced with γδTCR-Cl5 either alone or together with NKG2D wild type or the different NKG2D chimeras were incubated with a biotin-labeled anti-αβTCR antibody (clone BW242/412; Miltenyi Biotec, Bergisch Gladbach, Germany) and subsequently incubated with an anti-biotin antibody coupled to magnetic beads (anti-biotin MicroBeads; Miltenyi Biotec). Thereafter, the cell suspension was loaded onto an LD column and αβTCR+ T cells were depleted by MACS cell separation per the manufacturer's protocol (Miltenyi Biotec). After depletion, TEGs were expanded using a T cell rapid expansion protocol (REP)[12].

Selection of engineered T cells

After αβ-depletion, T cells were selected using human CD4 or CD8 microbeads and MS columns (Miltenyi Biotec). Procedure was carried out according to manufacturer´s protocol.

NKG2D ligand staining

The expression of NKG2D ligands in tumor cell lines and organoids was assessed using Recombinant Human NKG2D Fc Chimera Protein (R&D systems, Abingdon, UK). 10^5 tumor cells were incubated either with 0.5 μg of NKG2D Fc recombinant protein or IgG1-Fc during 30 min. Cells were washed with FACs buffer (1% BSA, 1% Na+azide) and secondary antibody IgG-PE (Southern Biotech, Alabama, USA) was added in a 1:200 dilution. Cells were fixed using 1% PFA in PBS. Samples were measured on a BD LSR Fortessa and FACSDiva (BD) software was used for data analysis.

Functional T cell assays

For CD69 expression, 200.000 T cells per well were incubated in a 96 wells plate precoated with 0,2 ug/ml anti-huCD3 (clone OKT3; 130-093-387, Miltenyi Biotec), 5 µg/ml anti-huNKG2D (clone 1D11; 320802, Biolegend) or a combination of the two. Cells were incubated for 24 hours after which they were incubated with anti-huCD69-APC (1:25; clone FN50; 2154550) from Sony Biotechnology during 30 min. Cells were washed with FACs buffer (1% BSA, 1% Na+azide) and fixed using 1% PFA in PBS. Samples were measured on BD FACs Canto and FACSDiva (BD) software was used for data analysis.

For cytokine detection 5 x 10^4 effector T cells were co-cultured for 18 hours with different tumor cell lines or organoids in a 1:1 or 1:3 effector-to-target ratios (E:T) respectively in round-bottom 96-well plates in presence of pamidronate. After incubation, supernatants were collected and either frozen or used to detect IFNγ levels straight away. ELISA was performed using IFN gamma Human Uncoated ELISA Kit (Thermo Fisher Scientific, Massachusetts, USA).

51 Chromium-release assay for cell-mediated cytotoxicity was previously described [9]. In brief, target cells were labeled for 2 hours with 100 µCu 51Cr and incubated for 4 to 5 hours with transduced T cells in five effector-to-target ratios (E:T) between 10:1 and 0.11:1 in the presence of 10-30 µM of pamidronate. Percentage of specific lysis was calculated as follows: (experimental cpm - basal cpm)/(maximal cpm - basal cpm) x100 with maximal lysis determined in the presence of 5% triton and basal lysis in the absence of effector cells.

For long term serial-killing assays, 5 x 10^3 RPMI 8226 or SCC9 cells expressing luciferase-GFP were co-cultured with effector T cells at 3:1 effector: target ratio in presence of 10 µM pamidronate. To asses ability of the different constructs to repetitively kill tumor cells, new targets were added every 24h hours. Luciferin was added at 12.5 ug/ml and luminescence signal was measured on Softmax pro machine at 24, 48, 72 and 96 hours.

In order to assess proliferation, T cells were resuspended at 1 x 10^6 cells/ml using a 2 µM solution of CellTrace™ Violet Cell Proliferation Kit (Thermo Fisher Scientific, Massachusetts, USA) in PBS. The cell suspension was incubated for 20 min at 37°C. Cells were washed two times with complete RPMI medium and resuspended in culture medium. For proliferation after stimulation with antibodies, 200.000 labeled T cells per well were incubated for 6 days in a 96 wells plate pre-coated with different concentrations of anti-huCD3 (clone OKT3; 130-093-387, Miltenyi Biotec), anti-huNKG2D (clone 1D11; 320802, Biolegend) or a combination of the two. For the proliferation assay with tumor cell lines, 2.5 x 10^5 labeled effector T cells were co-cultured together with 2.5 x 10^5 tumor cells in 48-well plates for 6 days, 100 µM pamidronate was added to cultures boost recognition. On day 6,

cells were analyzed by flow cytometry. For the proliferation assays with organoids, 1×10^5 labeled T cells were co-cultured with organoids in a E:T ratio of 1:1,5 in 96-U well plate in presence of pamidronate (100 µM) during 6 days. On day 6, proliferation was assessed by flow cytometry.

3D model

The 3D model was previously described in detail [27]. The RPMI 8226 tumor cells were stained with Vybrant DiO (Thermo Fisher, United States) and seeded in Matrigel (Corning, United States) together with multipotent mesenchymal stromal cells (MSCs) and endothelial progenitor cells (EPCs), both stained with Vybrant DiD (Thermo Fisher, United States). After four days, the different TEGs were stained with Vybrant DiI (Thermo Fisher, United States) and administered to the model together with and 10 µM PAM (Calbiochem, United States). Two and six days later, the Matrigel was dissolved using Dispase (Corning, United States) to retrieve the cells from the model. Tumor, T cells and stromal cells were quantified by FACS using Flow count Fluorospheres (Beckman Coulter, United States). Cell number were normalized to mock treatment.

Animal models

NOD.Cg-PrkdcscidIl2rgtm1Wjl/SzJ (NSG) mice originally obtained from Jackson Laboratory (Bar Harbor, ME, USA) were bred and housed in the breeding unit of the Central Animal Facility of Utrecht University. Experiments were conducted under institutional guidelines after permission from the local Ethical Committee and in accordance with the current Dutch laws on Animal Experimentation. Mice were housed in sterile conditions using an individually ventilated cage (IVC) system and fed with sterile food and water. Irradiated mice were given sterile water with antibiotic ciproxin for the duration of the experiment. Mice were randomized with equal distribution by sex and divided into 10-12 mice/group. Adult mice (16-30 weeks old) received sublethal total body irradiation (1.75 Gy) on Day -1. On Day 0, depending on the model, NSG mice were injected either intravenously with 5×10^6 RPMI 8226-luciferase cells resuspended in 100 ul of PBS or subcutaneously with $0,5 \times 10^6$ SCC9-luciferase tumor cells resuspended in mixture of matrigel and PBS (1:1). On days 1 and 6 mice were injected intravenously with 1×10^7 of different engineered T cells (TEGs). All mice received 0.6×10^6 IU of IL-2 (Proleukin; Novartis) in 100 µl incomplete Freund's adjuvant (IFA) subcutaneously together with the first TEGs injection and every 3 weeks until day 45. Pamidronate (10mg/kg body weight) was injected intravenously together with the T cell injections, and every 3 weeks until the end of the experiment, in order to enhance TEGs activation as previously reported [12]. Tumor growth was weekly monitored by bioluminescence. Furthermore, in the subcutaneous model tumor volumes were measured weekly and calculated by using the formula *tumor volume = 0.4x (length x width². In the RPMI

8226-luc model, mouse survival was assessed at least twice a week, by monitoring weight loss and symptoms of disease (sign of paralysis, weakness, reduced motility).

Results

Use of a type I design and CD28 transmembrane domain leads to optimal expression of NKG2D chimeras

We combined cancer metabolome-targeting TEG001 with targeting of cancer-associated stress antigens by designing three different NKG2D-derived chimeric co-receptors. As the natural orientation of NKG2D (a type II membrane protein) differs from the three chosen costimulatory proteins ICOS, CD28 and 4-1BB (all type I membrane proteins), two different types of chimeras were generated. A "Type I" design where the extracellular domain of NKG2D was fused to the hinge, transmembrane, and cytoplasmic domains of the different costimulatory proteins, or a "Type" II design where the cytoplasmic signaling domain of the costimulatory proteins was fused to the transmembrane and extracellular domain of NKG2D (Figure 1A). For "Type I" chimeras, differential expression was observed in Jurkat-76 cells when assessed by flow cytometry, with strongest surface expression for NKG2D-CD28$_{wt}$ and weakest for NKG2D-4-1BB$_{wt}$ chimera. Of the "Type II" designs, only one of the chimeras, NKG2D-CD28$_{wt}$, was marginally expressed (Figure 1B). Therefore, we next focused on the "Type I" NKG2D chimeras and NKG2D$_{wt}$, which were expressed equimolar in combination with the γδTCR-Cl5 in primary CD4+ αβT cells that lack endogenous NKG2D expression (CD4+ TEG001). Again, NKG2D-CD28$_{wt}$ showed increased surface expression compared to the other two chimeras and NKG2D$_{wt}$ (Figure 1C). As membrane expression of proteins can depend on their transmembrane domain [28], we hypothesized that the superior expression of the NKG2D-CD28$_{wt}$ chimera was a consequence of its transmembrane domain (TM). Using the same CD28 hinge and TM for all chimera's (Figure 1D) resulted in higher and more comparable surface expression (Figure 1E). Therefore, chimera designs with CD28 hinge and TM were selected for further testing.
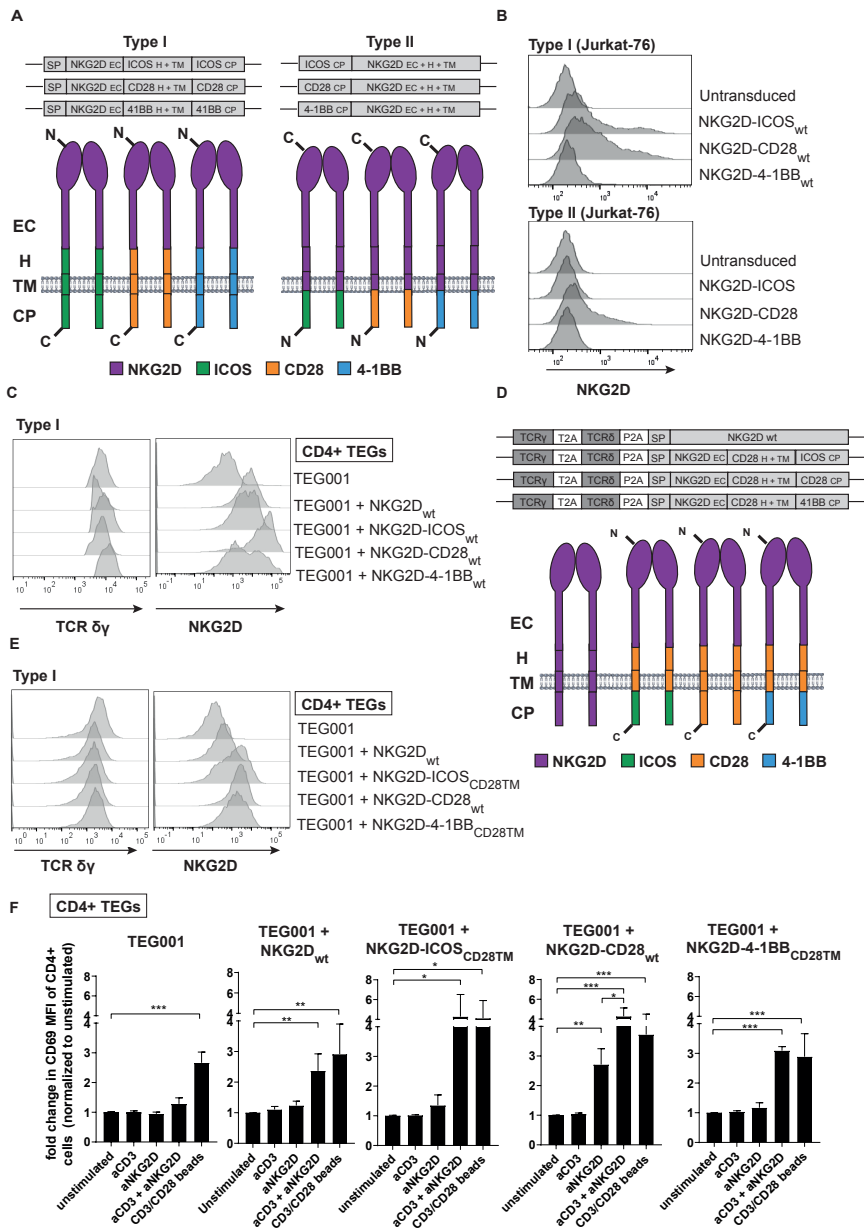
3

Figure 1. NKG2D chimeric co-receptors design, expression and activity upon CD3 and NKG2D stimulation. (A) Schematic diagram of type I and type II chimeric NKG2D co-receptors. Signal peptide (SP), ectodomain (EC), hinge (H), transmembrane (TM) and cytoplasmic (CP) domains are as indicated. N-terminal and C-terminal are represented by N and C respectively. NKG2D, ICOS, CD28 and 4-1BB domains are colored in purple, green, orange and blue respectively. (B) Expression of type I and type II chimeric NKG2D co-receptors in Jurkat-76 cells. (C) Surface expression of γδTCR-Cl5 and type I NKG2D co-

receptors or NKG2D$_{WT}$ on CD4+ T cells after transduction and αβ depletion, assessed by flow cytometry. (D) Schematic overview of three different type I chimeras and γδTCR transgene cassette in the retroviral vector pMP71. TCRδ chain was derived from clone 5 (d) and TCRy from clone G115 (g) and F2A (derived from the foot-and-mouth disease virus) and T2A (derived from the Thosea asigna virus) refer to two different 2A ribosomal skipping sequences. NKG2D, ICOS, CD28 and 4-1BB domains are colored in purple, green, orange and blue respectively. (E) Surface expression of γδTCR-Cl5 and NKG2D$_{WT}$ or type I NKG2D co-receptors containing CD28 transmembrane (TM) and hinge (H) domains, on CD4+ T cells after transduction and αβ depletion and assessed by flow cytometry. (F) Expression of CD69 upon stimulation with CD3 (0,2 µg/ml and/or NKG2D (5 µg/ml) antibodies, or CD3/CD28 dynabeads. MFI was measured by flow cytometry and fold change was calculated per type of cells as MFI relative to unstimulated condition. N=2 Error bars represent SD, significance was calculated using One way ANOVA with Dunnett correction for multiple comparisons. *P <0.05, **P < 0.01, ***P < 0,001.

NKG2D$_{wt}$ and NKG2D chimeras rescue activation of sub-optimally stimulated TEG001

Suboptimal TCR engagement is often a limitation for TCR-based cancer immune therapies [8, 29]. Therefore we assessed whether additional engagement of the different NKG2D chimeras or NKG2D$_{wt}$ can rescue activation of T cells when TCR engagement is limited. Within this context, we observed that combination of a suboptimal CD3 stimulation through low concentration of plate-bound anti-CD3 antibody with an antibody against NKG2D, only increased expression of CD69 in TEG001 when one of the NKG2D chimeras or NKG2D$_{wt}$ were co-expressed (Figure 1F). Of note, triggering of the NKG2D-CD28$_{wt}$ chimeric co-receptor in the absence of TCR engagement did lead to a small, but significant, upregulation of CD69 without CD3 stimulation, which is in line with earlier observations that antibody induced stimulation of CD28 can lead to the expression of CD69 [30].

Co-expression of NKG2D-4-1BB$_{CD28TM}$ in TEG001 improves IFNy release, but not short-term killing, in response to tumor cells expressing NKG2D ligands

We next investigated whether the increased signaling induced by the NKG2D chimeras is preserved when using tumor cells expressing natural NKG2D-ligands for the activation CD4$^+$ TEG001. A panel of tumor cell lines was selected based on their reported susceptibility to γ9δ2TCR mediated recognition [9, 12, 13, 31, 32] and characterized for NKG2D ligand expression by utilizing a NKG2D-Fc fusion protein (Supplementary Figure 1A). Three tumor cell line phenotypes were identified: (I) **recognized** by TEG001 and **low** NKG2D ligand expression (Daudi), (II) **recognized** by TEG001 and **high** NKG2D ligand expression (SCC9, K562 and RPMI 8226), (III) **not recognized** by TEG001 and **high** NKG2D ligand expression (HL60).

First, we assessed the impact of the NKG2D-chimeras on activation of CD4$^+$ TEGs in a co-culture with tumor cell lines expressing high or low levels of NKG2D-ligands, measured by IFNγ secretion. As additional control, NKG2D$_{wt}$ and the NKG2D

chimeras were also expressed together with the nonfunctional γδTCR LM1 [9], called TEG-LM1. The most prominent change in activity was observed for TEG001 co-expressing NKG2D-4-1BB$_{CD28TM}$ chimera, which secreted higher levels of IFNγ against NKG2D-ligand high expressing tumor cells K562 when compared to TEG001 (Figure supplementary figure 1B). This difference was visible for all tested pamidronate (PAM) concentrations, a modulator of accumulation of pAg in the tumor cell [33, 34], but most significant at the lower concentrations, implying again that co-stimulation becomes important once TCR ligand expression is limited. In contrast, there were no significant differences in killing observed between CD8+ TEG001 and TEG001 co-expressing the different chimeric co-receptors or NKG2D$_{wt}$ when using chromium (^{51}Cr) labeled HL60, Daudi, K562, RPMI 8226 and SCC9 tumor cells as targets (Supplementary figure 1C), indicating that the short-term killing potential of the TEGs is not influenced by these co-stimulatory chimeras or that endogenous NKG2D expression by CD8+ TEGs can overrule effects observed with CD4+ TEGs.

Co-expression of NKG2D chimeric co-receptors in TEG001 enhances proliferation capacity and overcomes low TCR-ligand density

It has been reported that variations in costimulatory signaling mainly impacts persistence and exhaustion of CAR-T cells [19, 35]. To assess whether this also holds true when a combined signaling of γδTCR and chimeric NKG2D molecules is used, we examined proliferation capacity of both CD4+ and CD8+ TEG001 cells co-transduced with NKG2D$_{wt}$ or the different NKG2D chimeras. At day 6, co-expression of NKG2D$_{wt}$ in CD4+ TEGs already resulted in a significant decrease in Cell Trace violet (CTV) MFI, indicating an enhanced proliferation ability when compared to conventional TEG001 (Figure 2A). Interestingly, co-expression of the NKG2D chimeras resulted in a further significant decrease in CTV MFI when compared to TEG001 co-expressing NKG2D$_{wt}$, emphasizing the importance of combining the extracellular ligand binding domain of NKG2D with the intracellular co-stimulatory signaling domains. Intriguingly, under most stringent conditions, thus low NKG2D antibody concentration (1 μg/ml), only CD4+ TEGs co-expressing NKG2D-CD28$_{wt}$ showed a significant increase in proliferation compared to TEGs expressing NKG2D$_{wt}$ (Figure 2A). By contrast, in CD8+ TEGs, with endogenous NKG2D expression, the anti-NKG2D Ab also induced proliferation of TEG001 and TEG-LM1, reducing the overall observed differences in proliferation (Supplementary Figure 2A). This suggests that the endogenous expression of NKG2D on these cells could partially overrule the effect of the chimeras. As differences were more profound in the absence of endogenous NKG2D, and stimulation by anti-NKG2D antibodies could again overestimate impact of co-receptor signaling, we next tested proliferation ability of CD4+ TEGs after stimulation with the natural ligands. As expected, CD4+ TEG001, but not CD4+ TEG-LM1 (mock), were able to proliferate when co-cultured with RPMI 8226 tumor cells (Figure 2B and Supplementary

figure 2B). Co-expression of NKG2D$_{wt}$, without modified co-stimulation domain, no longer showed a benefit when compared to conventional TEG001. However, once more, addition of the NKG2D chimeric co-receptors to CD4+ TEG001 significantly increased proliferation when compared to TEG001 co-expressing NKG2D$_{wt}$, highlighting the importance of the addition of costimulatory signaling domains to the natural receptor once natural ligands are engaged. As both RPMI-8226 and HL60 express high levels of NKG2D ligands, but only RPMI-8226 is recognized by TEG001, these data imply that γ9δ2TCR activation is essential for the additive effect of the NKG2D chimeras.
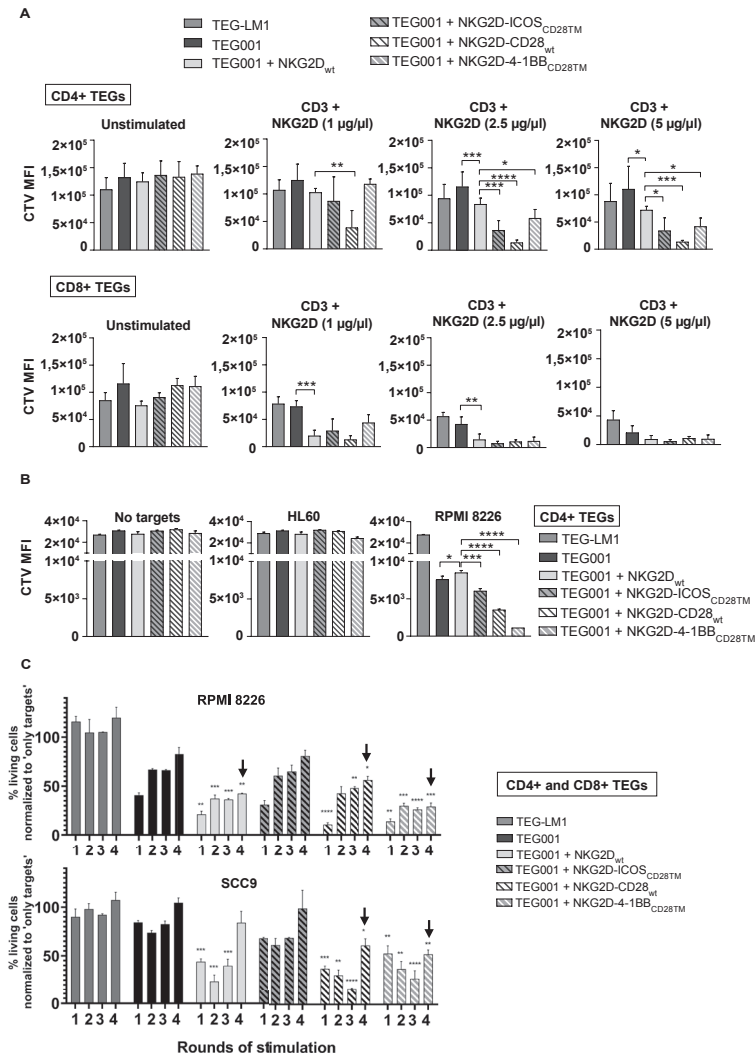
Figure 2. Introduction of NKG2D chimeric co-receptors improves proliferation and long-term killing activity of TEGs. (A) CD4+ and CD8+ transduced T cells were labeled with CTV and stimulated with CD3 and NKG2D antibodies during six days. On day 6 MFI was assessed by flow cytometry. N=3, data represent Trace violet MFI ± SD, significance was calculated using One Way ANOVA with Holm-sidak. (B) CD4+ transduced T cells were labeled with CTV and incubated either with HL60 or RPMI 8226 cells in presence of 100 μM PAM. On day 6 MFI was assessed by flow cytometry. Representative graph of two independent experiments. Data represent Cell Trace violet MFI ± SD, significance was calculated using One Way ANOVA with Holm-sidak (C) RPMI 8226 or SCC9 tumor cells expressing luciferase, were incubated with the different TEGs in 3:1 E:T ratio. TEGs were challenged every 24h with new targets cells and luciferase signal was measured at 24, 48, 72 and 96h. Representative graph of at least two independent experiments. Data represent mean ± SD, significance was calculated using One Way ANOVA with Dunnet correction comparing TEG001 to TEG001 co-expressing the NKG2D receptors. P <0.05, **P < 0.01, ***P < 0,001, ****P < 0,0001.

Increased serial killing in the presence of NKG2D$_{WT}$, NKG2D-CD28$_{wt}$ and NKG2D-4-1BB$_{CD28TM}$

Although we did not see enhanced short-term killing when co-expressing the different NKG2D chimera's (Supplementary figure 1C), we postulated that co-expression of the chimeric co-receptors would impact TEG serial killing over time as reported recently for T cells engineered with a FAS-4-1BB fusion protein [36]. As serial killing of tumor cells depends on both CD4+ and CD8+ engineered T cells [37], RPMI-8226 and SCC9 tumor cells expressing luciferase were incubated with a mixture of CD4+ and CD8+ (50%-50%) TEGs in 3:1 E:T ratio. TEGs were challenged every 24h with new targets cells and luciferase signal was measured after 24, 48, 72 and 96 hours. Overall, TEG001 co-expressing NKG2D$_{wt}$, NKG2D-CD28$_{wt}$, or NKG2D-4-1BB$_{CD28TM}$, showed increased killing ability even after the 4th re-challenge against RPMI-8226 and the latter two also against SCC9 (Figure 2C), while addition of NKG2D-ICOS$_{CD28TM}$ to TEG001 did not have any additive effect in killing ability when compared to TEG001.

NKG2D-CD28$_{WT}$ and NKG2D-4-1BB$_{CD28TM}$ improve persistence and specific tumor targeting of TEG001 in a bone marrow niche model

Expression of NKG2D-CD28$_{wt}$ or NKG2D-4-1BB$_{CD28TM}$ in TEG001 cells showed an additive effect in several functional readouts, in particular when assessing CD4+ TEGs in longer term assays. To further explore potential benefits of chimeric NKG2D designs we increased the difficulty for engineered immune to target tumor cells by mimicking a more physiological tumor microenvironment (TME) [38, 39] in a 3D bone marrow niche model [27]. After 3 days the models treated with TEG001 and TEG001 co-expressing NKG2D-chimeric receptors showed decreased tumor cell numbers compared to treatment with TEG-LM1, however, no differences in tumor control between functional constructs were observed (Figure 3A). On day 6 solely TEG001s co-expressing NKG2D-CD28$_{WT}$ or NKG2D-4-1BB$_{CD28TM}$ further significantly increased tumor lysis when compared to TEG001. As we observed in the previous set of experiments that chimeric co-stimulatory receptors had a direct impact on

proliferation of TEGs, the number of T cells was also assessed (Figure 3A). At day 3, all TEG001 variants had higher viable T cell numbers when compared to the non-functional TEG-LM1, while only TEG001 co-expressing NKG2D-CD28$_{WT}$ and NKG2D-4-1BB$_{CD28TM}$ showed significantly higher number of T cells when compared to TEG001 at day 6. In summary, the 3D model hinted towards superiority of TEG001-NKG2D-CD28$_{WT}$ and TEG001-NKG2D-4-1BB$_{CD28TM}$.

Combining targeting of the cancer metabolome and cancer-associated stress antigens do not harm healthy resting and stressed tissues

The 3D model (Figure 3) can also be used to assess the impact of the TEG treatment on healthy tissues, by quantification of the remaining viable stromal cells (MSCs). No differences were observed between all conditions in stromal cell number over time (Figure 3A, right panel), highlighting preservation of healthy tissues and the tumor specificity of TEGs in the very same experimental set up. To further preclude the potential risk of targeting healthy tissues, we extended the analyses to stressed healthy tissues, which can temporarily upregulate NKG2D-ligands [40]. Recognition of several healthy donor derived hematopoietic cell subsets was assessed in resting, stressed (irradiation or combined treatment with cyclophosphamide and fludarabine) or activated state (treated with huCD40LT, LPS or IFNγ). Expression of NKG2D ligands was assessed for all the conditions (Figure 3B). However, co-incubation of the differently treated healthy cell subsets with CD4+ TEGs expressing the different NKG2D chimeras did not result in recognition (Figure 3C), suggesting an advantageous safety profile of TEG001 co-expressing NKG2D-receptors.

Improved therapeutic effect of TEGs co-expressing NKG2D-4-1BB$_{CD28TM}$ and NKG2D-CD28$_{WT}$ against multiple myeloma *in vivo*

To assess whether differences between TEG001 and TEG001 co-expressing the different chimeric co-receptors translates into *in vivo* differences, we established a human multiple myeloma xenograft model utilizing the same target, RPMI-8226, as used in the 3D model (Figure 4A). Treatment with TEG001 co-expressing NKG2D-CD28$_{WT}$ and NKG2D-4-1BB$_{CD28TM}$ led to a further improved tumor control compared to TEG001 (Supplementary figure 3), while introduction of NKG2D$_{WT}$ or NKG2D-ICOS$_{CD28TM}$ did not improve ability of TEG001 to inhibit tumor growth *in vivo*. Importantly, the improvement in tumor control by introduction of NKG2D-CD28$_{WT}$ and NKG2D-4-1BB in TEG001 also translated into a significantly prolonged mouse survival time compared to treatment with TEG001 (Figure 4B). The net treatment effect for TEG001 compared to TEG-LM1 mock treatment, was 12 days, while for the groups treated with TEG001 co-expressing NKG2D-CD28$_{wt}$ or NKG2D-4-1BB$_{CD28TM}$ this was more than doubled, with a net treatment effect of 31.5 and 28 days respectively.
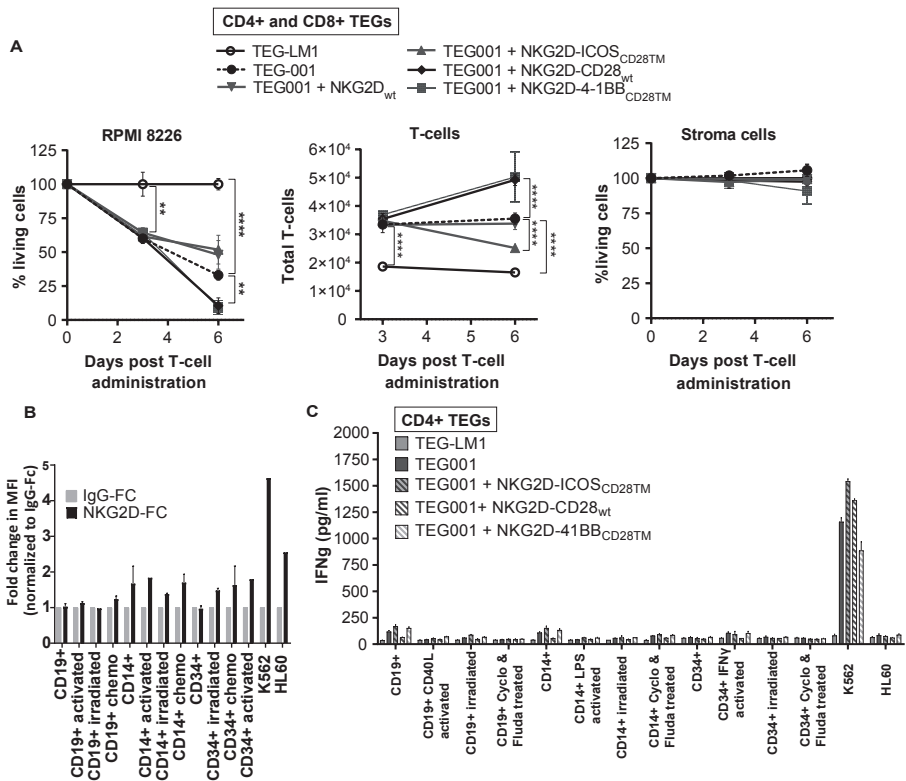
Figure 3. NKG2D-CD28$_{WT}$ and NKG2D-4-1BB$_{CD28TM}$ improve persistence and specific tumor targeting without harming healthy tissue. (A) RPMI 8226 tumor cell line expressing luciferase and stroma cells were cultured in matrigel constituting 3D bone marrow niche. After four days CD4+ and CD8+ TEGs were added together with PAM (10 µM PAM). Three and six days later, living tumor, stroma and T cells were quantified by FACs. Tumor and stroma cell numbers were normalized to mock treatment (TEG-LM1). N=2. Data represent mean ± SD. Significance was calculated using Two Way ANOVA with Dunnet correction (B) Surface expression of NKG2D ligands on healthy hematopoietic cells in resting, activated or stressed states. MFI was measured by flow cytometry using NKG2D-Fc and a IgG-Fc fusion proteins. Fold change was calculated per type of cells as MFI measured using NKG2D-Fc relative to IgG-Fc condition. (C) CD4+ TEG001 or TEG001 co-expressing NKG2D-ICOS$_{CD28TM}$, NKG2D-CD28$_{WT}$ and NKG2D-4-1BB$_{CD28TM}$ were co-cultured with healthy hematopoietic cells in resting, activated (CD40L, LPS, IFNγ) or stressed by irradiation or a combination treatment with cyclophosphamide and fludarabine, in presence of 100 µM pamidronate. IFNγ release was measured by ELISA. N=2. Data represent mean ± SD.

TEG dynamics *in vivo* substantially differs between all formats

To further investigate the effect of the introduction of NKG2D-CD28$_{WT}$ and NKG2D-4-1BB in TEG001 on TEG dynamics in vivo, the xenograft model using RPMI-8226 was modified by labeling TEGs administered in the second injection (day 7) with CTV (Figure 4C). In line with our observations in the long-term survival model, tumor burden, when assessed by BLI, was significantly reduced in mice treated

with TEGs co-expressing NKG2D-4-1BB$_{CD28TM}$ or NKG2D-CD28$_{WT}$ when compared to TEG001 (Figure 4D). The number of tumor cells (GFP+) measured by FACS in the bone marrow was significantly reduced for TEGs co-expressing NKG2D-4-1BB$_{CD28TM}$ (Figure 4E). The number of T cell was monitored in peripheral blood on days 8 and 15 (1 and 8 days respectively after the 2nd T cell injection). Interestingly, the number of TEG-LM1 (mock) cells increased overtime, while the amount of TEG001 cells in blood significantly decreased (Figure 4F), with a twofold higher number of TEG-LM1 cells in both bone marrow and spleen compared to TEG001 at day 15, and a significantly decreased MFI for CTV when compared to TEG001 (Figure 4G). This data implies that tumor encounter partially hampers homeostatic proliferation of engineered immune cells in vivo. When only comparing the functional chimeras, on day 15 T cell numbers in blood TEG001- NKG2D-CD28$_{WT}$ were significantly lower compared to day 8, while for TEG001- NKG2D-4-1BB$_{CD28TM}$ such a significant drop in T cell numbers was not observed (Figure 4H). Interestingly, mice treated with TEG001- NKG2D-CD28$_{WT}$ also had a lower number of TEGs both in bone marrow and spleen, when compared to TEG001 and TEG001-NKG2D-4-1BB$_{CD28TM}$. Analysis of MFI for CTV implied significant increased proliferation of TEG001-NKG2D-4-1BB$_{CD28TM,}$ compared to TEG001 in blood and spleen (Figure 4I). Altogether, differences observed between TEGs containing NKG2D-CD28$_{WT}$ or 4-1BB$_{CD28TM}$ chimeras in killing at early time points (Figure 4D-E) and in *in vivo* proliferation rate (Figure 4H-I) suggest that, *in vivo,* NKG2D-CD28$_{WT}$ chimera expressed in TEG001 induce strong and fast killing of tumor cells during the first days (Figure 4D-E) followed by the death of TEGs (Figure 4H), while cells co-expressing NKG2D-4-1BB$_{CD28TM}$ have an advantage during chronic antigen stimulation because of their enhanced capacity to proliferate despite cognate recognition of the tumor.

Improved tumor control of TEGs co-expressing NKG2D-4-1BB$_{CD28TM}$ against head and neck xenograft model

To extend the data on tumor control with our novel set of receptors, we next chose a solid tumor model, as targeting solid tumors using engineered immune cells remains a major clinical challenge [41]. For this, NSG mice were subcutaneously injected with SCC9-luciferase tumor cells and treated on days 1 and 7 with TEG-LM1 (mock), TEG001, TEG001 co-expressing the different chimeric co-receptors (NKG2D-CD28$_{WT}$ or NKG2D-4-1BB$_{CD28TM}$) (Figure 5A). Bioluminescence signal and tumor volume were both measured to monitor tumor growth. In this model, TEG001 co-expressing NKG2D-4-1BB$_{CD28TM}$ was the only design that consistently showed a significant decrease in tumor load when assessed by BLI (Figure 5B) and tumor volume (Figure 5C) compared to TEG-LM1 and TEG001.
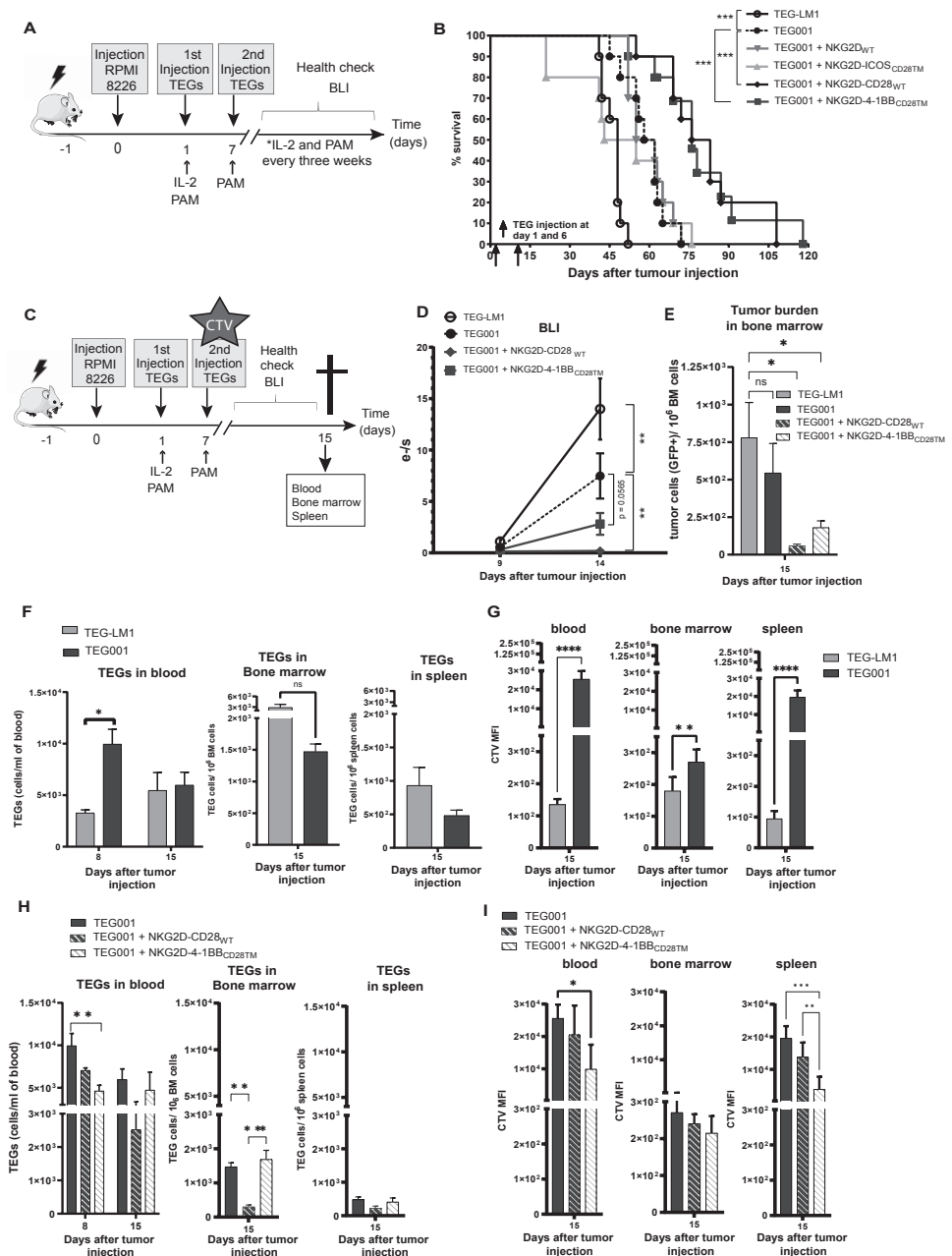
Figure 4. Study of *in vivo* therapeutic effects and proliferation of TEGs co-expressing NKG2D chimeric co-receptors in a multiple myeloma model. (A) Schematic diagram of experimental setup to evaluate efficacy of TEGs co-expressing NKG2D co-receptors against RPMI 8226 tumor. NSG mice were irradiated at day -1 and injected with 5 x 10⁶ RPMI 8226-luciferase tumor cells i.v. at day 0, followed by

3

10^7 TEGs expressing γδ-TCR-LM1 (mock), γδ-TCR-Cl5 alone or in combination with NKG2D$_{WT}$, NKG2D-ICOS$_{CD28TM}$, NKG2D-CD28$_{WT}$ and NKG2D-4-1BB$_{CD28TM}$ on days 1 and 7 in presence of PAM (n=10 mice per treatment group). Weekly BLI and bleeding were performed, and IL2 and PAM was administered every three weeks (B) Survival was assessed at least twice a week by monitoring weight loss and symptoms of disease. One mouse was censored at day 63 in NKG2D-4-1BB$_{CD28TM}$ treated group due to non-tumor related death. Significance was calculated by log-rank (Mantel-Cox) test; *P <0.05, **P < 0.01, ***P < 0,001 (C) Schematic diagram of experimental setup to evaluate *in vivo* proliferation of TEGs co-expressing NKG2D co-receptors against RPMI 8226 tumor. NSG mice were irradiated at day -1 and injected with 5 x 10^6 RPMI 8226-luciferase tumor cells i.v. at day 0, followed by 10^7 TEG-LM1 (mock), TEG001, TEG00-NKG2D-CD28$_{WT}$ or TEG001-NKG2D-4-1BB$_{CD28TM}$ on days 1 and 7 in presence of PAM (n=5 mice per treatment group). Second injection of TEGs was labeled with CTV. Mice were sacrificed at days 15-16 (stated as 15 for clarity). Tumor burden was measured by BLI (D), where statistical significances were calculated by a mixed-effects model, or number of GFP+ cells in bone marrow (E), significance was calculated using One Way ANOVA with Dunnet correction. P <0.05, **P < 0.01, ***P < 0,001, ****P < 0,0001 (F) Comparison between number of TEG-LM1 and TEG001 in blood, bone marrow and spleen. Significance was calculated using unpaired T test. P <0.05, **P < 0.01, ***P < 0,001, ****P < 0,0001. (G) Proliferation of TEG-LM1 and TEG001 in blood, bone marrow and spleen as measured by CTV MFI. Significance was calculated using unpaired T test. P <0.05, **P < 0.01, ***P < 0,001, ****P < 0,0001. (H) Comparison between number of TEG001, TEG001-NKG2D-CD28$_{WT}$ and TEG001-NKG2D-4-1BB$_{WT}$ in blood, bone marrow and spleen. Significance was calculated using One Way ANOVA with Bonferroni correction. P <0.05, **P < 0.01, ***P < 0,001, ****P < 0,0001 (I) proliferation of TEG001, TEG001-NKG2D-CD28$_{WT}$ and TEG001-NKG2D-4-1BB$_{WT}$ measured by CTV MFI decrease in blood, bone marrow and spleen. Significance was calculated using One Way ANOVA with Bonferroni correction. P <0.05, **P < 0.01, ***P < 0,001, ****P < 0,0001

Improved recognition of tumor organoids and increased proliferation by TEG001 cells co-expressing NKG2D-4-1BB$_{CD28TM}$

To further assess the power of engineered T cells we utilized 3D cell structures with tumor-derived organoids which have become valuable tools to investigate treatment responses [42]. Within this context we recently reported targeting of head and neck cancer derived organoids by TEG001 [43]. To assess whether TEG001 co-expression NKG2D-4-1BB$_{CD28TM}$ are also superior in this model, we used organoids derived from patients suffering from Head and Neck cancer (HN) and from other, difficult to treat, cancers such as hepatocellular carcinoma (HCC) and hepatoblastoma (HB). The expression of NKG2D ligands by the organoids was quantified by staining with an NKG2D-FC protein (Supplementary figure 4A). Co-expression of NKG2D-4-1BB$_{CD28TM}$ on TEG001 cells significantly increased IFNγ release against one of the recognized primary organoid cultures (Figure 5D). As we saw most profound effects of the NKG2D co-stimulation on proliferation, we next also labeled TEG001 with or without NKG2D-4-1BB$_{CD28TM}$ with CTV and measured T cell proliferation upon co-culture with four recognized and two non-recognized organoids (Figure 4E, Supplementary figure 4B). A significant increase in proliferation for TEG001 co-expressing NKG2D-4-1BB$_{CD28TM}$ compared to TEG001 against most of the organoids was observed, illustrated by a decrease in CTV signal. In conclusion, recognition of primary solid tumors by TEG001 can be improved by the addition of modulated NKG2D co-stimulation.
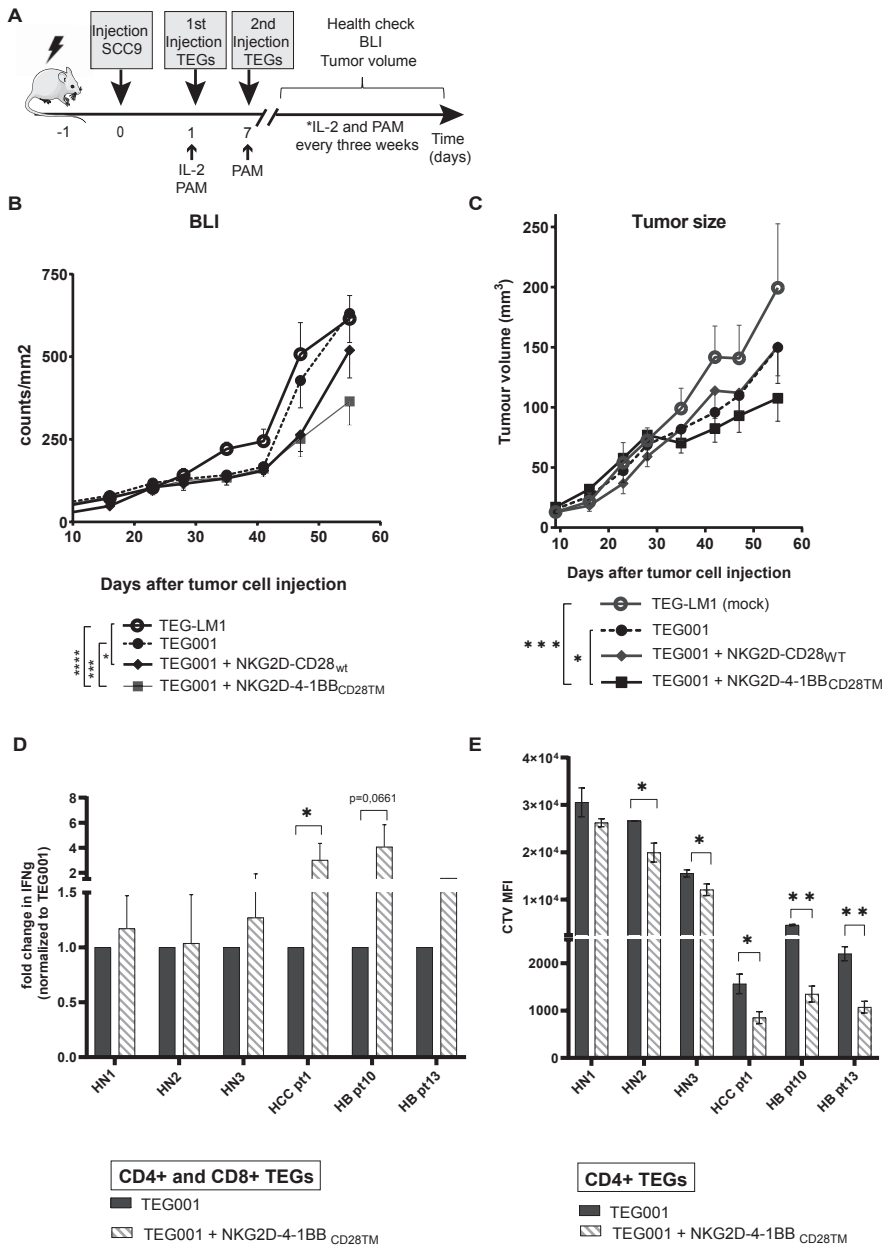
3

**Figure 5. In vivo therapeutic effects of TEGs co-expressing NKG2D chimeric co-receptors in head
and neck xenograft model.** (A) Schematic diagram of experimental setup to evaluate efficacy of TEGs
co-expressing NKG2D co-receptors against SCC9-luciferase tumor. NSG mice were irradiated and injected
s.c. with 0,5 x 10^6 SCC9 tumor cells. On days 1 and 7, mice were treated with 10^7 TEG-LM1 (mock) (n=12),
TEG001 (n=11), TEG001-NKG2D-CD28$_{WT}$ (n=11) or TEG-NKG2D-4-1BB$_{CD28TM}$ (n=11). Weekly BLI and bleeding

were performed, and IL2 and PAM were administered every three weeks. (D) BLI and (E) tumor volume were measured weekly to assess tumor outgrowth. Statistical significances were calculated by mixed-effects model with repeated measures. *P <0.05, **P < 0.01, ***P < 0,001, ****P < 0,0001. (C) Transduced CD4+ and CD8+ T cells were incubated with the different organoids with 30-60 µM PAM. After 18 hours, supernatants were harvested and analyzed for IFNγ secretion by ELISA. Data represent mean of fold change normalized to TEG001 ± SD. N=4 (HN-106T, HN-M20-400, HN-M21-0120, HCC pt1), N=2 (HB pt10) or N=1 (HB pt13). Significance was calculated using unpaired T test. P <0.05, **P < 0.01, ***P < 0,001, ****P < 0,0001. (D) Transduced CD4+ T cells were labeled with CTV and incubated with the different organoids as indicated, in presence of 100 µM PAM. On day 6 MFI was assessed by flow cytometry. Representative graphs of two independent experiments are shown. Data represent Cell Trace Violet MFI ± SD, significance was calculated using an unpaired T test.

Discussion

In this report we present a new strategy to further improve antitumor activity of TCR engineered immune cells, by combining cancer-metabolome targeting TEGs with stress-ligand sensing chimeric co-receptors, constructed by fusing the extracellular NKG2D domains to the hinge, transmembrane and signaling domains of different costimulatory proteins. Side by side comparison of different signaling domains for co-stimulation revealed that chimeric receptors based on CD28 or 4-1BB overcame suboptimal TCR engagement, enhanced TEG proliferation and serial killing *in vitro,* and resulted in superior tumor control in a 3D bone marrow model as well as *in vivo* in a multiple myeloma model. Both chimeras associated with different dynamics in vivo, but only 4-1BB-based co-stimulation led to improved tumor control in an *in vivo* solid tumor model.

It has been shown that co-expression of the 4-1BB receptor in αβTCR engineered αβ T cells led to improved antitumor activity [44]. Downside of this strategy however is the dependence on interaction with natural 4-1BB ligands, that are mainly expressed on professional antigen presenting cells, which could be overcome by our strategy, as NKG2D targets additional tumor-associated antigens expressed in 70-80% of all tumors. Expression of a PD1-CD28 chimeric receptor also enhanced activity of T cells transduced with a tumor reactive αβTCR [45], and most recently FAS-4-1BB fusion proteins have been shown to convert anergy- or death signals in αβTCR engineered T cells into pro-survival signals [36]. These studies however miss a direct comparison of different signaling domains within the context of the very same target alongside defined TCR signaling. Our direct comparison of different signaling domains within the context of identical TCR and ligands for the chimeric co-receptors, showed similar tumor control *in vivo* in a multiple myeloma model. However different dynamics were observed for TEGs co-expressing NKG2D-CD28$_{WT}$ and NKG2D-4-1BB$_{CD28TM}$ *in vivo* which has not been obvious in 3D models, emphasizing the need for different models to asses potency of engineered immune cells. TEGs co-expressing NKG2D-CD28$_{WT}$ showed a more rapid tumor control *in vitro* and *in vivo* but associated *in vivo* with partial loss of engineered immune cells. In contrast, TEG co-expressing NKG2D-4-1BB$_{CD28TM}$ exhibited not only enhanced

tumor control but also enhanced proliferation *in vivo,* resulting in a significantly better tumor control in both hematological as solid tumor models compared to TEG001. We also show that addition of the NKG2D chimeric co-receptors rescued suboptimal TCR-stimulation. Therefore, this strategy might be interesting to enhance recognition of tumors that have low TCR ligand density, not only for γδTCR, but also for αβTCR based strategies, as addition of these chimeras reduces the threshold of antigen density required for optimal activity.

Most studies dealing with co-stimulation do not analyze the functional impact of the co-stimulation seperately for different cell subsets. Within this context, our studies demonstrate that although the NKG2D-chimera's were expressed in both CD4+ and CD8+ TEGs, true functional impact of co-stimulation might primarily be important for engineered CD4+ T cells within the context of TCR stimulation. We cannot exclude that the expression of the natural NKG2D receptor in CD8+ TEG competed with the chimera, though addition of DAP10 was needed to harness the full potential of NKG2D in combination with CAR-T [46]. Improved CD4+ TEG function most likely provides help for CD8+TEG as shown for TEGs when using a CD8-dependent γδTCR [47], or when using class I restricted αβTCR [48].

In conclusion, our study provides strong *in vitro* and preclinical evidence that combining cancer-metabolome targeting TEGs with stress-ligand sensing chimeric co-receptors, in the form of NKG2D-CD28$_{wt}$ and NKG2D-4-1BB$_{CD28TM}$ co-receptors on TEGs, enhances antitumor activity for liquid tumors while preserving the safety profile, therefore making this concept also interesting for other TCR-based engineering concepts. However, both chimeric co-receptors acted mainly on CD4+ T cells and associated with different biology and dynamics *in vivo.* NKG2D-CD28$_{WT}$ chimera showed a more rapid liquid tumor control but also partial loss of engineered immune cells, while TEGs co-expressing NKG2D-4-1BB$_{CD28TM}$ displayed an improved control of both liquid and solid tumors *in vivo*, conjoined with an enhanced proliferation capacity despite cognate recognition of the tumor. Overall, this data implies that TEGs co-expressing NKG2D-4-1BB$_{CD28TM}$ would have an advantage during chronic antigen stimulation because of their proliferation capacity, and might therefore be an interesting candidate to treat patients with solid tumors

References

1. Sebestyen Z, Scheper W, Vyborova A, Gu S, Rychnavska Z, Schiffler M, et al. RhoB Mediates Phosphoantigen Recognition by Vγ9Vδ2 T Cell Receptor. Cell Rep. 2016;15(9):1973-85.

2. Rigau M, Ostrouska S, Fulford TS, Johnson DN, Woods K, Ruan Z, et al. Butyrophilin 2A1 is essential for phosphoantigen reactivity by gammadelta T cells. Science. 2020;367(6478).

3. Karunakaran MM, Willcox CR, Salim M, Paletta D, Fichtner AS, Noll A, et al. Butyrophilin-2A1 Directly Binds Germline-Encoded Regions of the Vgamma9Vdelta2 TCR and Is Essential for Phosphoantigen Sensing. Immunity. 2020;52(3):487-98 e6.

4. Gu S, Sachleben JR, Boughter CT, Nawrocka WI, Borowska MT, Tarrasch JT, et al. Phosphoantigen-induced conformational change of butyrophilin 3A1 (BTN3A1) and its implication on Vγ9Vδ2 T cell activation. Proc Natl Acad Sci U S A. 2017;114(35):E7311-e20.

5. Harly C, Guillaume Y, Nedellec S, Peigne CM, Monkkonen H, Monkkonen J, et al. Key implication of CD277/butyrophilin-3 (BTN3A) in cellular stress sensing by a major human gammadelta T-cell subset. Blood. 2012;120(11):2269-79.

6. Palakodeti A, Sandstrom A, Sundaresan L, Harly C, Nedellec S, Olive D, et al. The molecular basis for modulation of human Vgamma9Vdelta2 T cell responses by CD277/butyrophilin-3 (BTN3A)-specific antibodies. J Biol Chem. 2012;287(39):32780-90.

7. Sebestyen Z, Prinz I, Dechanet-Merville J, Silva-Santos B, Kuball J. Translating gammadelta (gammadelta) T cells and their receptors into cancer cell therapies. Nat Rev Drug Discov. 2020;19(3):169-84.

8. Vyborova A, Beringer DX, Fasci D, Karaiskaki F, van Diest E, Kramer L, et al. γ9δ2T cell diversity and the receptor interface with tumor cells. J Clin Invest. 2020;130(9):4637-51.

9. Gründer C, van Dorp S, Hol S, Drent E, Straetemans T, Heijhuurs S, et al. γ9 and δ2CDR3 domains regulate functional avidity of T cells harboring γ9δ2TCRs. Blood. 2012;120(26):5153-62.

10. Vyborova A, Janssen A, Gatti L, Karaiskaki F, Yonika A, van Dooremalen S, et al. γ9δ2 T-Cell Expansion and Phenotypic Profile Are Reflected in the CDR3δ Repertoire of Healthy Adults. Frontiers in Immunology. 2022;13.

11. van Diest E, Hernandez Lopez P, Meringa AD, Vyborova A, Karaiskaki F, Heijhuurs S, et al. Gamma delta TCR anti-CD3 bispecific molecules (GABs) as novel immunotherapeutic compounds. J Immunother Cancer. 2021;9(11).

12. Marcu-Malina V, Heijhuurs S, van Buuren M, Hartkamp L, Strand S, Sebestyen Z, et al. Redirecting alphabeta T cells against cancer cells by transfer of a broadly tumor-reactive gammadeltaT-cell receptor. Blood. 2011;118(1):50-9.

13. Straetemans T, Gründer C, Heijhuurs S, Hol S, Slaper-Cortenbach I, Bönig H, et al. Untouched GMP-Ready Purified Engineered Immune Cells to Treat Cancer. Clin Cancer Res. 2015;21(17):3957-68.

14. Majzner RG, Mackall CL. Clinical lessons learned from the first leg of the CAR T cell journey. Nat Med. 2019;25(9):1341-55.

15. Hartmann J, Schussler-Lenz M, Bondanza A, Buchholz CJ. Clinical development of CAR T cells-challenges and opportunities in translating innovative treatment concepts. EMBO Mol Med. 2017;9(9):1183-97.

16. Zhang E, Yang P, Gu J, Wu H, Chi X, Liu C, et al. Recombination of a dual-CAR-modified T lymphocyte to accurately eliminate pancreatic malignancy. J Hematol Oncol. 2018;11(1):102.

17. Sadelain M, Brentjens R, Rivière I. The basic principles of chimeric antigen receptor design. Cancer Discov. 2013;3(4):388-98.

18. Ruella M, Barrett DM, Kenderian SS, Shestova O, Hofmann TJ, Perazzelli J, et al. Dual CD19 and CD123 targeting prevents antigen-loss relapses after CD19-directed immunotherapies. J Clin Invest. 2016;126(10):3814-26.

19. Weinkove R, George P, Dasyam N, McLellan AD. Selecting costimulatory domains for chimeric antigen receptors: functional and clinical considerations. Clin Transl Immunology. 2019;8(5):e1049.

20. Liu H, Wang S, Xin J, Wang J, Yao C, Zhang Z. Role of NKG2D and its ligands in cancer immunotherapy. Am J Cancer Res. 2019;9(10):2064-78.

21. González S, López-Soto A, Suarez-Alvarez B, López-Vázquez A, López-Larrea C. NKG2D ligands: key targets of the immune response. Trends Immunol. 2008;29(8):397-403.

22. Baumeister SH, Murad J, Werner L, Daley H, Trebeden-Negre H, Gicobi JK, et al. Phase I Trial of Autologous CAR T Cells Targeting NKG2D Ligands in Patients with AML/MDS and Multiple Myeloma. Cancer Immunol Res. 2019;7(1):100-12.

23. Rincon-Orozco B, Kunzmann V, Wrobel P, Kabelitz D, Steinle A, Herrmann T. Activation of V gamma 9V delta 2 T cells by NKG2D. JImmunol. 2005;175(4):2144-51.

24. Orr MT, Lanier LL. Natural killer cell education and tolerance. Cell. 2010;142(6):847-56.

25. Huch M, Gehart H, van Boxtel R, Hamer K, Blokzijl F, Verstegen MM, et al. Long-term culture of genome-stable bipotent stem cells from adult human liver. Cell. 2015;160(1-2):299-312.

26. Driehuis E, Kretzschmar K, Clevers H. Establishment of patient-derived cancer organoids for drug-screening applications. Nat Protoc. 2020;15(10):3380-409.

27. Braham MVJ, Minnema MC, Aarts T, Sebestyen Z, Straetemans T, Vyborova A, et al. Cellular immunotherapy on primary multiple myeloma expanded in a 3D bone marrow niche model. Oncoimmunology. 2018;7(6):e1434465.

28. Fujiwara K, Tsunei A, Kusabuka H, Ogaki E, Tachibana M, Okada N. Hinge and Transmembrane Domains of Chimeric Antigen Receptor Regulate Receptor Expression and Signaling Threshold. Cells. 2020;9(5).

29. Xia A, Zhang Y, Xu J, Yin T, Lu XJ. T Cell Dysfunction in Cancer Immunity and Immunotherapy. Front Immunol. 2019;10:1719.

30. Vandenberghe P, Verwilghen J, Van Vaeck F, Ceuppens JL. Ligation of the CD5 or CD28 molecules on resting human T cells induces expression of the early activation antigen CD69 by a calcium- and tyrosine kinase-dependent mechanism. Immunology. 1993;78(2):210-7.

31. Vyborova A, Beringer DX, Fasci D, Karaiskaki F, van Diest E, Kramer L, et al. gamma9delta2T cell diversity and the receptor interface with tumor cells. J Clin Invest. 2020.

32. Johanna I, Straetemans T, Heijhuurs S, Aarts-Riemens T, Norell H, Bongiovanni L, et al. Evaluating in vivo efficacy - toxicity profile of TEG001 in humanized mice xenografts against primary human AML disease and healthy hematopoietic cells. J Immunother Cancer. 2019;7(1):69.

33. Kunzmann V, Bauer E, Feurle J, Weissinger F, Tony HP, Wilhelm M. Stimulation of gammadelta T cells by aminobisphosphonates and induction of antiplasma cell activity in multiple myeloma. Blood. 2000;96(2):384-92.

34. Luckman SP, Hughes DE, Coxon FP, Graham R, Russell G, Rogers MJ. Nitrogen-containing bisphosphonates inhibit the mevalonate pathway and prevent post-translational prenylation of GTP-binding proteins, including Ras. J Bone Miner Res. 1998;13(4):581-9.

35. Zhao Z, Condomines M, van der Stegen SJC, Perna F, Kloss CC, Gunset G, et al. Structural Design of Engineered Costimulation Determines Tumor Rejection Kinetics and Persistence of CAR T Cells. Cancer Cell. 2015;28(4):415-28.

36. Oda SK, Anderson KG, Ravikumar P, Bonson P, Garcia NM, Jenkins CM, et al. A Fas-4-1BB fusion protein converts a death to a pro-survival signal and enhances T cell therapy. J Exp Med. 2020;217(12).

37. Kuball J, Schmitz FW, Voss RH, Ferreira EA, Engel R, Guillaume P, et al. Cooperation of human tumor-reactive CD4+ and CD8+ T cells after redirection of their specificity by a high-affinity p53A2.1-specific TCR. Immunity. 2005;22(1):117-29.

38. Di Modugno F, Colosi C, Trono P, Antonacci G, Ruocco G, Nisticò P. 3D models in the new era of immune oncology: focus on T cells, CAF and ECM. J Exp Clin Cancer Res. 2019;38(1):117.

39. Tang H, Qiao J, Fu YX. Immunotherapy and tumor microenvironment. Cancer Lett. 2016;370(1):85-90.

40. Eagle RA, Jafferji I, Barrow AD. Beyond Stressed Self: Evidence for NKG2D Ligand Expression on Healthy Cells. Curr Immunol Rev. 2009;5(1):22-34.

41. Marofi F, Motavalli R, Safonov VA, Thangavelu L, Yumashev AV, Alexander M, et al. CAR T cells in solid tumors: challenges and opportunities. Stem Cell Res Ther. 2021;12(1):81.

42. Tuveson D, Clevers H. Cancer modeling meets human organoid technology. Science. 2019;364(6444):952-5.

3

43. Dekkers JF, Alieva M, Cleven A, Keramati F, Wezenaar AKL, van Vliet EJ, et al. Uncovering the mode of action of engineered T cells in patient cancer organoids. Nat Biotechnol. 2022.

44. Daniel-Meshulam I, Horovitz-Fried M, Cohen CJ. Enhanced antitumor activity mediated by human 4-1BB-engineered T cells. Int J Cancer. 2013;133(12):2903-13.

45. Ankri C, Shamalov K, Horovitz-Fried M, Mauer S, Cohen CJ. Human T cells engineered to express a programmed death 1/28 costimulatory retargeting molecule display enhanced antitumor activity. J Immunol. 2013;191(8):4121-9.

46. Li S, Zhao R, Zheng D, Qin L, Cui Y, Li Y, et al. DAP10 integration in CAR-T cells enhances the killing of heterogeneous tumors by harnessing endogenous NKG2D. Mol Ther Oncolytics. 2022;26:15-26.

47. Johanna I, Hernández-López P, Heijhuurs S, Scheper W, Bongiovanni L, de Bruin A, et al. Adding Help to an HLA-A*24:02 Tumor-Reactive γδTCR Increases Tumor Control. Front Immunol. 2021;12:752699.

48. Willemsen R, Ronteltap C, Heuveling M, Debets R, Bolhuis R. Redirecting human CD4+ T lymphocytes to the MHC class I-restricted melanoma antigen MAGE-A1 by TCR alphabeta gene transfer requires CD8alpha. Gene Ther. 2005;12(2):140-6.

Acknowledgements

Funding

Competing interests

JK is shareholder of Gadeta. JK, ZS, EvD, and DB are inventors on patents

Supplementary Figures
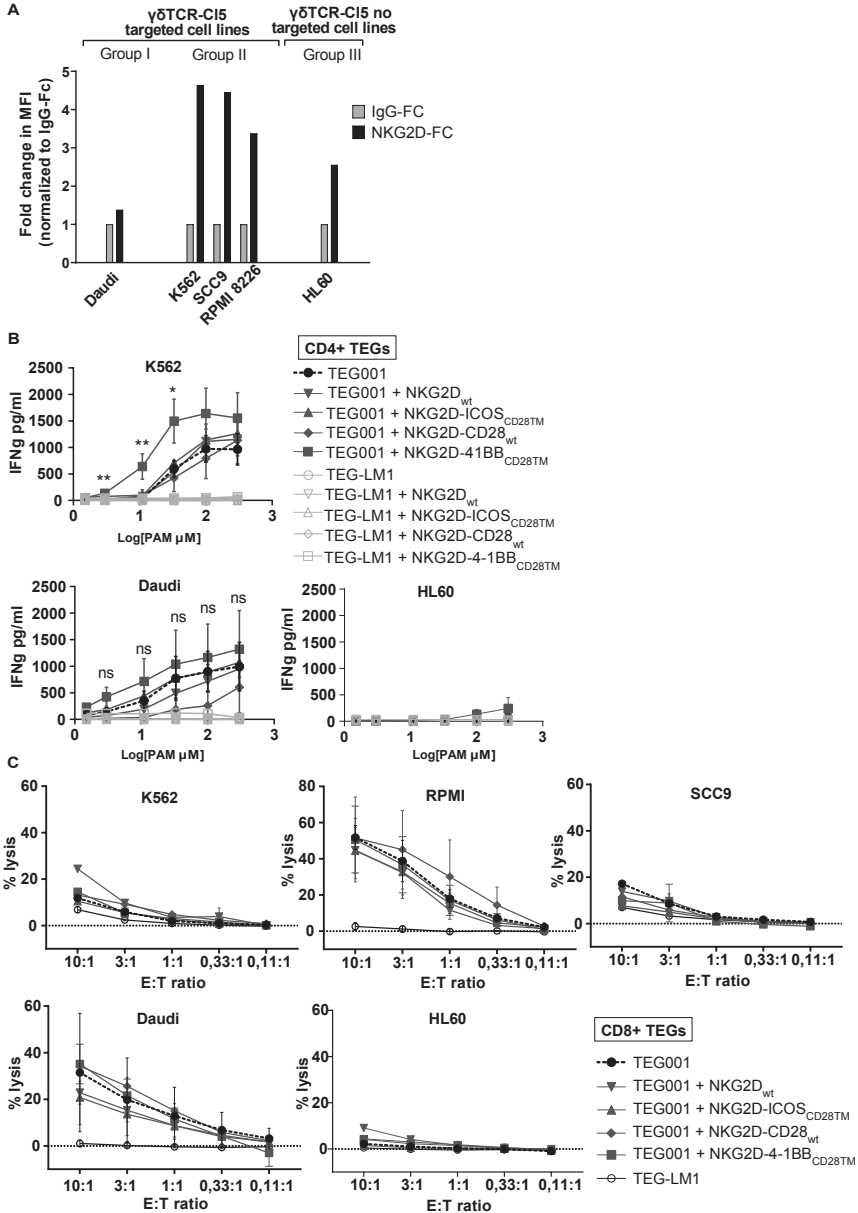
Supplementary Figure 1. Introduction of NKG2D-4-1BB chimeric co-receptor increases TEG001 IFNγ release in response to tumor cells expressing NKG2D ligands, but does not impact short term killing. (A) Surface expression of NKG2D ligands in TEG001 targeted (K562, SCC9, RPMI 8226 and Daudi) or not targeted (HL60) tumor cells. MFI was measured by flow cytometry using NKG2D-Fc and a

IgG-Fc fusion proteins. Fold change was calculated per type of cells as MFI measured using NKG2D-Fc relative to IgG-Fc condition. (B) Transduced CD4+ T cells were incubated with K562, Daudi or HL60 at several pamidronate concentrations. After 18 hours, supernatants were harvested and analyzed for IFNγ secretion by ELISA. N=3. Data represent mean ± SD, significance was calculated using Two Way ANOVA with Dunnet correction. Differences between T cells expressing only γδ-TCR-Cl5 or in combination with NKG2D receptors are indicated as *P <0.05, **P < 0.01. (C) Transduced CD8+ (75%) T cells were tested against K562, RPMI 8226, SCC9, Daudi and HL60 in a ^{51}Cr-release assay (E:T, 10:1, 3:1, 1:1, 0,33:1, 0,11:1). ^{51}Cr-release was measured in the supernatant after 5 hours. Specific lysis was calculated using the formula (experimental cpm - basal cpm)/(maximal cpm - basal cpm) x100 with maximal lysis determined in the presence of 5% triton and basal lysis in the absence of effector cells. N=2 for K562, SCC9 and HL60, N=1 with technical duplicates. Data represent mean ± SD, significance was calculated using Two Way ANOVA with Dunnet correction for the N=2 samples.
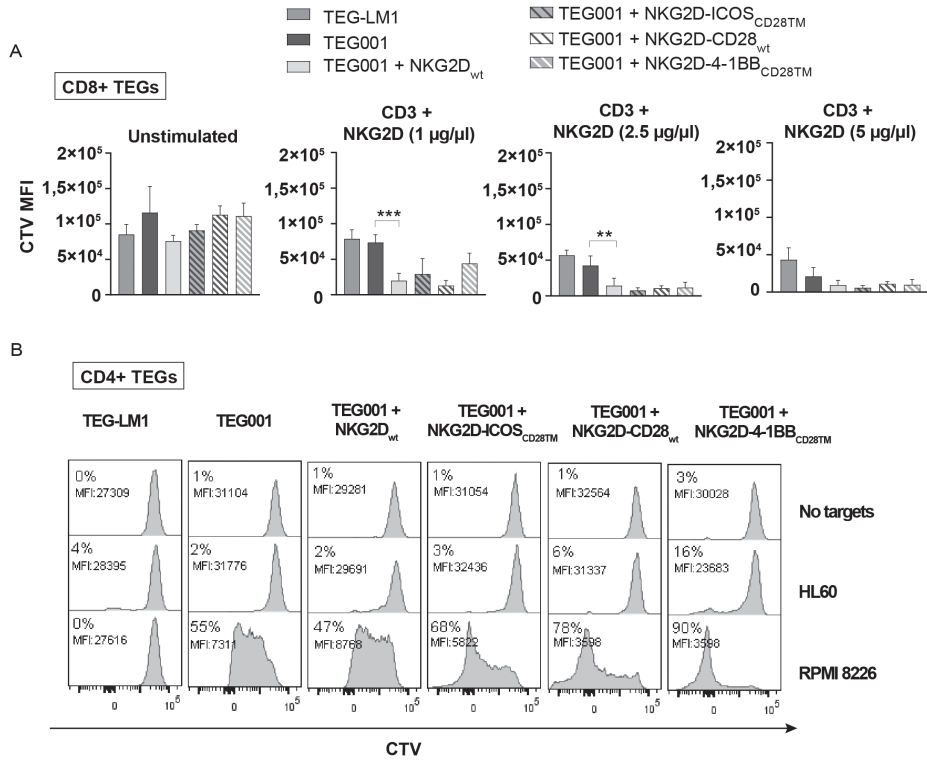
Supplementary Figure 2. In vitro assessment of TEGs. (A) CD8+ transduced T cells were labeled with CTV and stimulated with CD3 and NKG2D antibodies during six days. On day 6 MFI was assessed by flow cytometry. N=2. Data represent Cell Trace violet (CTV) MFI ± SD, significance was calculated using One Way ANOVA with Holm-sidak.. (B) CD4+ transduced cells were labeled using CTV and co-cultured with HL60 or RPMI 8226 tumor cells. On day 6, proliferation was assessed by flow cytometry. Histogram data shows CTV intensity and percentage of proliferating cells, taking LM1 without targets as control for gating
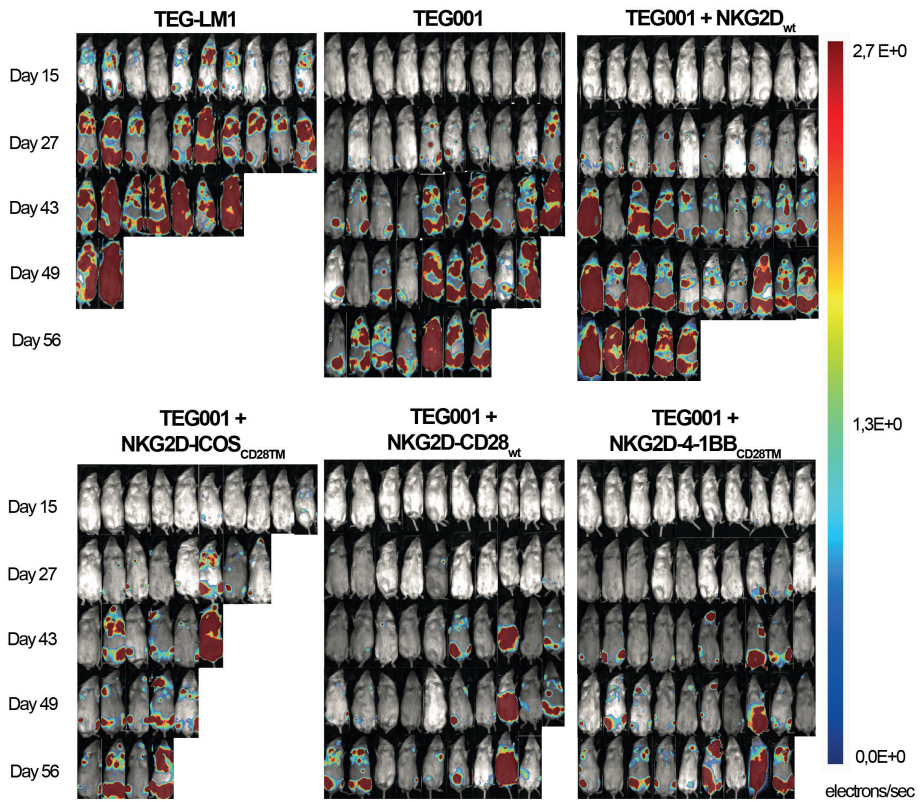
Supplementary Figure 3. *In vivo* **monitoring of tumor growth by BLI in multiple myeloma xenograft.** (A) RPMI 8226-luciferase tumor growth in NSG mice treated with different TEGs. Pictures show BLI signal of all the mice on days 15, 27, 43, 49, 56.
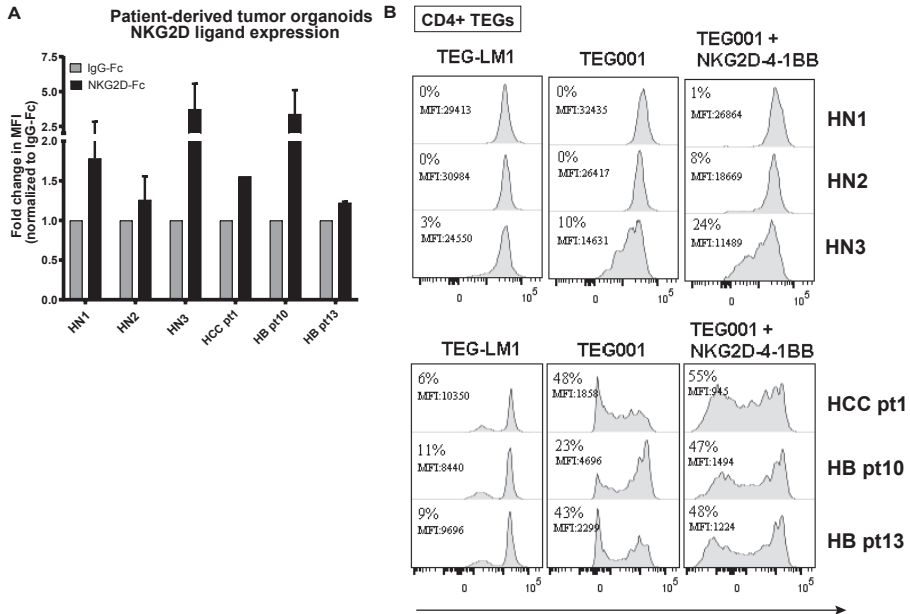
Supplementary Figure 4. *In vitro* **recognition of patient-derived tumor organoids by TEGs.** (**A**) Surface expression of NKG2D ligands in patient-derived liver and head neck tumor organoids. MFI was measured by flow cytometry using NKG2D-Fc and a IgG-Fc fusion proteins. Data represent mean of NKG2D-Fc staining relative to IgG-Fc condition ± SD. N=2 for all organoids but HCC pt1 (N=1) **(B)** CD4+ transduced cells were labeled using CTV and co-cultured with patient-derived liver and head and neck tumor organoids in presence of 100 μM PAM. On day 6, proliferation was assessed by flow cytometry. Histogram data shows CTV intensity and percentage of proliferating cells, taking LM1 without targets as control for gating.

3

CHAPTER 4

Gamma delta TCR Anti-CD3 Bispecific molecules (GABs) as novel immunotherapeutic compounds

Eline van Diest[1,*], Patricia Hernández López[1,*] Angelo Meringa[1],
Anna Vyborova[1], Effrosyni Karaiskaki[1], Sabine Heijhuurs[1], Jan Gumathi Bormin[1],
Sanne van Dooremalen[1], Mara J.T. Nicolasen[1], Lucrezia Gatti[1], Inez Johanna[1],
Trudy Straetemans[1], Zsolt Sebestyén[1], Dennis X. Beringer[1,#] and Jürgen Kuball[1,2, #]

[1] Center for Translational Immunology, University Medical Center Utrecht,
Utrecht University, 3584 CX Utrecht, The Netherlands
[2] Department of Hematology, University Medical Center Utrecht, Utrecht University,
3584 CX Utrecht, The Netherlands

* EvD and PHL contributed equally
# Shared senior authors

Abstract

Background: γ9δ2 T cells hold great promise as cancer therapeutics because of their unique capability of reacting to metabolic changes with tumor cells. However, it has proven very difficult to translate this promise into clinical success.

Methods: In order to better utilize the tumor reactivity of γ9δ2T cells and combine this with the great potential of T cell engager molecules, we developed a novel bispecific molecule by linking the extracellular domains of tumor-reactive γ9δ2TCRs to a CD3-binding moiety, creating gamma delta TCR anti-CD3 bispecific molecules (GABs). GABs were tested *in vitro* and *in vivo* for ability to redirect T lymphocytes to a variety of tumor cell lines and primary patient material.

Results: GABs utilizing naturally occurring high affinity γ9δ2TCRs efficiently induced αβT cell mediated phosphoantigen-dependent recognition of tumor cells. Reactivity was substantially modulated by variations in the Vδ2 CDR3-region and the BTN2A1-binding HV4-region between CDR2 and CDR3 of the γ-chain was crucial for functionality. GABs redirected αβT cells against a broad range of hematopoietic and solid tumor cell lines and primary acute myeloid leukemia. Furthermore, they enhanced infiltration of immune cells in a 3D bone marrow niche and left healthy tissues intact, while eradicating primary multiple myeloma cells. Lastly, GABs constructed from natural high affinity γ9δ2TCR sequences significantly reduced tumor growth in vivo in a subcutaneous myeloma xenograft model.

Conclusions: We conclude that GABs allow for the introduction of metabolic targeting of cancer cells to the field of T cell engagers.

Introduction

Among all immunological subtypes, γδT cells stand out in an unbiased computational analysis for their association with improved overall survival of patients with many different tumor types [1]. γδT cells are innate like T cells that are present in both blood and tissue, and are known to be important for recognition of foreign pathogens, stress signatures of infected cells, and of cancer cells [2]. *In vitro*, γδT cells display very potent and broad tumor recognition; they can target and lyse cancer cells of both hematological and solid origin [3, 4]. In contrast to αβT cells, γδT cells do not rely on HLA for target cell recognition [5]. γ9δ2 T cells, a γδ subset mainly present in the blood, are known to recognize an increase in intracellular phosphoantigens (pAg), which can be caused by microbial infections but are also found in many cancers [6]. Recognition of intracellular pAg levels by γ9δ2 TCRs relies on an inside out mechanism involving RhoB, BTN3A1, and BTN2A1 [7-11]. The metabolic targeting of tumor cells by γ9δ2 cells paves the way for novel tumor antigens for immunotherapy [12]. Unfortunately, the adoptive transfer of *ex vivo* expanded polyclonal γδT cells associates so far with few clinical responses [13], most likely because of a significantly underestimated diversity, and many mechanisms of tolerance in advanced cancer patients that act against this particular immune subset [12, 14]. Most recently, restoring the αβ / γ9δ2 T cell balance by BTN3A1 blocking antibodies has been suggested to hold great therapeutic promise as a new checkpoint inhibitor [15]; but only a fraction of tumors is infiltrated by γ9δ2 T cells [1]. T cells engineered to express a defined γδTCR (TEGs) have been proposed as an alternative strategy [11, 16-24] in line with the development of chimeric antigen receptor transduced T cells (CAR-T) [25, 26]. However, advanced therapy medicinal products (ATMPs) such as genetically engineered T cells are delivered to patients with a substantial price tag [27], and production processes, as well as clinical implementation are cumbersome [28].

To avoid the practical and economic challenges of ATMPs while still utilizing the immune system to attack cancer, an alternative strategy is currently employed for classical antigens like CD19. Bispecific antibodies (bsAb) have been developed, fusing a tumor-targeting domain to a T cell binding domain, to recruit cytotoxic T cells to tumors. Such a bispecific T cell engager (BiTE) combining an anti-CD19 and anti-CD3 domain is now used in daily clinical practice [29], and many other bsAb for cancer immunotherapy are in various phases of clinical development[30]. The selection of suitable tumor-associated target antigens for these novel therapies, however, remains very challenging, currently limiting the broad application of CAR-T and bsAb therapy [31].

An alternative T cell engager strategy arose by linking the extracellular domain of an αβTCR as a tumor antigen binding domain to a single chain variable fragment (scFv) of a CD3 antibody [32]. These αβTCR-bispecifics recognize intracellular

peptides presented by MHC molecules, creating the possibility of targeting novel tumor-specific antigens that are not expressed at the cell surface. HLA restriction, however, also limits the use of such αβTCR-bispecifics to tumors with high mutational loads and defined HLA-types. Furthermore, down-regulation of HLA is observed as an immune-escape mechanism in approximately 40 to 90% of all human tumors [33], thereby greatly limiting the applicability of therapies based on αβTCR mediated tumor recognition.

To overcome these limitations and to combine the tumor specificity and therapeutic potential of γδT cells with the recent success of T cell engagers, we fused the extracellular domain of a γ9δ2TCR to an anti-CD3 scFv. We demonstrate that these **G**dTCR **A**nti-CD3 **B**ispecific molecules (GABs) with natural high affinity γ9δ2TCR can mimic the rather complex more pattern-like mode of action mediated by a γ9δ2TCR [7, 8, 34] without the need of additional affinity maturation. GABs efficiently redirect αβT cells towards several tumor cell lines of both hematologic and solid origin, as well as primary patient material *in vitro*. Furthermore, we show significant reduction of tumor growth after GAB treatment in a subcutaneous myeloma xenograft model. We conclude that GABs open an avenue towards metabolic cancer targeting tumors with a bispecific format.

Material and Methods

Generation of Bispecific constructs

A customized pcDNA3-NEO vector, which allows consecutive expression of two genes of interest under their own CMV promoter, was a kind gift of Jan Meeldijk (LTI protein facility, UMC Utrecht, The Netherlands). First the antiCD3-scFv (OKT3) [35] gene was cloned into multiple cloning site one. In addition to the antiCD3-scFv gene, the DNA fragment also contained bases encoding, a $(G_4S)_3$ flexible linker at the 5' end and poly histidine tag on the 3' end. At the 5' end of the flexible linker a BsiWI restriction site was present for the subsequent introduction of the TCR gamma chain in the vector, resulting in the TCR gamma-CD3scFv fusion gene. The TCR delta chain was cloned into the second multiple cloning site. TCR domain boundaries were used as in Allison et al. [36]. Most γ9 and δ2 TCR sequences were reported previously [11, 24, 36], while other γδTCR sequences were obtained from randomly picked clones (Table 1).

Expression and purification of Bispecifics

His-tagged GABs were expressed in 293 F cells. 293 F cells were cultured in Gibco Freestyle Expression medium, as transfection reagent Polyethylenimine (PEI) (25 kDa linear PEI, Polysciences, Germany) was used. Transfection was done using 293 F cells at a density of 1.10^6 cells/ml mixed with 1.25 μg DNA and 3.75 μg PEI per

million cells. DNA and PEI were pre-mixed in freestyle medium (1/30 of transfection volume), incubated for 20 minutes, and added dropwise to the cell cultures. The cultures were maintained shaking at 37 °C 5% CO_2. Cell culture supernatant was harvested after 5 days and filtered through a 0.22 µm filter top (Milipore, United States). Supernatant was adjusted to 25 mM Tris (Sigma Aldrich, Germany), 150 mM NaCl (Sigma Aldrich, Germany) and 15 mM Imidazole (Merck, Germany) (pH 8). Supernatant was loaded on a 1 ml HisTrap FF column (GE healthcare, United States) using the ÄKTA start purification system (GE healthcare, United States). Column was washed with IMAC loading buffer (25 mM Tris,150 mM Nacl 15 mM Imidazole (pH 8), and protein was eluted using a linear imidazole gradient from 21 to 300 mM in 20 CV. Fractions containing the GAB were pooled, concentrated and buffer exchanged to TBS (25 mM tris, 150 mM NaCl, pH 8) using vivaspin 4 10 kD spin columns (Sartorius, Germany). Protein was diluted 100 times in IEX loading buffer (25 mM Tris pH 8), and loaded onto a HiTrap Q HP 1 ml column (GE healthcare, United states) using the ÄKTA start purification system, for a second purification step. Column was washed with 10 column volumes IEX loading buffer, and protein was eluted using a linear NaCl gradient form 50 to 300 mM in 25 CV. Fractions containing the GAB were pooled, concentrated using vivaspin 4 10 kD spin columns (Sartorius, Germany) and examined by SDS-PAGE and staining with Instant blue protein stain (Sigma Aldrich, Germany). Protein concentration was measured by absorbance on Nanodrop and corrected for the Extinction coefficients. Protein was snap frozen and stored at -80°C and thawed before use.

Cell lines, Flow cytometry, IFNy Elispot, CD107 degranulation assay, luciferase based cytotoxicity and the animal model are reported in supplementary methods.

In vitro **bone-marrow model**

The 3D model was previously described in detail [20]. In short: primary CD138+ were selected from the mononuclear cells (MNCs) of myeloma bone marrow from two patients by MACS separation using microbeads (Miltenyi Biotec, Germany). The CD138+ cells and the RPMI 8226 tumor cells were stained with Vybrant DiO (Thermo Fisher, United States) and seeded in Matrigel (Corning, United States) together with multipotent mesenchymal stromal cells (MSCs) and endothelial progenitor cells (EPCs), both stained with Vybrant DiD (Thermo Fisher, United States). After four days, T cells were stained with Vybrant DiI (Thermo Fisher, United States) and administered to the model together with CL5 or LM1 GAB (30 µg/ml) and 10 µM PAM (Calbiochem, United States). One day later the culture medium was refreshed with medium containg 30 µg/ml GAB. Tumor-, T - and stromal cells within and surrounding the matrigel were visualized two days later by confocal imaging. Afterwards, the Matrigel was dissolved using Dispase (Corning, United States) to retrieve the cells from the model. The cells were quantified by FACS using Flow count Fluorospheres (Beckman Coulter, United States), and normalized to mock treatment.

Results

Production of highly pure GABs

In line with the observation that not only antibodies but also high affinity αβTCR can be linked to anti-CD3scFvs to redirect T cells to tumor cells [32], we assessed whether the γ9δ2TCR CL5 (Table 1) was able to mediate anti-tumor reactivity in a bispecific format. **G**dTCR **A**nti-CD3 **B**ispecific molecule**s** (GABs) were cloned with an anti-CD3scFv derived from the anti-CD3ε antibody OKT3 linked to the C terminus of the gamma chain of a soluble γ9δ2TCR, using a flexible $(G_4S)_3$ linker (Figure 1A).

Table 1 GAB sequences. Depicted are sequences used for generation of GABs

GAB	REF	CDR3δ	CDR3γ
CL5	24	CACDALKRTDTDKLIF	CALWEIQELGKKIKVF
6_2	this report	CACDTLPGAGGADKLIF	CALWEVQELGKKIKVF
CL13	24	CACVPLLADTDKLIF	CALWEVIELGKKIKVF
G115	36	CACDTLGMGGEYTDKLIF	CALWEAQQELGKKIKVF
AJ8	this report	CACDTAGGSWDTRQMFF	CALWEAQQELGKKIKVF
A1	11	CACDTLLLLGDSSDKLIF	CALWEAQQELGKKIKVF
A3	11	CACDAWGHTDKLIF	CALWEAQQELGKKIKVF
A4	11	CACDALGDTGSDKLIF	CALWEAQQELGKKIKVF
C1	11	CACDPVPSIHDTDKLIF	CALWEAQQELGKKIKVF
C3	11	CACDTVSGGYQYTDKLIF	CALWEAQQELGKKIKVF
C4	11	CACDTLALGDTDKLIF	CALWEAQQELGKKIKVF
C5	11	CACDLLAPGDTSFTDKLIF	CALWEAQQELGKKIKVF
C7	11	CACDMGDASSWDTRQMFF	CALWEAQQELGKKIKVF
LM1	24	CACDTLLATDKLIF	CALWEAQQELGKKIKVF
DLC4	46	CACDPAILGDELSWDTRQMFF	CALWEVRQELGKKIKVF
MOP	38	CACDPVVLGDTGYTDKLIF	CALKELGKKIKVF
RIG1	9	CACDPVQVTGGYKVDKLIF	CALWEVHELGKKIKVF
RIG6	9	CACDPLIGSERLGDTGIDKLIF	CALWESQELGKKIKVF
DGSF68	45	CACDTVAHGGGTDKLIF	CALWEVGELGKKIKVF

CL5 GAB was expressed in mammalian freestyle 293F cells as secreted protein, and purified from the culture supernatant using His-tag purification, followed by a second ion exchange purification step, to ensure a highly pure protein product. As expected, the two different chains of the GAB, ectoGamma-CD3scFv and ectoDelta, were both clearly visible on gel (Figure 1B). This indicates that during expression, the two separate chains of the GAB associate properly, resulting in a heterodimeric bispecific molecule.

GABs bind to αβT cells

To further address proper folding of GABs, we employed a flow cytometry based analysis. αβT cells were incubated with CL5 GAB, followed by a secondary staining using fluorochrome labeled antibodies against Vδ2, Vγ9 or panγδ-TCR (Figure 1C). A strong and specific staining could by observed with all three antibodies, further indicating that the CD3scFv and both TCR chains are properly associated and folded. Following GAB binding on the cell surface of T lymphocytes that were coated with CL5 GAB over time, shows GAB binding up to four days after initial binding to CD3 (Figure 1D), with a declining signal after 2 days implying, as for other bispecific molecules [37], that continuous presence of the molecule will be needed to maintain efficacy.

4
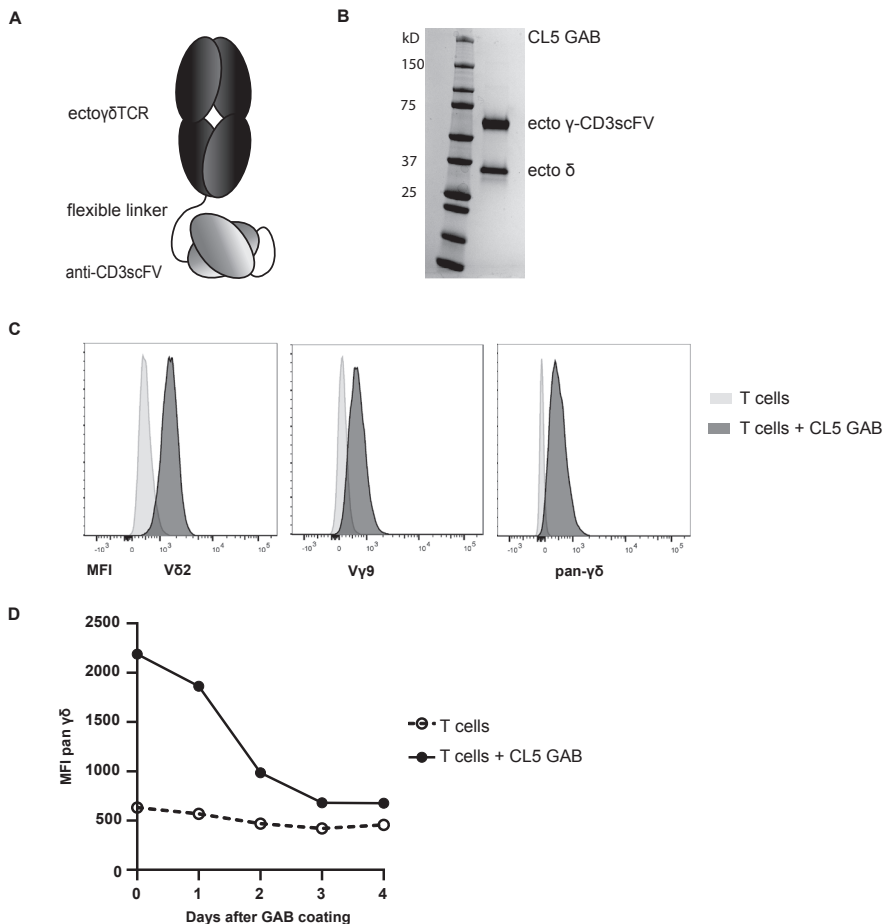
Figure 1. GAB design and binding to CD3+T cells. (A) Schematic representation of the GAB design, showing the extracellular γδTCR domain linked to an anti-CD3 scFv via a flexible linker. (B) Purified GAB was run on SDS-page gel and stained with Coomassie brilliant blue protein stain, visualizing the ectoγ-CD3scFv and ectoδ-chain. (C,D) Coating of αβT cells with GAB (10 μg/mL (C) or 90 μg/mL (D)), followed by staining with fluorochrome labeled anti-Vγ9, Vδ2 or pan γδ antibodies. MFI was measured by flow cytometry and represented in histograms. GAB, gamma delta TCR anti-CD3 bispecific molecules

GABs induce pAg-dependent tumor recognition by αβT cells which is influenced by variations in the Vδ2 TCR chain

γ9δ2T cells are known to recognize SCC9 cells, a squamous cell carcinoma cell line. This recognition can be enhanced by treating tumor cells with pamidronate (PAM), which causes an increase in the intracellular phosphoantigen (pAg) levels by inhibiting the mevalonate pathway [24]. To test whether GABs can also induce recognition of this cell line, αβT cells and SCC9 target cells were co-incubated with and without PAM, and CL5 or LM1 GAB. LM1 GAB was generated to serve as negative control, LM1 GAB harbors a γ9δ2 TCR where the CDR3 region of the δ chain is replaced by a single alanine, making the γ9δ2 TCR non-functional.[24] As anticipated, CL5 - but not LM1 GAB, induced recognition of SCC9 target cells by αβT cell in the presence of PAM (Figure 2A), suggesting that the mode of recognition by GABs is comparable to recognition mediated by γ9δ2TCRs expressed at a cell membrane [11]. We [11, 24] and others [38-40] reported on the impact of changes in the CDR3 region of δ2TCR chains on TCR function. To assess the impact of variations in the CDR3 region of the δ2TCR chain on GAB activity, we generated a larger panel of GABs, derived from previously published γ9δ2TCRs [11, 24, 36] and randomly picked γ9δ2T cell clones, varying in CDR3 δ-chain (Table 1). To assess activity, the different GABs were co-incubated with αβT cells and SCC9 target cells in the presence of PAM. Most GABs efficiently induced an IFNγ response, though activity substantially differed between different constructs (Figure 2B), although all showed similar binding to αβ T cells (Figure S1). GABs in which the CDR3δ was reduced to one alanine (LM1) did not induce IFNγ production at any concentration (Figure 2B). Titrating GAB concentrations allowed for further analysis of the differences in efficacy between the different CDR3δ sequences. We observed large differences in GAB activity with an EC_{50} of 0.8 μg/ml for the best performing GAB to an EC_{50} of 25 μg/ml for the lowest activity. EC_{50} of several non- or very low active receptors could not formally be assessed (Figure 2B and Table 2).
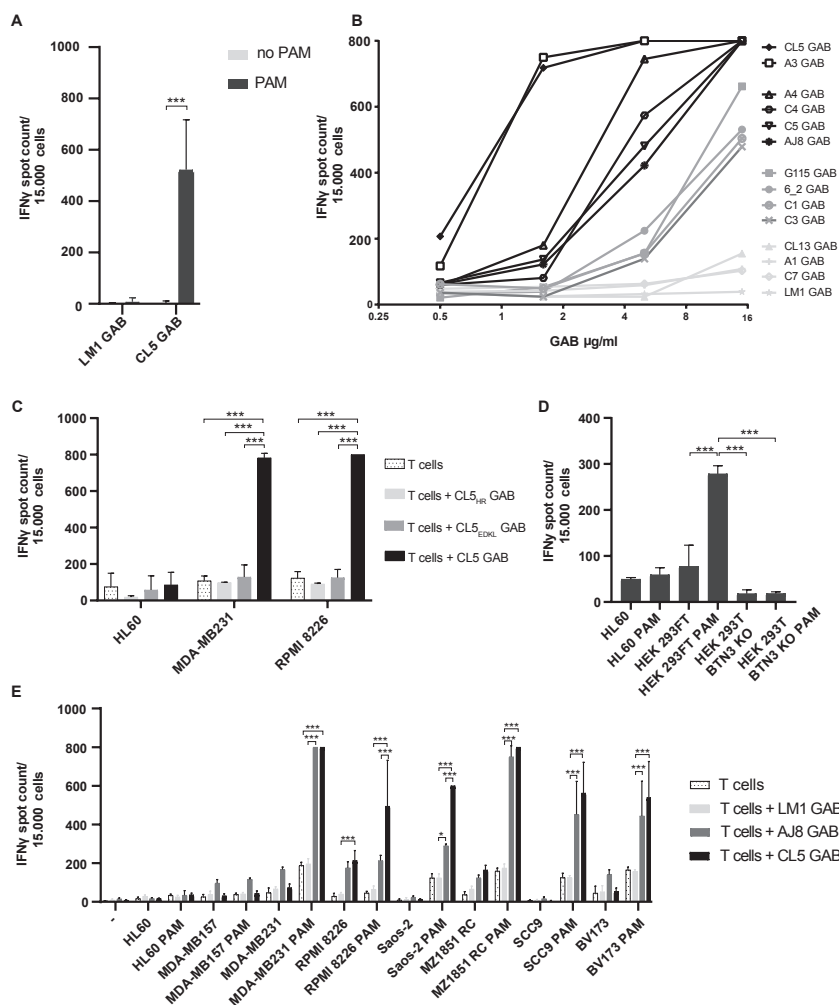
Figure 2. GABs induce pAg dependent tumor recognition by αβT cells. (A–E) IFNγ production was measured by elispot, if separate spots could not be distinguished, spot count was set to a maximum value of 800. (A) αβT cells were co-incubated with SCC9 target cells in the presence or absence of PAM (100 μM) and LM1 or CL5 GAB (10 ug/mL), values are corrected for T cells only (n=4). (B) T cells were incubated with SCC9 target cells, PAM (100 μM) and an increasing concentration of GABs derived from different Vγ9Vδ2TCRs. A representative experiment is shown. (C) γ-chain HV4 mutations shown to hamper TCR binding were tested in the GAB format, αβT cells and target cells were co-incubated with the wildtype or mutant GABs (10 μg/mL) and PAM (100 μM) n=2. (D) AJ8 GAB (10 μg/mL) was co-cultured with T lymphocytes, HL60, HEK293FT WT or BTN3A1 knockout cells with and without PAM (100 μM) n=1 in duplo. (E) CL5 and AJ8 GAB (10 μg/mL) were tested in a coculture of T cells and a larger panel of target cell lines with and without the addition of PAM (100 μM), and compared with mock GAB LM1 n=2. Error bars represent SD, significance was calculated using a multiple T test (A) or one-way ANOVA (C–E). * P<0.05,**p<0.001, ***p<0.0001. ANOVA, analysis of variance; GAB, gamma delta TCR anti-CD3 bispecific molecules; PAM, pamidronate.

Table 2 EC50 of GAB for IFNγ release. EC50 of GABs was calculated from Figure 2A. n.d. not determined.

GAB	EC$_{50}$ (µg/ml)	Confidence interval (µg/ml)	R^2
CL5	0.7524	0.6285 to 0.9086	0.9956
A3	0.8344	0.7055 to 0.9888	0.9637
A4	2.417	2.038 to 2.882	0.9851
C4	3.528	2.934 to 4.198	0.9916
C5	4.028	3.304 to 4.818	0.9801
AJ8	4.586	3.816 to 5.444	0.9777
G115	8.537	7.127 to 10.23	0.9923
6_2	9.811	7.777 to 12.17	0.9267
C1	11.46	9.356 to 13.81	0.9471
C3	12.30	10.14 to 14.74	0.9740
CL13	27.70	21.50 to 42.50	0.9301
A1	n.d.	n.d.	n.d.
C7	n.d.	n.d.	n.d.
LM1	n.d.	n.d.	n.d.

γ-TCR loop and BTN3A are critical for GAB mediated αβT cell activation

The HV4 region between the CDR2 and the CDR3 of the γ-chain is critical for γ9δ2TCR activity by binding to BTN2A1 expressed on target cells [9-11]. To assess whether GABs also depend on this mode of action, we focused on GAB CL5, one of the most active TCR sequences from the tested panel, and introduced two mutations in the γHV4 region of CL5 GAB (E$_{70}$D$_{72}$→K$_{70}$L$_{72}$ (CL5$_{EDKL}$GAB) and H$_{85}$→R$_{85}$ (CL5$_{HR}$GABs)), reported to cause loss of activity in membrane expressed γ9δ2TCRs [41]. CL5, CL5$_{EDKL}$ and CL5$_{HR}$ GABs were added to a co-culture of αβT cells with the well-described breast cancer cell line (MDA-MB231) or multiple myeloma cell line (RPMI 8226) [11, 24] in the presence of PAM. CL5$_{EDKL}$ and CL5$_{HR}$ GAB lost activity, assessed by IFNγ production, when compared to the wild type CL5 GAB (Figure 2C), highlighting the importance of the γHV4 region for target cell engagement by GABs.

BTN3A has also been recognized as a crucial factor in phosphoantigen dependent γ9δ2TCR reactivity. Loss of BTN3A membrane expression on target cell leads to a complete loss of membrane-bound γ9δ2TCR reactivity to pAgs [11, 42]. By testing GAB mediated recognition of HEK293FT WT and BTN3A knock-out, we confirmed that GAB induced recognition after PAM treatment also depends on BTN3A expression (Figure 2D). These findings support the assumption that there is a similar binding mode between membrane-expressed γ9δ2TCRs and GABs, both depending on encounter of BTN2A1 through the γ-chain and a second signal, which is pAg and BTN3A depended.

GABs retarget αβT cells to a wide variety of tumor cells

Next, we addressed whether GABs can redirect αβT cells to a broader variety of tumor cells, and whether GABs with different EC_{50} against SCC9 target cells also have different activities against a broader range of hematological and solid tumor cells. GABs with lower (AJ8) and higher (CL5) EC_{50} or the negative control LM1 GAB were co-incubated with αβT cells, and previously defined panel of tumors targets cells [43]. A significant increase in IFNγ production was observed for CL5 and AJ8 GABs against most tumor targets except for HL60 and MDA-MB157, while LM1 GAB did not induce cytokine secretion (Figure 2E). For most cell lines, CL5 GAB had a slightly higher activity compared to AJ8 GAB, although not always significant. Isolated CD4+ and CD8+ αβT cells induced IFNγ release after co-incubation with CL5 GAB (Figure S2A). However, as expected we observed that the relative contribution of CD4+ and CD8+ αβT cells differed between donors and target cells, with CD4+ αβT cells producing more cytokines in general.

As in blood up to 5% of the CD3+ T lymphocytes are comprised of Vδ2+ T cells, we next investigated GAB activity in combination with Vδ2+ and αβT cells side by side. Vδ2+ and αβT cells were isolated from a healthy donor and IFNγ release was measured after a co-culture with two recognized (RPMI8226, SCC9) and one unrecognized cell line (ML-1) with and without CL5 GAB and in the absence or presence of PAM (Figure S2B). LM1 GAB was added as extra control to the Vδ2+ T cells. As expected, the Vδ2+ T cells alone recognized the positive target cell lines after PAM treatment, surprisingly however this recognition was lower compared to αβT cells co-incubated with CL5 GAB. Activity of Vδ2+ T cells was not blocked by the addition of the mock LM1 GAB, and addition of GAB CL5 did not lead to a further increase in activation of the Vδ2+ T cells. These data imply that GABs will most likely not activate Vδ2+ T cells, which could be a consequence of the differences in CD3 composition of Vδ2+ T cells versus αβT cells [44]. This is also in line with the previous observation that Vδ2+T cell expansion protocols usually do not use CD3 engagers, but rather rely on agents that directly engage the TCR, such as phytohaemagglutinin (PHA) [4, 43].

To this point, IFNγ production was used as a read out for GAB activity. However, the clinical activity of bispecific molecules comes through their ability to mediate killing of target cells. Therefore, as the next step, we assessed CD8+ αβT cell-mediated toxicity by utilizing a degranulation assay detecting surface expression of the lysosomal-associate membrane glycoptrotein-1 (LAMP-1/CD107a) by FACS. αβT cells were co-cultured with three different target cell lines and CL5, AJ8 or negative control LM1 GAB, with and without PAM for 7 hours (Figure 3A). As an extra control, αβT cells and GABs were incubated together without target cells. Similar to the IFNγ release data, GABs induced degranulation of CD8+ αβT cells upon binding to a target cell line in a PAM dependent manner, while

4

no upregulation of CD107a was observed when co-incubated with the negative control cell line HL60. To formally asses the ability of GABs to kill tumor targets, we employed a luciferase-based cytotoxicity assay. RPMI 8226 and SCC9 tumor cells stably transduced with a luciferase gene were co-cultured with GABs and αβT cells at different effector to target (E:T) ratios. After a co-culture of 16 hours, the bioluminescence was measured by adding beetle luciferin to the co-culture. The amount of viable cells was determined by comparing the bioluminescence signal to untreated target cells (Figure 3B). Both CL5 and AJ8 GAB efficiently induced up to 60-80% lysis of the tumor cells at the lower effector to target cell ratios, while LM1 GAB had as little activity as αβT cells alone.

To extend our findings to GABs harboring sequences published by others [9, 38, 45, 46], a second set of five GABs were generated (Table 1) and tested for ability to induce target cell lysis after co-incubation with αβ T lymphocytes and the multiple myeloma target cell line RPMI 8226[11] in the presence of PAM. As benchmark we used the previously identified GABs with lower (AJ8) and higher (CL5) EC_{50} and as negative control LM1 GAB. Again, we observed differences in activity, GABs harboring sequences from CL5 were superior to all other tested GABs. Only the GABs derived from DGSF68 and MOP TCR were not significantly different from the lysis induced by AJ8 GAB, while the other 3 tested GABs were inferior to the AJ8 GAB (Figure S3).

GABs are active against primary leukemia but not against primary healthy tissues

To test whether GABs can mediate recognition of not only tumor cell lines, but also of primary tumors such as primary AML, αβT cells were co-cultured with AJ8 GAB and primary AML blasts of 4 patients, with and without PAM. GABs induced a significant increase in IFNγ production upon PAM treatment against two out of the four patient samples (Figure 4A).

Given the broad activity of GABs, we next assessed their ability to sense healthy tissues in a resting or stressed situation. To this end, we isolated B cells, monocytes and CD34+ cells from a healthy donor, and tested reactivity of CL5 and LM1 GAB against these cells and against healthy donor-derived fibroblasts in an IFNγ release assay. Recognition of the cells was tested in resting, but also activated or stressed conditions, such as after irradiation or chemotherapy treatment. Neither CL5 nor LM1 GAB induced recognition of healthy cells, in resting, activated or stressed conditions, while the positive control, RPMI 8226 tumor cells, induced cytokine release when incubated with CL5 GAB (Figure 4B).
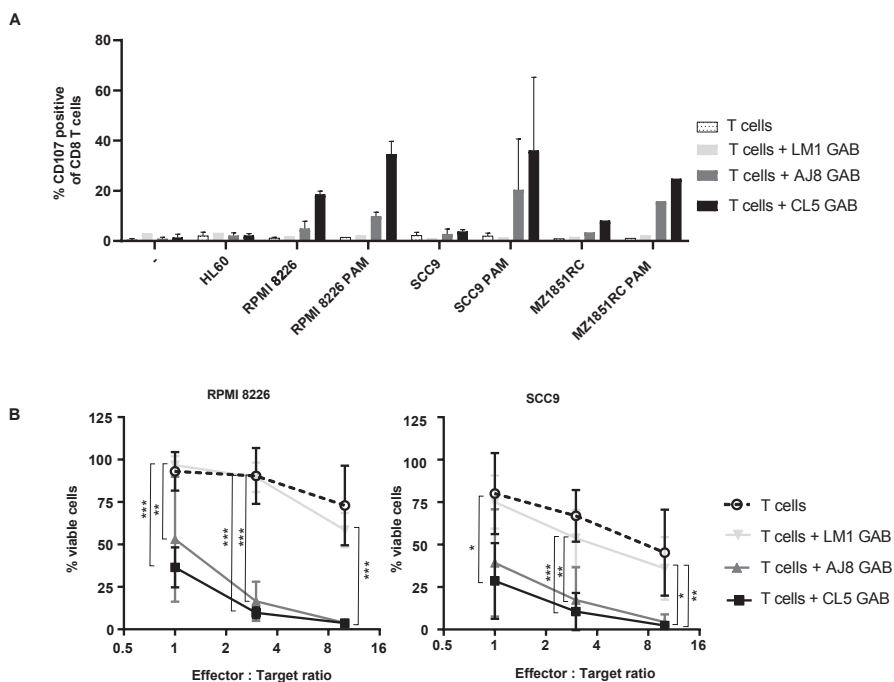
Figure 3 GABs induce T cell mediated lysis of cancer cell lines. (A) CD8+T cell degranulation was measured by staining with CD107a antibody during a 7-hour co-incubation of T cell effector and three different target cell lines in the presence and absence of GAB (10 μg/mL) and PAM (100 μM). Golgistop was added during the incubation. N=2 (for LM1 GAB and MZ1851RC N=1) significance was not calculated because of amount of data points. (B) T effector and luciferase transduced RPMI 8226 and SCC9 target cells were co-incubated for 16 hours in the presence and absence of GAB (10 μg/mL) and PAM (100 μM) at different E:T ratios. Percentage viable cells were determined by comparing luminescence signal to untreated target cells, representing 100% viability. N=3, error bars represent SD, significance was calculated using a one-way ANOVA. * P<0.05, **p<0.001, ***p<0.0001. ANOVA, analysis of variance; GAB, gamma delta TCR anti-CD3 bispecific molecules
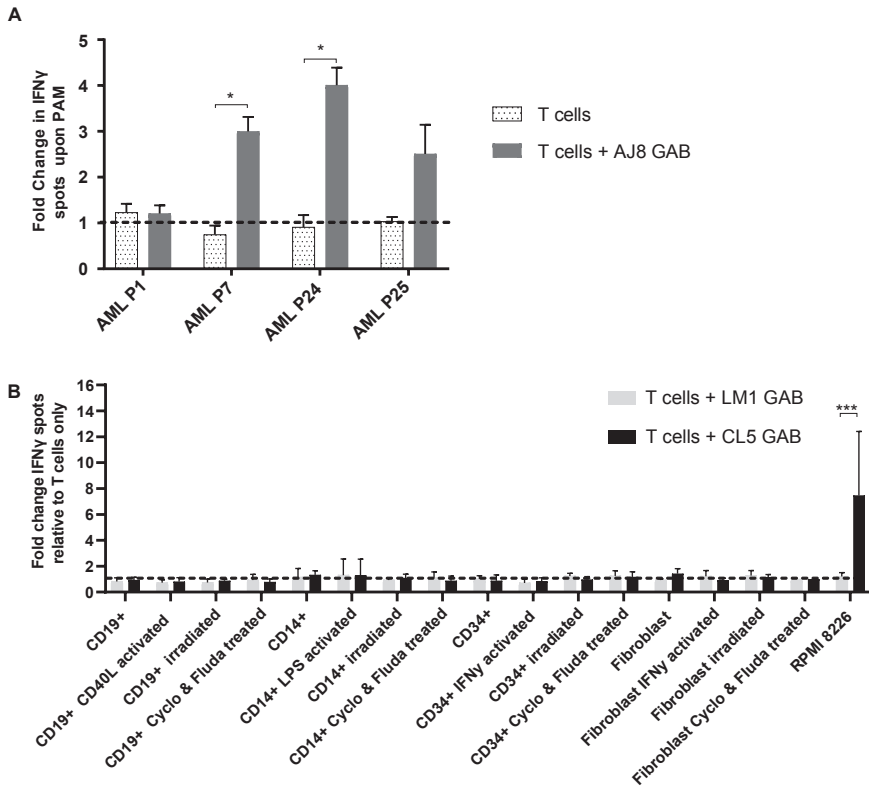
Figure 4 GABs induce recognition of primary AML samples but not of healthy hematopoietic cells or fibroblasts. (A) αβT cells were incubated with AML blasts with or without 100 µM PAM, and 10 µg/mL AJ8 GAB. IFNγ production was measured by elispot after 24 hours. Fold change in IFNγ production on addition of pamidronate was calculated N=1. (B) αβT cells were co-cultured with healthy hematopoietic cells or fibroblasts and LM1 or CL5 GAB (10 µg/mL). Target cells were activated as indicated, or stressed by irradiation or a combination treatment with cyclophosphamide (Cyclo) and fludarabine (Fluda). IFNγ release was measured by elispot. The figure represents pooled data from four different target cell donors (CD19+ and CD14+) or two donors (CD34+ and fibroblasts). αβT effector cells were derived from four different donors (CD19+ and CD14+) or two donors (CD34+ and fibroblasts). Error bars represent SD, significance was calculated using a multiple T test. * P<0.05, **p<0.001, ***p<0.0001. GAB, gamma delta TCR anti-CD3 bispecific molecules.

4
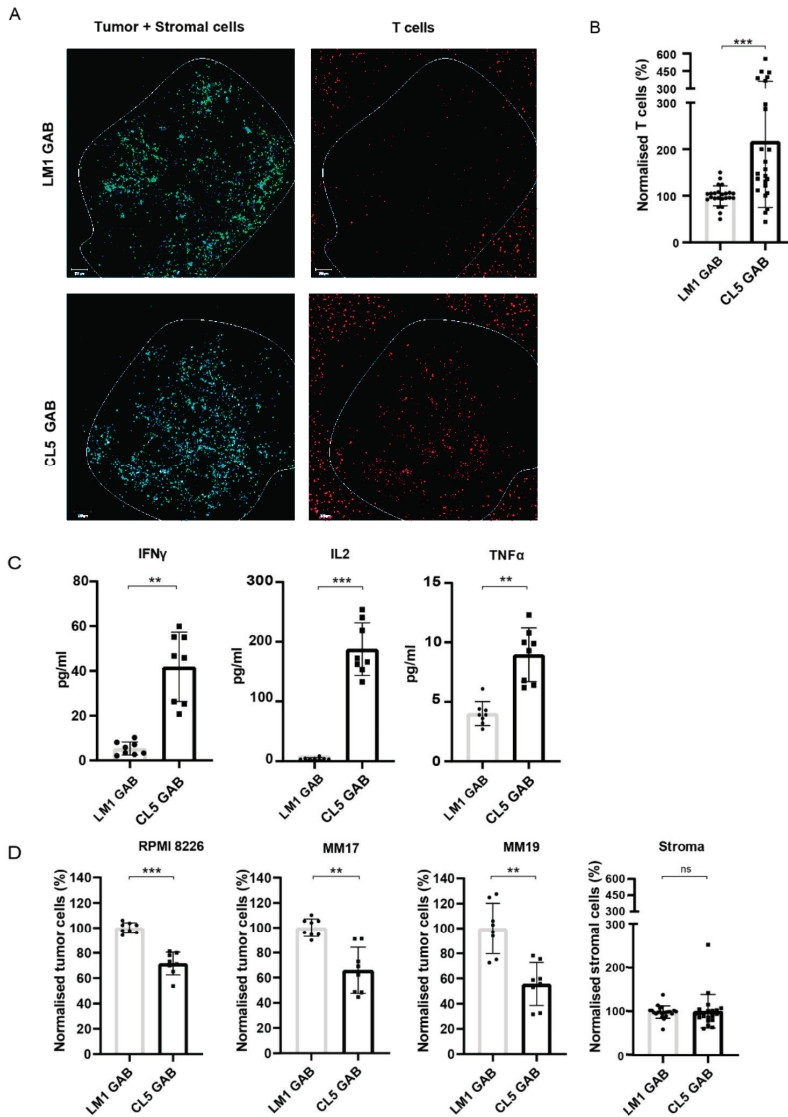
Figure 5. GABs mediate recognition and lysis of primary multiple myeloma in a 3D model. The RPMI 8226 tumor cell line or primary MM patient material was cultured in a 3D bone marrow niche consisting of matrigel and stromal cells. After 4 days, αβT cells were added together with PAM (10 μM PAM) and GAB (30 μg/mL). (A) Confocal images showing cell localization within and around the 3D model (boundaries indicated by the white line) with the tumor and stromal cells, respectively, in green and blue and T cells in red. (B) Two days after addition of the T cells, the matrigel was dissolved to retrieve the cells from the model. αβT lymphocytes were quantified by flow cytometry and normalized to mock treatment. (C) Cytokines were measured in the supernatant by luminex. (D) Tumor and stromal cells were collected from the dissolved matrigel and quantified by flow cytometry. Cell numbers were normalized to mock treatment. Significance was calculated by a paired T test. *P<0.05, **p<0.001, ***p<0.0001. N=4 with technical duplo's. GAB, gamma delta TCR anti-CD3 bispecific molecules

Favorable efficacy toxicity profile of GABs in the bone marrow niche

In vivo, the tumor microenvironment is often important for survival and proliferation of tumor cells. Therefore, we tested whether GABs can also eradicate primary tumor material without harming healthy tissues in a more natural environment, using a previously described 3D bone marrow niche model [20]. In this model, mesenchymal stem cells (MSC) and endothelial progenitor cells (EPC) are used as stromal support for the growth of a multiple myeloma (MM) cell line (RPMI 8226) or primary CD138+ MM cells derived from patients. CD138+ MM cells from two patients, and the MM cell line RPMI 8226 were stained and seeded in matrigel together with MSCs and EPCs. After four days, labeled αβT cells, together with CL5 or LM1 GAB and PAM were added to the model. One day later fresh medium with GABs was added to the model to ensure constant GAB coating on the αβT cells. After two days visualizing αβT cells infiltrated into the tumor bearing matrigel by confocal microscopy indicated an increased αβT cell infiltration in the presence of Cl5, but not LM1 GAB (Figure 5A). This observation was supported by a subsequent FACs based quantification of the αβT cells present in the matrigel (Figure 5B). To further study specific αβT cell activation by GABs, we measured several cytokines in the supernatant of the 3D model containing primary MM tumor cells. Next to IFNγ, we also observed a significant increase in the levels of other Th1 cytokines, IL2 and TNFα for the CL5 GAB condition (Figure 5C).

The most important measurement remains the elimination of tumor cells. Therefore, the amount of tumor cells remaining in the model after CL5 GAB treatment was determined by FACs analysis and cell numbers were normalized to treatment with mock LM1 GAB. Treatment with CL5 GAB induced a signification reduction of CD138+ MM cells compared to the mock treatment with LM1 GAB, for both patient samples and the MM cell line RPMI 8226. (Figure 5D). Healthy stromal cells were also quantified, showing no differences between CL5 or LM1 GAB treatment (Figure 5D), suggesting that surrounding healthy tissues are not affected by the treatment with active GAB.

GABs control tumor growth in vivo

To test whether treatment with GABs can also affect tumor growth *in vivo,* we established a xenograft model by injecting RPMI 8226 multiple myeloma cells subcutaneously (s.c) into NSG mice. For this in vivo experiment we generated RPMI 8226 B2M knock-out cells that we injected s.c, as in previous experiments i.v injected WT RPMI 8226 cells were rejected when co-engrafted with human PBMC, most likely due to allo-reactivity (Figure S4). One week after tumor cell injection, mice received an i.v injection of human PBMCs (Figure 6A). Next, the mice were randomized over two groups, based on tumor size, and received treatment for 7 consecutive days with CL5 GAB or the mock LM1 GAB. Moreover, an additional group in which mice received tumor and PBMCs but no GABs was included as extra control to monitor co-engraftment of PBMCs and tumor in NSG mice. Tumor volume was measured three times per week for 30 days. Treatment with CL5 GAB significantly decreased tumor growth compared to the control group treated with LM1 GAB (Figure 6B). Furthermore, mice treated with LM1 GAB showed similar tumor outgrowth compared to the PBMC only group. Persistence of GABs bound to αβ T cells in the blood was determined by flow cytometry 1, 2 and 8 days after GAB injection by calculating absolute number of αβTCR- and αβTCR/γδTCR double positive (GAB coated) T cells. Figure 6C shows that 24 hours after the first GAB injection (day 10), and 48 hours after the last GAB injection (day 17), around 30% of the total αβTCR positive cells are αβTCR/γδTCR double positive, meaning that there are still GABs bound to the T cells. Furthermore, we found that 8 days after the last GAB injection (day 23) this double positive population was no longer present.

4
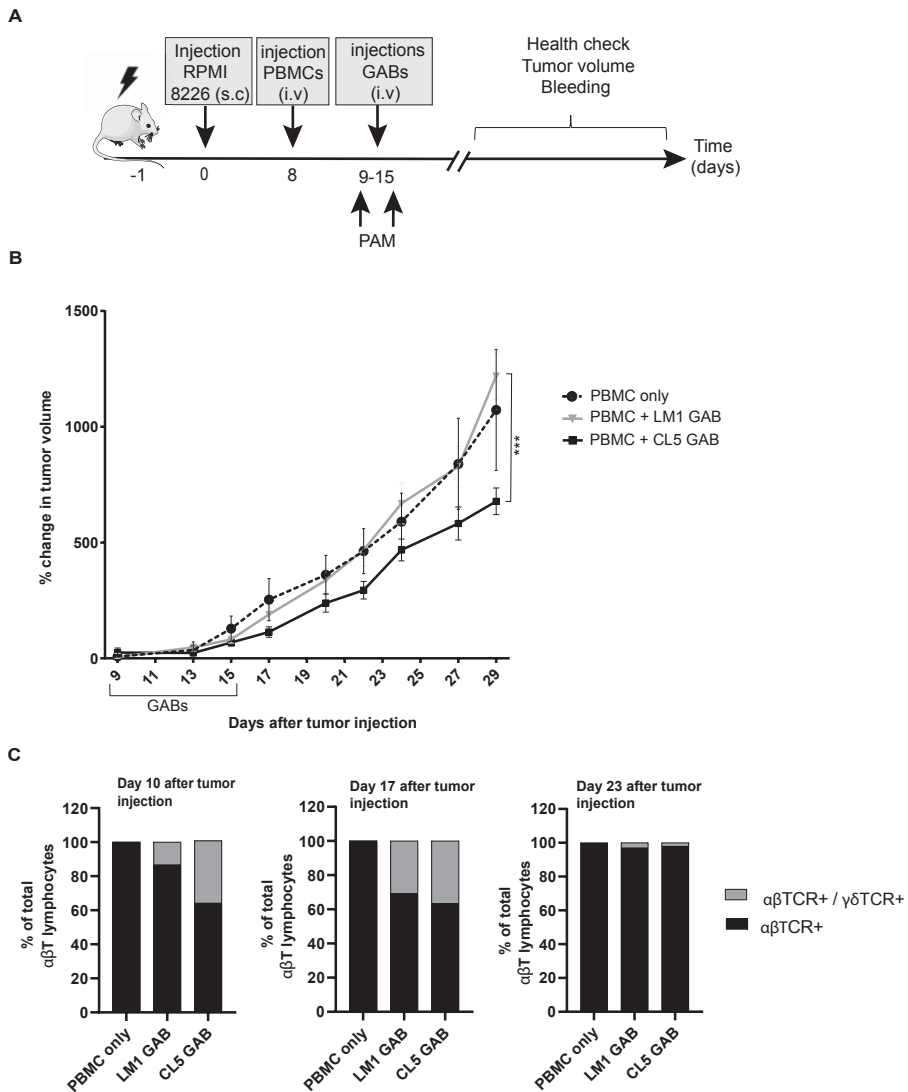
Figure 6. In vivo control of tumor growth by GABs. (A) Schematic representation of experimental design. NSG mice were irradiated at day −1, and injected subcutaneous (s.c) with 10*106 RPMI 8226 tumor cells 1 day later. After 7 days, the mice were randomized over three groups, based on tumor size (N=10). From day 9 to 15, mice in two groups were treated with one intravenous injection per day of CL5 or LM1 GAB (2,7 mg/kg). Tumor size was measured three times per week for 3 weeks after start of the GAB treatment (B) and is plotted as percent change in tumor volume compared with the initial tumor volume at the start of the GABs treatment. (C) Amount of αβTCR single positive and αβTCR/γδTCR double positive cells in the mice was determined by flow cytometry on day 10, 17 and 23 after tumor injection, which corresponds to 24 hours after the first GAB injection and 48 hours and 8 days after the last GAB injection. Data are shown as mean of percentage of total αβTCR positive cells. PBMC only N=4, LM1/CL5 GAB N=10. Error bars represent SEM, significance was calculated by mixed-effects model with repeated measures. * P<0.05, **p<0.001, ***p<0.0001. GAB, gamma delta TCR anti-CD3 bispecific molecules.

Discussion

In this study we developed a novel bispecific T cell engager format, **G**dTCR **A**nti-CD3 **B**ispecific molecules (GABs), based on the fusion of a soluble γδ2 TCR to an anti-CD3 scFv. With GABs, we introduce the targeting of cancer as a metabolic disease to the field of bispecific T cell engagers. GAB activity against tumor but not healthy tissues was observed when utilizing naturally occurring high affinity γ9δ2 TCR and relied, as for membrane bound γ9δ2 TCR, on the complex orchestration of BTN2A1 and BTN3A1 and was modified by intracellular phosphoantigen levels [8, 11, 12].

Most T cell engagers use tumor targeting domains with binding affinities in the nanomolar range, a 10-100 fold affinity maturation has been reported to further enhance activity [37, 47]. For T cell engagers with an αβTCR as tumor binding domain, affinity maturation from the micromolar to picomolar range is needed to overcome the rather low overall avidity mediated by a low density of tumor associated molecules within the context of MHC molecules, in order to create functional T cell engagers [48]. Therefore, it was initially surprising that a γ9δ2TCR is active in the bispecific format without artificial affinity maturation, while natural αβTCR showed only a little activity [32]. Most recent studies estimated the binding affinity of the γ9 chain to BTN2A1 to be around 40 μM [9] which is in the range of αβTCRs [49]. However, the number of BTN2A1 molecules that are present on the cell surface for binding to the γ9 TCR chain is most likely substantially higher compared to tumor associated antigens in HLA complexes, potentially generating a higher avidity for γ9δ2TCR based T cell engagers compared to αβTCRs. This however does not explain why, in our data set, only a selected group of defined γ9δ2 TCR clones was active in the GAB format.

The reported affinity of the γ9 chain to BTN2A1 [9] is presumably an underestimation of the binding affinity of the γ9δ2 TCR to its complete interacting complex, as the TCR binding is not solely mediated by the γ9-chain. This assumption is supported by our previous observation that apart from the γ-chain, variations in the CDR3 region of the δ2 chain also contribute substantially to the overall functional avidity of γ9δ2 TCRs once expressed in a T cell [11, 24]. δ2TCR sequences that were previously reported to mediate high overall efficacy when expressed at the cell membrane [11], also mediated high activity when used in the GAB format, *e.g* CL5 and A3. Vice versa, sequences which mediated lower efficacy in the TEG format were even poorer performers in the GAB format, *e.g.* A1. Thus, as both the γ9- and δ2-chain contribute to the affinity of a γ9δ2 TCR to its complex, a careful selection of δ2TCR sequences is needed guarantee a functional GAB.

Transforming cold- into hot tumors is a key success factor for immune therapies.[50] Novel αβTCR based biologics have been reported to warm "cold" tumors [51]. By using a 3D bone marrow niche model for primary MM cells [20], we provide evidence that γ9δ2TCR, when provided in the GAB format, can initiate infiltration of immune

4

cells into the tumor microenvironment. This was further confirmed by the in vivo model, showing that GABs can reduce tumor growth of a subcutaneously growing RPMI 8226 tumor.

Furthermore, as the utilized 3D model was comprised of healthy MSC and EPC to guarantee survival and proliferation of MM cells *in vitro* [20], this model also allowed us to assess the impact of GABs on healthy tissues, and extended our *in vitro* safety data for GAB. This current data confirms the previously reported lack of toxicity of targeting BTN2A1 and BTN3A1 when utilizing a high affinity γ9δ2TCR in the TEG format [17, 20, 23, 24] or when administering BTN3A1 targeting antibodies[15].

In this report we tested the reactivity of GABs to patient material from several AML patients, and found that GABs were reactive to two out of the four samples. This observation is in line with our previous report assessing larger tumor panels, including 16 AML patients, which suggest that approximately 50% of all tumor cells are recognized by primary γδT cells or TEGs [23]. Mode of action studies investigating requirements for γ9δ2TCR mediated tumor cell recognition, conducted in order to elucidate this differential tumor recognition, pointed to multiple factors such as pAg dependent rearrangement of the BTN2-BTN3 complex involving RhoB and the intracellular B30.1 domain of BTN3A1 [9-11]. However, these studies also imply that a yet to be defined second ligand, binding to the CDR3δ is most likely involved. Thus, although a lot of knowledge has been obtained over the past years, tumor recognition mediated by a γ9δ2TCR cannot be fully explained and predicted yet [11]. Therefore, further investigation into the complex γ9δ2TCR mediated target cell recognition, and the identification of novel biomarkers that can help identifying patient populations that are susceptible to γδ based therapies will be key for a successful clinical translation [12].

The GAB format outperformed natural γ9δ2T cells, as reported previously for TEGs [11, 43], most likely reflecting the careful selection of a high affinity γ9δ2TCR in the GAB or TEG design. Despite this superior activity, a limiting factor for γ9δ2TCR mediated target cell recognition remains the requirement for pAg accumulation, also GAB mediated recognition of many cancer cells required additional treatment with amino-bisphosphonates to increase pAg levels. To elucidate why tumor cells differ in the dependence on PAM to enhance γ9δ2TCR recognition further investigation will be needed, but it is most likely a consequence of different availabilities of all the characterized key components for γ9δ2TCR binding, including, but not limited to, the intracellular accumulation of pAgs. The dependence on increased intracellular pAg levels for recognition of many tumors, does however imply that γ9δ2TCR based therapeutic strategies most likely need to be combined with amino-bisphosphonate treatment, a state of the art drug safely combined with many different treatments including γ9δ2T infusions [12].

In conclusion, we have shown that a γ9δ2TCR bispecific format can mimic the rather complex metabolic cancer targeting usually mediated by membrane bound γ9δ2TCR [7, 8, 34], though requires a very careful selection of the used sequences and then allows for the introduction of the unique tumor targeting potential of γ9δ2T cells to the field of bispecific T cell engagers. Our findings imply also that, in contrast to previously reported data for αβTCR derived bispecifics, selecting an endogenously occurring high affinity γ9δ2TCR for use in a bispecific format could omit the need for affinity maturation. Since the use of affinity matured TCRs poses the risk of altering the TCR specificity or introducing cross-reactivity [52, 53], using a therapy based on the endogenous TCR affinity could be a preferred strategy. This approach might overcome cumbersome engineering efforts, and provide with GABs and TEGs, two complementary or even additive strategies as reported for CAR-T.

Acknowledgements

4

Funding

Conflict of interest statement

J.K. is shareholder of Gadeta (www.gadeta.nl). Jürgen Kuball, Zsolt Sebestyen, Dennis X Beringer, Anna Vyborova, and Eline van Diest are authors on several patent applications.

References

1. Gentles AJ, Newman AM, Liu CL, Bratman SV, Feng W, Kim D, et al. The prognostic landscape of genes and infiltrating immune cells across human cancers. Nat Med. 2015;21(8):938-45.

2. Bonneville M, O'Brien RL, Born WK. Gammadelta T cell effector functions: a blend of innate programming and acquired plasticity. NatRevImmunol. 2010;10(7):467-78.

3. Scheper W, Grunder C, Straetemans T, Sebestyen Z, Kuball J. Hunting for clinical translation with innate-like immune cells and their receptors. Leukemia. 2014;28(6):1181-90.

4. Scheper W, van Dorp S, Kersting S, Pietersma F, Lindemans C, Hol S, et al. gammadeltaT cells elicited by CMV reactivation after allo-SCT cross-recognize CMV and leukemia. Leukemia. 2013;27(6):1328-38.

5. Simões AE, Di Lorenzo B, Silva-Santos B. Molecular Determinants of Target Cell Recognition by Human γδ T Cells. Front Immunol. 2018;9:929.

6. Gober HJ, Kistowska M, Angman L, Jenö P, Mori L, De Libero G. Human T cell receptor gammadelta cells recognize endogenous mevalonate metabolites in tumor cells. J Exp Med. 2003;197(2):163-8.

7. Gu S, Sachleben JR, Boughter CT, Nawrocka WI, Borowska MT, Tarrasch JT, et al. Phosphoantigen-induced conformational change of butyrophilin 3A1 (BTN3A1) and its implication on Vgamma9Vdelta2 T cell activation. Proc Natl Acad Sci U S A. 2017;114(35):E7311-E20.

8. Sebestyen Z, Scheper W, Vyborova A, Gu S, Rychnavska Z, Schiffler M, et al. RhoB Mediates Phosphoantigen Recognition by Vgamma9Vdelta2 T Cell Receptor. Cell Rep. 2016;15(9):1973-85.

9. Rigau M, Ostrouska S, Fulford TS, Johnson DN, Woods K, Ruan Z, et al. Butyrophilin 2A1 is essential for phosphoantigen reactivity by gammadelta T cells. Science. 2020;367(6478).

10. Karunakaran MM, Willcox CR, Salim M, Paletta D, Fichtner AS, Noll A, et al. Butyrophilin-2A1 Directly Binds Germline-Encoded Regions of the Vgamma9Vdelta2 TCR and Is Essential for Phosphoantigen Sensing. Immunity. 2020;52(3):487-98.e6.

11. Vyborova A, Beringer DX, Fasci D, Karaiskaki F, van Diest E, Kramer L, et al. gamma9delta2T cell diversity and the receptor interface with tumor cells. J Clin Invest. 2020.

12. Sebestyen Z, Prinz I, Dechanet-Merville J, Silva-Santos B, Kuball J. Translating gammadelta (gammadelta) T cells and their receptors into cancer cell therapies. Nat Rev Drug Discov. 2020;19(3):169-84.

13. Deniger DC, Moyes JS, Cooper LJ. Clinical applications of gamma delta T cells with multivalent immunity. Front Immunol. 2014;5:636.

14. Scheper W, Sebestyen Z, Kuball J. Cancer Immunotherapy Using gammadeltaT Cells: Dealing with Diversity. Front Immunol. 2014;5:601.

15. Payne KK, Mine JA, Biswas S, Chaurio RA, Perales-Puchalt A, Anadon CM, et al. BTN3A1 governs antitumor responses by coordinating alphabeta and gammadelta T cells. Science. 2020;369(6506):942-9.

16. Johanna I, Hernandez-Lopez P, Heijhuurs S, Bongiovanni L, de Bruin A, Beringer D, et al. TEG011 persistence averts extramedullary tumor growth without exerting off-target toxicity against healthy tissues in a humanized HLA-A*24:02 transgenic mice. J Leukoc Biol. 2020;107(6):1069-79.

17. Johanna I, Straetemans T, Heijhuurs S, Aarts-Riemens T, Norell H, Bongiovanni L, et al. Evaluating in vivo efficacy - toxicity profile of TEG001 in humanized mice xenografts against primary human AML disease and healthy hematopoietic cells. J Immunother Cancer. 2019;7(1):69.

18. Kierkels GJJ, Scheper W, Meringa AD, Johanna I, Beringer DX, Janssen A, et al. Identification of a tumor-specific allo-HLA-restricted gammadeltaTCR. Blood Adv. 2019;3(19):2870-82.

19. Straetemans T, Janssen A, Jansen K, Doorn R, Aarts T, van Muyden ADD, et al. TEG001 Insert Integrity from Vector Producer Cells until Medicinal Product. Mol Ther. 2020;28(2):561-71.

20. Braham MVJ, Minnema MC, Aarts T, Sebestyen Z, Straetemans T, Vyborova A, et al. Cellular immunotherapy on primary multiple myeloma expanded in a 3D bone marrow niche model. Oncoimmunology. 2018;7(6):e1434465.

21. Straetemans T, Kierkels GJJ, Doorn R, Jansen K, Heijhuurs S, Dos Santos JM, et al. GMP-Grade Manufacturing of T Cells Engineered to Express a Defined gammadeltaTCR. Front Immunol. 2018;9:1062.

22. Kierkels GJ, Straetemans T, de Witte MA, Kuball J. The next step toward GMP-grade production of engineered immune cells. Oncoimmunology. 2016;5(2):e1076608.

23. Straetemans T, Gründer C, Heijhuurs S, Hol S, Slaper-Cortenbach I, Bönig H, et al. Untouched GMP-Ready Purified Engineered Immune Cells to Treat Cancer. Clin Cancer Res. 2015;21(17):3957-68.

24. Grunder C, van DS, Hol S, Drent E, Straetemans T, Heijhuurs S, et al. gamma9 and delta2CDR3 domains regulate functional avidity of T cells harboring gamma9delta2TCRs. Blood. 2012;120(26):5153-62.

25. June CH, O'Connor RS, Kawalekar OU, Ghassemi S, Milone MC. CAR T cell immunotherapy for human cancer. Science. 2018;359(6382):1361-5.

26. Singh AK, McGuirk JP. CAR T cells: continuation in a revolution of immunotherapy. Lancet Oncol. 2020;21(3):e168-e78.

27. Chabannon C, Kuball J, McGrath E, Bader P, Dufour C, Lankester A, et al. CAR-T cells: the narrow path between hope and bankruptcy? Bone Marrow Transplant. 2017;52(12):1588-9.

28. McGrath E, Chabannon C, Terwel S, Bonini C, Kuball J. Opportunities and challenges associated with the evaluation of chimeric antigen receptor T cells in real-life. Curr Opin Oncol. 2020;32(5):427-33.

29. Batlevi CL, Matsuki E, Brentjens RJ, Younes A. Novel immunotherapies in lymphoid malignancies. Nat Rev Clin Oncol. 2016;13(1):25-40.

30. Krishnamurthy A, Jimeno A. Bispecific antibodies for cancer therapy: A review. Pharmacol Ther. 2018;185:122-34.

31. Abbott RC, Cross RS, Jenkins MR. Finding the Keys to the CAR: Identifying Novel Target Antigens for T Cell Redirection Immunotherapies. Int J Mol Sci. 2020;21(2).

32. Liddy N, Bossi G, Adams KJ, Lissina A, Mahon TM, Hassan NJ, et al. Monoclonal TCR-redirected tumor cell killing. Nat Med. 2012;18(6):980-7.

33. Bubenik J. Tumour MHC class I downregulation and immunotherapy (Review). Oncol Rep. 2003;10(6):2005-8.

34. Sandstrom A, Peigne CM, Leger A, Crooks JE, Konczak F, Gesnel MC, et al. The intracellular B30.2 domain of butyrophilin 3A1 binds phosphoantigens to mediate activation of human Vgamma9Vdelta2 T cells. Immunity. 2014;40(4):490-500.

35. Arakawa F, Kuroki M, Kuwahara M, Senba T, Ozaki H, Matsuoka Y, et al. Cloning and sequencing of the VH and V kappa genes of an anti-CD3 monoclonal antibody, and construction of a mouse/human chimeric antibody. J Biochem. 1996;120(3):657-62.

36. Allison TJ, Winter CC, Fournie JJ, Bonneville M, Garboczi DN. Structure of a human gammadelta T-cell antigen receptor. Nature. 2001;411(6839):820-4.

37. Goebeler ME, Bargou RC. T cell-engaging therapies - BiTEs and beyond. Nat Rev Clin Oncol. 2020;17(7):418-34.

38. Starick L, Riano F, Karunakaran MM, Kunzmann V, Li J, Kreiss M, et al. Butyrophilin 3A (BTN3A, CD277)-specific antibody 20.1 differentially activates Vgamma9Vdelta2 TCR clonotypes and interferes with phosphoantigen activation. Eur J Immunol. 2017;47(6):982-92.

39. Wang H, Fang Z, Morita CT. Vgamma2Vdelta2 T Cell Receptor recognition of prenyl pyrophosphates is dependent on all CDRs. JImmunol. 2010;184(11):6209-22.

40. Yamashita S, Tanaka Y, Harazaki M, Mikami B, Minato N. Recognition mechanism of non-peptide antigens by human gammadelta T cells. Int Immunol. 2003;15(11):1301-7.

41. Willcox CR, Vantourout P, Salim M, Zlatareva I, Melandri D, Zanardo L, et al. Butyrophilin-like 3 Directly Binds a Human Vgamma4(+) T Cell Receptor Using a Modality Distinct from Clonally-Restricted Antigen. Immunity. 2019.

42. Harly C, Guillaume Y, Nedellec S, Peigné CM, Mönkkönen H, Mönkkönen J, et al. Key implication of CD277/butyrophilin-3 (BTN3A) in cellular stress sensing by a major human γδ T-cell subset. Blood. 2012;120(11):2269-79.

43. Marcu-Malina V, Heijhuurs S, van Buuren M, Hartkamp L, Strand S, Sebestyen Z, et al. Redirecting αβ T cells against cancer cells by transfer of a broadly tumor-reactive γδT-cell receptor. Blood. 2011;118(1):50-9.

44. Morath A, Schamel WW. αβ and γδ T cell receptors: Similar but different. J Leukoc Biol. 2020;107(6):1045-55.

4

45. Tanaka Y, Morita CT, Tanaka Y, Nieves E, Brenner MB, Bloom BR. Natural and synthetic non-peptide antigens recognized by human gamma delta T cells. Nature. 1995;375(6527):155-8.

46. De Libero G, Casorati G, Giachino C, Carbonara C, Migone N, Matzinger P, et al. Selection by two powerful antigens may account for the presence of the major population of human peripheral gamma/delta T cells. J Exp Med. 1991;173(6):1311-22.

47. Ellerman D. Bispecific T-cell engagers: Towards understanding variables influencing the in vitro potency and tumor selectivity and their modulation to enhance their efficacy and safety. Methods. 2019;154:102-17.

48. Li Y, Moysey R, Molloy PE, Vuidepot AL, Mahon T, Baston E, et al. Directed evolution of human T-cell receptors with picomolar affinities by phage display. NatBiotechnol. 2005;23(3):349-54.

49. Birnbaum ME, Mendoza JL, Sethi DK, Dong S, Glanville J, Dobbins J, et al. Deconstructing the peptide-MHC specificity of T cell recognition. Cell. 2014;157(5):1073-87.

50. Duan Q, Zhang H, Zheng J, Zhang L. Turning Cold into Hot: Firing up the Tumor Microenvironment. Trends Cancer. 2020;6(7):605-18.

51. Lowe KL, Cole D, Kenefeck R, I OK, Lepore M, Jakobsen BK. Novel TCR-based biologics: mobilising T cells to warm 'cold' tumours. Cancer Treat Rev. 2019;77:35-43.

52. Riley TP, Baker BM. The intersection of affinity and specificity in the development and optimization of T cell receptor based therapeutics. Semin Cell Dev Biol. 2018;84:30-41.

53. Cameron BJ, Gerry AB, Dukes J, Harper JV, Kannan V, Bianchi FC, et al. Identification of a Titin-Derived HLA-A1-Presented Peptide as a Cross-Reactive Target for Engineered MAGE A3-Directed T Cells. SciTranslMed. 2013;5(197):197ra03.

54. Choi BD, Yu X, Castano AP, Bouffard AA, Schmidts A, Larson RC, et al. CAR-T cells secreting BiTEs circumvent antigen escape without detectable toxicity. Nat Biotechnol. 2019;37(9):1049-58.
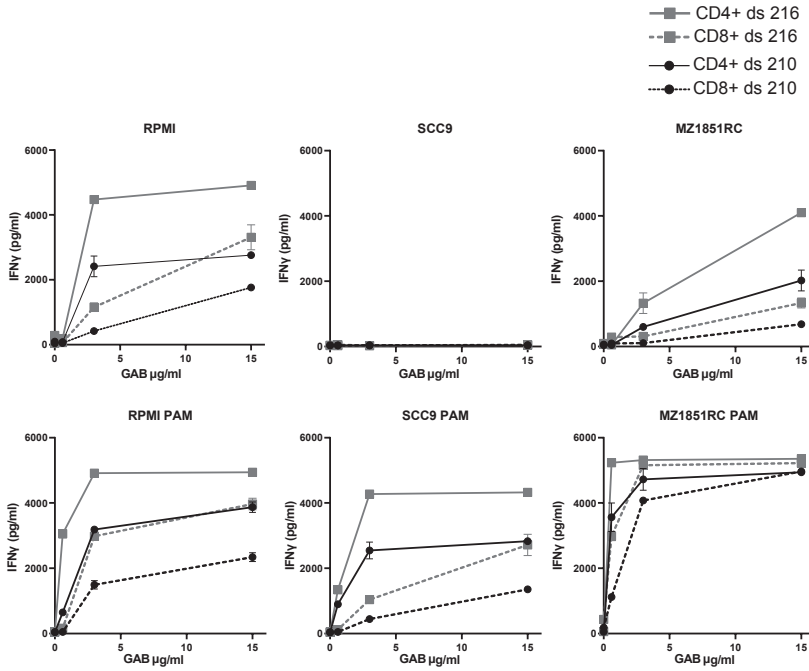
Supplementary Material
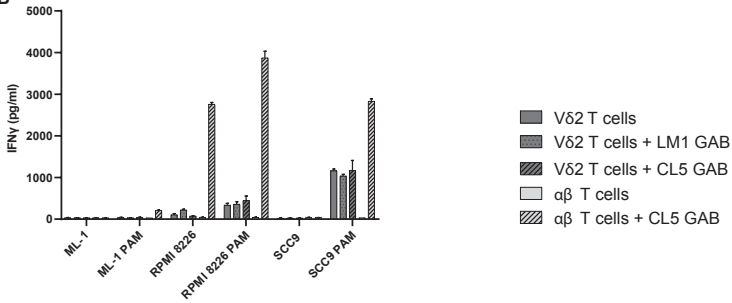
Supplementary Figures
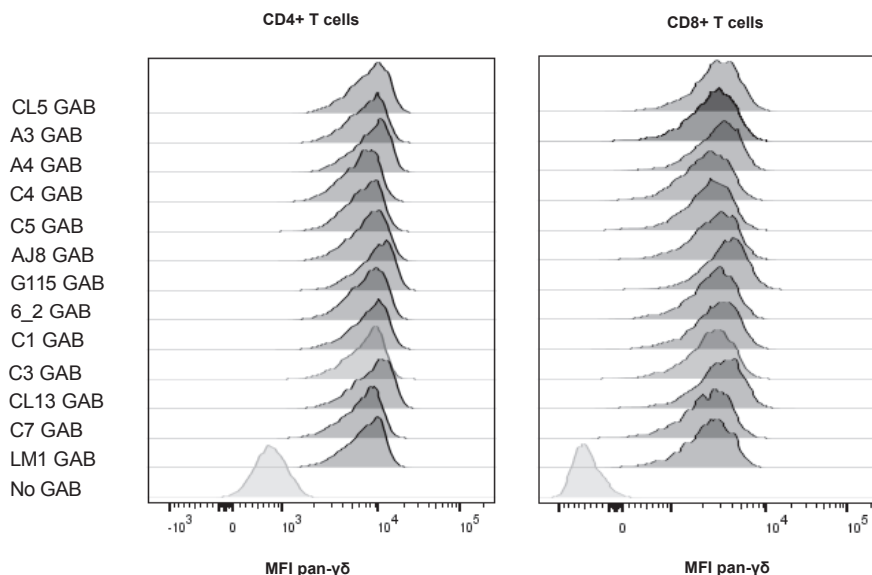
Supplementary Figure 1. GAB coating of CD4 and CD8+ αβT cells. Coating of αβT cells with GAB (90 µg/ml), followed by staining with fluorochrome labeled anti pan γδ, CD4 and CD8 antibodies. MFI was measured by flow cytometry, histograms represent MFI for γδ for CD4+ and CD8+ T lymphocytes.

Supplementary Figure 2. Differential GAB mediated activation of CD4+, CD8+ αβ T cells and Vδ2+ T cells. IFNγ release was measured using ELISA after a co-culture of (A) MACS separated CD4 and CD8 αβ T cells from 2 different T cells donors with 3 different target cells in the presence of different concentration of CL5 GAB, with and without PAM (100 µM). (B) bulk αβ T cells or bulk Vδ2+ T cells with 2 recognized (RPMI 8226 + SCC9) and 1 unrecognized cell line (ML-1) with and without LM1/CL5 GAB (15 µg/ml) and PAM (100 µM). N=1 error bars represent SD from technical duplicates.
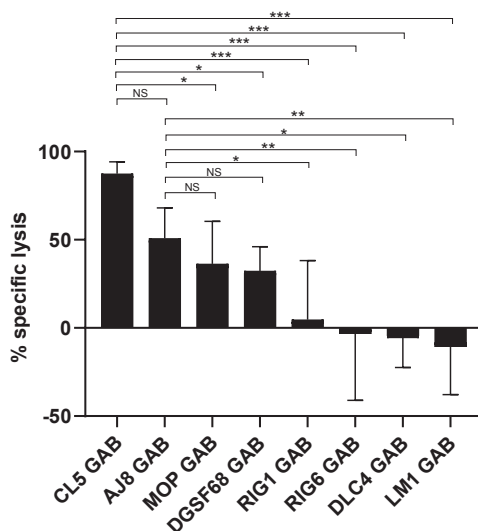
Supplementary Figure 3. Higher activity CL5 GAB compared to GABs derived from publicly available γ9δ2 TCRs. A) T effector and luciferase transduced RPMI 8226 cells were co-incubated for 16 hours in the presence of GABs (10 µg/ml) derived from different Vγ9Vδ2 TCRs and PAM (30 µM) at 10:1 E:T ratio. Percentage specific lysis was determined by comparing luminescence signal to untreated target cells, representing 100% viability. N=2, with technical duplos error bars represent SD, significance was calculated using a one-way ANOVA; * P<0.05, **P<0.001, ***P<0.0001

4
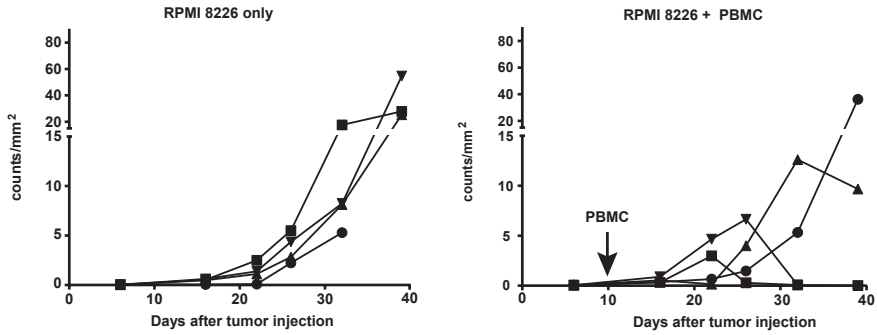
Supplementary Figure 4. Poor outgrowth of IV injected RPMI 8226 in NSG mice when co-engrafted with huPBMCs. NSG mice were irradiated at day -1, and injected intra venous (i.v) with 10*10^6 RPMI 8226 tumor cells one day later, after 10 days the mice were randomized over two groups. One group was injected i.v with 10*10^6 huPBMCs (n=5 right panel) while the other group received no further treatment (n=4 left panel). Tumor growth was monitored by bioluminescence imaging (BLI) once a week and plotted overtime, each line represents one mouse.

Supplementary Material and Methods

Cells, Cell lines, and Primary Material

PBMCS were isolated by Ficoll-Paque (GE Healthcare, Eindhoven, The Netherlands) from buffy coats obtained from Sanquin Blood Bank (Amsterdam, The Netherlands). αβT cells were expanded from PBMCs using CD3/CD28 dynabeads (Thermo Fisher scientific, United States) and (1.7×10^3 IU/ml of MACS GMP Recombinant Human interleukin (IL)-7 (Miltenyi Biotec, Germany), and 1.5×10^2 IU/ml MACS GMP Recombinant Human IL-15 (Milteny Biotec, Germany). CD4+ and CD8+ αβT cells were selected using MACS isolation with CD4- and CD8- microbeads respectively (Miltenyi Biotec, Germany). γδ T cells were first selected from PBMCs by MACS isolation using TCR γδ+ isolation kit (Miltenyi Biotec, Germany), after which the Vδ2+ T cells were isolated via FACS sort based on positive staining for Vδ2-FITC (clone B6, Biolegend). Vδ2+ cells were expanded using the previously described rapid expansion protocol [1] RPMI 8226 stably expressing GFP-luciferase was generated by a previously described retroviral transduction protocol [2]. The plasmid containing the GFP and luciferine transgenes was kindly provided by Jeanette Leusen (UMC Utrecht, Utrecht, Netherlands). The following cell lines were obtained from ATCC between 2010 and 2018, HL60 (CCL-240), ML-1 (CVCL_0436), MDA-MB231 (HTB-26), RPMI 8226 (CCL-155), Saos-2 (HTB-85), SCC9 (CRL-1629), HEK293T (CRL-3216). HEKBTN3 knock-out was a gift from Erin Adams (Chicago, United States). BV173 (ACC 20) was obtained from DSMZ. MZ1851RC was a kind gift from Barbara Seliger (University Halle, Germany). MDA-MB157 was kindly provided in 2016 by Thordur Oskarsson (Deutschen Krebsforschungszentrum, Heidelberg, Germany). Freestyle 293-F cells (R790-07) were obtained from Invitrogen (United States). HL60, RPMI 8226 ML-1 and BV173 were cultured in RPMI (Gibco, United states), 10% FCS (Bodinco, Alkmaar, The Netherlands), 1% Pen/Strep (Invitrogen, United States). Freestyle 293-F in Freestyle expression medium (Gibco). All other cell lines in DMEM, 10% FCS, 1% Pen/Strep. RPMI 8226 B2M knockout was created using Alt-R Crispr-CAS9 system (IDT, United States) according to the manufacturers protocol, with guide RNA sequence AAGTCAACTTCAATGTCGGA. Transfection was done with Neon Transfection system (Thermo Fisher Scientific) using the following settings: pulse voltage 1050 V, pulse width 20, 3 pulses.

Primary Material

Primary acute myeloid leukemia and multiple myeloma blasts were obtained from the biobank of the University Medical Center, Utrecht in accordance with good clinical practice and the Declaration of Helsinki regulations. All patients gave their consent prior to storage in the biobank (TCBio 16-088). B cells and monocytes were isolated from PBMCs by MACS-separation using CD19 and CD14-microbeads (Miltenyi Biotec, Germany) respectively, according to the manufacturers' protocol.

Fibroblasts were a kind gift from Marieke Griffioen (Leiden University Medical Centre, Leiden, The Netherlands) and cultured in DMEM medium containing 10% FCS, 100 U/ml penicillin and 100 µg/ml streptomycin. Multipotent mesenchymal stromal cells (MSCs) were isolated from healthy bone marrow (Hematology Department, UMC Utrecht, The Netherlands) by adherence to tissue culture flasks, and cultured in MSC-medium; α-minimal essential media (Gibco, USA) containing 0.2 mM L-ascorbic acid 2-phosphate, 10% FCS, 100 U/ml penicillin and 100 µg/ml streptomycin. Endothelial progenitor cells (EPCs) were isolated from healthy umbilical cord blood by density-gradient centrifugation using Ficoll-paque. The isolated MNCs were seeded on collagen I-coated tissue flasks and expanded in EGM-2 medium (Lonza, Switzerland) containing 10% FCS, 100 U/ml penicillin and 100 µg/ml streptomycin CD34+ were isolated from human umbilical cord blood using magnetic bead selection (Milteny Biotec, Germany). Umbilical cord blood was obtained after informed consent and approval by the ethics committee of the University Medical Center Utrecht (TC-bio 15-345). To induce stress, cells were irradiated with 3500 cGy, or treated with 5mM cyclophosphamide (Sigma Aldrich, Germany) and 20 µM fludarabine (Sigma Aldrich) Activation was done with huCD40LT (Milteny Biotec, Germany) 400 ng/ml for 72 hours prior to assay (CD19+), IFNγ (R&D systems, Canada) 1000IU/ml 16 hours prior to assay (CD34+, Fibroblasts), LPS 100ng/ml (Invitrogen, United States) added during the assay (CD14+).

Flow cytometry

0.2*10^6 T cells were incubated with GAB (10 µg/ml if not indicated differently) in 20 µl FACS buffer (PBS, 1% BSA (Sigma Aldrich, Germany), 0.01 % sodium azide (Severn Biotech Ltd, United Kingdom) for 30 minutes at room temperature. Cells were washed once in FACS buffer and incubated with the appropriate secondary antibody mix for 30 minutes at room temperature. Cells were washed 2 times in FACS buffer and fixed in 1% paraformaldehyde (Merck, Germany) in PBS. Data acquisition was done on FACS Canto and analyzed using FACS Diva software (BD, United States) or FlowJo. Antibodies that were used are pan-γδTCR-PE (Beckman Coulter, United States, clone IMMU510, 1:10), pan-γδTCR APC (BD Pharmigen, United States, clone B1,1:5), Vδ2-FITC (Biolegend, United States, clone B6, 1:10) and Vγ9-PE (BD pharmingen, clone B3, 1:25).

IFNγ Elispot

15.000 effector cells and 50.000 target cells were incubated together, with or without GAB (10 µg/ml if not indicated differently) for 16 hours at 37 °C 5% CO_2. In PAM conditions, 100 µM PAM (Calbiochem, United States) was added to the cells. The co-culture was done in nitrocellulose-bottomed 96-well plates (Millipore, United States) pre-coated with α-IFNγ antibody (clone 1-D1K) (Mabtech, Sweden). After 16 hours, the plates were washed with PBS and incubated with mAb7-B6-1

(II; Mabtech, Sweden) followed by Streptavadin-HRP (Mabtech, Sweden) IFNγ spots were visualized with TMB substrate (Mabtech, Sweden) and analyzed using A.EL.VIS ELISPOT wcanner and analysis software (A.EL.VIS, Germany).

CD107 degranulation assay

300.000 target cells were incubated with 100.000 T cells, GAB (10 µg/ml) and 100 µM PAM (Calbiochem, United States) in the presence of aCD107α-PE (BD, United States, clone AB4, 1:200) for 7 hours, after 2 hours Golgistop (BD, United States) was added (1:1500). After 7 hours, cells were washed in FACs buffer and stained with aCD3-eFluor450 (eBioscience, United states, clone OKT3, 1:50) and aCD8-PerCP-Cy5.5 (Biolegend, United States, clone RPA-T8, 1:1000). Cells were washed 2 times in FACS buffer and fixed in 1% paraformaldehyde (Merck, Germany) in PBS. Data acquisition was done on FACS Canto and analyzed using FACS Diva software (BD)

Luciferase based cytotoxicity

5000 RPMI 8226 target cells stably expressing luciferase were incubated with T cells at different E:T ratios (1:1 to 1:30), with or without 10 µg/ml GAB in the presence of 0.1 mM PAM (calbiochem, United States). After 16 hours, beetle luciferin (Promega, United States) was added to the wells (125 µg/ml) and bioluminescence was measured on SoftMax Pro plate reader. The signal in treatment wells was normalized to the signal measured for untreated targets, which was assumed to represent 100% living cells.

Animal model

NOD.Cg-PrkdcscidIl2rgtm1Wjl/SzJ (NSG) mice were obtained from Jackson Laboratory (Bar Harbor, ME, USA). Experiments were conducted under institutional guidelines after permission from the local Ethical Committee and in accordance with the current Dutch laws on Animal Experimentation. Mice were housed in sterile conditions using an individually ventilated cage (IVC) system and fed with sterile food and water. Irradiated mice were given sterile water with antibiotic ciproxin for the duration of the experiment. Adult female mice (16 weeks old) received sublethal total body irradiation (1.75 Gy) on Day -1. For the iv model, mice received a subcutaneous injection of 10×10^6 RPMI 8226-luc cells in PBS on day 0. Ten days later, mice were randomized into two groups of 4 or 5 mice and one group was intravenously injected with 10×10^6 huPBMCs. Tumor growth was measured once a week by bioluminescence imaging (BLI). For the subcutaneous model, mice received a subcutaneous injection of 10×10^6 RPMI 8226-luc B2M knockout cells in PBS, on day 0. One week later, mice were randomized based on tumor volume into two groups of 10 mice and intravenously injected with 10×10^6 huPBMCs. Next, mice received 7 consecutive injections of either CL5 GAB

or LM1 GAB (2,7 mg/kg body weight). Pamidronate (10 mg/kg body weight) was injected together with the GABs on days 9 and 12. Moreover, an extra group (n=4) that received tumor and huPBMCs but no GABs was included as additional control. Tumor volume was measured three times a week as primary outcome measure. Percent change in tumor volume was calculated using the formula: (Vf-V0)/V0*100, where V0 = volume at the beginning of the treatment, and Vf = final volume. Mouse peripheral blood samples were obtained via cheek vein (maximum 50–80 µl/mouse) once a week. Red blood cell lysis was performed for blood samples using 1× RBC lysis buffer (Biolegend) before cell staining. Blood samples were stained with γδTCR-PE (clone RPA-T4, Biolegend), αβTCR-FITC (Clone IP26, Invitrogen), huCD45-PB (Clone HI30, Sony). The persistence of GABs bound to αβ T cells was measured in peripheral blood by quantifying the absolute αβTCR positive and αβTCR[+]/γδTCR double positive cell number by flow cytometry using using Flow-count Fluorospheres (Beckman Coulter).

Supplementary references

1. Marcu-Malina V, Heijhuurs S, van Buuren M, Hartkamp L, Strand S, Sebestyen Z, *et al.* Redirecting αβ T cells against cancer cells by transfer of a broadly tumor-reactive γδT-cell receptor. Blood 2011;118:50-9

2. Grunder C, van DS, Hol S, Drent E, Straetemans T, Heijhuurs S, *et al.* gamma9 and delta2CDR3 domains regulate functional avidity of T cells harboring gamma9delta2TCRs. Blood 2012;120:5153-62

4
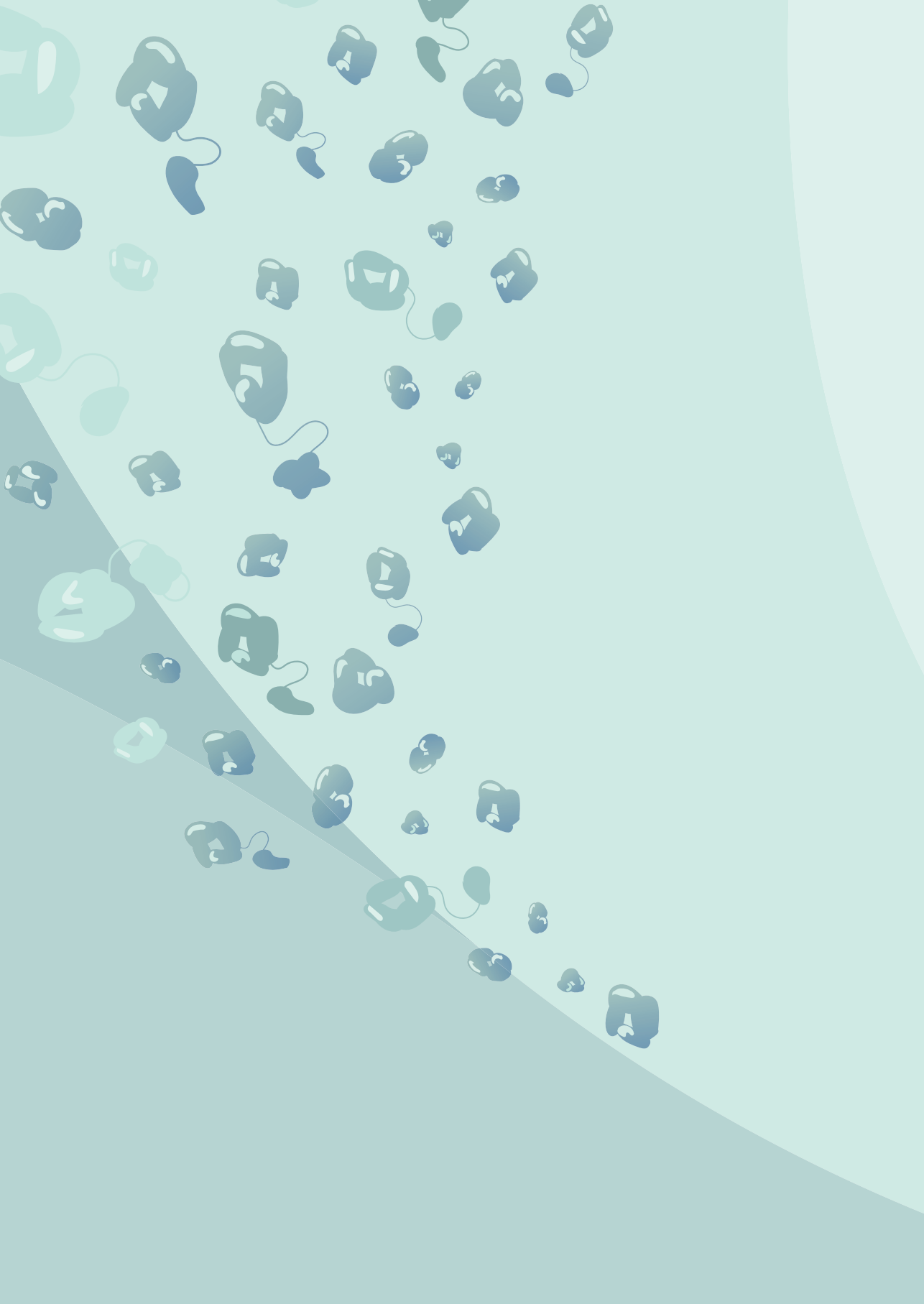
CHAPTER 5

The making of multivalent gamma delta TCR anti-CD3 bispecific T cell engagers

Eline van Diest[1#], Mara J.T. Nicolasen[1#], Lovro Kramer[1], Jiali Zheng[1],
Patricia Hernández-López[1], Dennis X Beringer[1*], Jürgen Kuball[1,2*].

1. Center for Translational Immunology, University Medical Center Utrecht,
Utrecht University, The Netherlands
2. Department of Hematology, University Medical Center Utrecht,
Utrecht University, The Netherlands

#These authors share first authorship
*These authors share senior authorship

Abstract

We have recently developed a novel T cell engager concept by utilizing γ9δ2TCR as tumor targeting domain, named Gamma delta TCR anti-CD3 bispecific molecule (GAB), targeting the phosphoantigen-dependent orchestration of BTN2A1 and BTN3A1 at the surface of cancer cells. To explore alternative designs to enhance effectivity of current GABs, made by the fusion of the ectodomains of a γδTCR to an anti-CD3 single chain variable fragment (scFv) (γδ$_{ECTO}$-αCD3), we first attempted to link only the variable domains of the γ and δ chain to an anti-CD3 scFv (γδ$_{VAR}$-αCD3). Multimerizing γδ$_{VAR}$-αCD3 proteins would in theory allow us to increase the tumor binding valency. However, γδ$_{VAR}$-αCD3 proteins were poorly expressed, and while the addition of stabilizing mutations based on findings for αβ single chain formats increased expression, generation of meaningful amounts of γδ$_{VAR}$-αCD3 protein was not possible. As an alternative strategy, we explored the natural properties of the original GAB design (γδ$_{ECTO}$-αCD3), and observed the spontaneous formation of γδ$_{ECTO}$-αCD3-monomers and -dimers during expression. We successfully enhanced the fraction of γδ$_{ECTO}$-αCD3-dimers by shortening the linker length between the heavy and light chain in the anti-CD3 scFv, though this also decreased protein yield by 50%. Finally, we formally demonstrated with purified γδ$_{ECTO}$-αCD3-dimers and -monomers, that γδ$_{ECTO}$-αCD3-dimers are superior in function when compared to similar concentrations of monomers, and do not induce T cell activation without simultaneous tumor engagement. In conclusion, a γδ$_{ECTO}$-αCD3-dimer based GAB design has great potential, though protein production needs to be further optimized before preclinical and clinical testing.

Introduction

During the last decade, the introduction of immunotherapy has led to a significant improvement in treatment options for cancer patients. Many of these therapies aim to improve T lymphocyte mediated tumor recognition, for example by relieving the breaks on these cells by checkpoint inhibition, or by arming T cells with chimeric antigen receptors that induce cancer cell recognition [1]. Another opportunity to use T cells for cancer therapy arose from the discovery that T cells can be redirected to tumor cells by a bispecific hybrid antibody [2], and since this initial discovery, many different bispecific antibodies to redirect T cells towards tumor cells have been developed [3]. In general, bispecific antibodies combine a tumor binding domain, directed to a tumor associated antigen, with a T cell recruitment domain, most often binding to CD3ε. These bispecific antibodies, also called T cell engagers (TCE), can induce T cell mediated cytotoxicity towards tumor cells by simultaneously binding to the target antigen and CD3, without specific T cell receptor (TCR) - MHC engagement [4]. Blinatumomab, a TCE directed against CD19 and CD3 is the first TCE construct that is FDA approved for the treatment of patients with refractory or relapsed pre-B-acute lymphoid leukemia [5]. Recently a second TCE, Tebentafusp, targeting a gp100 peptide in HLA-A*02:01 and CD3, was FDA approved for the treatment of unresectable or metastatic uveal melanoma [6]. Next to these two TCEs, a plethora of novel TCEs with different designs and tumor targets is currently in various stages of clinical development [7, 8].

The majority of TCEs utilize antibody-derived tumor binding domains, in the form of single chain variable fragments, antigen binding fragments, or full length antibodies [9]. These antibody-derived binding domains can be engineered to bind to tumor associated antigens with very high affinity, which has been reported as beneficial for the development of highly potent TCEs [10, 11]. A challenge that remains, however, is the selection of novel suitable target antigens for TCEs. On-target off-tumor toxicity remains a concern for high affinity TCEs when low levels of the target antigen are expressed on healthy tissue [12].

Most recently, we have developed a novel TCE concept, so called **G**amma Delta TCR **a**nti-CD3 **B**ispecific molecules (**GABs**) by fusing ectodomains of a γδ T cell receptor (TCR) to an anti-CD3 single chain variable fragment ($γδ_{ECTO}$-αCD3) [13]. This concept is based on the anti-tumor activity of γ9δ2 T cells, which are important players in the recognition of foreign pathogens, virally infected cells, and also cancer cells [14]. Vγ9δ2 T cells, a specific γδT cell subset mainly found in the blood, recognize members of the butyrophilin (BTN) family, namely BTN2A1, through the gamma chain of their Vγ9δ2TCR, and additionally require BTN3A1 expression on the tumor cells for full activation[15-17]. Recognition of the BTN2A1-BTN3A1 complex is induced by an intra-cellular accumulation of phosphoantigens (pAg) that can bind to the intracellular B30.2 domain of BTN3A1, which is modulated by RhoB [18, 19].

5

pAg accumulation can be caused by microbial infection, but is also associated with cancerous transformation of cells [20]. *In vitro,* Vγ9δ2T cells recognize and lyse a broad spectrum of solid and hematological tumor cells [21, 22] and therefore provide an interesting tool box for the development of anti-cancer therapies [23]. However, the activity of Vγ9δ2T cells is diverse when analyzed in a clonal population [17], and can be hampered by many inhibitory receptors, like NKG2A [24].

GABs are a means to utilize the favorable clonal properties of natural Vγ9δ2T cells, and, by engaging mainly αβ T lymphocytes, make it possible to overcome the general poor functionally of Vγ9δ2T cells in advanced stage cancer patients. Furthermore, GAB mediated tumor recognition is independent of the mutational load or tumor associated antigen expression of the tumor cells, thus introduces a novel tumor targeting concept to the TCE field. This concept would also overcome extensive and expensive T cell engineering concepts with defined Vγ9δ2TCRs [23, 25].

Critical for the GAB concept remains the rather low affinity of the Vγ9δ2 TCR for its ligands, which has been reported in the µM range [15, 16], a couple of magnitudes lower than the high affinity antibody derived domains generally used for tumor binding in TCEs. For αβTCR based TCEs, like Tebentafusp, the consensus is that affinity maturation of the αβTCR from µM to pM is required to create a functional TCE [26]. While we have shown that for the GAB, affinity maturation of the γδTCR is not essential when naturally selected high affinity CDR3 sequences of the δ chain are used [13], we hypothesized that increasing the tumor binding avidity of the Vγ9δ2 TCR would further improve the effectivity of a GAB.

Most TCEs combine only one tumor- and one T cell engaging domain, similar to our original GAB design, however there are also higher valency constructs currently being developed [9, 27, 28]. Often the rationale behind the use of these higher valency constructs is to increase the potency of the TCE by increasing the tumor binding avidity rather than the direct affinity maturation of the tumor binding domain [29]. In this light, we report here on the failure and success of different strategies to create multivalent GABs, and show that while attempts to express the γ and δ variable domains as a single chain linked to an anti-CD3 single chain variable fragment (γδ$_{VAR}$αCD3) were not successful, we observed γδ$_{ECTO}$-αCD3-dimers as a side product during the production process with the original γδ$_{ECTO}$-αCD3 GAB design, incorporating the full length γδTCR ectodomains. Although it is a technical challenge to achieve meaningful yields of γδ$_{ECTO}$-αCD3-dimers, γδ$_{ECTO}$-αCD3-dimers have improved *in vitro* potency compared to the monomeric form, while there is no evidence for non-specific T cell activation by bivalent CD3 engagement.

Material and Methods

Generation of Bispecific constructs

Design of the original γδ$_{ECTO}$-αCD3 construct was reported previously [13]. To force dimerization, the 3(G4S) linker between the OKT3 variable heavy and light chain was replaced by a G4S linker. To create the γδ$_{VAR}$-αCD3, the variable domains of the γ and δ chain linked to an anti-CD3 single chain variable fragment were cloned into a modified pcDNA3 vector (kind gift from protein facility LTI; UMCU) using BswI and SalI restriction sites, containing a 3' biotin acceptor peptide and His-tag after the SalI restriction site. From the N- to C-terminus the γδ$_{VAR}$ –αCD3 had the following design, Vδ-3(G4S)-Vγ-3(G4S)-VH-3(G4S)-VL. For constructing the single chain γδ$_{VAR}$ the C-terminus of the Vδ chain was linked to the N-terminus Vγ chain by a flexible linker with the sequence GSADDAKKDAAKKDGKS. Unless indicated otherwise, the TCR sequences used for the GAB constructs are derived from CL5 TCR [30] (γδ$_{VAR}$ and γδ$_{VAR}$-αCD3) or AJ8 TCR (γδ$_{ECTO}$-αCD3) [13]. CDR3 sequences of all the TCRs used are indicated in Table 1. The anti CD3 single chain variable fragment (αCD3) was derived from the mAb OKT3 [31].

Cells and Cell lines

PBMCS were isolated by Ficoll-Paque (GE Healthcare, cat no. Cytvia 17-1440-03) from buffy coats obtained from Sanquin Blood Bank). αβT cells were expanded from PBMCs using CD3/CD28 dynabeads (Thermo Fisher scientific, cat no. 40203D) and 1.7×10^3 IU/ml of MACS GMP Recombinant Human interleukin IL-7 (Miltenyi Biotec, cat no. 130-095-361), and 1.5×10^2 IU/ml MACS GMP Recombinant Human IL-15 (Milteny Biotec, cat no. 130-095-762). HL60, RPMI 8226, and SSC9 stably expressing GFP-luciferase was generated by a previously described retroviral transduction protocol [30]. The plasmid containing the GFP and luciferase transgenes was kindly provided by Jeanette Leusen (UMC Utrecht, Utrecht, Netherlands). The following cell lines were obtained from ATCC between 2010 and 2018, HL60 (CCL-240), RPMI 8226 (CCL-155), SCC9 (CRL-1629) and Daudi (CCL-213). Freestyle 293-F cells (R790-07) were obtained from Invitrogen . ML-1, HL60, RPMI 8226 and Daudi were cultured in RPMI (Gibco, cat no. 12017599) , 10% FCS (Bodinco), 1% Pen/Strep (Invitrogen, cat no. 11548876). Freestyle 293-F in Freestyle expression medium (Gibco, cat no. 10319322). SCC9 in DMEM (Gibco, cat no. 31966047) 10% FCS, 1% Pen/Strep.

Expression and purification of Bispecifics

Bap and His-tagged γδ$_{VAR}$ –αCD3, γδ$_{VAR}$, or γδ$_{ECTO}$-αCD3 were expressed in 293 F cells. 293 F cells were cultured in Gibco Freestyle Expression medium, as transfection reagent Polyethylenimine (PEI) (25 kDa linear PEI, Polysciences, cat no. 23966-1) was used. Transfection was performed using 293 F cells at a density of 1.10^6 cells/ml mixed with 1.25 µg DNA, 3.75 µg PEI and per million cells. DNA and PEI were pre-

mixed in freestyle medium (1/30 of transfection volume), incubated for 20 minutes, and added dropwise to the cell cultures. The cultures were maintained shaking at 37 °C 5% CO_2. To biotinylate the protein during expression, a vector containing the bacterial biotin ligase BirA was added to the transfection mix (10% of total DNA), and six hours after transfection, the medium was supplemented with 100 µM Biotin. Cell culture supernatant was harvested after 5 days and filtered through a 0.22 µm filter top (Milipore, Cat no. S2GPT02RE). Supernatant was adjusted to 25 mM Tris (Sigma Aldrich, cat no. 1185-53-1), 150 mM NaCl (Sigma Aldrich, 7647-14-5) and 15 mM Imidazole (Merck, 288-32-4) (pH 8) and loaded on a 1 ml HisTrap HP column (GE healthcare, cat no. 17-5247-01) using the ÄKTA start purification system (GE healthcare). The column was washed with IMAC loading buffer (25 mM Tris,150 mM Nacl 15 mM Imidazole (pH 8), and protein was eluted using a linear imidazole gradient from 21 to 300 mM in 20 CV. Fractions containing the expressed protein were pooled, concentrated and buffer exchanged to TBS (25 mM tris, 150 mM NaCl, pH 8) using vivaspin 20 30kD spin columns (Sartorius, cat no. VS2022). Protein was diluted 100 times in IEX loading buffer (25 mM Tris pH 8), and loaded onto a HiTrap Q HP 1 ml column (GE healthcare, cat no. 17-1153-01) using the ÄKTA start purification system, for a second purification step. The column was washed with 10 column volumes IEX loading buffer, and protein was eluted using a linear NaCl gradient form 50 to 300 mM in 25 CV. Fractions containing the GAB were pooled, concentrated using vivaspin 20 30kD spin columns and examined by SDS-PAGE and staining with Instant blue protein stain (Sigma Aldrich, cat no. ISB1L). Protein concentration was measured by absorbance on Nanodrop and corrected for the Extinction coefficients. The protein was snap frozen and stored at -80°C and thawed before use.

Beads coated with variable domains of the γ and δ chains (γδ$_{VAR}$) for target cell staining

Biotinylated soluble γδ$_{VAR}$ was mixed with 5-7µm streptavidin-coated UV-beads (Spherotech) in excess to ensure fully coated beads, 10 µg γδ$_{VAR}$/mg microspheres. $7.5*10^4$ cells, ML1 or K562, were incubated with 20 µl γδ$_{VAR}$ -UV beads (0.33 mg beads/ml) for 30 minutes at RT. The mixtures were fixed by adding 20 µl 2% formaldehyde for 15 minutes. The samples were washed once with 1% formaldehyde and analyzed on a BD FACSCanto II (BD).

Size exclusion chromatography and Multi Angle light scattering (SEC/ SEC-MALS)

Size exclusion chromatography was perfomed on a Yarra 3 uM SEC 3000 column (Phenomenex) using the high Performance Liquid Chromatography system (Shimadzu). The column was washed with SEC running buffer (100 mM Sodium Phosphate 150 mM NaCl pH 6.8) before loading of the samples. Protein samples

were 5x diluted in SEC running buffer and filtered through a 0.22 μM centrifugal filter before loading on the column. For molecular weight characterization SEC was performed with online static light scattering (miniDAWN TREOS, Wyatt Technology) and differential refractive index (dRI, Shimadzu RID-10A) on a Shimadzu HPLC system. Data were analyzed using the ASTRA software suite v.6.1.5 (Wyatt Technology).

IFNγ ELISA/Elispot

15.000 (Elispot) or 50.000 (ELISA) effector cells and 50.000 target cells were incubated together with or without GAB (different concentrations) for 16 hours at 37 °C 5% CO_2. 30 or 100 μM pamidronate (calbiochem, cat no. 109552-15-0) was added to the target cells. For ELISA the supernatant was harvested after 16 hours, and the level of IFNγ was determined using the IFN gamma Human Uncoated ELISA Kit (Invitrogen, cat no. 15541107). For the Elispot assay the co-culture was done in nitrocellulose-bottomed 96-well plates (Millipore, cat no. MSIPN4550) precoated with α-IFNγ antibody (Mabtech, 3420-3-1000, clone 1-D1K 1:200). After 16 hours, the plates were washed with PBS and incubated with mAb7-B6-1 (II; Mabtech, cat no. 3420-6-1000) followed by Streptavadin-HRP (Mabtech, cat no. 3310-9) IFNγ spots were visualized with TMB substrate (Mabtech, cat no. 3651-10) and analyzed using A.EL.VIS ELISPOT Scanner and analysis software (A.EL.VIS).

Luciferase based cytotoxicity

5000 or 10000 target cells stably expressing luciferase were incubated with T cells at a 3:1 or 5:1 T cell to target cell ratio, with different $γδ_{ECTO}$-αCD3 concentrations (as indicated) in the presence of 30 or 100 μM pamidronate (calbiochem, cat no. 109552-15-0). After 16 hours, beetle luciferin (Promega, E1602) was added to the wells (125 μg/ml) and bioluminescence was measured on SoftMax Pro plate reader. The signal in treatment wells was normalized to the signal measured for targets and T cells only, which was assumed to represent 100% living cells.

Results

Variable domains of the γ and δ chains ($γδ_{VAR}$) are poorly expressed as a single chain fragment

The GAB design published to date is a fusion of ectodomains of a γδ T cell receptor (TCR) to an anti-CD3 single chain variable fragment ($γδ_{ECTO}$-αCD3) (Figure 1A) [13]. We next explored strategies to increase the valency of GABs, in an effort to further increase potency. Multivalent tumor binding could be achieved, for example, by generating shorter single chain variable fragments as tumor- and T cell binding domains, and linking these in tandem with the desired stoichiometry [32]. To test the feasibility of this approach, we constructed variable domains of the γ and

δ chain (γδ$_{VAR}$) linked to an anti-CD3 single chain variable (αCD3) fragment with 1:1 stoichiometry (γδ$_{VAR}$-αCD3) (Figure 1B). γδ$_{VAR}$-αCD3 and the αCD3 alone (as a positive control) were expressed in HEK293F cells, and protein production was evaluated on a SDS gel after His-tag purification. While there was a visible band for the αCD3 alone around 30kD, we did not observe expression of the γδ$_{VAR}$-αCD3, which is expected at 62kD (Figure 1B left panel). We were able to visualize a band for the γδ$_{VAR}$-αCD3 using Western blot, indicating that this design does result in expressed protein, but yields are not comparable to quantities produced for αCD3 alone (Figure 1B right panel).
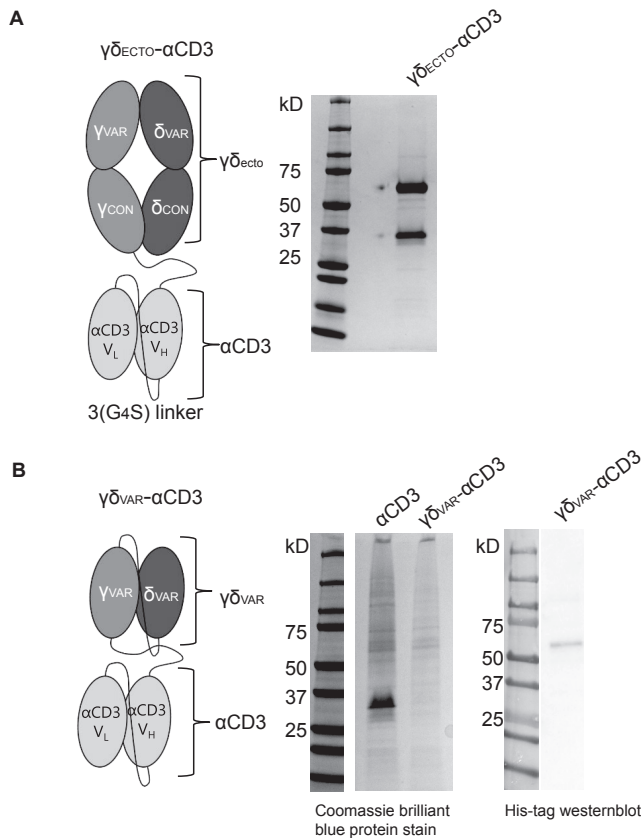
Figure 1. Expression of a γδ$_{VAR}$–αCD3 bispecific molecule A) Schematic representation of the γδ$_{ECTO}$-αCD3, showing the extracellular (ecto) γδTCR (top), with the TCRγ chain connected to an anti-CD3 single chain variable fragment (αCD3) with the variable light (V$_L$)and heavy (V$_H$) and light chain (bottom) via a flexible linker. Purified GAB was run on SDS-page gel and stained with coomassie brilliant blue protein stain: visualizing the ectoγ-CD3scFV (59kD) and ectoδ chain (26 kD). B) Schematic representation of the γδ$_{VAR}$–αCD3 with the Vδ-Vγ single chain TCR fragment (scTv) (top) linked to an anti-CD3 scFv (bottom) via a flexible linker. After HIS-tag purification the CD3scFv and γδ$_{VAR}$–αCD3 samples were run on SDS gel and visualized with coomassie brilliant blue protein stain. (left) or His-Tag westernblot (right)

Stabilizing mutations reported from αβ variable T cell receptor single chains increase expression of γδ$_{VAR}$-αCD3 by three-fold.

For αβTCR-derived single chains, expression yields are often very low compared to antibody-derived single chains, due to aggregation and misfolding of the protein [32]. Therefore, introduction of stabilizing mutations is, in general, required to achieve successful expression of αβTCR-derived single chains [33-35]. These stabilizing mutations are often unique for each TCR, and are usually identified by large random mutagenesis PCR screens. In an attempt to identify a more broadly applicable engineering strategy, Richman et al compared stabilizing mutations found for several different αβTCR-derived single chains, and identified amino acids that were mutated in more than one stabilized αβTCR-derived single chain [34]. To determine which of the regular occurring stabilizing mutation in single chain αβTCR would be suitable to include in our γδ$_{VAR}$, we aligned the sequences of variable domains of αβTCR 2C (PDB 1TCR) and γδTCR G115 (PDB 1HXM) (Supplementary Figure 1A) and their corresponding protein structures in PyMOL. Based on the location and chemical environment of the residues in the γδTCR and the potential benefit of mutations that are present in single chain αβTCRs, we selected six mutations to introduce in the γδTCR variable chains (γδ$_{VAR-MUT}$) (Supplementary Figure 1B). Three out of five mutations in the gamma chain were localized in the region of the variable domain that interacts with the constant domain in the full length TCR. These three mutations have the potential to either change polarity/hydrophobicity (γK$_{13}$V in orange and γI$_{99}$S blue) or flexibility (γV$_{49}$E in green) of the variable gamma chain (Supplementary Figure 1B) [34]. Two other gamma chain mutations (γV$_{49}$E in blue and γI$_{50}$L in red) plus the delta chain mutation (δM$_{50}$P in red) are located in in the variable γ- variable δ interface (in red, Supplementary Figure 1B).

γδ$_{VAR}$-αCD3 and γδ$_{VAR-MUT}$-αCD3 were expressed in HEK293F cells, and protein production was evaluated by western blot (Figure 2A). Introduction of the six mutations approximately tripled the expression yield of γδ$_{VAR-MUT}$-αCD3 when compared to γδ$_{VAR}$-αCD3 (Figure 2B). Despite the rather modest increase in expression by only threefold, we next performed a large-scale production and purification of the γδ$_{VAR-MUT}$-αCD3 (Figure 2C). To assess activity, the purified γδ$_{VAR-MUT}$-αCD3 and γδ$_{ECTO}$-αCD3 (as a positive control) were added to a co-culture of T lymphocytes, and the target cell line Daudi, previously shown to be recognized by γ9δ2 T cells [36]. The unrecognized cell line ML-1 was used as a negative control, and additionally the Daudi cells were treated with the mevalonate pathway inhibitor pamidronate (PAM) to enhance γ9δ2TCR mediated recognition [30]. While the γδ$_{ECTO}$-αCD3 only induced T cell activation against Daudi cells treated with PAM (Figure 2D), the γδ$_{VAR-MUT}$-αCD3 did not induce differential recognition of the target cell lines (Figure 2E). In one experiment the γδ$_{VAR-MUT}$-αCD3 induced nonspecific T cell activation, which could imply the presence of larger protein aggregates

5

that can trigger T cell activation without target cell engagement. Size exclusion chromatography (SEC) of γδ$_{VAR-MUT}$-αCD3 protein confirmed that in addition to the monomeric γδ$_{VAR-MUT}$-αCD3 peak at 9 minutes, a large proportion of the γδ$_{VAR-MUT}$-αCD3, ~25%, was eluted before this monomeric peak, indicative of aggregated γδ$_{VAR-MUT}$-αCD3 (Figure 2F).
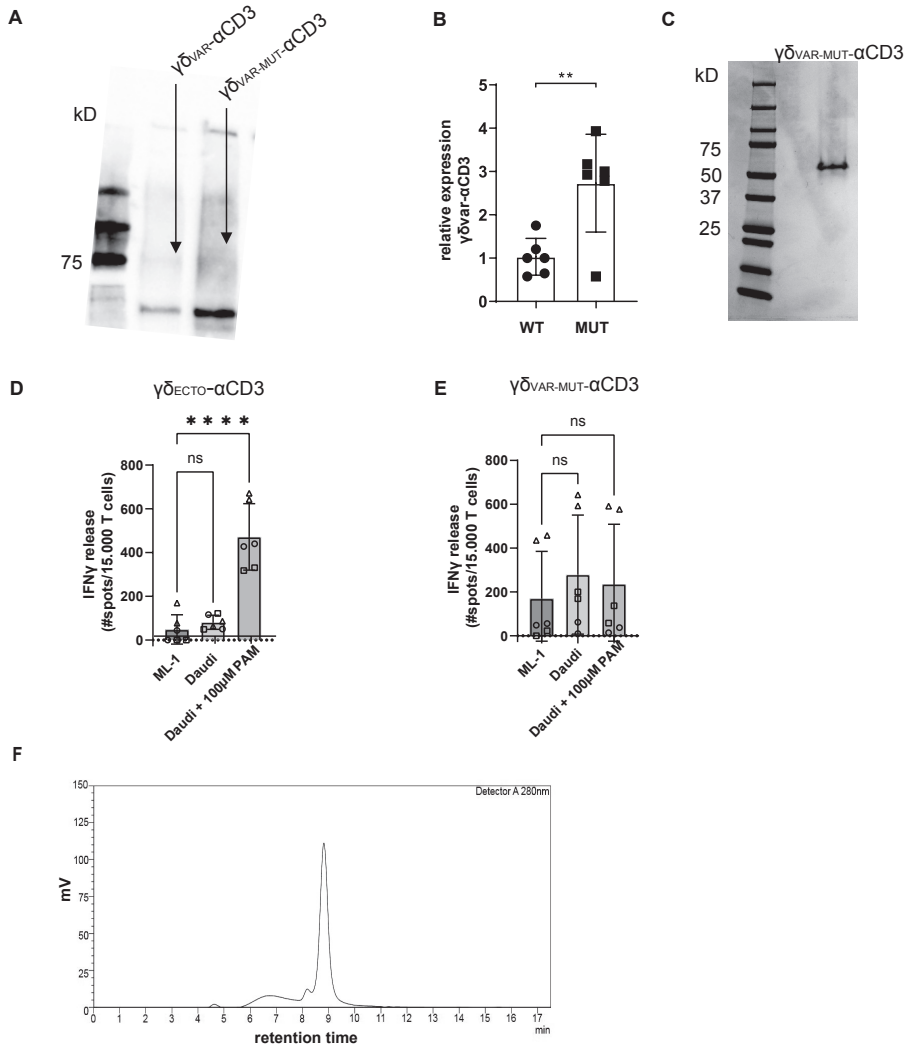
Figure 2. γδ$_{VAR-MUT}$–αCD3 does not redirect T cells to tumor cells A) γδ$_{VAR}$–αCD3 WT or with six stabilizing mutations, were expressed in HEK293F cells, and protein expression was visualized using His-Tag westernblot. B) Expression of γδ$_{VAR}$–αCD3 6mut relative to the WT γδ$_{VAR}$–αCD3. N=6 error bars represent SD, significance was calculated using an unpaired T-test **= p≤ 0.01. C) SDS-PAGE analysis of purified

γδ$_{VAR-MUT}$–αCD3. D\E) T lymphocytes were co-incubated with D) γδ$_{ECTO}$-αCD3 or E)γδ$_{VAR-MUT}$–αCD3 (5-10 µg/ml) and target cells ML-1 or Daudi, -/+ 100 µM pamidronate (PAM). IFNγ release was measured by ELISPOT. The different symbols represent three different experiments (two technical replicates). N=3, error bars represent SEM, significance was calculated using one-way ANOVA, ****= ≤ 0.0001 ns=not significant p>0.5. F) Size exclusion chromatogram of the γδ$_{VAR-MUT}$–αCD3.

To assess the expression and folding properties of the γδ$_{VAR-MUT}$ specifically, γδ$_{VAR-MUT}$ was expressed in HEK293F cells and purified using ion exchange chromatography. The γδ$_{VAR-MUT}$ was eluted in several peaks (Figure 3A), indicating that there is a variation in the physical properties of the protein, which could have an influence on its functionality. When the different fractions were evaluated on SDS gel, all contained the γδ$_{VAR-MUT}$ (Figure 3B). We have previously shown that it is possible to assess γ9δ2 TCR binding to target cells by coating soluble γδ$_{ECTO}$ on fluorescent streptavidin beads and evaluation of bead binding by flow cytometry [17]. To test the γδ$_{VAR-MUT}$ in the different elution peaks for binding activity, the protein fractions corresponding to the separate peaks were coated on fluorescent streptavidin beads and assessed for K562 target cell binding by flow cytometry, ML-1 cells were used as a negative control. No staining was observed for beads coated with any of the γδ$_{VAR-MUT}$ elution peaks of the two cell lines, while beads coated with γδ$_{ECTO}$ specifically stained K562 cells and not the negative control cell line ML-1 (Figure 3C and D). Based on these results we can conclude that, similar to previous findings for αβTCR-derived single chains, in order for a γδ$_{VAR}$-αCD3 to be expressed and functional, extensive work would have to be performed to stabilize the γδ variable domain single chain format.

γδ$_{ECTO}$-αCD3 -dimer formation occurs naturally and is impacted by the linker length between the heavy and light chain of αCD3

As alternative strategy to increase valency of GABs, we next considered possibilities to generate a multivalent GAB by using the original γδ$_{ECTO}$-αCD3 design (Figure 1A). It has been reported previously that single chain fragments can cause protein oligomerization due to inter-chain variable heavy and light chain interactions, instead of the intended intra-chain heavy and light chain association (Figure 4A) [37, 38]. To test whether the current γδ$_{ECTO}$-αCD3 design harboring an anti-CD3 single chain variable fragment with the heavy and light chain linked with a 3(G4S) flexible linker (γδ$_{ECTO}$-αCD3) results in multimerization of the γδ$_{ECTO}$-αCD3 molecules, γδ$_{ECTO}$-αCD3 were analyzed, using size exclusion chromatography (SEC) (Figure 4B). The SEC chromatogram of γδ$_{ECTO}$-αCD3 showed three peaks, with the peak at the highest retention time (peak 3) containing the most protein, implying that there are indeed more size variants in the protein product. Separate analysis of the two major protein peaks (2 and 3) on SDS-PAGE showed the presence of both protein chains in the peaks, with no difference in relative signal intensity between the chains (Supplementary Figure 2A). The SEC was repeated with different protein batches, always resulting in a similar chromatogram, with a comparable ratio between

the percentage area under the curve (AUC) of the 2 major peaks (Supplementary Figure 2B). Furthermore, varying the TCR sequence either by changing the CDR3 region of the Vδ2 or the complete Vγ9 or Vδ2 chain (Clone 5, 6_2, EPCR-reactive γδTCR) in the γδ$_{ecto}$-αCD3, did not influence the ratio of percentage AUC of the two size variants (Table 1 and Supplementary Figure 2C).

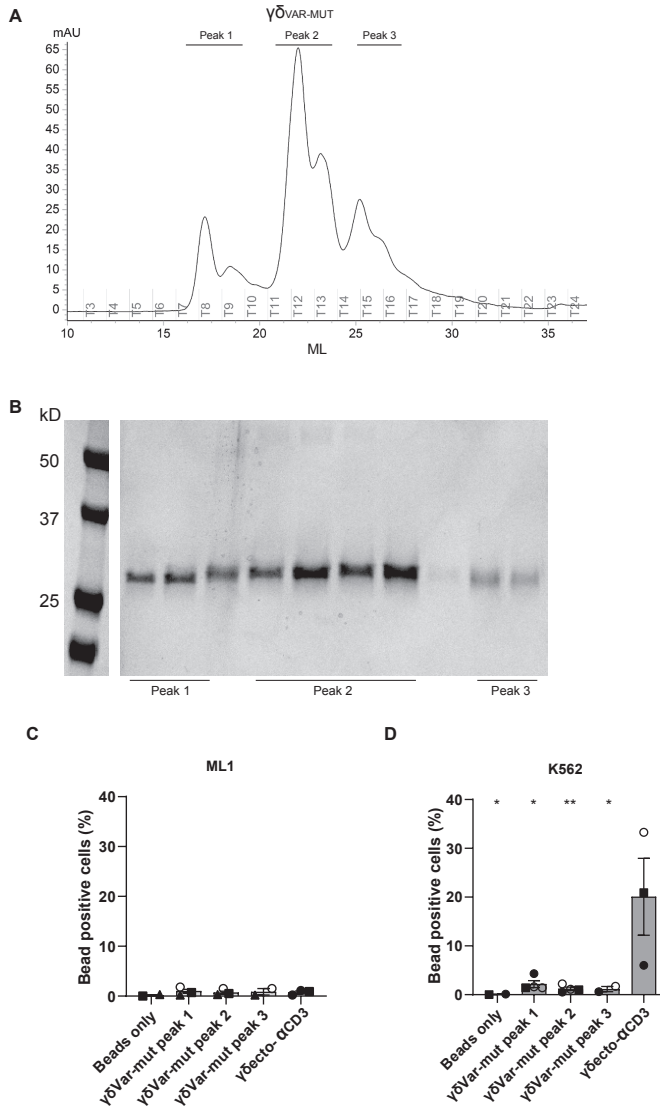**Figure 3. Expression and misfolding of single chain γδ$_{VAR-MUT}$.** A) γδ$_{VAR}$ with stabilizing mutations (γδ$_{VAR-MUT}$) were expressed in HEK29F cells and purified using ion exchange chromatography B) the different protein elution fractions after ion exchange chromatography (IEX) were run on SDS gel and visualized

To determine the size of the GAB variants in both peaks we first used SEC-reference standards, containing 5 different molecules with known molecular weight. Based on the calibration curve the GAB variant peak 2 would have a molecular weight of around 310 kDa and the GAB variant in peak 3 would have a molecular mass of around 115 kDa (Supplementary Figure 2D). Assuming that the peak 3 would contain monomeric GAB, with a theoretical molecular mass of 85 kDa, this number deviates substantially. These large deviations in molecular mass are not uncommon when using SEC as the retention time is not only dictated by the size of the protein, but also by the shape [39]. To formally determine the exact size of the γδ$_{ECTO}$-αCD3 protein in the SEC peaks, we performed size exclusion chromatography with multi angle light scattering (SEC-MALS). The MALS analysis provided the molar masses for the 2 major sized peaks, with peak 2 consisting of a protein with a molar mass 176.7 kDa, and peak 3 of a protein with a molar mass of 88.45 kDa, corresponding to dimeric and monomeric γδ$_{ECTO}$-αCD3 respectively (Supplementary Figure 2E), the small deviation from the theoretical molar mass, 171 kDa and 85.5 kDa, can be attributed to N-linked glycosylation of γδ$_{ECTO}$-αCD3 (Supplementary Figure 2F). While not determined in the SEC-MALS analysis, due to the small size, this means that peak 1 most likely contains trimerized γδ$_{ECTO}$-αCD3.

One of the factors influencing the single chain folding is the length of the linker between the two variable chains, with shorter linkers sterically hindering intra-chain interaction and thereby promoting inter-chain interactions (Figure 4A). Therefore, the flexible linker between the heavy and light chain of αCD3 was shortened from 15 to 5 amino acids (3(G4S) to G4S, γδ$_{ECTO}$-αCD3$_{G4S}$). After production and purification, a sample of the γδ$_{ECTO}$-αCD3$_{G4S}$ was analyzed by SEC (Figure 4C), showing an increase in the relative amount of dimeric γδ$_{ECTO}$-αCD3$_{G4S}$ to over 50% of the total protein.

We conclude that it is possible to enhance the formation of naturally dimerized γδ$_{ECTO}$-αCD3 from approximately 20%, to over 50% by decreasing the linker length. Of note, there was no clear indication that larger aggregated oligomers, which could potentially cause non-specific T cell activation as seen for the γδ$_{VAR}$-αCD3, are present in either γδ$_{ECTO}$-αCD3 product.

5

A

αCD3 intra-chain fold   αCD3 inter-chain fold

3(G4S) linker   G4S linker

B

γδ$_{ECTO}$-αCD3

Detector A 280nm

mV

retention time

peak	1	2	3
retention time	6.76	7.23	8.25
area fraction %	1.4%	24%	74.5%

C

γδ$_{ECTO}$-αCD3$_{G4S}$

Detector A 280nm

mV

retention time

peak	1	2	3
retention time	6.76	7.23	8.31
area fraction %	9.2%	56.3%	34.5%
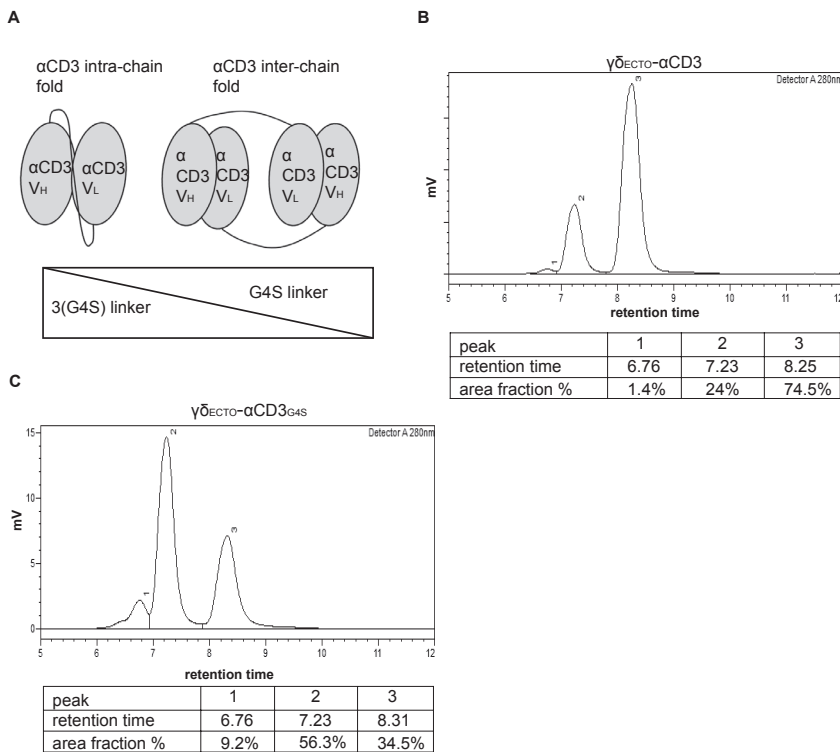
Figure 4. γδ$_{ECTO}$-αCD3-dimers are formed by αCD3 dimerization, which is influenced by linker length between the heavy and the light chain. A) schematic representation of αCD3 either folded by with intra-chain interaction (left) or with inter-chain interaction of two αCD3s (right). B+C) Size exclusion chromatography of γδ$_{ECTO}$-αCD3 comprising the linker 3(G4S) (B) or γδ$_{ECTO}$-αCD3$_{G4S}$ (C).

γδ$_{ECTO}$-αCD3$_{G4S}$ production is less efficient than γδ$_{ECTO}$-αCD3

Unfortunately, although the shorter G4S linker led to a higher percentage of dimer formed during protein expression, it also decreased total protein expression, as shown in a side by side comparison of expression medium of γδ$_{ECTO}$-αCD3 and γδ$_{ECTO}$-αCD3$_{G4S}$ by western blot (Figure 5A). On average, the relative expression of the γδ$_{ECTO}$-αCD3$_{G4S}$ compared to γδ$_{ECTO}$-αCD3 was decreased by two-fold, meaning that overall, while the G4S linker approximately doubles the proportion of formed dimer, it also causes a two-fold decrease in protein expression.

γδ$_{ECTO}$-αCD3-dimers are functionally superior to monomers

Despite the lower efficiency in the production of γδ$_{ECTO}$-αCD3$_{G4S}$ compared to γδ$_{ECTO}$-αCD3, we tested whether, without further purification of the monomer and dimer fraction, differences in the activity between both constructs could be

observed. $\gamma\delta_{ECTO}$-αCD3 and $\gamma\delta_{ECTO}$-αCD3$_{G4S}$ were therefore titrated in a co-culture of T lymphocytes and SCC9 target cell line, and IFNγ release was determined by ELISPOT (Figure 5B). The $\gamma\delta_{ECTO}$-αCD3$_{G4S}$ showed a slight increase in functional avidity, defined as IFNγ release, compared to the $\gamma\delta_{ECTO}$-αCD3, probably due to the higher percentage of dimer present in the $\gamma\delta_{ECTO}$–αCD3$_{G4S}$ protein product. Next, we also tested the $\gamma\delta_{ECTO}$-αCD3 and $\gamma\delta_{ECTO}$-αCD3$_{G4S}$ for direct target cell killing, using a luciferase-based cytotoxicity assay. Luciferase transduced target cell lines (RPMI8226 and SCC9) were co-cultured with T cells and different concentrations of $\gamma\delta_{ECTO}$-αCD3 and $\gamma\delta_{ECTO}$-αCD3$_{G4S}$, and the amount of viable cells was determined (Figure 5C). Again, we observed a slight, but not significant, increase in target cell killing of the $\gamma\delta_{ECTO}$-αCD3$_{G4S}$ compared to $\gamma\delta_{ECTO}$-αCD3.
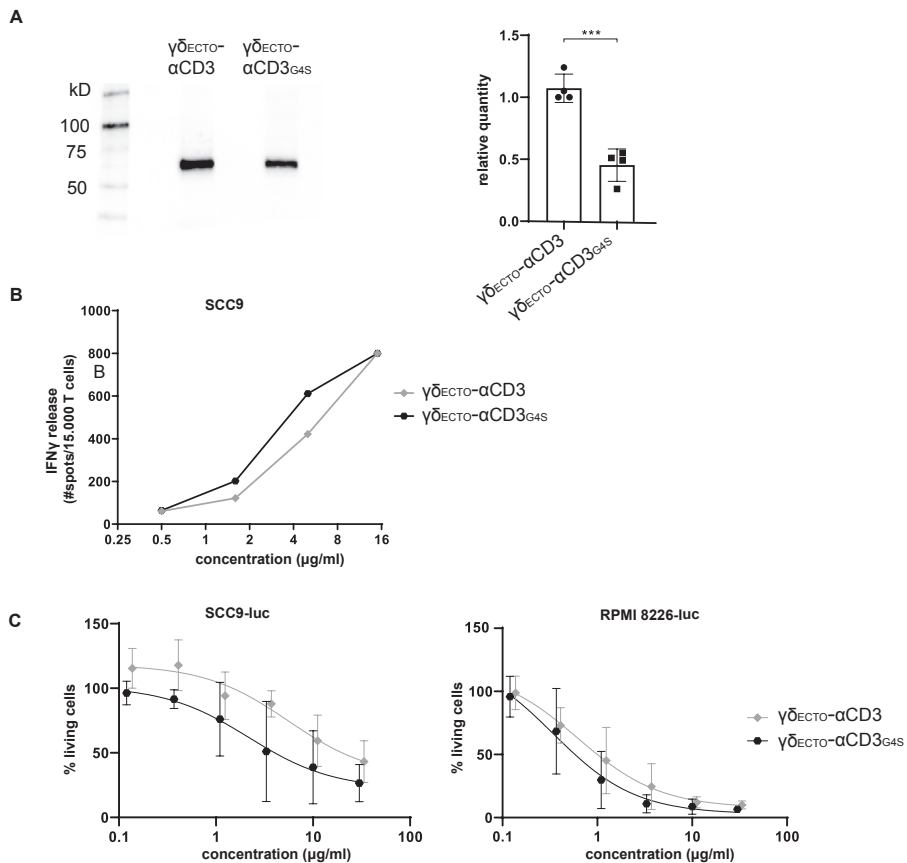
Figure 5. Functionality and expression of $\gamma\delta_{ECTO}$-αCD3 and $\gamma\delta_{ECTO}$-αCD3$_{G4S}$. A) Westernblot of unpurified expression medium with $\gamma\delta_{ECTO}$-αCD3 and $\gamma\delta_{ECTO}$-αCD3$_{G4S}$ GAB. The γ_{ECTO}αCD3 chain is visualized by α-HIS westernblot. Representative blot is shown in the left panel, graph showing relative quantity determined in four independent blots is shown on the right B) T lymphocytes were co-incubated with SCC9 target cells

in the presence of PAM (100 µM) and γδ$_{ECTO}$-αCD3 or γδ$_{ECTO}$-αCD3$_{(G4S)}$ (0.5-15 µg/ml) overnight. IFNy was measured by ELISPOT C) Effector and luciferase transduced RPMI 8226 were co-incubated for 16 hours in the presence and absence of γδ$_{ECTO}$-αCD3 or γδ$_{ECTO}$-αCD3$_{(G4S)}$ at different concentrations and PAM (30 µM). Percentage viable cells was determined by comparing luminescence signal to the untreated condition, representing 100% viability. N=4 (A), N=2 (B), N=4 (C), error bars represent SD. Significance was calculated using an unpaired T-test *** =P≤ 0.001

We hypothesized that the lack of significance in activity was most likely a consequence of the still rather limited difference in the amount of dimers (20% and 50% dimer; Figure 4B-C), which made it difficult to formally asses the true value of dimers, when compared to monomers. As the shortening of the G4S linker also significantly decreased the expression efficiency of the γδ$_{ECTO}$-αCD3 protein, we decided to assess the impact of purified dimer and monomer fractions derived from the original design, namely γδ$_{ECTO}$-αCD3.

Preparative size exclusion chromatography was used to separate monomeric and dimeric γδ$_{ECTO}$-αCD3. As dimeric γδ$_{ECTO}$-αCD3 are, in theory, not only bivalent for tumor binding, but also for CD3 binding, the binding properties of monomeric and dimeric γδ$_{ECTO}$-αCD3 to T lymphocytes were first evaluated. Purified monomeric and dimeric γδ$_{ECTO}$-αCD3 were titrated and incubated with T lymphocytes, followed by a secondary staining using fluorochrome labeled panγδ-TCR antibody (Figure 6A). A comparison of the MFI between the dimer and the monomer showed an increase in T cell binding at lower γδ$_{ECTO}$-αCD3 concentrations for the dimeric form, compared to the monomer. This could be attributed to an increase in the CD3 binding avidity of the dimer protein, but might also be partially explained by the presence of two binding epitopes for the panγδ-TCR antibody in each dimeric γδ$_{ECTO}$-αCD3.

To test whether dimeric GABs are more potent than monomeric GABs to specifically activate T lymphocytes, we titrated monomeric or dimeric γδ$_{ECTO}$-αCD3 in a co-culture with T cells and target cells, either the non-recognized cell line HL60 [36] or one of the previously used recognized cell line RPMI8226 or SCC9. This titration showed that the dimeric γδ$_{ECTO}$-αCD3 was more potent compared to monomeric γδ$_{ECTO}$-αCD3, inducing more IFNγ release compared to monomer in a co-culture with recognized target cells, RPMI8226 and SCC9, while no IFNγ release was detected in the presence of the non-recognized target cell line HL60 for either dimeric or monomeric γδ$_{ECTO}$-αCD3 (Figure 6B). IFNγ release by T cells was significantly increased for dimeric γδ$_{ECTO}$-αCD3 at concentrations ≥ 0.6 µg/ml when co-cultured with RPMI8226 and SCC9 (Figure 6C).

A luciferase based killing assay was performed to directly compare the dimers and monomers of γδ$_{ECTO}$-αCD3 for the ability to induce target cell lysis. Luciferase transduced HL60, RPMI8226, and SCC9 targets cells were co-cultured with T cells

and an increasing protein concentration. Neither monomeric nor dimeric γδ$_{ECTO}$-αCD3 did induce T cell mediated killing of the non-recognized target cell line HL60, in line with the lack of T cell activation in the cytokine release assay. Dimeric γδ$_{ECTO}$-αCD3 induced more target cell killing at lower protein concentrations for both tested recognized target cell lines RPMI8226 and SCC9, while monomeric γδ$_{ECTO}$-αCD3 induced efficient target cell lysis only at higher concentrations (Figure 6D), which is also reflected in the significant difference in EC$_{50}$ between γδ$_{ECTO}$-αCD3 monomer and dimer (Figure 6E). In conclusion, our data shows that increasing the avidity of the γδTCR binding in the GAB format enhanced the potency *in vitro,* with the dimeric form of γδ$_{ECTO}$-αCD3 being superior to the monomeric form. Furthermore, bivalent CD3 engagement alone does not cause T cell activation, but requires target cell engagement.

5

A

γδECTO-αCD3	EC$_{50}$ µg/ml	95% CI µg/ml
monomer	3.22	1.225 to 4.829
dimer	0.17	0.06422 to 0.4118

B

C

D

E
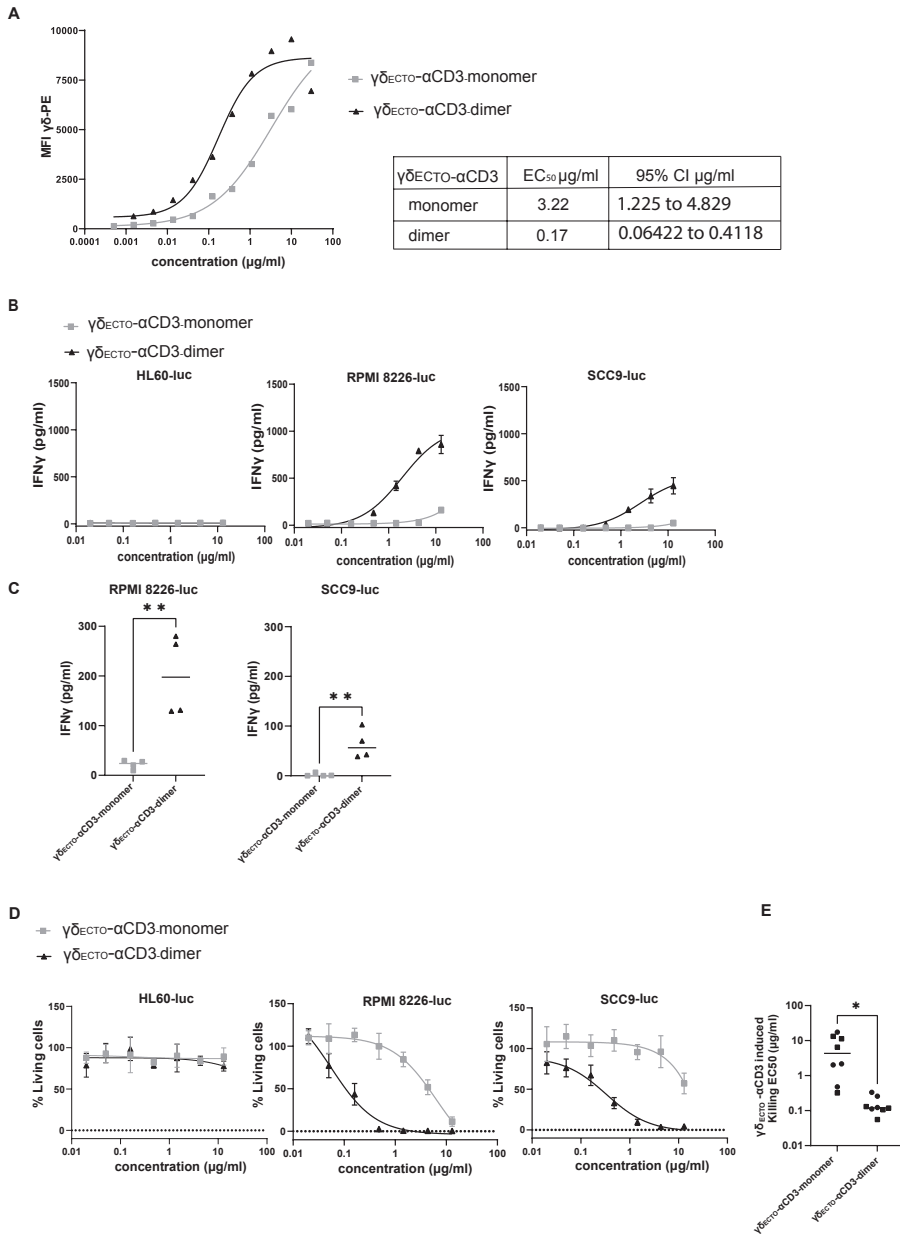
Figure 6. γδ$_{ECTO}$-αCD3-dimers are functionally superior A) Coating of T lymphocytes with γδ$_{ECTO}$-αCD3-monomers or dimers, followed by staining with fluorochrome labeled anti pan-γδ antibody. MFI was measured by flow cytometry, representative figure is shown N=3. B) T cells were incubated with target cells, PAM (30 µM) and γδ$_{ECTO}$-αCD3-monomers or dimers (0.02-15 µg/ml) for 20 hours. IFNγ release was measured by ELISA. Plots present mean + SD of duplicates of a representative assay, N=4 for all cell lines. C) IFNγ release at a γδ$_{ECTO}$-αCD3 concentration at 0.6 µg/ml (as in B) for RPMI8226-luc and SCC9-

luc. Unpaired t test was used to determine significance between the γδ$_{ECTO}$-αCD3 monomer and dimer conditions, ** P-value <0.01 (GraphPad Prism). Each dot represents the mean of biological replicates. D) T lymphocytes and luciferase transduced HL60, RPMI8226, and SCC9 target cells were co-incubated for 20 hours in the presence and absence of γδ$_{ECTO}$-αCD3-monomers or dimers at different concentrations and PAM (10 µM) at an E:T ratio of 5:1. Percentage viable cells was determined by comparing luminescence signal to the no GAB condition, representing 100% viability. Plots present mean + SD of triplicates of a representative assay, N=4 for all cell lines. E) EC$_{50}$ for each killing assay was determined in GraphPad Prism for RPMI8226-luc and SCC9-luc. Unpaired t test was used to determine significance between the γδ$_{ECTO}$-αCD3 monomer and dimer conditions, * P-value <0.05 (GraphPad Prism).

Discussion

In this report we have explored different possibilities to increase the binding valency of previously described GABs [13]. We show that dimers are a natural by-product of the recently reported γδ$_{ECTO}$-αCD3 design, and that γδ$_{ECTO}$-αCD3-dimers have higher activity when compared to γδ$_{ECTO}$-αCD3-monomers. However, all efforts to generate meaningful amounts of γδ$_{ECTO}$-αCD3-dimers, and strategies to increase valency by generating single chain formats derived from the variable domains the of the γδTCR (γδ$_{VAR}$-αCD3) were jeopardized by the lack of efficiency, and misfolding during protein production.

Identifying a means to increase valency of the GABs without compromising protein yields will be critical for further clinical translation, in order to guarantee sufficient amounts of protein during GMP-grade production, and to enter a clinical trial with the most active compound. There are several other TCEs described in literature that are multivalent in tumor binding, for example tandem diabodies [40] with two separate chains interacting to form four linked single chain variable fragments, or immunoglobulins with one or two extra antigen binding fragments attached [41, 42]. These designs are, however, not easily translated to the GAB format, as we have shown here that the expression yield of a single chain γδ$_{VAR}$ was very low, and most of the expressed single chain γδ$_{VAR}$ was misfolded and not functional. This is not surprising, given the long journey required to develop stabilized αβTCR-derived single chains [33-35]. While we have shown that the introduction of mutations, based on stabilizing mutations for αβTCR-derived single chains, increased expression efficiency of γδ$_{VAR}$ three-fold, further attempts to stabilize the single chain γδ$_{VAR}$ will be needed. Due to the inherent differences in sequence between variable domains of the αβ and γδ chains, non-optimal choices might have been made.

We next focused on the original γδ$_{ECTO}$-αCD3 design because of its sufficient stability, and observed spontaneous formation of monomers and dimers during expression. γδ$_{ECTO}$-αCD3-dimers are most likely formed by dimerization of αCD3 domains from two γδ$_{ECTO}$-αCD3 molecules. This assumption was supported by our observation that dimer formation could be enhanced by shortening the linker length between the variable heavy and light chain of the αCD3 fragment

5

(γδ$_{ECTO}$-αCD3$_{G4S}$). With a linker of 15 amino acids 20% of the γδ$_{ECTO}$-αCD3 protein was dimerized, which could be increased to over 50% by decreasing the linker length to only 5 amino acids in γδ$_{ECTO}$-αCD3$_{G4S}$. The functional benefit of increased dimerization of the γδ$_{ECTO}$-αCD3$_{G4S}$ was rather limited, and significant functional benefits could only be observed for γδ$_{ECTO}$αCD3-dimers when comparing purified dimers with purified monomers. Introduction of the shorter linker also decreased expression efficiency of the γδ$_{ECTO}$-αCD3$_{G4S}$, which could be because this shorter linker is also more prone to cause larger misfolded oligomers that will be excluded during protein purification [37]. Further clinical testing and development of the multivalent GABs using this αCD3 dimerized format is therefore not feasible. Addition of a dimerization domain to the C terminus of the αCD3 to induce association of two monovalent γδ$_{ECTO}$-αCD3 to form a dimer, as reported for other TCEs, could be a more efficient alternative [27, 43, 44].

Common dimerization domains cause symmetric dimerization of two identical molecules, thereby inducing a symmetric multivalent γδ$_{ECTO}$-αCD3 containing two tumor engaging- and two CD3 binding domains. We have shown in this report that the dimerized αCD3 of γδ$_{ECTO}$-αCD3 did not result in a non-specific T cell activation, in line with observations for other TCE harboring two CD3 binding domains [40, 44]. However, dual CD3 engagement and the risk for subsequent target cell independent T cell activation remains a concern in the field, and needs to be thoroughly investigated when designing a next generation of TCEs [29]. In this light, the dock-and-lock method would be an interesting strategy to explore for the creation of a 2:1 valency GAB [43].

Despite the fact that our data imply that dimers are the preferred choice for further exploration to improve the potency of GABs, a potential downside of the introduction of additional multimerization domains in the GAB is that these larger multimers might substantially increase the space between the tumor- and CD3-binding domains, which could lead to a decreased activation efficacy, due to suboptimal immune synapse distances. The remarkable high potency of the FDA approved TCE blinatumomab is partially attributed to its small size, causing the formation of very tight immune synapses that are indistinguishable from naturally formed TCR-MHC synapses after target and T cell engagement [45]. The overall effect of TCE size on efficacy is, however, also dependent on the exact binding epitope on the ligand. Chen et al. showed that while a smaller TCE was more efficient when binding to a membrane distal epitope, this effect was reversed when the binding epitope was more membrane proximal [46]. As the exact binding mechanism and ligands for the γ9δ2 TCR are not yet completely elucidated [17], the optimal size and design for GABs is hard to predict, and is probably best determined by an experimental approach.

In conclusion, our data imply that dimerization of GAB is an interesting strategy for further preclinical development, however the road towards clinical translation is challenging, as engineering meaningful yields of dimers remains challenging.

Acknowledgements

Funding

Conflict of interest statement

JK reports grants from Gadeta, Novartis, and Miltenyi Biotech and is the inventor on patents dealing with γδT cell related aspects, as well as the co-founder and shareholder of Gadeta. EvD and DB are inventor on patents dealing with γδT cell-related aspects. The remaining authors declare that the research was conducted in the absence of any commercial or financial relationships that could be construed as a potential conflict of interest

5

References

1. Waldman AD, Fritz JM, Lenardo MJ. A guide to cancer immunotherapy: from T cell basic science to clinical practice. Nat Rev Immunol. 2020;20(11):651-68.

2. Staerz UD, Bevan MJ. Hybrid hybridoma producing a bispecific monoclonal antibody that can focus effector T-cell activity. Proc Natl Acad Sci U S A. 1986;83(5):1453-7.

3. Trabolsi A, Arumov A, Schatz JH. T Cell-Activating Bispecific Antibodies in Cancer Therapy. J Immunol. 2019;203(3):585-92.

4. Brischwein K, Parr L, Pflanz S, Volkland J, Lumsden J, Klinger M, et al. Strictly target cell-dependent activation of T cells by bispecific single-chain antibody constructs of the BiTE class. J Immunother. 2007;30(8):798-807.

5. Przepiorka D, Ko CW, Deisseroth A, Yancey CL, Candau-Chacon R, Chiu HJ, et al. FDA Approval: Blinatumomab. Clin Cancer Res. 2015;21(18):4035-9.

6. Nathan P, Hassel JC, Rutkowski P, Baurain JF, Butler MO, Schlaak M, et al. Overall Survival Benefit with Tebentafusp in Metastatic Uveal Melanoma. N Engl J Med. 2021;385(13):1196-206.

7. Labrijn AF, Janmaat ML, Reichert JM, Parren P. Bispecific antibodies: a mechanistic review of the pipeline. Nat Rev Drug Discov. 2019;18(8):585-608.

8. Thakur A, Huang M, Lum LG. Bispecific antibody based therapeutics: Strengths and challenges. Blood Rev. 2018;32(4):339-47.

9. Brinkmann U, Kontermann RE. The making of bispecific antibodies. MAbs. 2017;9(2):182-212.

10. Root AR, Cao W, Li B, LaPan P, Meade C, Sanford J, et al. Development of PF-06671008, a Highly Potent Anti-P-cadherin/Anti-CD3 Bispecific DART Molecule with Extended Half-Life for the Treatment of Cancer. Antibodies (Basel). 2016;5(1).

11. Ellwanger K, Reusch U, Fucek I, Knackmuss S, Weichel M, Gantke T, et al. Highly Specific and Effective Targeting of EGFRvIII-Positive Tumors with TandAb Antibodies. Front Oncol. 2017;7:100.

12. Middelburg J, Kemper K, Engelberts P, Labrijn AF, Schuurman J, van Hall T. Overcoming Challenges for CD3-Bispecific Antibody Therapy in Solid Tumors. Cancers (Basel). 2021;13(2).

13. van Diest E, Hernández López P, Meringa AD, Vyborova A, Karaiskaki F, Heijhuurs S, et al. Gamma delta TCR anti-CD3 bispecific molecules (GABs) as novel immunotherapeutic compounds. J Immunother Cancer. 2021;9(11).

14. Bonneville M, O'Brien RL, Born WK. Gammadelta T cell effector functions: a blend of innate programming and acquired plasticity. NatRevImmunol. 2010;10(7):467-78.

15. Rigau M, Ostrouska S, Fulford TS, Johnson DN, Woods K, Ruan Z, et al. Butyrophilin 2A1 is essential for phosphoantigen reactivity by γδ T cells. Science. 2020;367(6478).

16. Karunakaran MM, Willcox CR, Salim M, Paletta D, Fichtner AS, Noll A, et al. Butyrophilin-2A1 Directly Binds Germline-Encoded Regions of the Vγ9Vδ2 TCR and Is Essential for Phosphoantigen Sensing. Immunity. 2020;52(3):487-98.e6.

17. Vyborova A, Beringer DX, Fasci D, Karaiskaki F, van Diest E, Kramer L, et al. γ9δ2T cell diversity and the receptor interface with tumor cells. J Clin Invest. 2020;130(9):4637-51.

18. Sebestyen Z, Scheper W, Vyborova A, Gu S, Rychnavska Z, Schiffler M, et al. RhoB Mediates Phosphoantigen Recognition by Vγ9Vδ2 T Cell Receptor. Cell Rep. 2016;15(9):1973-85.

19. Gu S, Sachleben JR, Boughter CT, Nawrocka WI, Borowska MT, Tarrasch JT, et al. Phosphoantigen-induced conformational change of butyrophilin 3A1 (BTN3A1) and its implication on Vγ9Vδ2 T cell activation. Proc Natl Acad Sci U S A. 2017;114(35):E7311-e20.

20. Gober HJ, Kistowska M, Angman L, Jenö P, Mori L, De Libero G. Human T cell receptor gammadelta cells recognize endogenous mevalonate metabolites in tumor cells. J Exp Med. 2003;197(2):163-8.

21. Scheper W, Grunder C, Straetemans T, Sebestyen Z, Kuball J. Hunting for clinical translation with innate-like immune cells and their receptors. Leukemia. 2014;28(6):1181-90.

22. Scheper W, van Dorp S, Kersting S, Pietersma F, Lindemans C, Hol S, et al. gammadeltaT cells elicited by CMV reactivation after allo-SCT cross-recognize CMV and leukemia. Leukemia. 2013;27(6):1328-38.

23. Sebestyen Z, Prinz I, Dechanet-Merville J, Silva-Santos B, Kuball J. Translating gammadelta

(gammadelta) T cells and their receptors into cancer cell therapies. Nat Rev Drug Discov. 2020;19(3):169-84.

24. Vyborova A, Janssen A, Gatti L, Karaiskaki F, Yonika A, van Dooremalen S, et al. γ9δ2 T-Cell Expansion and Phenotypic Profile Are Reflected in the CDR3δ Repertoire of Healthy Adults. Front Immunol. 2022;13:915366.

25. Dekkers JF, Alieva M, Cleven A, Keramati F, Wezenaar AKL, van Vliet EJ, et al. Uncovering the mode of action of engineered T cells in patient cancer organoids. Nat Biotechnol. 2022.

26. Liddy N, Bossi G, Adams KJ, Lissina A, Mahon TM, Hassan NJ, et al. Monoclonal TCR-redirected tumor cell killing. Nat Med. 2012;18(6):980-7.

27. Harwood SL, Alvarez-Cienfuegos A, Nuñez-Prado N, Compte M, Hernández-Pérez S, Merino N, et al. ATTACK, a novel bispecific T cell-recruiting antibody with trivalent EGFR binding and monovalent CD3 binding for cancer immunotherapy. Oncoimmunology. 2017;7(1):e1377874.

28. Bacac M, Colombetti S, Herter S, Sam J, Perro M, Chen S, et al. CD20-TCB with Obinutuzumab Pretreatment as Next-Generation Treatment of Hematologic Malignancies. Clin Cancer Res. 2018;24(19):4785-97.

29. Ellerman D. Bispecific T-cell engagers: Towards understanding variables influencing the in vitro potency and tumor selectivity and their modulation to enhance their efficacy and safety. Methods. 2019;154:102-17.

30. Grunder C, van DS, Hol S, Drent E, Straetemans T, Heijhuurs S, et al. gamma9 and delta2CDR3 domains regulate functional avidity of T cells harboring gamma9delta2TCRs. Blood. 2012;120(26):5153-62.

31. Arakawa F, Kuroki M, Kuwahara M, Senba T, Ozaki H, Matsuoka Y, et al. Cloning and sequencing of the VH and V kappa genes of an anti-CD3 monoclonal antibody, and construction of a mouse/human chimeric antibody. J Biochem. 1996;120(3):657-62.

32. Robinson RA, McMurran C, McCully ML, Cole DK. Engineering soluble T-cell receptors for therapy. Febs j. 2021.

33. Gunnarsen KS, Kristinsson SG, Justesen S, Frigstad T, Buus S, Bogen B, et al. Chaperone-assisted thermostability engineering of a soluble T cell receptor using phage display. Sci Rep. 2013;3:1162.

34. Richman SA, Aggen DH, Dossett ML, Donermeyer DL, Allen PM, Greenberg PD, et al. Structural features of T cell receptor variable regions that enhance domain stability and enable expression as single-chain ValphaVbeta fragments. Mol Immunol. 2009;46(5):902-16.

35. Aggen DH, Chervin AS, Insaidoo FK, Piepenbrink KH, Baker BM, Kranz DM. Identification and engineering of human variable regions that allow expression of stable single-chain T cell receptors. Protein Eng Des Sel. 2011;24(4):361-72.

36. Marcu-Malina V, Heijhuurs S, van Buuren M, Hartkamp L, Strand S, Sebestyen Z, et al. Redirecting αβ T cells against cancer cells by transfer of a broadly tumor-reactive γδT-cell receptor. Blood. 2011;118(1):50-9.

37. Yamauchi S, Kobashigawa Y, Fukuda N, Teramoto M, Toyota Y, Liu C, et al. Cyclization of Single-Chain Fv Antibodies Markedly Suppressed Their Characteristic Aggregation Mediated by Inter-Chain VH-VL Interactions. Molecules. 2019;24(14).

38. Arndt KM, Müller KM, Plückthun A. Factors influencing the dimer to monomer transition of an antibody single-chain Fv fragment. Biochemistry. 1998;37(37):12918-26.

39. Burgess RR. A brief practical review of size exclusion chromatography: Rules of thumb, limitations, and troubleshooting. Protein Expr Purif. 2018;150:81-5.

40. Reusch U, Duell J, Ellwanger K, Herbrecht C, Knackmuss SH, Fucek I, et al. A tetravalent bispecific TandAb (CD19/CD3), AFM11, efficiently recruits T cells for the potent lysis of CD19(+) tumor cells. MAbs. 2015;7(3):584-604.

41. Bacac M, Fauti T, Sam J, Colombetti S, Weinzierl T, Ouaret D, et al. A Novel Carcinoembryonic Antigen T-Cell Bispecific Antibody (CEA TCB) for the Treatment of Solid Tumors. Clin Cancer Res. 2016;22(13):3286-97.

42. Slaga D, Ellerman D, Lombana TN, Vij R, Li J, Hristopoulos M, et al. Avidity-based binding to HER2 results in selective killing of HER2-overexpressing cells by anti-HER2/CD3. Sci Transl Med. 2018;10(463).

5

43. Chang CH, Rossi EA, Goldenberg DM. The dock and lock method: a novel platform technology for building multivalent, multifunctional structures of defined composition with retained bioactivity. Clin Cancer Res. 2007;13(18 Pt 2):5586s-91s.

44. Ahmed M, Cheng M, Cheung IY, Cheung NK. Human derived dimerization tag enhances tumor killing potency of a T-cell engaging bispecific antibody. Oncoimmunology. 2015;4(4):e989776.

45. Kufer P, Lutterbüse R, Baeuerle PA. A revival of bispecific antibodies. Trends Biotechnol. 2004;22(5):238-44.

46. Chen W, Yang F, Wang C, Narula J, Pascua E, Ni I, et al. One size does not fit all: navigating the multi-dimensional space to optimize T-cell engaging protein therapeutics. MAbs. 2021;13(1):1871171.

47. Willcox CR, Pitard V, Netzer S, Couzi L, Salim M, Silberzahn T, et al. Cytomegalovirus and tumor stress surveillance by binding of a human γδ T cell antigen receptor to endothelial protein C receptor. Nat Immunol. 2012;13(9):872-9.

Supplementary Figures and Tables

Supplementary Table 1 GAB sequences. Depicted are the CDR3 sequences used for generation of γδ$_{ECTO}$-αCD3

GAB	REF	CDR3δ	CDR3γ
AJ8	13	CACDTAGGSWDTRQMFF	CALWEAQQELGKKIKVF
LM1	30	CACDTLLATDKLIF	CALWEAQQELGKKIKVF
A3	17	CACDAWGHTDKLIF	CALWEAQQELGKKIKVF
C4	17	CACDTLALGDTDKLIF	CALWEAQQELGKKIKVF
C5	17	CACDLLAPGDTSFTDKLIF	CALWEAQQELGKKIKVF
C7	17	CACDMGDASSWDTRQMFF	CALWEAQQELGKKIKVF
A3	17	CACDAWGHTDKLIF	CALWEAQQELGKKIKVF
CL5	30	CACDALKRTDTDKLIF	CALWEIQELGKKIKVF
6_2	13	CACDTLPGAGGADKLIF	CALWEVQELGKKIKVF
EPCR reactive γ4δ5 TCR	47	CAASSPIRGYTGSDKLIF	CATWDGFYYKKLFGSG

5

A

```
Variable Alpha/Delta

α2C      .QSVTQPDARVTVSEGASLQLRCKYSYSA......TPYLFWYVQYPRQGLQLLLKYYSG..DPVVQGV.....
δG115    AIELVPEHQTVPVSIGVPATLRCSMKGEAI....GNYYINWYRKTQGNMTFIYREK.......DIYGPGFK.


α2C      NGFEAEFSKSNSSFHLRKASVHWSDSAVYFCAVSGF......ASALTFGSGTKVIVLP..
δG115    DNFQGDIDIAKNLAVLKILAPSERDEGSYYCACDTLGMGGEYTDKLIFGKGTRVTVEP..


Variable Bèta/Gamma

β2C      EAAVTQSPRNKVAVTGGKVTLSCNQTNNH.......NNMYWYRQDTGHGLRLIHYSYG....
γG115    AGHLEQPQISSTKTLSKTARLECVVSGITI....SATSVYWYRERPGEVIQFLVSISYD...


β2c      AGSTEKGDIP.DGYKASRP.SQENFSLILELATPSQTSVYFCASGGG......GTLYFGAGTRLSVL
γG115    GTVRKESGIPSGKFEVDRIPETSTSTLTIHNVEKQDIATYYCALWEAQQELGKKIKVFGPGTKLIIT
```
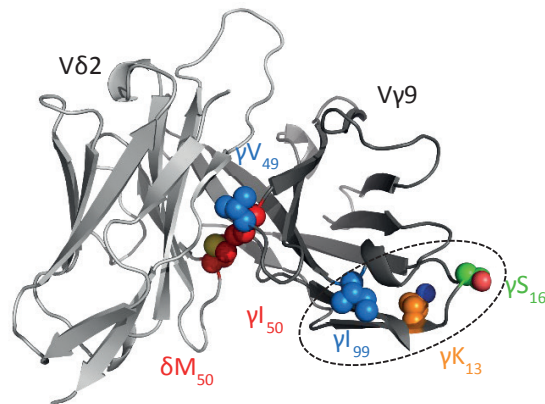
B

Supplementary Figure 1. Alignment of variable αβ- and γδ-chains and structure of G115 TCR with selected residues to be mutated to generate γδ$_{VAR-MUT}$. A) Example alignment of a variable αβ TCR 2C, (PDB 1TCR) and γδ TCR G115 (PDB 1hxm). The selected frequently mutated amino acids identified in αβ variable T cell receptor single chains by Richman et al are indicated in bold. Corresponding amino acids in the γ9- or δ2-chains of the G115 TCR are indicated in bold, and color coded as shown in B. B) Structure of G115 TCR with selected AA highlighted in spheres, the dashed oval indicates the would-be Vγ-Cγ interface. (I) γI$_{99}$S; in blue: Changing the hydrophobic isoleucine to the more polar serine could make the variable gamma chain more stable when solvent exposed, a serine at this position is also highly conserved in Vβ genes of human and mouse. (II) γK$_{13}$V; in orange: Changing the positively charged amino-acid lysine to the smaller and more hydrophobic valine could potentially stabilize the variable gamma domain, because the valine can point more inward and can be buried within the variable domain. Moreover, in many stabilized TCRs and in all variable heavy and light genes, there is a small hydrophobic residue at this position (III) γS$_{16}$G; in green: most antibodies have glycine at this position, which could be important for flexibility. (IIII) γV$_{49}$E; in blue: glutamic acid is the second most common amino acid at this position in the Vβ gene, and in two single chain αβTCRs a mutation from glycine to glutamic acid resulted in more stable protein. (V+VI) γI$_{50}$L+ δM$_{50}$P; in red: The introduced leucine and proline in the gamma and delta chain respectively could interact and potentially stabilize the variable gamma- delta interface.

5
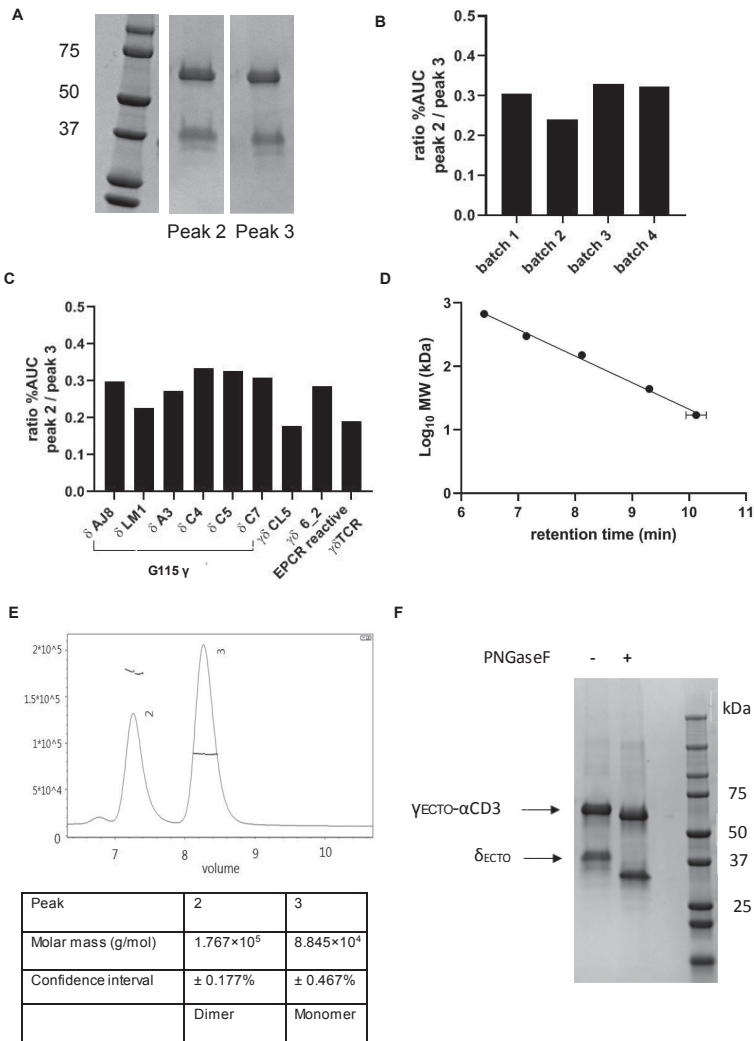
Supplementary Figure 2. γδ$_{ECTO}$-αCD3-dimer formation is reproducible and independent from γδTCR sequence A) γδ$_{ECTO}$-αCD3 purified protein from SEC peak 2 and 3 was run on SDS-page gel under reducing conditions and stained with coomassie brilliant blue protein stain B+C) The ratio between the % area under the curve (AUC) of the SEC peak 2 and 3 is plotted after size exclusion chromatography of B) different batches of γδ$_{ECTO}$-αCD3 C) γδ$_{ECTO}$-αCD3 derived from different γδ TCRs (AJ8 to C7 GAB: unique δ2 chain+ γ9 chain from G115 TCR, 6_2+ CL5 GAB: unique γ9δ2 TCRs and C132 GAB: unique γ4δ5 TCR) D) Retention times of SEC mass standards (AL0-3042, Phenomenex) plotted against their mass (in kDa) each point represent the mean of 4 separate SEC runs, error bar represents the standard deviation. Linear regression was done in GraphPad Prism v9.30; R^2= 0.9948; "Log$_{10}$MW= -0.4190*(ret.time) + 5.514" E) SEC-MALS experiment to determine molecular size of protein in peak 2 and 3 visible after SEC, determining that the peak 2 corresponds to γδ$_{ECTO}$-αCD3-dimer (1.77 ×10^5 g/mol) while peak 3 consists of γδ$_{ECTO}$-αCD3-monomer form (8.85×10^4 g/mol). F) SDS-PAGE analysis of the deglycosylation with PNGaseF under reducing conditions of γδ$_{ECTO}$-αCD3
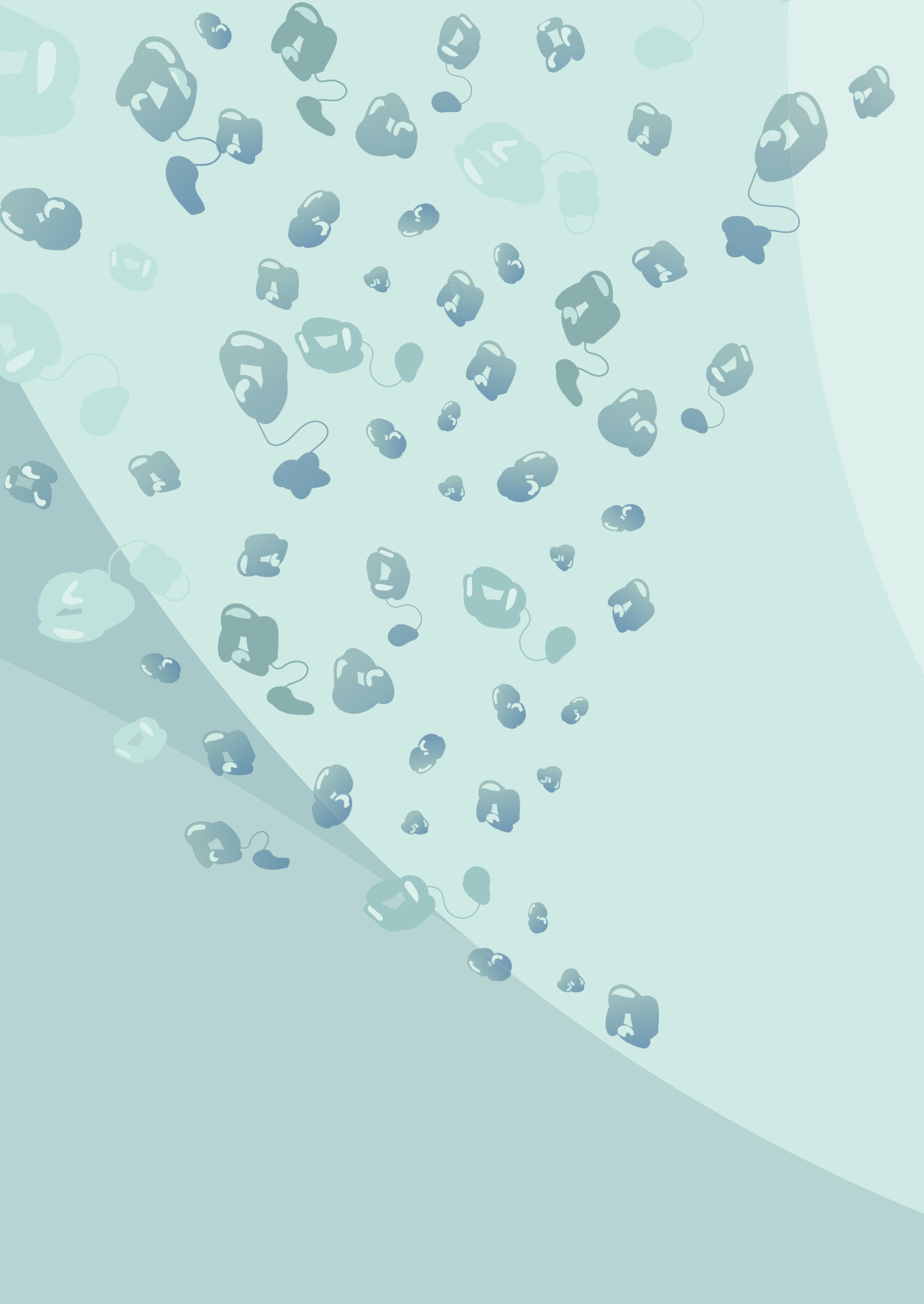
CHAPTER 6

Impact of CD3 binding affinity on the potency of Gamma delta TCR Anti-CD3 Bispecific T cell engagers (GABs)

Eline van Diest[1+], Patricia Hernández-López[1+], Mara J.T. Nicolasen[1], Laura Bongiovani[2], Alain de Bruin[2,3], Effrosyni Karaiskaki[1], Koen Bots[1], Sabine Heijhuurs[1], Anita Kumari[1], Trudy Straetemans[1], Dennis X Beringer[1*], Jürgen Kuball[1,4]*

[1]Center for Translational Immunology, University Medical Center Utrecht, The Netherlands
[2]Department of Biomolecular Health Sciences, Dutch Molecular Pathology Center, Faculty of Veterinary Medicine, Utrecht University, Utrecht, Netherlands.
[3]Department of Pediatrics, University Medical Center Groningen, University of Groningen, Groningen, Netherlands.
[3]Department of Hematology, University Medical Center Utrecht, The Netherlands

[+] Shared first authors
*Equally contributed

Abstract

We previously developed a novel T cell engager construct: **G**amma Delta TCR **A**nti-CD3 **B**ispecific T cell engager molecule (GAB), by fusing the ectodomains of a Vγ9Vδ2 TCR to an anti-CD3 single chain variable fragment (scFv). GABs mirror the unique tumor sensing capacity of Vγ9Vδ2T cells, which is mediated by BTN2A1, and a phosphoantigen- and RhoB-dependent orchestration of BTN3A1 at the cell membrane of target cells. Amongst various variables, the binding affinity of the anti-CD3 scFv has been identified as an important determinant of *in vitro* and *in vivo* potency of bispecific T cell engagers. In this light, we explored the effect of several anti-CD3scFvs, with different binding characteristics, on GAB effectivity. We show that *in vitro* GAB potency correlated with CD3 binding strength, and that increasing CD3 binding strength also increased GAB-induced IFNγ release and tumor cell killing. Within this context we describe a Vγ9Vδ2TCR-aCD3scFv combination that, *in vitro,* observed a low EC50 for tumor cell killing, and a 10-fold higher EC50 for cytokine secretion. GABs comprised of a high affinity anti-CD3 scFv and a high affinity anti-CD3 binding arm also showed improved efficacy *in vivo* in a xenograft model. We detected prolonged GAB binding to T cells *in* vivo for this construct, which might have contributed to the increased efficacy, but was, however, also accompanied by a temporary lymphopenia that resolved over time. In conclusion, we show that increasing CD3 binding affinity in combination with a high affinity Vγ9Vδ2 TCR increases the potency of the GAB molecules, both *in vitro* and *in vivo,* with an acceptable safety toxicity profile.

Introduction

A variety of immunotherapeutic strategies are currently being developed for the treatment of cancer, including checkpoint inhibitors, adoptive T cell transfer of TCR or CAR-engineered T cells, and bispecific T cell engagers. Bispecific T cell engagers (TCEs) combine a tumor targeting domain with a T cell binding domain, often specific for CD3, and can thereby redirect T lymphocytes to tumor cells, independent of specific TCR-MHC binding [1, 2]. Blinatumomab and tebentafusp are currently the only two FDA-approved TCE constructs [3, 4], but many other TCEs are under development [2]. However, other difficulties are currently hampering further TCE development, including the identification of novel suitable target antigens, and the occurrence of treatment related toxicities, like, for example, cytokine release syndrome.

We previously developed a novel T cell engager construct: **G**amma Delta TCR **A**nti-CD3 **B**ispecific T cell engager molecule (GAB), by fusing the ectodomains of a Vγ9Vδ2TCR to an anti-CD3 single chain variable fragment (scFv) [5]. GABs duplicate the unique tumor sensing capacity of Vγ9Vδ2T cells, which is mediated by the direct interaction of the Vγ9Vδ2TCR with BTN2A1, further modulated by the phosphoantigen-dependent orchestration of BTN3A at the cell membrane of target cells [6-8]. Phosphoantigen accumulation is found in infected cells, but is also often seen during transformation of tumor cells [9], and orchestrates BTN3A turnover together with RhoB [10]. GABs can efficiently induce αβT cell mediated phosphoantigen-dependent recognition of tumor cells, and redirect αβT cells against a broad range of hematopoietic and solid tumor cell lines, and primary acute myeloid leukemia or multiple myeloma [5]. Affinity of Vγ9Vδ2TCR to their ligand complex can, however, substantially differ [8, 11]. We have shown that selection of naturally occurring higher affinity Vγ9Vδ2TCR is important for GAB effectivity [5], which is in line with the consensus that higher affinity target cell engagement is preferred, to achieve potent T cell redirection [12]. It was nonetheless surprising that GABs are functional when using Vγ9Vδ2TCR. Though GABs were constructed with Vγ9Vδ2TCR that are considered as high affinity within the context of Vγ9Vδ2TCR, their binding affinity is substantially lower (in the mM range) when compared to αβTCR based TCEs, for which affinity maturation to the pM range is necessary to create potent TCEs [13]. Different requirements of TCR affinity for γδ- and αβTCR based TCEs might simply reflect the higher expression of the respective ligands, as the total amount of surface expressed Vγ9Vδ2TCR ligand complex likely exceeds the amount of MHC presented peptides for a specific αβTCR.

In addition to the target binding arm, the choice of CD3 binding domain, often an scFv derived from an anti-CD3 monoclonal Ab (mAb), has also been reported to influence effectivity of TCEs [12]. The interest in determining the optimal anti-CD3

6

scFv for TCEs originated from the first clinical trials using bispecific T cell engagers, showing only a short therapeutic window, due to early occurrence of cytokine release syndrome (CRS), which was at least partially attributed to the high affinity binding of the TCE's to CD3 [14]. Many of the several subsequent reports on the effect of CD3 binding affinity on TCE effectivity and tolerability concluded that lowering CD3 binding affinity improved *in vivo* biodistribution, tumor control, toxicity, and kinetics of several TCE formats [15-19]. Another interesting report showed that, by careful anti-CD3 scFv selection, it was possible to completely uncouple the TCE mediated tumor cell lysis from cytokine release, which would significantly reduce the risk for CRS [20].

Most of such CD3 scFv affinity studies with TCEs were conducted with TCEs that combine the CD3 engaging arm with a very high affinity tumor target binding domain, which might not reflect the situation in which a lower affinity target binding domain is used, like, for example the Vγ9Vδ2TCR in the GABs. Thus, more studies are needed to assess the right balance when the affinity of the tumor binding arm is lower, as biological properties of both arms are likely to contribute to overall TCE potency [12, 21].

In this report, we investigated how different anti-CD3 scFvs in the GAB format influence GAB potency *in vitro* and *in vivo*. We showed superior T cell activation and tumor cell lysis by GABs with a higher affinity anti-CD3 scFv *in vitro*, which demonstrated improved tumor control *in vivo*, when combined with a higher affinity Vγ9Vδ2TCR.

Material and methods

Generation and production of GABs

The construction of the GAB molecule was described earlier [5]. The different CD3scFv were interchanged in the GAB-containing vector using a 5' FSEI site and 3' SALI site. The scFvs sequence were constructed by linking the 3' variable heavy chain via a flexible $3(G_4S)$ linker to the variable light chain (TR66, 7196,7232 and OKT3) or in the opposite order (UCHT1). The scFv sequences can be found in Table 1. TCR domain boundaries were used as in Allison et al. [22]. The γ9 and δ2 TCR sequences used were reported previously AJ8 [5] as low affinity TCR (γδTCR$_{LO}$), and high affinity A3 *in vitro* [8], and CL5 for the *in vivo* experiments (γδTCR$_{HI}$) [23]. GAB expression and purification have been extensively described [5].

Cells and Cell lines

PBMCS were isolated by Ficoll-Paque (GE Healthcare, Eindhoven, The Netherlands) from buffy coats obtained from Sanquin Blood Bank (Amsterdam, The Netherlands).

αβT cells were expanded from PBMCs using CD3/CD28 dynabeads (Thermo Fisher scientific, United States) and 1.7×10^3 IU/ml of MACS GMP Recombinant Human interleukin (IL)-7 (Miltenyi Biotec, Germany), and 1.5×10^2 IU/ml MACS GMP Recombinant Human IL-15 (Milteny Biotec, Germany). Mock TCR transduced T cells and RPMI 8226 and SCC9 stably expressing GFP-luciferase were generated via a retroviral transduction protocol described earlier [23]. The plasmid containing the GFP and luciferine transgenes was kindly provided by Jeanette Leusen (UMC Utrecht, Utrecht, Netherlands). The following cell lines were obtained from ATCC between 2010 and 2018, HL60 (CCL-240), RPMI 8226 (CCL-155), SCC9 (CRL-1629), K562 (CCL-243) and MDA-MB231 (HTB-26). Freestyle 293-F cells (R790-07) were obtained from Invitrogen (United States). HL60, RPMI 8226 and K562 were cultured in RPMI (Gibco, United states), 10% FCS (Bodinco, Alkmaar, The Netherlands), 1% Pen/Strep (Invitrogen, United States). Freestyle 293-F in Freestyle expression medium (Gibco). SCC9 and MDA-MB231 in DMEM, 10% FCS, 1% Pen/Strep.

Flow cytometry

0.2×10^6 bulk αβT cells were incubated with GAB at different concentrations, in 20 µl FACS buffer PBS, 1% BSA (Sigma Aldrich, Germany), 0.01% sodium azide (Severn Biotech Ltd, United Kingdom) for 30 minutes at room temperature. Cells were washed once in FACS buffer, and incubated with pan-γδTCR-PE (Beckman Coulter, United States, clone IMMU510, 1:10) for 30 minutes at room temperature. Cells were washed 1 time in FACS buffer and fixed in 1% paraformaldehyde (Merck, Germany) in PBS. Data acquisition was done on FACS Canto and analyzed using FACS Diva software (BD, United States).

IFNγ ELISA

50.000 effector cells and 50.000 target cells were incubated together, with or without GAB (different concentrations, as indicated) for 16 hours at 37 °C 5% CO_2, 0.1 mM PAM (calbiochem) was added to the target cells. The supernatant was harvested after 16 hours, and the level of IFNγ was determined using the IFN gamma Human Uncoated ELISA Kit (Invitrogen).

Luciferase-based cytotoxicity

5000 target cells stably expressing luciferase were incubated with T cells transduced with a mock TCR at 3:1 target cell ratio, with different GAB concentrations (as indicated) in the presence of 0.1 mM PAM (calbiochem, United States). After 16 hours, beetle luciferin (Promega, United States) was added to the wells (125 µg/ml) and bioluminescence was measured on SoftMax Pro plate reader. The signal in treatment wells was normalized to the signal measured for targets and T cells only, which was assumed to represent 100% living cells.

6

Animal model, *in vivo* cytokine analyses and mouse pathology

NOD.Cg-PrkdcscidIl2rgtm1Wjl/SzJ (NSG) mice were obtained from Jackson Laboratory (Bar Harbor, ME, USA). Experiments were conducted under institutional guidelines after permission from the local Ethical Committee and in accordance with the current Dutch laws on animal experimentation. Mice were housed in sterile conditions using an individually ventilated cage (IVC) system, and fed with sterile food and water. Irradiated mice were given sterile water with antibiotic ciproxin for the duration of the experiment. Adult female mice (13 weeks old) received sublethal total body irradiation (1.75 Gy) on Day -1. Mice received a subcutaneous injection of 10×10^6 RPMI 8226-luc B2M KO cells in PBS on day 0. For the tumor treatment model, the mice were randomized, based on tumor size, into three groups of 10 mice on day 7, and were intravenously injected with 10×10^6 huPBMCs. Next, mice received 7 GAB injections every other day, starting at day 8 (2.7 mg/kg body weight). Pamidronate (10 mg/kg body weight) was injected together with the GABs on days 8 and 14. Moreover, an extra group (n=5) that received tumor and huPBMCs, but no GABs was included as an additional control. Tumor volume was measured three times a week as the primary outcome measure. For the second, short mouse model, mice were randomized over four groups of 5 mice, and received two GAB injections on day 8 and 10. Peripheral blood samples were obtained via cheek vein (maximum 50–80 µl/mouse) on indicated days. Red blood cell lysis was performed for blood samples using 1× RBC lysis buffer (Biolegend) before cell staining. Blood samples were stained with γδTCR-PE (clone IMMU510, Beckman Coulter), αβTCR-FITC (Clone IP26, Invitrogen), huCD45-PB (Clone HI30, Sony), CD4-APC (clone RPA-T4, Biolegend) and CD8 (clone RPA-T8, Biolegend). The persistence of GABs bound to αβT cells was measured in peripheral blood by quantifying the absolute αβTCR positive and αβTCR+/γδTCR double positive cell number by flow cytometry, using Flow-count Fluorospheres (Beckman Coulter). Plasma was collected and luminex was performed to measure cytokine levels for IL2, IL6, IL10, TNFα, IFNγ, MCP1, MIP1α, MIP1β, CXCL1, and IP10. Tumors were collected at the end of the experiment (day 12) and fixed in formalin. Fixed tumors were embedded in paraffin and cut into 4 um sections, and hematoxylin and eosin (H&E) staining were performed, following the previously described protocol [24]. The following histologic features were evaluated: number of mitotic figures and apoptotic cells: expressed as a range per high-power fields (HPFs), calculated in the same, randomly selected 5 HPFs, 40×); extension of the necrotic tumor tissue was expressed as the percentage considering the entire tumor mass. Images were taken using an Olympus BX45 microscope with the Olympus DP25 camera, and analyzed using DP2-BSW (version.2.2) software. T cell infiltration was determined using immunofluorescent (IF) staining. For IF, after deparaffinization and dehydration, slides were pretreated with 10 mM citrate buffer pH 6.0 for 15 min, followed by cooling at room temperature for 30 min. Staining was done using anti-human Anti-Nuclei Antibody (clone 3E1.3, Merck

Millipore BV) and anti-human CD3 polyclonal antibody (Agilent Technologies). Slides were mounted in VECTASHIELD Antifade Mounting Medium with DAPI (Vector Laboratories). Slides were scanned by an Olympus VS200 research slide scanner and analyzed by the Olyvia (Olympus) imaging software. The total number of double positive cells was counted in the entire tissue section, and expressed as a number.

Results

Anti-CD3 scFv panel with different CD3 binding affinity

To study the effect of CD3 binding affinity on GAB activity, we selected five anti-CD3 scFvs (αCD3) to couple to the previously characterized low affinity Vγ9Vδ2TCR AJ8 (TCR$_{LO}$)[5]. The selected scFvs were derived from three anti-CD3 antibodies that have been historically used in different TCEs, listed from low to high CD3 affinity: TR66, OKT3 and UCHT1 (Supplementary Table 1)[25]. In addition, two CD3 scFv sequences, 7195 and 7232, were chosen based on their binding kinetics[26]. 7195 is a high affinity scFv with a long half-life of 117 minutes, while the intermediate affinity scFv 7232 has a short half-life of only 7 minutes. After expression and purification, the different TCR$_{LO}$-αCD3 GABs were analyzed on SDS gel, all showing similar bands for the TCRδ$_{LO}$- and TCRγ$_{LO}$-αCD3 chain, confirming proper expression of all constructs (Figure 1A).

We first assessed T cell binding of the TCR$_{LO}$-αCD3 GABs by flow cytometry. GABs were titrated and incubated with T lymphocytes and the T cells bound by GABs were assessed using a pan-γδTCR antibody (Figure 1B). Titration of GABs allowed us to determine EC$_{50}$ values, showing, in line with earlier reports, that GABs containing one of the high affinity scFvs UCHT1 and 7195 were the strongest binders, with an EC$_{50}$ of 0.2-0.3 μg/ml (Table 1). GABs containing one of the intermediate affinity scFvs 7232 and OKT3 showed similar intermediate binding with an EC$_{50}$ around 1 μg/ml, and GABs constructed with the low affinity TR66 had the lowest EC$_{50}$ at 2.2 μg/ml. Based on these data, we selected three scFvs with different CD3 binding affinity for further functional testing: the high affinity scFv UCHT1 (αCD3$_{HI}$), OKT3 as intermediate binder (αCD3$_{MED}$) and TR66 with low binding affinity (αCD3$_{LO}$).
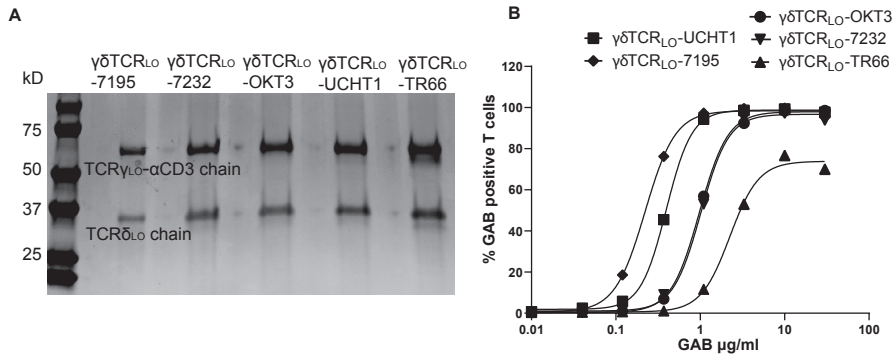
6

Figure 1. Expression and T cell binding of the GAB molecules with different anti-CD3 scFvs (A) After HIS-tag purification, the GABs containing a low affinity γδTCR with different anti-CD3 scFvs (γδTCR$_{LO}$-αCD3) were run on SDS gel, and visualized with Coomassie brilliant blue protein stain. Showing a band for the TCRγ$_{LO}$-αCD3 chain at 59 kD and the TCRδ$_{LO}$ chain at 24 kD (B) Coating of T lymphocytes with GABs containing the different αCD3 scFvs, followed by staining with fluorochrome labeled anti pan-γδ antibody, percentage positive T cells was determined by flow cytometry. The EC$_{50}$ was calculated using a non-linear regression model, depicted in the table as μg/ml and mol/L (M) for each anti-CD3 scFv. N=2, a representative figure is shown

Table 1 EC$_{50}$ of GABs with different CD3scFvs in T cell binding in (μg/ml) and (M)

CD3scFv	EC$_{50}$ (μg/ml) T cell binding	EC$_{50}$ (M) T cell binding
UCHT1	0.396 μg/ml	4.7 * 10^{-9} M
7195	0.222 μg/ml	2.6 * 10^{-9} M
OKT3	0.979 μg/ml	1.2 * 10^{-8} M
7232	1.017 μg/ml	1.2 * 10^{-8} M
TR66	2.241 μg/ml	2.7 * 10^{-8} M

GABs using a high affinity CD3 scFv are more potent in inducing IFNγ release by T cells, mainly when combined with a lower affinity γδTCR

To test impact of the anti-CD3 scFv binding affinity on *in vitro* potency of the GABs, we first assessed the TCR$_{LO}$-αCD3$_{HI/MED/LO}$ GABs in an IFNy release assay. The GABs were titrated in a co-culture of T lymphocytes and the recognized target cell lines MDA-MB231 and SCC9. There was a clear impact of the different anti-CD3 scFvs on GAB potency against both cell lines, γδTCR$_{LO}$-αCD3$_{HI}$ GAB could already induce IFNy release at low concentrations, starting from 0.1 μg/ml. γδTCR$_{LO}$-αCD3$_{MED}$ and γδTCR$_{LO}$-αCD3$_{LO}$ were only able to induce IFNy release at the higher concentrations, from 10 μg/ml against SCC9 or 1 μg/ml against MDA-MB231, and did not reach a plateau (Figure 2A).

The different anti-CD3 scFvs were also tested in combination with a higher affinity TCR ($\gamma\delta TCR_{HI}$) [5]. There was again a difference in potency between $\gamma\delta TCR_{HI}$-$\alpha CD3_{HI}$ and $\gamma\delta TCR_{HI}$-$\alpha CD3_{LO}$ GAB. Combining the $\gamma\delta TCR_{HI}$ with the $\alpha CD3_{MED}$, resulted in a GAB with intermediate potency (Figure 2B). $\gamma\delta TCR_{HI}$-$\alpha CD3_{HI}$ induced more IFNy release at concentrations below 10 µg/ml compared to $\gamma\delta TCR_{HI}$-$\alpha CD3_{MED}$, but at higher concentrations, the GAB with $\alpha CD3_{MED}$ induced similar or even higher levels of IFNy against both targeted cell lines.

To test whether activation of T cells through GABs occurs only in the presence of the molecular target and is not due to the higher affinity CD3 binding only, GABs with the different anti-CD3 scFvs were incubated at a fixed concentration of 10 µg/ml with HEK293T-BTN3KO cells, a cell line which lacks one of the ligands crucial for Vγ9Vδ2TCR mediated activation. RPMI 8226 was used as a positive control, and IFNy release was assessed (Figure 2C). Overall, none of the GABs induced IFNy when co-incubated with the negative target cell line HEK293T-BTN3AKO, while they did induce recognition when co-incubated with the positive control cell line RPMI 8226. This confirms that for all of the anti- CD3 scFvs used here, single T cell engagement is not sufficient to induce cytokine release.

6
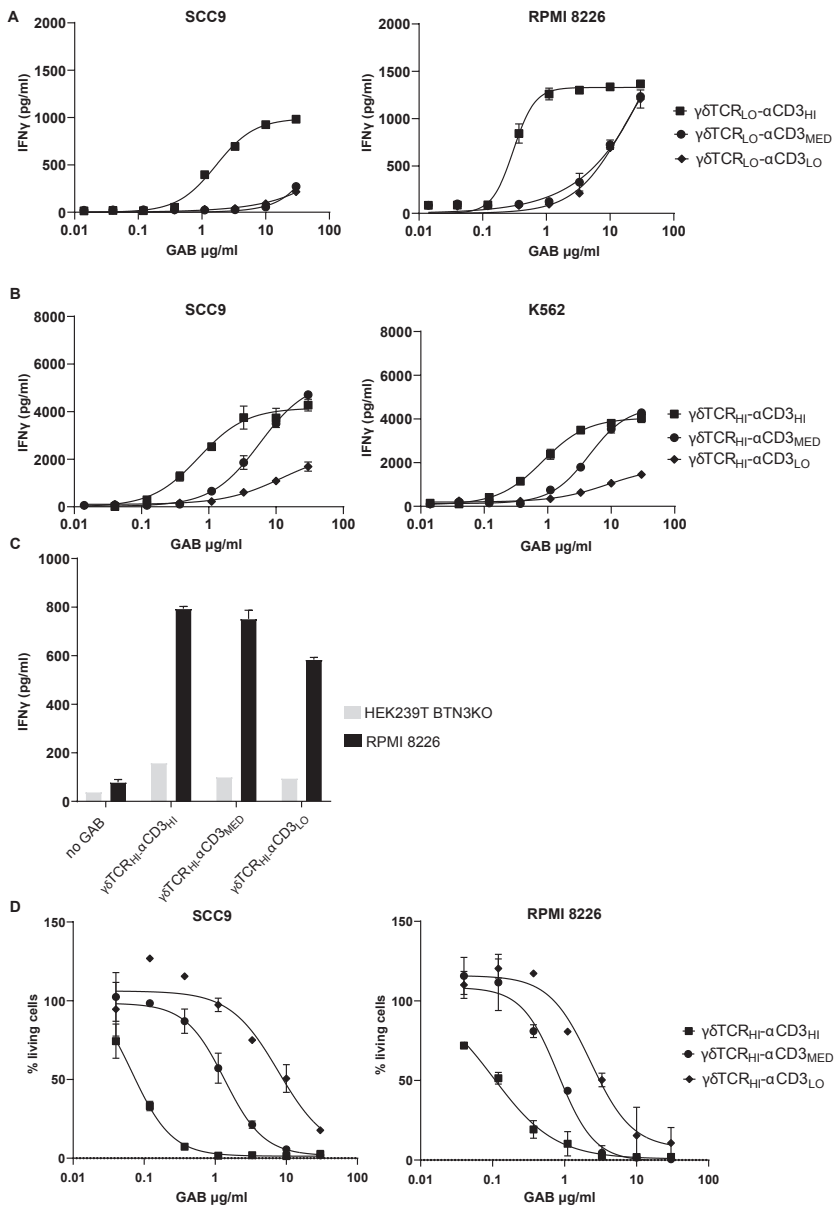
Figure 2. GAB with higher affinity CD3 binding is more potent in induction of IFNγ release and tumor cell lysis. (A+B) IFNγ release was determined after 16 hours 1:1 co-culture of T cells (A) with RPMI 8226 or SCC9 targets cells and a titration of GABs with a lower affinity γδTCR (γδTCR$_{LO}$) combined with an anti-CD3 scFv with high (αCD3$_{HI}$), intermediate (αCD3$_{MED}$) or low affinity (αCD3$_{LO}$) in the presence of PAM (100 μM). (B) or with K562 and SCC9 target cells and a titration of GABs with high affinity γδTCR (γδTCR$_{HI}$) coupled to αCD3$_{HI}$ /αCD3$_{MED}$ /αCD3$_{LO}$ in the presence of PAM (100 μM). (C) GABs with γδTCR$_{HI}$ coupled to αCD3$_{HI}$ /αCD3$_{MED}$ /αCD3$_{LO}$ (10 μg/ml) were incubated with HEK293T BTN3KO or RPMI 8226 target cells

and T cells, and IFNγ release was measured after 16 hours. (D) T lymphocytes and luciferase transduced RPMI 8226 and SCC9 target cells were co-incubated for 16 hours with γδTCR$_{HI}$ coupled to αCD3$_{HI}$/αCD3$_{MED}$/αCD3$_{LO}$ at different concentrations and PAM (30 µM) at an E:T ratio of 3:1. Percentage viable cells was determined by comparing luminescence signal to the no-GAB condition, representing 100% viability. N=1 Error Bars represent SD from technical duplicates.

GABs using higher affinity anti-CD3 scFvs are more potent in inducing tumor cell lysis, and increase the EC$_{50}$ ratio between killing and cytokine secretion

Creating a more favorable balance for induction of tumor cell killing is the most important aspect for TCEs. Therefore, we tested all of the different TCR$_{HI}$-αCD3 GABs for their ability to induce tumor cell lysis, using two recognized tumor cell lines: RPMI 8226 and SCC9. The amount of living cells was determined after a co-culture of T cells, target cells and GABs at different concentrations. In line with the IFNγ release data, γδTCR$_{HI}$-αCD3$_{HI}$ was most potent in inducing tumor cell lysis, inducing killing at concentrations as low as 0.1 µg/ml (Figure 2D). Again γδTCR$_{HI}$-αCD3$_{MED}$ GAB displayed an intermediate phenotype, able to efficiently induce lysis, but at a higher concentration compared to the GABs with a high affinity scFvs. GABs with the αCD3$_{LO}$ were able to induce lysis only at the highest concentrations.

Toxicity of TCE is frequently induced by excessive cytokine secretion, and therefore TCE's with reduced cytokine secretion relative to killing capacity are developed [19, 27, 28]. Within this context, we analyzed EC$_{50}$ in target cell lysis and IFNγ release for the γδTCR$_{HI}$-αCD3 GABS with high, medium or low CD3 affinity, using the target cell line SCC9 (Table 2). Interestingly, the EC$_{50}$ for target cell lysis was substantially lower compared to IFNγ release for all tested anti-CD3 scFvs. The largest difference in EC$_{50}$ values was observed for γδTCR$_{HI}$-αCD3$_{HI}$, with 10-fold less GABs needed for target cell killing when compared to IFNγ release, while the other tested GABs had smaller differences, a 4.4 fold difference for γδTCR$_{HI}$-αCD3$_{MED}$ and a 1.5 fold difference γδTCR$_{HI}$-αCD3$_{LO}$. Our data imply that, despite having the strongest activity for both killing and cytokine secretion, γδTCR$_{HI}$-αCD3$_{HI}$ could have the best therapeutic efficacy/toxicity window for later clinical application.

Table 2 EC50 γδ$_{HI}$-αCD3$_{HI/MED/LO}$ GABs IFNγ release and target cell lysis with SCC9 target cells

	EC$_{50}$ IFNγ release	EC$_{50}$ Target cell lysis
γδ$_{HI}$-αCD3$_{HI}$	0.712 µg/ml	0.068 µg/ml
γδ$_{HI}$-αCD3$_{MED}$	5.722 µg/ml	1.350 µg/ml
γδ$_{HI}$-αCD3$_{LO}$	12.18 µg/ml	7.755 µg/ml

6

GABs with the high affinity anti-CD3 scFv show better *in vivo* tumor control compared to GABs with an intermediate affinity.

Others reported that selecting the most potent *in vitro* T cell engager does not necessarily result in the best *in vivo* efficacy in mice [16]. Therefore, we tested whether the most potent GAB, with the best efficacy-toxicity profile when assessed *in vitro* ($\gamma\delta TCR_{HI}$-$\alpha CD3_{HI}$), was superior *in vivo* when compared to the less potent GAB *in vitro* ($\gamma\delta TCR_{HI}$-$\alpha CD3_{MED}$). To this end, NSG mice were injected with the multiple myeloma cell line RPMI 8226-β2M KO subcutaneously, and human PBMC intravenously one week later to reconstitute the human immune system (Figure 3A) as described previously [5]. Starting from day 8, the mice received injections with $\gamma\delta TCR_{HI}$-$\alpha CD3_{HI}$, $\gamma\delta TCR_{HI}$-$\alpha CD3_{MED}$, or $\gamma\delta TCR_{MOCK}$-$\alpha CD3_{MED}$, with mock TCR LM1 [23] coupled to $\alpha CD3_{MED}$ as a negative control, every second day until day 20. Tumor size was determined until day 35, showing that both $\gamma\delta TCR_{HI}$-$\alpha CD3_{HI}$ and $\gamma\delta TCR_{HI}$-$\alpha CD3_{MED}$ significantly reduced tumor size compared $\gamma\delta TCR_{MOCK}$-$\alpha CD3_{MED}$, while the mock group did not differ significantly from the PBMC only group (Figure 3B). Moreover, the GAB with $\alpha CD3_{HI}$ was significantly better in tumor control, compared to the $\alpha CD3_{MED}$.

Superior *in vivo* performance of $\gamma\delta TCR_{HI}$-$\alpha CD3_{HI}$ could be due not only to its increased killing efficacy (e.g. Table 2), but also potentially to extend persistence in the bloodstream due to prolonged binding to T cells. To investigate this hypothesis, mice were bled on day 9,10 and 21, 22 and 24, corresponding to 24 plus 48 hours after the first GAB injection and 24, 48 and 96 hours after the seventh and last GAB injection respectively. Total human T lymphocytes per ml of blood was determined, and these T cells were divided in T cells that stained single for positive for αβTCR, and αβTCR/γδTCR double positive, corresponding to T cells coated with GAB protein (Figure 3C). $\gamma\delta TCR_{HI}$-$\alpha CD3_{HI}$ showed higher and longer *in vivo* T cell coating compared to the other groups. Almost all T cells were still bound by GABs 48 hours after the first or the last injection in this group. Strikingly, the total T cell numbers in the group treated with $\gamma\delta TCR_{HI}$-$\alpha CD3_{HI}$ was consistently lower compared to either $\alpha CD3_{MED}$ GAB or PBMCs-only group, with a strong drop within the first 24 hours after each injection, and did not differ between CD4+ or CD8+ T cells (Figure 3C and Figure S1A and B). However, 96 hours after $\gamma\delta TCR_{HI}$-$\alpha CD3_{HI}$ injections, T cell counts started to recover. We also monitored weight loss and survival of the mice until the end of the experiment at day 35, as these factors could indicate toxicity due to overstimulation of T cells, and we saw no significant differences between the groups (Figure S1 C and D) in line with the favorable toxicity and efficacy profile observed *in vitro*.
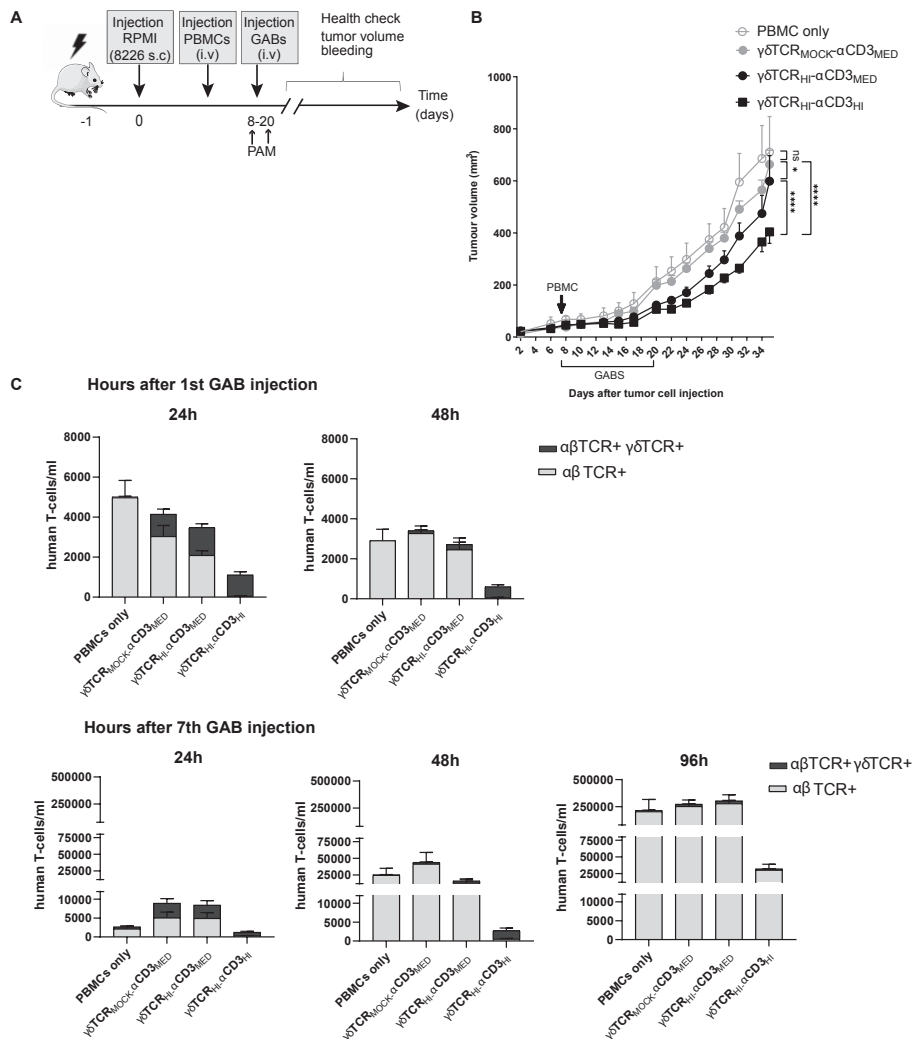
Figure 3. Superior *in vivo* tumor control and T cell coating by GABs with higher affinity CD3 binding
(A) Schematic representation of experimental design. NSG mice were irradiated at day -1, and injected subcutaneously (s.c) with 10*10^6 RPMI 8226 tumor cells one day later. After 7 days the mice were randomized over three groups of 10 and one group of 5 (PBMC only), based on tumor size. All groups were injected with 10*10^6 huPBMCs i.v on day 7. From day 8 to 20 three groups were treated with i.v injections of γδTCR$_{HI}$-αCD3$_{HI}$, γδTCR$_{HI}$-αCD3$_{MED}$ or γδTCR$_{MOCK}$-αCD3$_{MED}$ every other day for a total of 7 injections (2,7 mg/kg). The PBMC only group did not receive additional treatment (B) Tumor size was measured three times a week for five weeks after tumor cell injection. (C) Amount of αβTCR single positive and αβTCR/γδTCR double positive cells in the mice was determined by flow cytometry on day 9, 10, 21, 22 and 24 after tumor injection, which corresponds to 24 and 48h after the first GAB injection and 24, 48 and 96 hours after the last GAB injection respectively. PBMC only N=5, γδTCR$_{HI}$-αCD3$_{HI}$, γδTCR$_{HI}$-αCD3$_{MED}$ or γδTCR$_{MOCK}$-αCD3$_{MED}$ N=10. Error bars represent SEM, significance was calculated by mixed-effects model with repeated measures. * P<0.05, ** P<0.001, ***P<0.0001.

GABs with the high affinity anti-CD3 scFv do not induce enhanced cytokine release or T cell infiltration compared to GABs with an intermediate affinity i*n vivo*.

To further investigate the different *in vivo* treatment effects of GABs with either -αCD3$_{MED}$ or αCD3$_{HI,}$ we performed a second, two-week mouse model in which, after tumor and PBMC injection, GABs were injected twice, and blood and tumor were collected. The potential risk of T cell overstimulation by high affinity CD3 binding, was addressed by determining the presence of 10 cytokines and chemokines, associated with cytokine release syndrome (CRS), 4 and 48 hours after injection of γδTCR$_{HI}$-αCD3$_{MED}$ and γδTCR$_{HI}$-αCD3$_{HI}$. For four of the selected cytokines and chemokines, IFNγ, MCP1, MIP1β, and CXCL1, the plasma levels were below the detection limit of the luminex assay in all samples. Overall, for the other six cytokines and chemokines, 4 hours after GAB injection, we observed no significant differences between mice injected with mock- or functional GAB, nor between mice injected with GAB with -αCD3$_{MED}$ or -αCD3$_{HI}$ (Figure 4B). We only observed a decrease in IP-10 level in mice treated with γδTCR$_{MOCK}$-αCD3$_{HI}$ mice compared to γδTCR$_{MOCK}$-αCD3$_{MED}$, which was, however, not seen for the groups treated with γδTCR$_{HI}$-αCD3$_{MED}$ or γδTCR$_{HI}$-αCD3$_{HI}$. This low level of induced cytokines by the different GABs was also observed 48 hours after the second GAB injection (Figure S2).

To assess whether we observed either a difference in T cell infiltration after GAB injection, or an enhanced killing of tumors between different groups, histopathologic analysis of tumor sections were performed. We observed a significant decrease in mitotic figures and apoptotic cells in mice treated with functional GAB (γδTCR$_{HI}$), compared to mock treatment (γδTCR$_{MOCK}$), while there were no differences observed between αCD3$_{MED}$ or -αCD3$_{HI}$ treated groups or in the percentage necrosis between all the groups. These data implied, in line with the recently described apoptotic paradox [29], an improved tumor control early after functional GAB injections, though no differences in tumor control were observed between different active GABs at this early time point. We also did not observe any significant differences in T cell infiltration between the different treatment groups, implying that GABs do not attract T cells to the tumor site during this early treatment phase, and that the improved tumor control of γδTCR$_{HI}$-αCD3$_{HI}$ might be a consequence of longer exposure over time with GAB -coated T cells, rather than of an increase in effector cell infiltration.

In conclusion, we show that γδTCR$_{HI}$-αCD3$_{HI}$ has the most favorable efficacy toxicity profile, with improved tumor control *in vivo,* with no signs of increased inflammation or treatment related toxicity.
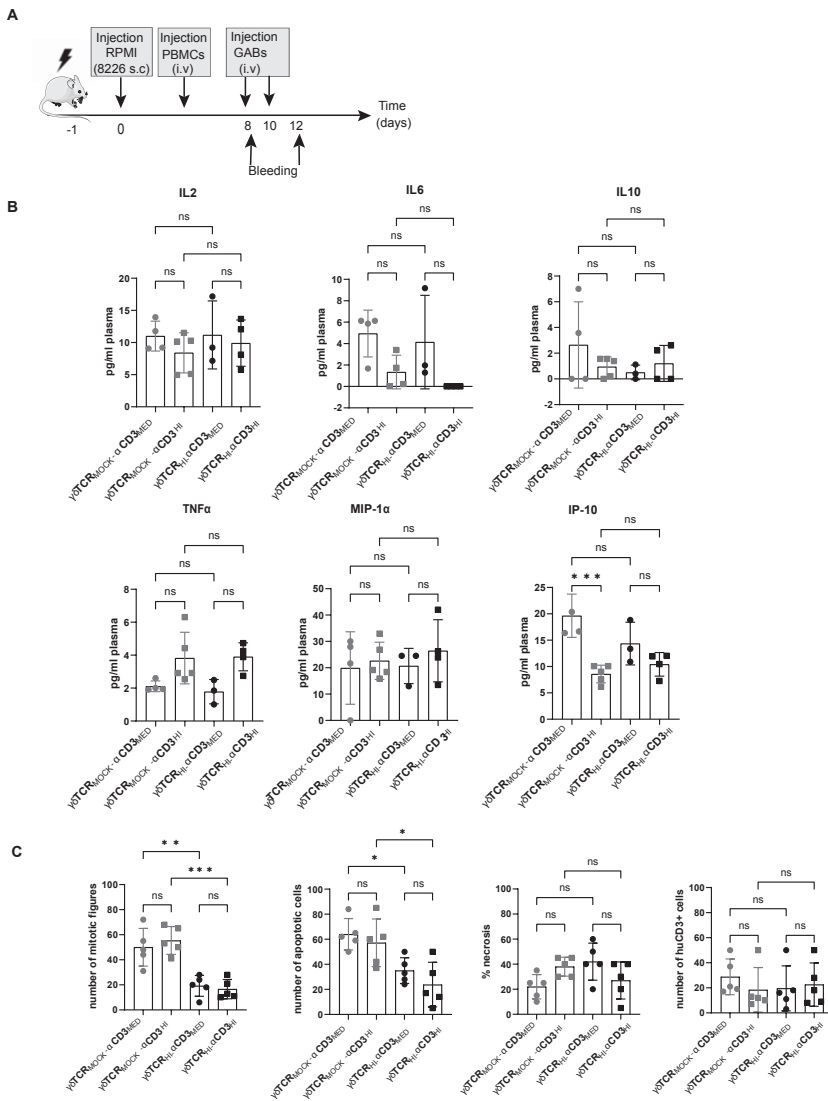
Figure 4. GABs with high affinity CD3 binding do not increase production of cytokines associated with cytokine release syndrome or tumor T cell infiltration (A) Schematic representation of experimental design. NSG mice were irradiated at day -1, and injected subcutaneously (s.c) with 10*10^6 RPMI 8226 tumor cells one day later. After 7 days the mice were randomized over four groups of 5 mice and injected with 10*10^6 huPBMCs (i.v), and day 8 and 10 the mice were injected with γδTCR_{HI/MOCK}-αCD3_{MED/HI.} (B) blood was drawn on day 8 (4 hours after the first GAB injection) and cytokine levels were measured using luminex. (C) Tumor tissue was collected on day 12 and the number of mitotic figures, amount of apoptotic cells and % necrosis was determined based and HE staining. Tumor infiltrated human T cells were visualized and quantified using HNF and CD3 staining and immunofluorescent microscopy. N=3,4 or 5, error bars represent SD, significance was calculated using one way ANOVA. * P<0.05, ** P<0.001, ***P<0.0001

6

Discussion

During the pre-clinical development of bispecific T cell engagers, many factors can be optimized to create the molecule with most beneficial properties [12, 21], and over the past several years, interest in the selection of CD3 binding domains with optimal properties to incorporate in TCEs has increased significantly [14]. A factor considered to be important for this selection is the relative potency of the TCE in induction of tumor cell lysis versus cytokine release, with the overall goal to reduce the risk of cytokine release syndrome [20, 28]. But the *in vivo* biodistribution of the TCE is also considered, with the assumption that the relative binding affinities of the tumor- and T cell binding arm will have a large impact on distribution and thereby potency of the TCE *in vivo* [15, 18].

Within this context, we further developed our most recently described TCE concept of GABs [5] and describe now a next generation of GAB that is optimized for the balance between the tumor binding- Vγ9Vδ2TCR ectodomain, and the anti-CD3 scFv T cell binding affinity.

To accomplish this goal, in this report we tested the influence of different binding strengths of the CD3 arm in the GABs, in combination with different Vγ9Vδ2TCR affinities, on the *in vitro* and *in vivo* potency. We found a strong correlation between CD3 binding affinity and *in vitro* potency of the GAB. GABs incorporating a higher affinity CD3scFv more efficiently induced cytokine release as well as tumor cell lysis. However, in addition to an overall increase in potency, we also observed a change in the window between the relative EC_{50} for induction of IFNγ release versus lysis, as reported by others [17, 20, 30]. This observation would allow for the treatment of patients with a lower amount of GAB protein, and thereby allow for a better distinction dissection between toxicity and cytokine secretion. We could not, however, identify specific Vγ9Vδ2TCR-CD3scFv combinations where cytokine secretion was abolished, while tumor toxicity was maintained.

Part of the success was also testing different anti-CD3 scFvs with either a high- (γδ$_{HI}$) or lower affinity (γδ$_{LO}$) Vγ9Vδ2TCR. The loss of potency when using lower affinity anti-CD3 scFvs, although observed for both GABs, seemed more pronounced in the γδ$_{LO}$ GAB, and mainly reduced the window between EC_{50} for induction of IFNγ release versus lysis. This observation is in line with a report showing that decreased binding avidity of the tumor engaging arm of HER2-CD3 TCEs, by using a tumor cell line with low HER2 expression, resulted in greater differences in TCE potency, while in a high avidity situation, by using a HER2 high tumor cell line, CD3 affinity did not affect the TCE potency [27].

In line with our *in vitro* assays, we also found superior *in vivo* tumor control by γδTCR$_{HI}$-αCD3$_{HI}$ compared to γδTCR$_{HI}$-αCD3$_{MED}$. This finding is in contrast to recent reports showing that TCEs with higher CD3 binding affinity, regardless of *in vitro* potency, do not show improved tumor control *in vivo* [18, 19]. Non-optimal biodistribution of the TCEs, bound to T cells, to lymph nodes and secondary lymphoid organs rather than to the tumor, is one of the concerns when using high binding affinity to CD3 *in vivo* [15]. We also observed a rapid decline in T cells in the blood after γδTCR$_{HI}$-αCD3$_{HI}$ treatment. However, this phenomenon was only temporary, did not associate with cytokine release, and did not impair, but rather associated with improved efficacy. Thus, while for other TCE's, strong binding to T cells is viewed as sub-optimal, this might not be the case for the GAB molecules, which need to overcome low affinity binding of the γδTCR to the tumor, which is even with "higher affinity" γδTCR most likely in the μM range. Therefore, prolonged circulation when binding on T cells might be important to achieve long term exposure of tumor tissues to GABs, as suggested by our observation that in the early phase, we neither observed increased T cell infiltration between all GABs, nor differences in mitotic or apoptotic signals between functional GABs at the tumor site in mice. Increasing the binding affinity of the γδTCR to its ligand complex could still be an interesting alternative strategy to improve GAB potency, though it could be challenging, given the lack of understanding of the full composition of the TCR-ligand complex.

In conclusion, here we show that increasing the binding affinity of the anti-CD3 scFv in the GAB format, in combination with a high affinity γδTCR, leads to increased potency *in vitro* and *in vivo*. Though *in vivo* temporary drops in T cell counts were observed as compared to other constructs, this did not associate with increased toxicity, but rather with improved tumor control, most likely through increased killing and a prolonged exposure of tumor cells to GAB coated T cells.
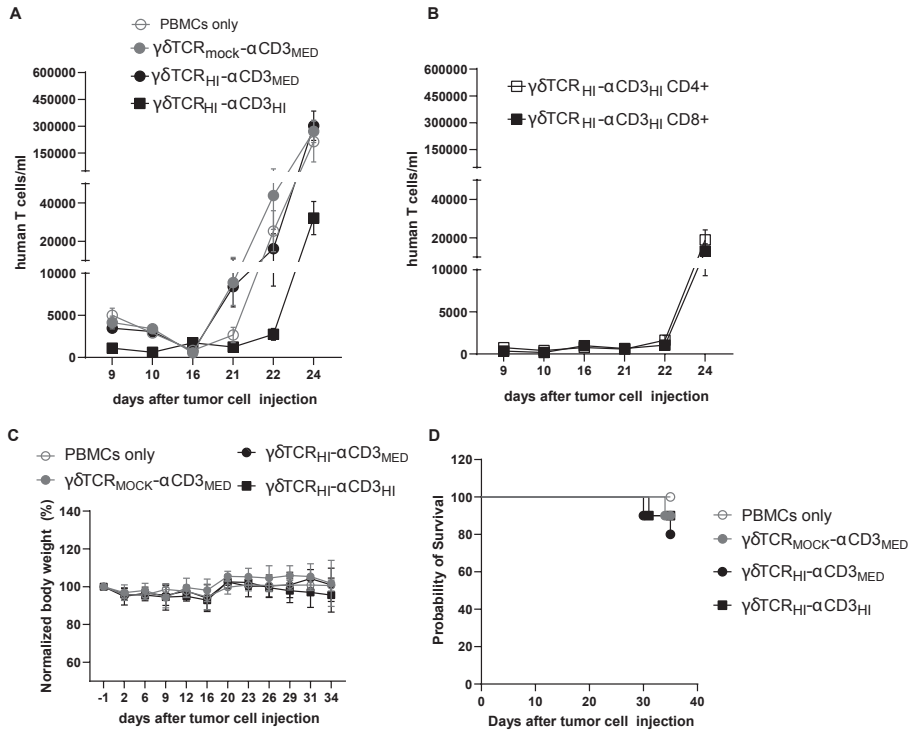
6

References

1. Goebeler ME, Bargou RC. T cell-engaging therapies - BiTEs and beyond. Nat Rev Clin Oncol. 2020;17(7):418-34.

2. Trabolsi A, Arumov A, Schatz JH. T Cell-Activating Bispecific Antibodies in Cancer Therapy. J Immunol. 2019;203(3):585-92.

3. Przepiorka D, Ko CW, Deisseroth A, Yancey CL, Candau-Chacon R, Chiu HJ, et al. FDA Approval: Blinatumomab. Clin Cancer Res. 2015;21(18):4035-9.

4. Dhillon S. Tebentafusp: First Approval. Drugs. 2022;82(6):703-10.

5. van Diest E, Hernández López P, Meringa AD, Vyborova A, Karaiskaki F, Heijhuurs S, et al. Gamma delta TCR anti-CD3 bispecific molecules (GABs) as novel immunotherapeutic compounds. J Immunother Cancer. 2021;9(11).

6. Karunakaran MM, Willcox CR, Salim M, Paletta D, Fichtner AS, Noll A, et al. Butyrophilin-2A1 Directly Binds Germline-Encoded Regions of the Vgamma9Vdelta2 TCR and Is Essential for Phosphoantigen Sensing. Immunity. 2020;52(3):487-98.e6.

7. Rigau M, Ostrouska S, Fulford TS, Johnson DN, Woods K, Ruan Z, et al. Butyrophilin 2A1 is essential for phosphoantigen reactivity by gammadelta T cells. Science. 2020;367(6478).

8. Vyborova A, Beringer DX, Fasci D, Karaiskaki F, van Diest E, Kramer L, et al. γ9δ2T cell diversity and the receptor interface with tumor cells. J Clin Invest. 2020.

9. Gober HJ, Kistowska M, Angman L, Jenö P, Mori L, De Libero G. Human T cell receptor gammadelta cells recognize endogenous mevalonate metabolites in tumor cells. J Exp Med. 2003;197(2):163-8.

10. Sebestyen Z, Scheper W, Vyborova A, Gu S, Rychnavska Z, Schiffler M, et al. RhoB Mediates Phosphoantigen Recognition by Vgamma9Vdelta2 T Cell Receptor. Cell Rep. 2016;15(9):1973-85.

11. Vyborova A, Janssen A, Gatti L, Karaiskaki F, Yonika A, van Dooremalen S, et al. γ9δ2 T-Cell Expansion and Phenotypic Profile Are Reflected in the CDR3δ Repertoire of Healthy Adults. Front Immunol. 2022;13:915366.

12. Ellerman D. Bispecific T-cell engagers: Towards understanding variables influencing the in vitro potency and tumor selectivity and their modulation to enhance their efficacy and safety. Methods. 2019;154:102-17.

13. Liddy N, Bossi G, Adams KJ, Lissina A, Mahon TM, Hassan NJ, et al. Monoclonal TCR-redirected tumor cell killing. Nat Med. 2012;18(6):980-7.

14. Vafa O, Trinklein ND. Perspective: Designing T-Cell Engagers With Better Therapeutic Windows. Front Oncol. 2020;10:446.

15. Mandikian D, Takahashi N, Lo AA, Li J, Eastham-Anderson J, Slaga D, et al. Relative Target Affinities of T-Cell-Dependent Bispecific Antibodies Determine Biodistribution in a Solid Tumor Mouse Model. Mol Cancer Ther. 2018;17(4):776-85.

16. Leong SR, Sukumaran S, Hristopoulos M, Totpal K, Stainton S, Lu E, et al. An anti-CD3/anti-CLL-1 bispecific antibody for the treatment of acute myeloid leukemia. Blood. 2017;129(5):609-18.

17. Dang K, Castello G, Clarke SC, Li Y, Balasubramani A, Boudreau A, et al. Attenuating CD3 affinity in a PSMAxCD3 bispecific antibody enables killing of prostate tumor cells with reduced cytokine release. J Immunother Cancer. 2021;9(6).

18. Haber L, Olson K, Kelly MP, Crawford A, DiLillo DJ, Tavaré R, et al. Generation of T-cell-redirecting bispecific antibodies with differentiated profiles of cytokine release and biodistribution by CD3 affinity tuning. Sci Rep. 2021;11(1):14397.

19. Staflin K, Zuch de Zafra CL, Schutt LK, Clark V, Zhong F, Hristopoulos M, et al. Target arm affinities determine preclinical efficacy and safety of anti-HER2/CD3 bispecific antibody. JCI Insight. 2020;5(7).

20. Trinklein ND, Pham D, Schellenberger U, Buelow B, Boudreau A, Choudhry P, et al. Efficient tumor killing and minimal cytokine release with novel T-cell agonist bispecific antibodies. MAbs. 2019;11(4):639-52.

21. Chen W, Yang F, Wang C, Narula J, Pascua E, Ni I, et al. One size does not fit all: navigating the multi-dimensional space to optimize T-cell engaging protein therapeutics. MAbs. 2021;13(1):1871171.

22. Allison TJ, Winter CC, Fournie JJ, Bonneville M, Garboczi DN. Structure of a human gammadelta T-cell

antigen receptor. Nature. 2001;411(6839):820-4.

23. Grunder C, van DS, Hol S, Drent E, Straetemans T, Heijhuurs S, et al. gamma9 and delta2CDR3 domains regulate functional avidity of T cells harboring gamma9delta2TCRs. Blood. 2012;120(26):5153-62.

24. Johanna I, Hernández-López P, Heijhuurs S, Bongiovanni L, de Bruin A, Beringer D, et al. TEG011 persistence averts extramedullary tumor growth without exerting off-target toxicity against healthy tissues in a humanized HLA-A*24:02 transgenic mice. J Leukoc Biol. 2020;107(6):1069-79.

25. Wu Z, Cheung NV. T cell engaging bispecific antibody (T-BsAb): From technology to therapeutics. Pharmacol Ther. 2018;182:161-75.

26. Smith E, inventoranti-CD3 antibodies, bispecific antigen-binding molecules that bind CD3 and CD20, and used thereof 2017.

27. Poussin M, Sereno A, Wu X, Huang F, Manro J, Cao S, et al. Dichotomous impact of affinity on the function of T cell engaging bispecific antibodies. J Immunother Cancer. 2021;9(7).

28. Li J, Piskol R, Ybarra R, Chen YJ, Li J, Slaga D, et al. CD3 bispecific antibody-induced cytokine release is dispensable for cytotoxic T cell activity. Sci Transl Med. 2019;11(508).

29. Morana O, Wood W, Gregory CD. The Apoptosis Paradox in Cancer. Int J Mol Sci. 2022;23(3).

30. Zuch de Zafra CL, Fajardo F, Zhong W, Bernett MJ, Muchhal US, Moore GL, et al. Targeting Multiple Myeloma with AMG 424, a Novel Anti-CD38/CD3 Bispecific T-cell-recruiting Antibody Optimized for Cytotoxicity and Cytokine Release. Clin Cancer Res. 2019;25(13):3921-33.

Supplementary Figures and Tables

Supplementary Table 1 anti-CD3 scFv sequence and reported affinity

Anti-CD3 scFv	Amino acid sequence	Reported K_D single arm
UCHT1	DIQMTQTTSSLSASLGDRVTISCRASQDIRNYLNWYQQKPDGTVKLLIYYTSRL HSGVPSKFSGSGSGSGTDYSLTISNLEQEDIATYFCQQGNTLPWTFAGGTKLEIK GGGGSGGGGSGGGGSQVQLQQSGPELVKPGASMKISCKASGYSFTGYTMN WVKQSHGKNLEWMGLINPYKGVSTYNQKFKDKATLTVDKSSSTAYMELLSLT SEDSAVYYCARSGYYGDSDWYFDVWGQGTTLTVFSVD	51 *10[-9] M [1]
OKT3	QVQLVQSGGGGVVQPGRSLRLSCKASGYTFTRYTMHWVRQAPGKGLEWIGYI NPSRGYTNYNQKFKDRFTISRDNSKNTAFLQMDSLRPEDTGVYFCARYYDDH YCLDYWGQGTPVTVSSGGGGSGGGGSGGGGSQIQMTQSPSSLSASVGDRV TITCSASSSVSYMNWYQQTPGKAPKRWIYDTSKLASGVPSRFSGSGSGTDYT FTISSLQ PEDIATYYCQQWSSNPFTFGQGTKLQITRVD	2.73 *10[-6] M [2]
TR66	QIQLVQSGAEVAKPGASVKVSCKASGYTFTRYTMHWVRQRPGQGLEWIGYI NPSRGYTNYNQKFKDRATLTTDKSTSTAYMELSSLTSEDTAVYYCARYYDD HYCLDYWGQGTTVTVSSGGGGSGGGGSGGGGSDIQLTQSPSSLSASVGDR VTITCRASSSVSYMNWYQQKSGTAPKRWIYDTSKVASGVPYRFSGSGSGTS YTLTISSLQPEDAATYYCQQWSSNPLTFGGGTKVEIKVD	2.6×10^{-7} M [3]
7195	QVQLVESGGGGLVQPGRSLRLSCAASGFTFADYTMHWVRQAPGKGLEWVSD ISWNSGSIAYADSVKGRFTISRDNAKNSLYLQMNSLRTEDTAFYYCAKDSRGY GHYKYLGLDVWGQGTTVTVSSGGGGSGGGGSGGGGSDIQMTQSPSSLSAS VGDRVTITCRASQSISSYLNWYQQKPGKAPKLLIYAASSLQSGVPSRFSGSGS GTDFTLTISSLQPEDFATYYCQQSYSTPPITFGQGTRLEIKV D	3.19*10[-9] M [4]
7232	QVQLVESGGGGLVHPGRSLRLSCAASGFTFDDYTMHWVRQAPGKGLEWVSDI SWNSGSRGYADSVKGRFTISRDNAENSLYLQMNSLRAEDTALYYCAKDKSGY GHYYYYAMDVWGQGTTVTVSSGGGGSGGGGSGGGGSDIQMTQSPSSLSAS VGDRVTITCRASQSISSYLNWYQQKPGKAPKLLIYAASSLQSGVPSRFSGSGS GTDFTLTISSLQPEDFATYYCQQSYSTPPITFGQGTRLEIKVD	2.2*10[-7] M [4]

6

Supplementary Figure 1. Human T cell outgrowth in vivo, and mouse survival and weight (A) total number of human T cells recorded in the mice model described in figure 3. For each (treatment) group or (B) γδTCR$_{HI}$-αCD3$_{HI}$ treatment group CD4+ and CD8+T lymphocytes separate. (C) Survival of the mice until the endpoint at day 35. (D) Body weight of the mice until the endpoint at day 35. Error bars represent SEM (A) or SD (C). N=10 or N=5 (PBMC only).
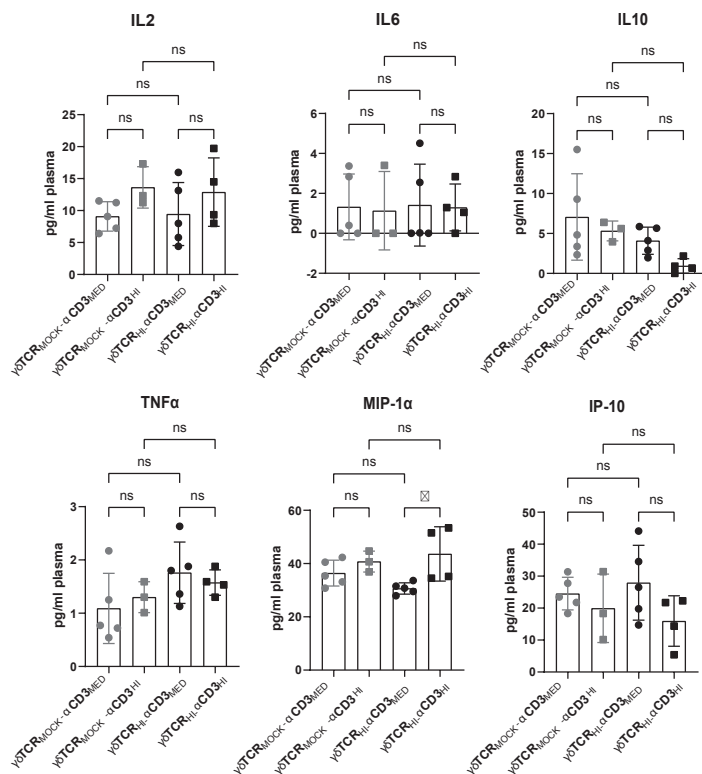
Supplementary Figure 2. GABs with higher affinity CD3 binding do not induce increased T cell infiltration in tumor tissue. Tumor tissue was collected and infiltrated. Human T cells were visualized and quantified using HNF and CD3 staining and immunofluorescent microscopy. N=5 Error bars represent SD, significance was calculated using student T test. ns= not significant.

6

Supplementary References

1. Li Q, Hapka D, Chen H, Vallera DA, Wagner CR. Self-assembly of antibodies by chemical induction. Angew Chem Int Ed Engl. 2008;47(52):10179-82.

2. Kjer-Nielsen L, Dunstone MA, Kostenko L, Ely LK, Beddoe T, Mifsud NA, et al. Crystal structure of the human T cell receptor CD3 epsilon gamma heterodimer complexed to the therapeutic mAb OKT3. Proc Natl Acad Sci U S A. 2004;101(20):7675-80.

3. Moore PA, Zhang W, Rainey GJ, Burke S, Li H, Huang L, et al. Application of dual affinity retargeting molecules to achieve optimal redirected T-cell killing of B-cell lymphoma. Blood. 2011;117(17):4542-51.

4. Smith E, inventoranti-CD3 antibodies, bispecific antigen-binding molecules that bind CD3 and CD20, and used thereof 2017.
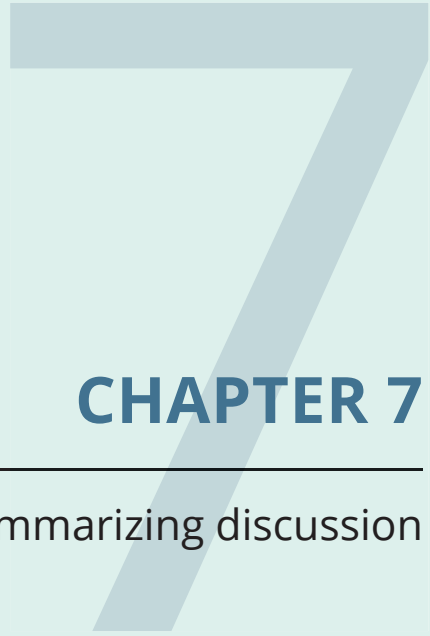
CHAPTER 7

Summarizing discussion

Immunotherapy for cancer treatment has undergone drastic development over the past decades, and several strategies are now entering and changing clinical practice. Since the initial introduction of adoptive T cell therapy (ACT) using tumor infiltrating lymphocytes (TILs) and treatment with checkpoint inhibitors, the field has further progressed. In **chapter 1** the development of different T lymphocyte based immunotherapeutic strategies were discussed, highlighting recent advances as well as hurdles that still need to be overcome.

αβTCR engineered T cells

In **chapter 2** we described a novel GMP grade method to purify αβTCR engineered T cells, based on a strategy initially developed for the purification of αβT cells engineered to express a γδTCR [1]. Currently most CAR-T cell manufacturing protocols do not include a step to purify the engineered T cells, meaning that infusion products also contain non- or poorly engineered T cells, still expressing the endogenous αβTCR [2]. This might influence effectivity of the infused product, and increases the risk of graft versus host disease (GvHD) by unwanted specificity of the residual endogenous αβTCR expression [3]. Though not general practice, there are several strategies described to achieve a pure engineered T cell infusion product, either by purification of engineered cells [4-6] or by gene-editing to eliminate endogenous TCR expression [7].

Inspired by these strategies, we developed an elegant approach for the purification of αβTCR engineered T cells, the mutation of two amino-acids in the βTCR chain abrogated binding of a GMP-grade antibody which can be then used to deplete all non- or poorly engineered T cells. This strategy omits the need for the introduction of extra artificial proteins and tags for purification or additional gene-editing steps that could pose extra risks for immunogenicity or unwanted side-effects.

As ACT therapy with engineered T cells always poses a risk for severe toxicities, such as cytokine release syndrome (CRS) or on-target off-tumor toxicity, possibilities to deplete infused T cells are important. Several strategies have been developed for engineered T cells, including incorporation of suicide genes [8] or introduction of an additional epitope that can be targeted with antibodies to deplete the engineered cells [6]. In this light, we also explored the possibility to allow binding of an anti-murine βTCR antibody that could be used for quick depletion of the αβTCR engineered cells in case of toxicity, by mutation of additional amino-acids in the βTCR. We were able to show depletion of engineered T cells *in vitro* by coupling a toxin to the depletion antibody, although this did not reach 100% efficiency. Future opportunities could arise from improving the binding affinity of the depletion antibody by introducing some additional mutations in the βTCR around the antibody binding epitope, or alternatively by further alterations of the

antibody. Additionally other toxins could be coupled to the antibody in an attempt to induce cell death more efficiently.

γδTCR transduced T cells

In chapter 3 we show that introduction of an extra co-stimulatory receptor can improve functionality of T cells engineered to express a defined γδTCR (TEGs). TEGs were introduced by our group in an attempt to overcome some of the hurdles limiting efficacy of γδT cell mediated therapy, including in vivo functional diversity of the γδT cell population, lack of γδT cell tumor infiltration and loss of proliferative capacity [9]. Since this initial study several reports have further shown the potential of TEGs in immunotherapy [10-12]. However, despite the unique tumor recognition mechanism of TEGs, this strategy is likely not insensitive to obstacles described for other engineered T cell strategies. These include difficulties in homing to- and infiltration of solid tumors, overcoming the suppressive tumor micro-environment (TME), occurrence of T cell exhaustion and lack of long term T cells persistence. In a report from our group it has indeed been shown that for TEGs expressing a HLA-A*24:02 reactive γδTCR (TEG011), long-term in vivo tumor control correlated with T cell persistence, with non-persisting mice developing extramedullary tumor masses comparable to mock treated mice [13].

In the CAR-T field researchers have established that co-stimulation is crucial for CAR mediated T cell activation. Since the development of the first-generation CARs with CD3ζ as sole signaling domain, with only limited activity, different co-stimulation domains have been added to the CAR design to increase anti-tumor efficacy and *in vivo* T cell persistence [14,15]. Different from CAR-T cells, TCR engineered T cells rely on the natural activation machinery of the T cell, and therefore on the endogenous expression of co-stimulatory receptors. The availability of ligands for these co-stimulatory receptors is however often limited in tumors, and chronic TCR stimulation combined with the absence of co-stimulation can lead to T cell exhaustion and anergy within the tumor and low persistence of T cells [16].

In **chapter 3** we showed that adding a chimeric co-receptor, with the extracellular domain of NKG2D fused to an intracellular co-stimulation domain, to TEG cells led to enhanced T cell proliferation and serial killing *in vitro*, and better tumor control *in vivo*. This effect was most robust when using the 41BB co-stimulation domain, CD28 co-stimulation showed a similar *in vitro* benefit, but in a solid tumor xenograft model it was not able to enhance tumor control as seen for 41BB co-stimulation. Comparisons between CAR-T cells harboring CD28 or 41BB co-stimulation domains have shown that these different signals can have profound downstream effects on T cell fitness and phenotype. While both CAR types are often very efficient in stimulating T cells and eradicating tumors, providing CD28 co-stimulation in general

7

creates CAR-T cells with more pronounced effector functions, while 41BB induces long term T cell persistence [17, 18]. Indeed we showed that while CD28 co-stimulation improved the TEG anti-tumor effect *in vivo,* this did co-inside with a loss of the engineered cells over time, and effect that was not seen for 41BB co-stimulation. Moreover, engineered cells co-stimulated with 41BB also showed enhanced *in vivo* proliferation compared to WT or CD28 co-stimulated TEG.

Another co-stimulation domain shown to increase CAR-T cell persistence and anti-tumor effectivity is ICOS [19]. Surprisingly, co-stimulation with ICOS did not improve TEG cells *in vitro* or *in vivo*, different from reports using CAR-T cells showing that an ICOS based CAR enhanced T cell persistence *in vivo* [19]. These researchers however also concluded that this effect was most profound when the ICOS domain was situated membrane proximal in the CAR, and the endogenous ICOS transmembrane (TM) region was used. In our experiments the CD28 TM domain was incorporated in all chimeric-co-receptors to reach equal receptor expression, but this might explain why ICOS is this case does not induce enhanced tumor targeting or T cell proliferation.

In this report NKG2D was chosen as extracellular binding domain, since NKG2D ligands are broadly expressed on tumors, and NKG2D is also an endogenous co-stimulatory receptor expressed on CD8+ T cells [20]. In a solid tumor xenograft model we showed that introducing NKG2D-41BB chimera into the TEGs resulted in tumor control, while we did not see a significant effect on tumor growth by the TEG cells without additional co-receptor. We can speculate that in addition to the improved T cell fitness by the 41BB signaling, the addition of the NKG2D receptor also improves T cell infiltration in the tumor. However, as survival was followed during this experiment we could not formally compare T cell infiltration in the tumor between groups at the same time point, it would however be interesting to perform such an experiment in the future.

Another interesting concept making use of additional stimulatory chimeric receptors to improve T cell function, are the inhibitory-to-stimulatory switch receptors [21]. These combine the extracellular binding domains of inhibitory receptors like PD1 or CTLA-4, with the intracellular domains of co-stimulatory receptors, such as 41BB or CD28, converting the would-be inhibitory signal to co-stimulatory support. As these inhibitory signals are often expressed in the context of TME of solid tumors, suppressing the activity of infiltrating T cells, such an approach would also be interesting to test for TEGs in the context of solid tumors.

Developing γδTCR anti-CD3 bispecific molecules as addition to gene transfer therapy

Redirection of T lymphocytes to towards tumor cells can also be achieved by bispecific T cell engager (TCEs) as investigated in **chapter 4, 5, and 6**. TCEs can redirect T lymphocytes towards tumor cells regardless of T cell specificity, and are being developed for various target antigens, many overlapping with CAR-T cells therapies. An interesting example of TCE versus ACT for T cell redirection, is the simultaneous development of the CD19 CAR-T cells therapy (tisagenlecleucel) and the anti-CD19 BiTE (Blinatumomab), both approved for treatment of B cell acute lymphoblastic leukemia (B-ALL) [22].

TCEs form an attractive alternative to ACT treatment since they omit the need for laborious and expensive ex- vivo engineering techniques and can be produced as large batches and provided to the patient as off-the shelf therapy, dramatically reducing the time a patient has to wait to start the therapy. Furthermore, the short *in vivo* half-life of most TCEs have the benefit that treatment can be stopped immediately in case of adverse events. On the other hand, this short half-life also means that there is no long term treatment effect with TCEs, while long term persistence has been reported for CAR-T cells, potentially resulting in long term tumor surveillance. Moreover, TCEs rely on the activity of endogenous T lymphocytes, while adoptively transferred T cells can be skewed to a more functional and long-lived cell phenotype during the *ex vivo* culture period. Overall, we can conclude that both strategies have benefits and drawbacks [23, 24], also illustrated by two reviews published simultaneous in blood advances titled 'CAR T cells better than BiTEs' and 'BiTEs better than CAR T cells' [25, 26]. While some patients might benefit from TCE therapy, others could be better off with CAR treatment, which might depend on tumor type, amount and phenotype of the circulating T cells and stage of the disease.

In this light, in **chapter 4** we developed a novel TCE concept: the Gamma delta TCR Anti-CD3 Bispecific (GAB), as addition to the previously described TEGs. Similar to TEGs for adoptive transfer of genetically engineered T cells, with GABs we introduce metabolic tumor targeting to the TCE field. The previously described difficulties in the identification of suitable target antigen for engineered T cells also apply to TCEs, and therefore we believe that using the unique, broadly applicable, tumor targeting potential of γδTCRs for a bispecific T cell engager holds great promise. We have shown that GABs can retarget T cells to a broad range of tumor cells *in vitro* and induce tumor control in a 3D bone marrow niche- and xenograft model.

7

Strategies to improve GAB potency

In **chapter 4** the ecto-γ9δ2TCRs was used as target binding domain to create the GABs, the precise binding affinity of the γ9δ2TCR is not yet known, but it has been determined that the γ-chain binds to BTN2A1 with an affinity of 40μM [27]. The overall γ9δ2TCR binding affinity is most likely somewhere in the μM range, comparable to αβTCRs, which is substantially lower compared to the target binding domain in most TCE formats. Also, for TCEs using tumor reactive αβTCRs, the TCRs have to be affinity enhanced to the pM range in order to achieve activity [28]. It is therefore interesting that γ9δ2TCRs can function in a TCE format using their endogenous 'low' affinity. We can speculate about the reason for this difference between αβ- and γδTCRs, which might include (I) differences in ligand density on target cells (II) the unique binding properties of the γ9δ2TCRs potentially binding to two distinct ligands on target cells (III) differences in ligand size and binding epitope distance to the membrane, all implicated to influence TCE activity [29].

We have however also found that there are differences in activity when comparing different γ9δ2TCRs within the GAB format, likely due to naturally occurring affinity differences. In light of this observation, it would be interesting to test whether γ9δ2TCRs with higher affinity compared to the TCRs used in the current report can further increase GAB potency *in vitro*, and more importantly *in vivo*. Despite many efforts in our group over the past years to identify potent tumor reactive γ9δ2TCRs [30, 31], we have yet to find a higher efficacy γ9δ2TCR than the clone 5 and A3 γ9δ2TCRs used in chapter 4.

Another means to obtain high affinity γ9δ2TCRs is to introduce affinity enhancing mutations in the γ9δ2TCR, as described previously for αβTCRs [32, 33]. Such strategies to identify high affinity TCRs are generally based on large library screens making use of phage- or yeast display [34, 35]. This first requires stable expression of soluble single chain variable TCR fragment, or double chain ecto-TCR protein, which can then be displayed on the yeast or phage surface. Despite our attempts to express these single- (sc) or double chain (dc) soluble γδTCRs with the purpose to use in phage display, this has not led to a successful protocol for γδTCRs thus far[36]. However, as the γδT cell field is relatively young compared to the research into αβT cells and the αβTCR, and interest in γδT cells has been increasing during the past years, this will undoubtedly lead to novel insights into γδTCR biology and subsequent developments in the field of TCR engineering that can also be beneficial for further affinity maturation of the γδTCR. Though, as adverse effects have been seen due to on- or off-target recognition by affinity matured αβTCRs after ACT [37, 38], extensive safety testing will have to be implemented to characterize affinity enhanced γδTCRs.

In **chapter 5** we have described an alternative strategy to improve the overall binding affinity of the GABs, by increasing the avidity rather than affinity. This strategy, also explored for other TCE formats [39, 40], would omit the need for affinity maturation which might be preferred in light of safety aspects. However, as discussed in chapter 5, we have not yet identified the optimal format to create an avidity increased GAB. While it was possible to induce the dimerization of GAB in the αCD3 scFv domain, this also led to a large compromise in protein production yield. As manufacturability is also a big challenge in the development of TCEs, developing a multivalent GAB design without decreasing the production yield would be crucial. Furthermore, the increase in potency of the GAB described for the dimeric form was approximately 5 fold *in vitro*, future xenograft studies should however be conducted to test the impact of this on *in vivo* GAB induced tumor targeting.

In addition to characteristics of the tumor antigen binding domain, the binding epitope and affinity to CD3 on T cells has also been recognized as critical for TCE activity. Originally, most TCEs made use of anti-CD3 scFvs derived from historically described CD3 mAb such as, UCHT1, OKT3 and SP34. Recently there have however been multiple reports showing that careful selection of the anti-CD3 scFv, mostly with lower binding affinities, often results in better pharmacokinetics and less toxicity *in vivo*, while retaining antitumor efficacy [41-43]. Simply lowering the CD3 affinity is however probably not beneficial for all TCE concepts, as researchers have speculated that optimal effectivity of TCEs is a balance between relative tumor antigen- and CD3 binding affinities, and is also influenced by other characteristics such as the TCE design and the specific target antigen [44, 45].

In this light, in **chapter 6** we investigated the effect of anti-CD3 scFvs with different binding affinities on GAB potency *in vitro* and *in vivo*. We found that GABs with the high affinity scFv UCHT1 had increased potency *in vitro* as well as in an multiple myeloma xenograft model compared to GABs with scFvs with lower CD3 binding affinity. Interestingly, this contrasts some of the literature on other TCE designs showing improved *in vivo* potency by lowering CD3 affinity binding [42, 43, 46], which might reflect the influence of the tumor binding domain, that is several folds lower in affinity in the GABs compared to most used TCEs.

Overall, to further develop the GABs multiple factors can be influenced, including design, binding valency, and tumor and CD3 binding affinity. In the end, careful consideration of these factors individually, but more importantly how these are best combined for an optimal effectivity will be crucial. Extensive *in vivo* testing of different GAB designs to determine optimal tumor effectivity, combined with pharmacokinetic and toxicity profiling will be pivotal for further pre-clinical development of the GABs.

7

In summary, in this thesis we aimed to advance immunotherapeutic strategies using αβ- or γδTCRs for tumor cell recognition. We developed a novel concept to purify and deplete αβTCR engineered T cells, a strategy that could contribute to improving the quality and safety of *ex vivo* manufactured αβTCR cell therapies. Furthermore, we improved *in vitro* and *in vivo* potency of T cells engineered with a γδTCR (TEG), by the introduction of an additional chimeric co-stimulation receptor. This will hopefully add to clinical efficacy of this cell product in the future, a strategy that might also be applicable to other cell therapies. Lastly, we introduced a novel concept to the fast-growing field of γδTCR mediated immunotherapy, and explored strategies to further improve this new treatment. With the γδTCR-αCD3 bispecific T cell engager we provide an alternative strategy to translate the promise of γδTCRs into anti-cancer therapy, with the potential to be a broadly applicable and off-the shelve therapy.

References

1. Straetemans T, Gründer C, Heijhuurs S, Hol S, Slaper-Cortenbach I, Bönig H, et al. Untouched GMP-Ready Purified Engineered Immune Cells to Treat Cancer. Clin Cancer Res. 2015;21(17):3957-68.

2. Lock D, Mockel-Tenbrinck N, Drechsel K, Barth C, Mauer D, Schaser T, et al. Automated Manufacturing of Potent CD20-Directed Chimeric Antigen Receptor T Cells for Clinical Use. Hum Gene Ther. 2017;28(10):914-25.

3. Kebriaei P, Singh H, Huls MH, Figliola MJ, Bassett R, Olivares S, et al. Phase I trials using Sleeping Beauty to generate CD19-specific CAR T cells. J Clin Invest. 2016;126(9):3363-76.

4. Casucci M, Falcone L, Camisa B, Norelli M, Porcellini S, Stornaiuolo A, et al. Extracellular NGFR Spacers Allow Efficient Tracking and Enrichment of Fully Functional CAR-T Cells Co-Expressing a Suicide Gene. Front Immunol. 2018;9:507.

5. Bister A, Ibach T, Haist C, Smorra D, Roellecke K, Wagenmann M, et al. A novel CD34-derived hinge for rapid and efficient detection and enrichment of CAR T cells. Mol Ther Oncolytics. 2021;23:534-46.

6. Valton J, Guyot V, Boldajipour B, Sommer C, Pertel T, Juillerat A, et al. A Versatile Safeguard for Chimeric Antigen Receptor T-Cell Immunotherapies. Sci Rep. 2018;8(1):8972.

7. Rafiq S, Hackett CS, Brentjens RJ. Engineering strategies to overcome the current roadblocks in CAR T cell therapy. Nat Rev Clin Oncol. 2020;17(3):147-67.

8. Yu S, Yi M, Qin S, Wu K. Next generation chimeric antigen receptor T cells: safety strategies to overcome toxicity. Mol Cancer. 2019;18(1):125.

9. Marcu-Malina V, Heijhuurs S, van Buuren M, Hartkamp L, Strand S, Sebestyen Z, et al. Redirecting αβ T cells against cancer cells by transfer of a broadly tumor-reactive γδT-cell receptor. Blood. 2011;118(1):50-9.

10. Straetemans T, Kierkels GJJ, Doorn R, Jansen K, Heijhuurs S, Dos Santos JM, et al. GMP-Grade Manufacturing of T Cells Engineered to Express a Defined γδTCR. Front Immunol. 2018;9:1062.

11. Johanna I, Straetemans T, Heijhuurs S, Aarts-Riemens T, Norell H, Bongiovanni L, et al. Evaluating in vivo efficacy - toxicity profile of TEG001 in humanized mice xenografts against primary human AML disease and healthy hematopoietic cells. J Immunother Cancer. 2019;7(1):69.

12. Braham MVJ, Minnema MC, Aarts T, Sebestyen Z, Straetemans T, Vyborova A, et al. Cellular immunotherapy on primary multiple myeloma expanded in a 3D bone marrow niche model. Oncoimmunology. 2018;7(6):e1434465.

13. Johanna I, Hernández-López P, Heijhuurs S, Bongiovanni L, de Bruin A, Beringer D, et al. TEG011 persistence averts extramedullary tumor growth without exerting off-target toxicity against healthy tissues in a humanized HLA-A*24:02 transgenic mice. J Leukoc Biol. 2020;107(6):1069-79.

14. Kowolik CM, Topp MS, Gonzalez S, Pfeiffer T, Olivares S, Gonzalez N, et al. CD28 costimulation provided through a CD19-specific chimeric antigen receptor enhances in vivo persistence and antitumor efficacy of adoptively transferred T cells. Cancer Res. 2006;66(22):10995-1004.

15. Milone MC, Fish JD, Carpenito C, Carroll RG, Binder GK, Teachey D, et al. Chimeric receptors containing CD137 signal transduction domains mediate enhanced survival of T cells and increased antileukemic efficacy in vivo. Mol Ther. 2009;17(8):1453-64.

16. Gaissmaier L, Elshiaty M, Christopoulos P. Breaking Bottlenecks for the TCR Therapy of Cancer. Cells. 2020;9(9).

17. Kawalekar OU, O'Connor RS, Fraietta JA, Guo L, McGettigan SE, Posey AD, Jr., et al. Distinct Signaling of Coreceptors Regulates Specific Metabolism Pathways and Impacts Memory Development in CAR T Cells. Immunity. 2016;44(2):380-90.

18. Weinkove R, George P, Dasyam N, McLellan AD. Selecting costimulatory domains for chimeric antigen receptors: functional and clinical considerations. Clin Transl Immunology. 2019;8(5):e1049.

19. Guedan S, Posey AD, Jr., Shaw C, Wing A, Da T, Patel PR, et al. Enhancing CAR T cell persistence through ICOS and 4-1BB costimulation. JCI Insight. 2018;3(1).

20. Prajapati K, Perez C, Rojas LBP, Burke B, Guevara-Patino JA. Functions of NKG2D in CD8(+) T cells: an opportunity for immunotherapy. Cell Mol Immunol. 2018;15(5):470-9.

7

21. Guo J, Kent A, Davila E. Chimeric non-antigen receptors in T cell-based cancer therapy. J Immunother Cancer. 2021;9(8).

22. Aldoss I, Bargou RC, Nagorsen D, Friberg GR, Baeuerle PA, Forman SJ. Redirecting T cells to eradicate B-cell acute lymphoblastic leukemia: bispecific T-cell engagers and chimeric antigen receptors. Leukemia. 2017;31(4):777-87.

23. Slaney CY, Wang P, Darcy PK, Kershaw MH. CARs versus BiTEs: A Comparison between T Cell-Redirection Strategies for Cancer Treatment. Cancer Discov. 2018;8(8):924-34.

24. Strohl WR, Naso M. Bispecific T-Cell Redirection versus Chimeric Antigen Receptor (CAR)-T Cells as Approaches to Kill Cancer Cells. Antibodies (Basel). 2019;8(3).

25. Molina JC, Shah NN. CAR T cells better than BiTEs. Blood Adv. 2021;5(2):602-6.

26. Subklewe M. BiTEs better than CAR T cells. Blood Adv. 2021;5(2):607-12.

27. Rigau M, Ostrouska S, Fulford TS, Johnson DN, Woods K, Ruan Z, et al. Butyrophilin 2A1 is essential for phosphoantigen reactivity by γδ T cells. Science. 2020;367(6478).

28. Liddy N, Bossi G, Adams KJ, Lissina A, Mahon TM, Hassan NJ, et al. Monoclonal TCR-redirected tumor cell killing. Nat Med. 2012;18(6):980-7.

29. Ellerman D. Bispecific T-cell engagers: Towards understanding variables influencing the in vitro potency and tumor selectivity and their modulation to enhance their efficacy and safety. Methods. 2019;154:102-17.

30. Gründer C, van Dorp S, Hol S, Drent E, Straetemans T, Heijhuurs S, et al. γ9 and δ2CDR3 domains regulate functional avidity of T cells harboring γ9δ2TCRs. Blood. 2012;120(26):5153-62.

31. Vyborova A, Beringer DX, Fasci D, Karaiskaki F, van Diest E, Kramer L, et al. γ9δ2T cell diversity and the receptor interface with tumor cells. J Clin Invest. 2020;130(9):4637-51.

32. Li Y, Moysey R, Molloy PE, Vuidepot AL, Mahon T, Baston E, et al. Directed evolution of human T-cell receptors with picomolar affinities by phage display. Nat Biotechnol. 2005;23(3):349-54.

33. Weber KS, Donermeyer DL, Allen PM, Kranz DM. Class II-restricted T cell receptor engineered in vitro for higher affinity retains peptide specificity and function. Proc Natl Acad Sci U S A. 2005;102(52):19033-8.

34. Smith SN, Harris DT, Kranz DM. T Cell Receptor Engineering and Analysis Using the Yeast Display Platform. Methods Mol Biol. 2015;1319:95-141.

35. Zhao Q, Ahmed M, Tassev DV, Hasan A, Kuo TY, Guo HF, et al. Affinity maturation of T-cell receptor-like antibodies for Wilms tumor 1 peptide greatly enhances therapeutic potential. Leukemia. 2015;29(11):2238-47.

36. Kramer L, Demuysere M, van Diest E, Beringer DX, Kuball J. Challenges of γ9δ2TCR affinity maturation when using phage display. bioRxiv. 2021:2021.05.20.445024.

37. Linette GP, Stadtmauer EA, Maus MV, Rapoport AP, Levine BL, Emery L, et al. Cardiovascular toxicity and titin cross-reactivity of affinity-enhanced T cells in myeloma and melanoma. Blood. 2013;122(6):863-71.

38. Parkhurst MR, Yang JC, Langan RC, Dudley ME, Nathan DA, Feldman SA, et al. T cells targeting carcinoembryonic antigen can mediate regression of metastatic colorectal cancer but induce severe transient colitis. Mol Ther. 2011;19(3):620-6.

39. Harwood SL, Alvarez-Cienfuegos A, Nuñez-Prado N, Compte M, Hernández-Pérez S, Merino N, et al. ATTACK, a novel bispecific T cell-recruiting antibody with trivalent EGFR binding and monovalent CD3 binding for cancer immunotherapy. Oncoimmunology. 2017;7(1):e1377874.

40. Bacac M, Colombetti S, Herter S, Sam J, Perro M, Chen S, et al. CD20-TCB with Obinutuzumab Pretreatment as Next-Generation Treatment of Hematologic Malignancies. Clin Cancer Res. 2018;24(19):4785-97.

41. Staflin K, Zuch de Zafra CL, Schutt LK, Clark V, Zhong F, Hristopoulos M, et al. Target arm affinities determine preclinical efficacy and safety of anti-HER2/CD3 bispecific antibody. JCI Insight. 2020;5(7).

42. Dang K, Castello G, Clarke SC, Li Y, Balasubramani A, Boudreau A, et al. Attenuating CD3 affinity in a PSMAxCD3 bispecific antibody enables killing of prostate tumor cells with reduced cytokine release. J Immunother Cancer. 2021;9(6).

43. Haber L, Olson K, Kelly MP, Crawford A, DiLillo DJ, Tavaré R, et al. Generation of T-cell-redirecting bispecific antibodies with differentiated profiles of cytokine release and biodistribution by CD3 affinity tuning. Sci Rep. 2021;11(1):14397.

44. Chen W, Yang F, Wang C, Narula J, Pascua E, Ni I, et al. One size does not fit all: navigating the multi-dimensional space to optimize T-cell engaging protein therapeutics. MAbs. 2021;13(1):1871171.

45. Poussin M, Sereno A, Wu X, Huang F, Manro J, Cao S, et al. Dichotomous impact of affinity on the function of T cell engaging bispecific antibodies. J Immunother Cancer. 2021;9(7).

46. Mandikian D, Takahashi N, Lo AA, Li J, Eastham-Anderson J, Slaga D, et al. Relative Target Affinities of T-Cell-Dependent Bispecific Antibodies Determine Biodistribution in a Solid Tumor Mouse Model. Mol Cancer Ther. 2018;17(4):776-85.

7
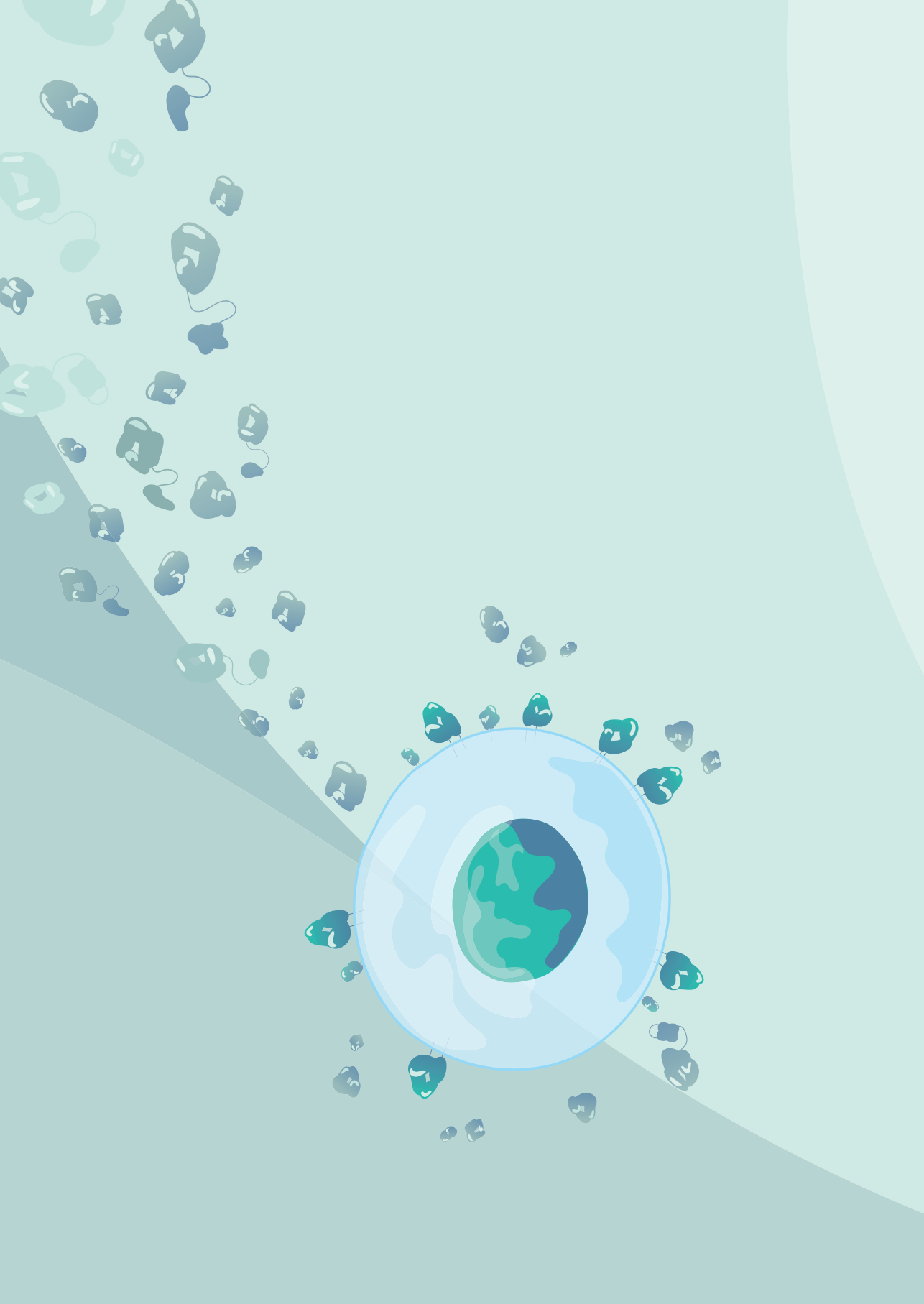
APPENDICES

Nederlandse samenvatting
Acknowledgement / Dankwoord
List of publications
Curriculum vitae

Nederlandse samenvatting

Ondanks alle grote stappen die zijn gezet in het verbeteren van kanker therapieën, zijn er nog steeds veel kankerpatiënten die niet kunnen worden genezen. Bovendien hebben de meeste kankermedicijnen, zoals bijvoorbeeld chemo- of radiotherapie, vervelende tijdelijke bijwerkingen zoals misselijkheid en haaruitval, en is er ook een risico op het optreden van ernstige blijvende schade aan het lichaam. Om deze redenen is het belangrijk dat er nieuwe, betere kankerbehandelingen worden ontwikkeld.

Het menselijke immuunsysteem is cruciaal in bescherming tegen bacteriën en virussen, maar speelt ook een belangrijke rol in het opruimen van kankercellen. Immunotherapie is een nieuwe vorm van kankerbehandeling, die gebaseerd is op dit natuurlijke vermogen van immuuncellen om kankercellen te herkennen en op te ruimen. Hoewel deze nieuwe therapievorm nog volop in ontwikkeling is, wordt het ook al toegepast in de dagelijkse kliniek, waar het voor veel patiënten een verbetering van de behandelopties betekent.

Immunotherapie met T cellen

In **hoofdstuk 1** van deze thesis worden verschillende immunotherapie-strategieën tegen kanker besproken, welke momenteel in verschillende stadia van ontwikkeling zijn. Allereerst de zogenaamde cellulaire immunotherapie met T lymfocyten, oftewel T cellen. T cellen zijn immuuncellen met een antenne, T cel receptor (TCR) genoemd, op hun oppervlakte, waarmee ze andere cellen in het lichaam afspeuren op zoek naar geïnfecteerde of gemuteerde kankercellen. Elke TCR past op een uniek stukje eiwit op het oppervlakte van een andere cel, en als de T cel dit stukje eiwit heeft gevonden en heeft gebonden, is dat een teken voor de T cel dat deze cel opgeruimd moet worden. Er zijn ook T cellen met een TCR die past op een eiwit dat vaak op kankercellen zit, deze cellen noemen we kankerspecifieke T cellen.

In het verleden is geprobeerd deze kankerspecifieke T cellen te isoleren uit een patiënt, ze te vermeerderen in het laboratorium om deze vervolgens weer terug te brengen in het lichaam als therapie, transfusie genoemd. Hoewel dit goed werkte voor sommige patiënten, was het bij de meesten moeilijk kankerspecifieke T cellen te vinden, of om ze uit laten groeien in het laboratorium.

Als oplossing is er een nieuwe techniek bedacht, namelijk het genetisch modificeren van T cellen met een kankerspecifieke TCR. Met deze techniek is het mogelijk veel T cellen te isoleren uit het bloed van een patiënt om deze vervolgens allemaal dezelfde, kankerspecifieke, TCR te geven. Deze gemodificeerde cellen kunnen vervolgens middels transfusie teruggegeven worden aan een patiënt, waarna ze de kankercellen kunnen herkennen en opruimen.

Gamma delta T cellen

De meeste T cellen in het lichaam zijn alfa bèta (αβ) T cellen (met een αβTCR op hun oppervlakte) , maar ongeveer 5% van de T cellen in het bloed zijn van een ander type: het gamma delta (γδ) type. Deze γδ T cellen zijn heel interessant voor immunotherapie, omdat is gebleken dat γδ T cellen in het bijzonder belangrijk zijn voor het herkennen en bestrijden van kankercellen. γδ T cellen hebben een unieke manier om gezonde cellen te onderscheiden van kankercellen, waarmee ze in staat zijn subtiele veranderingen in de metabole staat van kankercellen te herkennen. Dit mechanisme stelt γδ T cellen in staat verschillende typen kankercellen te herkennen, in tegenstelling tot (αβ) T cellen die in de regel slechts één specifiek eiwit herkennen van één specifieke kankersoort. Ondanks deze interessante anti-kanker werking van γδ T cellen, waren de eerste resultaten van onderzoeken waarin deze cellen werden gebruikt als therapie teleurstellend, waardoor er gedurende de laatste jaren verschillende nieuwe ideeën zijn ontwikkeld voor het gebruik van γδ T cellen als immunotherapie.

Een voorbeeld hiervan is een nieuw soort therapie ontwikkeld in ons lab, waarbij αβ T cellen genetisch gemodificeerd worden om een specifieke, kankerreactieve γδ TCR tot expressie te brengen, deze cellen worden TEGs genoemd. Met deze techniek is het mogelijk om de beste kwaliteiten van αβ T cellen te combineren met het unieke anti-kanker mechanisme van γδ T cellen. Momenteel worden de eerste patiënten behandeld met deze therapie in een klinische studie. Hierbij worden αβ T cellen uit het bloed van patiënten gehaald, deze worden dan in een celtherapie faciliteit gemodificeerd met een speciale kankerreactieve γδ TCR. Vervolgens worden de cellen vermeerderd in het lab waarna ze worden teruggegeven aan de patiënt waar ze vervolgens kankercellen kunnen herkennen en opruimen.

Bi-specifieke antilichamen

Met bi-specifieke antilichamen, hebben onderzoekers een nieuwe manier gevonden T cellen te gebruiken om kankercellen aan te vallen, zonder dat het nodig is voor de T cellen om een TCR te hebben die kankerreactief is. Deze bi-specifieke antilichamen zijn zo gemaakt dat ze tegelijkertijd aan kankercellen en aan T cellen kunnen binden. Door dit te doen vormen ze een soort bruggetje tussen de kanker- en de T cel, dit zorgt ervoor dat de T cel actief wordt en de kankercel gaat aanvallen, zonder dat het nodig is een kankerreactieve TCR te hebben die kan binden aan de kankercellen. Dit is een veelbelovende therapie, die momenteel al wordt gebruikt om kankerpatiënten te behandelen. Anders dan bij genetische modificatie, is het bij bi-specifieke antilichaamtherapie niet nodig om cellen uit het bloed van de patiënt te halen, de bi-specifieke antilichamen kunnen simpelweg toegediend worden met een infuus or injectie. Dit maakt de behandeling in theorie een stuk sneller en potentieel minder belastend voor de patiënt.

A

Samenvatting van de belangrijkste resultaten:

In **hoofdstuk 2** bespreken we een techniek die door ons is ontwikkeld om het produceren van αβ TCR gemodificeerde T cellen te verbeteren. Het proces om genetisch gemodificeerde cellen te maken is nooit 100 procent effectief, waardoor er aan het einde van het proces een mix van gemodificeerde cellen (met de kankerspecifieke TCR) en on-gemodificeerde cellen (met hun originele TCR) overblijft. Dit zou er voor kunnen zorgen dat de therapie minder effectief is, omdat een gedeelte van de cellen die aan de patiënt wordt gegeven niet de gewenste kankerreactieve TCR op zijn oppervlakte heeft, en dus niet zal reageren op de kankercellen. Wij hebben een techniek ontwikkeld om na de genetische modificatie de genetisch gemodificeerde cellen te scheiden van de on-gemodificeerde cellen. Hierdoor is het mogelijk alleen de gemodificeerde cellen, die nu kankerreactief zijn, terug te geven aan de patiënt als therapie. Dit hebben we gedaan door een paar veranderingen (mutaties) aan te brengen in de geïntroduceerde kankerreactieve TCR, waardoor deze onderscheiden kan worden van de originele (endogene) TCR van de T cellen.

Met dit soort anti-kanker therapieën is er altijd een risico dat patiënten bijwerkingen ervaren van de therapie, bijvoorbeeld omdat de gemodificeerde cellen te actief zijn of naast de kankercellen, ook andere gezonde lichaamscellen gaan aanvallen. Als dit gebeurt, is het belangrijk een manier te hebben om de gemodificeerde cellen uit te schakelen. In dit hoofdstuk laten we ook zien dat het mogelijk is specifiek alleen de gemodificeerde T cellen, en niet alle lichaamseigen T cellen, te herkennen en uit te schakelen. We hebben laten zien dat dit ook mogelijk is door gebruik te maken van de mutaties in de geïntroduceerde TCR.

In **Hoofdstuk 3** beschrijven we een manier om de in ons lab ontwikkelde TEG therapie (αβ T cellen genetisch gemodificeerd om een specifieke, kankerreactieve γδ TCR tot expressie te brengen) te verbeteren. We laten zien dat door een extra receptor, de zogenoemde co-stimulatie receptor, te introduceren naast de kankerreactieve γδ TCR, de TEG cellen beter worden in het herkennen en opruimen van kankercellen. Dit komt doordat, met de extra co-stimulatie receptor, de cellen minder snel 'vermoeid' raken en daardoor langer door kunnen gaan met kankercellen herkennen en opruimen. Tevens vermeerderen ze sneller wat ook belangrijk is voor hun effectiviteit. Uiteindelijk laten we zien dat in een experiment met muizen de nieuwe TEGs met co-stimulatie langer actief blijven en beter zijn in het aanvallen van de kankercellen. In dit onderzoek hebben we verschillende type co-receptoren getest, waarbij we duidelijke verschillen vonden tussen de geteste co-receptoren. Uiteindelijk hebben we één type receptor gevonden die in al onze experimenten de beste resultaten gaf. De uitkomst van dit onderzoek zijn niet alleen belangrijk voor onze TEGs, maar zouden ook van nut kunnen zijn voor andere therapieën die gebruik maken van gen modificatie met kankerreactieve TCRs.

In **hoofdstuk 4** introduceren we een nieuw bi-specifiek antilichaam concept, gebruikmakend van een γδ TCR voor kankerbinding. Normaal gesproken zitten γδ TCRs vast op het oppervlakte van een cel, maar in dit hoofdstuk laten we zien dat het ook mogelijk is om met wat aanpassingen, de γδ TCR los te maken van het celoppervlak. Deze zogenaamde *soluble* TCR kan nog steeds binden aan kankercellen, en door vervolgens de TCR te koppelen aan een stukje antilichaam dat kan binden aan T cellen, creëren we een bi-specifiek antilichaam. We noemen dit nieuwe bi-specifieke antilichaam GAB, wat staat voor **G**amma delta TCR **A**nti-CD3 **B**ispecific antibody. In dit hoofdstuk laten we zien dat toevoeging van GABs kan zorgen voor het herkennen en opruimen van kankercellen door αβ T cellen die zelf geen kankerreactieve TCR hebben, en zonder de GAB dus de kankercellen niet zouden herkennen. We laten eerst zien dat dit concept werkt in het lab (*in vitro*) en later laten we ook zien dat het inspuiten van GABs in muizen met een kanker ook leidt tot reductie in kankergroei *(in vivo)*.

In de twee volgende hoofdstukken van deze thesis bespreken we twee manieren die we onderzocht hebben om de werking van GABs te verbeteren. In **hoofdstuk 5** laten we zien dat het mogelijk is de activiteit van de GABs te verbeteren door er een dimeer van te maken. De GABs beschreven in hoofdstuk 4, hebben één kankerbindingsdomein (de γδ TCR) en één T cell bindingsdomein (de anti-CD3), dit noemen we een monomeer. In hoofdstuk 5 laten we zien dat het mogelijk is de GAB als dimeer te maken, waardoor elke GAB bestaat uit twee γδ TCRs voor kankerbinding en twee anti-CD3s voor T cel binding. We laten zien dat *in vitro* (in het lab) deze dimeer beter werkt dan de monomeer, waarbij je veel minder GAB hoeft te gebruiken om hetzelfde anti-kanker effect te bereiken. Dit komt waarschijnlijk doordat de GAB sterker kan binden aan de kankercellen met twéé bindingsdomeinen in vergelijking met één, een effect dat bekend is als het aviditeiteffect. Hoewel deze bevinding zeer interessant is, was het een stuk moeilijker om deze GAB dimeren in dezelfde hoeveelheden als de GAB monomeren te maken.

In hoofdstuk 6 vergelijken we GABs met verschillende T cel bindingsdomeinen (anti- CD3s). In de literatuur is beschreven dat voor andere bi-specifieke antilichamen, de keuze voor de anti-CD3 een groot effect kan hebben op de effectiviteit van het bi-specifieke antilichaam. Daarom hebben we in hoofdstuk 6 GABs gemaakt met vijf verschillende anti-CD3s en deze vergeleken voor effectiviteit. Deze verschillende anti-CD3s verschillen vooral in sterkte van binding aan de T cellen, bindingsaffiniteit genoemd. We laten zien dat *in vitro* de GABs met hoge bindingsaffiniteit aan T cellen, beter werken dan GABs met een lagere T cel bindingsaffiniteit. Vervolgens testen we dit ook *in vivo* in muizen, waarbij we hetzelfde effect zien. Interessant is dat dit in contrast staat met sommige bevindingen van andere onderzoekers, waarbij ze laten zien dat hoewel hoge T cel

A

bindingaffiniteit in vitro een beter resultaat geeft, dit *in vivo* juist andersom is en lagere affiniteit beter is. Onze hypothese is dat dit te maken heeft met verschillen in het kanker bindingsdomein. Waar veel bi-specifieke antilichamen gemaakt worden met hele hoge bindingsaffiniteit voor de kanker, heeft de GAB juist een vrij lage bindingaffiniteit voor de kankercellen. Dit zou de verschillen tussen onze bevindingen en die van andere onderzoekers kunnen verklaren.

In het laatste hoofdstuk, **hoofdstuk 7**, worden de resultaten ten slotte samengevat, en in een breder perspectief geplaatst door vergelijkingen te maken met de huidige literatuur.

Acknowledgement / Dankwoord

Dear **Jürgen**, first of all I would like to thank you for all your guidance and support during my PhD. I admire your work ethic, and your endless endeavor to form one strong group of scientists that work together and share their successes. Thinking back, I can imagine you sometimes had a hard time with Dennis and myself during meetings, where we could be very skeptical (and maybe even negative) about new data, and you then had to convince us that it looked promising and we should definitely explore this further. I did always enjoy the discussions, and learned that sometimes it also okay to agree to disagree. I had a lot of fun skiing together in Canada, nice to get to know you also in a different way. I wish you and the Kuball group all the best for the future, and hopefully we will still run in to each other every now and then.

Dear **Dennis** without you this thesis would definitely not have become what it is now. You are always calm and collected, and if I was lost in what to do or what try next, I knew walking by your office would always help the project (or me) back on track. From you I learned that being stressed doesn't help, and to just solve whatever problem needs solving. Sometimes I worry too much, and are hard on myself, and having your support and seeing your down-to-earth approach to the scientific world definitely helped me throughout my PhD, and all the set-backs we had to deal with during those times. I hope you can successfully continue with the soluble TCR/GAB projects, I look forward to seeing new publications in the future.

Dear **Dr. Zsolt** thanks to you I ended up performing my PhD in the Kuball group**.** You gave me the opportunity to perform my master internship under your supervision in the Kuball group, and that's how I ended up sticking around a lot longer. Although we didn't work as closely together during my PhD, you always had helpful input during meetings and feedback on manuscripts, thank you for that. And sorry that I ended up being a lot like Dennis in your opinion, however I think that was my character all along, I just hid it better during my internship.

Dear **Patricia**, what started as providing some assistance in testing GABs *in vivo,* ended up being a multiple years, multiple projects collaboration. Thank you for your hard work and perseverance in running al the failed GAB *in vivo* experiments we had to do before being successful in the end. It was always great working with you, you are easygoing, kind and willing to put in a lot of work without ever complaining. I hope the other story we worked on together, though in the basis your project, the NKG2D paper will be published in a great journal, you definitely deserve that. All the best luck in finishing your thesis, and the continuation of your work in the Kuball group as postdoc.

A

Dear **Inez**, we started our PhD at the same time. And while our projects were very different, and you went through it faster than I did, it was always nice to have someone to go to with questions and concerns. You often made me laugh with your unfiltered comments, I will never forget your eye candy remark in front of the entire group!

Great science is performed together, so I want to thank all other members of the Kuball group. **Sabine**, thank you for all the help with the *in vivo* experiments, and your genuine believe that we could get it to work and your enthusiasm when we did. **Trudy** you helped from the side-line with in *in vivo* experiments: thank you for all the good input, and the fun we had skiing in Canada. **Tineke**, thank you for always being available for questions and advice, and ofcourse for teaching me the legendary elispot assay and helping me reviving the luciferase based killing assays. **Angelo,** the 3D model you set-up helped to publish multiple stories in our group, including the GAB paper. Thank you for always making time to help out with this, even if you were already dealing with a full agenda. Good luck with finishing you thesis. **Astrid**, I don't think we ever worked together on a project, which is an accomplishment since you were there my entire time at the Kuball group, thank you for always hosting the Christmas drinks and the nice talks we had in the protein lab. **Mara and Jiali,** thanks to you we managed to publish the dimer paper, thank you for the work you put in to that. And to the other PhD students, **Lucrezia** and **Konstantinos:** we only overlapped a bit at the end of my PhD, when I might not have been the most approachable person in the lab, sorry for that. I am actually quite friendly, and I really can't help that serious face I have when walking down the hallways. I wish you all the best for your projects, I hope you are both successful. **Froso,** thank you for all the work you put into different chapters of this thesis, mainly chapter six wouldn't have finished without your pipetting skills. **Anke** and **Anna**, running buddies, I really enjoyed our Friday lunch runs together, and ofcourse the fun times together in Bordeaux during the gamma delta conference.

Also a big thanks to the students that helped me during my PhD: **Anita** and **Koen**, thanks to you we managed to clone a lot of different GAB constructs that ended up being the foundation for chapter 6 of this thesis.

Lieve Roomies, nu kan het in het Nederlands want we waren wat dat betreft niet zo inclusief. Na het eerste jaar van mijn PhD kwam ik bij jullie in de kamer terecht, en ik heb het hier ontzettend naar mijn zin gehad. **Kevin:** de pater familias, met wie ik altijd heerlijk kon kletsen als we de eersten op het kantoor waren, over alle bouwprojecten in Utrecht en het nieuwe seizoen van een huis vol bijvoorbeeld. **Thomas** en **Niels** jullie zie ik toch een beetje als duo en vooral mijn hardloop maatjes, Niels ik vond het zo leuk dat ik je kon verslaan met hardlopen in het

begin, maar later durfde ik me er niet meer aan te wagen. En Thomas, lekker hoe jij altijd wat olie op het vuur kon gooien van onze competitie drang. Ik hoop dat jullie beiden je PhD binnenkort ook succesvol af zullen ronden, heel veel succes hierbij. **Mitchell,** ik heb vooral gelachen om- en een beetje gegruwd van jouw eet-, of voornamelijk, opruim gewoontes. Maar had bewondering voor de hoeveelheid werk die je altijd hebt verricht, zowel tijdens je PhD als erna als postdoc. **Anne,** samen moesten wij een beetje weerstand bieden aan al het testosteron in de kamer, we hebben in ieder geval ons best gedaan met plantjes en opruim acties. Hopelijk kom ik jullie allemaal zo nu en dan nog tegen in het UMC, of ergens anders in Utrecht.

Allerliefste **Papa** en **Mama**, hoewel ik jullie niet erg gedetailleerd op de hoogte hield van de vorderingen tijdens mijn PhD, was het fijn om te weten dat jullie er waren als ik het nodig had en jullie trots op me zijn. Ik heb geluk met zulke lieve ouders, waar je altijd op terug kan vallen als het even tegenzit, die je helpen waar nodig, en die met je mee dansen als er iets te vieren valt.

En mijn lieve zusjes en broer. **Inge** en **Sjaakie,** een tijdlang woonden we alle drie in Utrecht, en ontstond de traditie om elke week samen te eten. Hoewel de frequentie hiervan inmiddels een stukje lager is, en Sjaakie weer terug naar Wageningen is getrokken, proberen we de traditie in stand te houden. Zo fijn om twee zussen te hebben waar je altijd terecht kunt voor leuke en minder leuke dingen. En Inge, sorry dat ik nooit wilde praten over mijn PhD, hopelijk maakt de Nederlandse samenvatting die ik heb geschreven voor dit boekje dit een beetje goed. Lieve **Bob**, van student die ik regelmatig dronken in de kroeg tegenkwam naar een ontzettend lieve vader van twee kleine apenkopjes. Ik vind het heel jammer dat Jolien en jij niet bij mijn verdediging zullen zijn, maar ik gun jullie het Bali avontuur van harte, en hoop dat jullie daar een geweldige tijd gaan hebben!

Lieve **Léon** en **Maria**, ik leerde jullie kennen aan het begin van mijn PhD als ontzettend lieve schoonouders, die betrokken en geïnteresseerd waren in mijn werk en probeerden te snappen waar ik allemaal mee bezig was. Jullie hebben een ontzettend lieve en slimme zoon opgevoed, dankjewel daarvoor!

Lieve **Opa & Oma**, vanaf mijn eerste rapport op de basisschool tot nu, het behalen van mijn PhD, jullie hebben het allemaal meegemaakt en zijn overal bij geweest. Ik ben ontzettend blij met zulke lieve en betrokken grootouders, en ik hoop dat jullie nog veel meer mijlpalen mee kunnen maken.

Opa Tom, of prof dr. ir. A van Diest, het is ontzettend jammer dat jij deze promotie dag niet meer mee kan maken. Je was trots toen ik tijdens mijn master stage ging lopen in Amerika, het herinnerde je aan jouw tijd in Amerika, waar je je PhD hebt

A

behaald en later nog als postdoc hebt gewerkt. Veel was natuurlijk veranderd sinds die tijd, maar toch waren er ook gelijkenissen. Ik kwam terug uit Amerika om aan mijn promotie te gaan beginnen, en daar was jij natuurlijk ook zeer geïnteresseerd in tot op het laatst. Helaas hebben we afscheid van je moeten nemen, maar we zullen aan je denken vandaag.

En dan mijn vriendinnen, **de Prinsjes**, tijdens onze studietijd begon het plezier bij Histos, en inmiddels zijn we heel al wat koophuizen, kinderen en een bruiloft verder, maar nog steeds bij elkaar. Ik was natuurlijk een beetje 'the odd one out' met mijn studie biomedische wetenschappen en daarna mijn promotie traject, maar dat betekende niet dat jullie niet geïnteresseerd waren in wat ik allemaal uitspookte in het lab. Jullie moet ik vooral bedanken voor alle afleiding en leuke momenten die ik met jullie heb beleeft tijdens mijn PhD, dat kon ik af en toe heel goed gebruiken! Lieve **Aniek, His, Mijke, Nina, Plien, Eef, Liz, Siem, El, Riep en Lien**, dank jullie wel.

En dan ten slotte de man die ik het meeste moet bedanken: **Matti.** Wij leerden elkaar kennen toen ik pas net begonnen was met mijn PhD, en gelukkig wilde je voor mij je mening over PhD studenten wel bijstellen. Jij bent door de jaren heen steeds meer mijn steun en toeverlaat geworden, waar je hard je best voor hebt moeten doen, want ook met jou deelde ik niet veel over werk. Zo kwam je er pas na twee jaar achter dat ik aan bispecifics werkte, en niet aan biospecifics. Ondanks mijn weerstand af en toe, heb je me ontzettend geholpen gedurende de jaren en zeker tijdens het afronden van mijn thesis, waar ik het af en toe best moeilijk mee heb gehad. Lieve schat, zonder jouw hulp en rotsvaste vertrouwen in mij was dit allemaal een stuk lastiger geweest en daar ben ik je heel dankbaar voor.

List of Publications

This Thesis

Kierkels GJJ*, <u>van Diest E</u>*, Hernández-López P*, Scheper W*, de Bruin ACM, Frijlink E, Aarts-Riemens T, van Dooremalen SFJ, Beringer DX, Oostvogels R, Kramer L, Straetemans T, Uckert W, Sebestyén Z, Kuball J. Characterization and modulation of anti-αβTCR antibodies and their respective binding sites at the βTCR chain to enrich engineered T cells. Mol Ther Methods Clin Dev. 2021 Jun 24 ;22:388-400.

Hernández-López P*, <u>van Diest E</u>*, Brazda P, Johanna I, Meringa A, Heijhuurs S , Nicolasen MJT, Kluiver T.A, Millen R, Karaiskaki E, Straetemans T, Clevers H, de Bree R, Stunnenberg HG, Peng W.C, Sebestyén Z, Beringer DX[#], Kuball[#] Combining targeting of the cancer metabolome and cancer-associated stress antigens impacts engineered T cell dynamics and efficacy. Manuscript in preparation, Januari 2023

<u>van Diest E</u>*, Hernández López P*, Meringa AD, Vyborova A, Karaiskaki F, Heijhuurs S, Gumathi Bormin J, van Dooremalen S, Nicolasen MJT, Gatti LCDE, Johanna I, Straetemans T, Sebestyén Z, Beringer DX, Kuball J. Gamma delta TCR anti-CD3 bispecific molecules (GABs) as novel immunotherapeutic compounds. J Immunother Cancer. 2021 Nov;9(11):e003850. Erratum in: J Immunother Cancer. 2021 Dec;9(12)

<u>van Diest E</u>*, Nicolasen MJT*, Kramer L, Zheng J, Hernandez-Lopez P, Beringer DX[#] and Kuball J[#]. The making of multivalent gamma delta TCR anti-CD3 bispecific T cell engagers. Front. Immunol. 2023 13:1052090

<u>van Diest E</u>*, Hernández López P*, Karaiskaki F, Bots K, Heijhuurs S, Kumari A, Straetemans T, Beringer DX[#], Kuball J[#]. Impact of CD3 binding affinity on potency of Gamma delta TCR Anti-CD3 Bispecific T cell engagers (GABs). Manuscript in preparation, Januari 2023

*These authors share first authorship
[#]These authors share senior authorship

Other

Hanke L, Knockenhauer KE, Brewer RC, <u>van Diest E</u>, Schmidt FI, Schwartz TU, Ploegh HL. The Antiviral Mechanism of an Influenza A Virus Nucleoprotein-Specific Single-Domain Antibody Fragment. mBio. 2016 Dec 13;7(6):e01569-16.

A

Janssen A, Villacorta Hidalgo J, Beringer DX, van Dooremalen S, Fernando F, <u>van Diest E</u>, Terrizi AR, Bronsert P, Kock S, Schmitt-Gräff A, Werner M, Heise K, Follo M, Straetemans T, Sebestyen Z, Chudakov DM, Kasatskaya SA, Frenkel FE, Ravens S, Spierings E, Prinz I, Küppers R, Malkovsky M, Fisch P, Kuball J. γδ T-cell Receptors Derived from Breast Cancer-Infiltrating T Lymphocytes Mediate Antitumor Reactivity. Cancer Immunol Res. 2020 Apr;8(4):530-543.

Vyborova A, Beringer DX, Fasci D, Karaiskaki F, <u>van Diest E</u>, Kramer L, de Haas A, Sanders J, Janssen A, Straetemans T, Olive D, Leusen J, Boutin L, Nedellec S, Schwartz SL, Wester MJ, Lidke KA, Scotet E, Lidke DS, Heck AJ, Sebestyen Z, Kuball J. γ9δ2T cell diversity and the receptor interface with tumor cells. J Clin Invest. 2020 Sep 1;130(9):4637-4651.

Janssen A, <u>van Diest E</u>, Vyborova A, Schrier L, Bruns A, Sebestyen Z, Straetemans T, de Witte M, Kuball J. The Role of γδ T Cells as a Line of Defense in Viral Infections after Allogeneic Stem Cell Transplantation: Opportunities and Challenges. Viruses. 2022 Jan 10;14(1):117.

Wachsmann TLA, Wouters AK, Remst DFG, Hagedoorn RS, Meeuwsen MH, <u>van Diest E</u>, Leusen J, Kuball J, Falkenburg JHF, Heemskerk MHM. Comparing CAR and TCR engineered T cell performance as a function of tumor cell exposure. Oncoimmunology. 2022 Feb 1;11(1):2033528.

Curriculum vitae

Eline van Diest was born on the 27th of July 1993 in Maastricht. In 2011 she completed her secondary education at the Sint-Maartenscollege in Maastricht (VWO-Atheneum). She then moved to Utrecht to study Biomedical Sciences at Utrecht University. After completing her bachelor in 2014 cum laude, Eline enrolled in the master program Infection and Immunity. As part of this program she performed a nine month internship under the supervision of dr. Zsolt Sebestyèn on CD20 CAR T cells. Afterwards, she performed a 6 month internship in the group of prof. dr. Hidde Ploegh at the Whitehead institute in Cambridge, Massachusetts. Here she worked on disrupting the influenza viral life cycle by intracellular expression of camelid derived single domain antibodies. After obtaining her MSc in 2016, she started her PhD training in the group of prof. dr. Jürgen Kuball at the Center for Translational Immunology at the University Medical Center Utrecht, where she worked on different strategies to improve immunotherapeutic therapies against cancer, including bispecific T cell engagers and TCR gene therapy with αβ and γδ TCRs. The results of this work are described in this thesis.

Currently, Eline is working as scientist cellular immunology and nanocell therapeutics, where she continuous to contribute to the development of novel immunotherapeutic strategies against cancer.

A